Geomorphic Studies of the Storm and Flood of November 3–5, 1985, in the Upper Potomac and Cheat River Basins in West Virginia and Virginia

U.S. GEOLOGICAL SURVEY BULLETIN 1981

Geomorphic Studies of the Storm and Flood of November 3–5, 1985, in the Upper Potomac and Cheat River Basins in West Virginia and Virginia

ROBERT B. JACOBSON, Editor

Chapters A through E are published as a
single volume and are not available separately

U.S. GEOLOGICAL SURVEY BULLETIN 1981

U.S. DEPARTMENT OF THE INTERIOR
BRUCE BABBITT, Secretary

U.S. GEOLOGICAL SURVEY
Dallas L. Peck, Director

UNITED STATES GOVERNMENT PRINTING OFFICE: 1993

For sale by
U.S. Geological Survey, Map Distribution
Box 25286, MS 306, Federal Center
Denver, CO 80225

Library of Congress Cataloging in Publication Data

Geomorphic studies of the storm and flood of November 3–5, 1985, in the upper Potomac and Cheat River basins in West Virginia and Virginia / Robert B. Jacobson, editor.
p. cm.—(U.S. Geological Survey bulletin; 1981) "A multidisciplinary study of the geomorphic effects of a severe storm in a mountainous area of the Appalachians."
Includes bibliographical references.
1. Landslides—Potomac River Watershed. 2. Landslides—Cheat River Watershed (W.Va. and Pa.). 3. Severe storms—Appalachian Mountains. 4. Floods—Potomac River Watershed. 5. Floods—Cheat River Watershed (W. Va. and Pa). 6. Geomorphology—Appalachian Mountains. I. Jacobson, Robert B. II. Series.
QE75.B9 no. 1981
[QE599.U5]
557.3 s—dc20
[551.3'07'0975491]

91–14451
CIP

CONTENTS

[Letters designate the chapters]

Chapter A

Introduction: Geomorphic Studies of the Storm and Flood of November 3–5, 1985, in the Upper Potomac and Cheat River Basins

By ROBERT B. JACOBSON

A multidisciplinary study of the geomorphic effects of a severe storm in a mountainous area of the Appalachians

U.S. GEOLOGICAL SURVEY BULLETIN 1981

GEOMORPHIC STUDIES OF THE STORM AND FLOOD OF NOVEMBER 3–5, 1985, IN THE UPPER POTOMAC AND CHEAT RIVER BASINS IN WEST VIRGINIA AND VIRGINIA

CONTENTS

PLATE

Introduction: Geomorphic Studies of the Storm and Flood of November 3–5, 1985, in the Upper Potomac and Cheat River Basins

By Robert B. Jacobson

INTRODUCTION

The heavy rains of November 3–5, 1985, produced record floods and extensive landsliding in the Potomac and Cheat River basins in West Virginia and Virginia (pl. 1). Although rainfall intensity was moderate, the storm covered a very large area and produced record floods for basins in the size range of 1000–10,000 km^2. In addition, thousands of landslides were triggered on slopes underlain by shale bedrock. The total social cost of the storm amounted to 70 lives lost and an estimated $1.3 billion in damage to homes, businesses, roads, and productive land in West Virginia and Virginia (Federal Emergency Management Agency (FEMA) 1985a, b). These extreme costs were incurred despite the fact that the affected area is sparsely populated.

To understand the origins and geomorphic effects of the 1985 storm, studies were undertaken by the U.S. Geological Survey, University of Maryland, West Virginia University, Cornell University, University of Virginia, The Johns Hopkins University, and Carleton College. Personnel were also consulted from the National Weather Service, Nuclear Regulatory Commission, U.S. Army Corps of Engineers, Soil Conservation Service, and Interstate Commission on the Potomac River basin.

This cooperative effort serves to document the effects of the storm as an example of an extreme geomorphic event in the central Appalachian Mountains. The following chapters comprise observations and preliminary analyses for some of the observed phenomena. Subsequent publications by the contributors to this volume will expand the scope of this research.

SOCIAL COSTS AND MITIGATION ISSUES

Cataclysmic storms that trigger floods and landslides are rare on human time scales, and memory of the catastrophic effects of storms appears to fade quickly. Despite a regional history of destructive floods in the central Appalachians, including well-publicized events in 1936, 1949, 1955, 1969, and 1972, homes and businesses are concentrated in valley bottoms, and public awareness of flood and landslide hazards is low. Interagency reports following the 1985 flood concluded that local and federal flood-plain management and disaster preventiveness programs have not been effective in reducing the risks to inhabitants of the region (FEMA, 1985a). When floodwaters swept through the narrow valleys of the Potomac and Cheat River basins November 4–6, 1985, inhabitants were ill prepared for the severity of the storm (FEMA, 1985a, p. 16).

The storm and flood caused an estimated $1.3 billion in damages in West Virginia and Virginia, including 70 deaths (FEMA, 1985a, b). In West Virginia, estimated damages totaled $577 million; 45 percent was to homes (9,000 homes, most of which were mobile homes in flood plains), 17 percent to agriculture, 20 percent to businesses, and 18 percent to public structures, primarily roads and bridges (FEMA, 1985a). In Virginia, estimated damages totaled $753 million; 62 percent was to private nonagricultural, 20 percent to agricultural, and 17 percent to public land and structures (FEMA, 1985b). Total disaster assistance from 14 federal agencies amounted to $285 million (Government Accounting Office, 1988).

In the wake of the 1985 flood, interagency flood-hazard mitigation reports stressed several key aspects of the problem of flooding in steep mountainous areas (FEMA, 1985a, b). The primary factor that leads to loss of life is the inhabitants' lack of perception of the hazard of flash floods. Hazard perception is a particular problem in steep basins, where channels are normally dry or have small flows. Inhabitants are not aware that steep basins can produce heavy flows with high concentrations of sediment and debris. To increase perception of the hazards of flood-prone areas, the reports stressed increased implementation of flood-warning evacuation systems and public awareness campaigns. Other factors addressed were siting of structures

Manuscript approved for publication February 22, 1991.

to avoid both inundation and erosional damage, design of bridges and highways to minimize impact of large, high-energy floods with high sediment loads, implementation of flood-control structures (both impoundments and protective levees), and restoration of stream channels and agricultural lands (FEMA, 1985a, b).

THE NOVEMBER 1985 STORM AS A GEOMORPHIC EXPERIMENT

Many of the mitigation strategies proposed for recovery from the 1985 event, and for dealing with similar events in the future, require understanding of the processes that create destructive floods and landslides in the central Appalachians. The meteorological conditions that lead to severe rainfall are poorly understood, and the recurrence frequencies of severe rainfall intensities and durations are only broadly predictable. Poor estimates of the recurrence frequencies of extreme floods stem from the fact that frequency analysis must rely on short historical flood records (most less than 50 yr). Landslide recurrence frequencies are mostly unknown. General models for geologic, geomorphic, and land-use controls on where flood and landslide damage occur do not exist, although evidence from many past floods indicates that the geomorphic effects of extreme storms are not randomly distributed on the landscape. No general strategy or methodology exists for adequately mapping flood and landslide hazards in the central Appalachian Mountains.

Because the November 1985 storm and its effects were unusually well documented by stream gages, rain gages, and poststorm aerial photography, the cataclysmic event could be studied in detail. In the study area, the storm consisted of a large, fairly homogeneous area of precipitation that can be resolved with existing rain gage data (pl. 1). Colucci and others (chapter B, this volume) discuss the meteorological context of the 1985 storm.

One of the main areas of high rainfall was located astride the Wills Mountain anticline, a structure that involves a variety of bedrock lithologies. Thus the influences of very different rocks and regoliths on landslide occurrence could be investigated along a well-defined rainfall gradient. Jacobson and others (chapter C, this volume) discuss the occurrence of landslides triggered by the 1985 storm.

Substantial rain fell on both the Potomac and Cheat River basins. The Cheat River basin is in the nearly flat-lying sedimentary rocks of the Appalachian Plateau physiographic province, whereas most of the affected parts of the Potomac River basin are in the folded Valley and Ridge physiographic province. This varied physiography has permitted study of flood effects in basins with very different geologic controls on valley geometry, sediment supply, and hydrologic response. Kite and Linton (chapter D, this volume) discuss these effects in the Cheat River basin and Miller and Parkinson (chapter E, this volume) discuss flood effects in the Potomac River basin.

Geomorphic Effects of the 1985 Storm and Natural Hazard Mitigation

Geomorphologists seek to understand the landscape in terms of mechanics, magnitude, and frequency of erosional and depositional processes. These concepts are also critical to design of policies that can mitigate hazards of severe storms like the November 1985 event.

Colucci and others (chapter B, this volume) analyzed the November 1985 storm event in terms of the size and recurrence of severe storms in the central Appalachians. They show that the 1985 storm resulted from a complex, but recognizable, series of meteorological events. Analysis of the genesis of the storm should be of use in future monitoring of meteorological conditions and should aid in prediction of severe rainfall. Simple frequency analysis of 2-day rainfall totals yielded a range of recurrence intervals (for rainfall at a point) from 80 to nearly 300 yr. The constraints on the frequency analysis point to the need for more long-term rainfall data. This chapter also contains a description of how "flash floods" can be triggered by long-duration as well as intense, short-duration rainfall.

Jacobson and others (chapter C, this volume) concentrate on magnitude and frequency of landslides, and the geologic, geomorphic, and land-use factors that control where landslides were triggered by the storm. Their results include (1) characterization of physical properties that were responsible for stability or instability of some regoliths, (2) evaluation of the bedrock, surficial geologic, land cover, and topographic factors that controlled where landslides occurred, (3) determination of the rainfall totals that triggered landslides on several regoliths, (4) determination of the relation between total rainfall and number of slope movements triggered, (5) construction of a statistical model for the recurrence frequency with which different areal densities of landslides can be expected in the future, and (6) evaluation of the influence of the considerable numbers of landslides that mobilized into debris flows and delivered sediment to streams to cause flood-related geomorphic changes.

Evaluation of the sensitivity of slope stability to various combinations of bedrock geology, surficial geology, land cover, and topography is necessary for establishing land management policies concerned with minimizing erosion, sedimentation, and hazards. Data on the recurrence frequency of landslides are important to evaluate future hazards and sediment supply from landslides. Landslides were not a particular concern in FEMA (1985a, b) reports, presumably because they occurred mostly on agricultural and forested land rather than in populated areas. However, much of the damage from flooding was due to large deposits of sediment and debris, which possibly originated from

landslides. Furthermore, in at least eight instances, debris flows reached stream channels and continued downstream, where their high bulk density could be expected to exert high shear stresses on channel beds and banks. The hypothesis that landslides may have contributed significantly to geomorphic changes in stream channels was tested by Jacobson and others, who found that landslides did have a measurable effect on these changes.

Kite and Linton (chapter D, this volume) and Miller and Parkinson (chapter E, this volume) discuss where and how flood damage occurs in these steep mountain basins. The December 1985 interagency report on flood-hazard mitigation for West Virginia states, "The unprecedented flood waters affected both floodprone areas and areas that had not known serious flooding in the past..." and that floodwater velocity, and not simply inundation, was responsible for much of the flood damage (FEMA, 1985a). Both chapters contain analyses of the hydraulic situations that created the most severe flood-plain erosion and deposition. Flow patterns and flow velocities were better than inundated area in predicting where the most severe flood-plain erosion and associated deposition occurred. In certain hydraulic situations, floodwaters caused channel avulsion and severe lateral erosion of valley bottom sediments. Lateral erosion was effective in removing parts of alluvial terraces and fans, whose surfaces were far above the presumed 100-yr flood levels. Other low-lying areas of valley bottoms were covered by several meters of slow-moving floodwater but experienced insignificant deposition or erosion. These observations suggest that step-backwater modeling of 100-yr flood stages may not be the best method to measure potential hazards in steep headwater drainage basins.

Kite and Linton's analysis of slack-water deposits from the 1985 storm illustrates the limitations of paleoflood hydrology in the central Appalachians. If calculation had been based on the altitudes of slack-water sediments deposited by the flood, the discharge of the 1985 flood on the Cheat River would have been significantly underestimated.

The conclusions of these two chapters have implications for (1) where to place public facilities, roadways, and bridges in valley bottoms to minimize risk from high-velocity flows, (2) design criteria for flood control structures, (3) design criteria for wet floodproofing, (4) the potential effects of upstream channelization on downstream hazards, and (5) the importance of valley-bottom land use in determining flood damage.

Geomorphic Effects of the 1985 Storm and Long-Term Landscape Evolution

The effects of the 1985 storm also provide information to construct models of long-term landscape evolution. The primary questions at issue in the central Appalachian Mountains are (1) the relative importance of rare and severe versus more common, low-magnitude geomorphic events in sculpting the landscape and (2) the importance of the present-day climate versus the effects of ancient climates.

Erosional and depositional features similar to those created by the 1985 event are replicated elsewhere in the landscape. Many debris flows from small landslides in 1985 were deposited on colluvial wedges and debris fans; these features are composed of multiple layers from previous events, although the bulk of the deposits may date from the transition between the Pleistocene and Holocene (Jacobson and others, 1989a, b). Flows from a small number of large debris avalanches that were triggered high on ridgetops are similar to more extensive prehistoric debris deposits (see pl. 1*B*, in Jacobson and others, chapter C, this volume). Similarly, prehistoric anastomosing channel patterns, channel avulsion scars, and levee and splay deposits attest to the fact that floods like the 1985 flood have occurred in the past in this area. Radiocarbon dates from two sites in Petersburg and Moorefield, W. Va., indicate that most of the existing sediment in the valley bottom is middle to late Holocene, but that islands and terraces of older sediments are also present (Jacobson and others, 1989a). In fact, most distinct features in the central Appalachian landscape are erosional or depositional features from processes similar to those triggered by the 1985 storm. From these observations, Jacobson and others (1989b) argued that rare, catastrophic, storm-generated events are the most effective in sculpting the central Appalachian landscape under the present-day climate, although extensive older deposits also attest to the importance of ancient climates.

REFERENCES CITED

Federal Emergency Management Agency, 1985a, Interagency flood hazard mitigation report in response to the November 7, 1985, disaster declaration (West Virginia): Report FEMA–743–DR–WV, 56 p.

———1985b, Interagency flood hazard mitigation report for the Commonwealth of Virginia: Report FEMA–755–DR–Virginia, 59 p.

Government Accounting Office, 1988, Disaster assistance—Response to West Virginia's November 1985 flood shows need for improvements: Report to Congressional Requesters GAO/RCED–88–5, 90 p.

Jacobson, R.B., Linton, R.C., and Rubin, Meyer, 1989a, Alluvial stratigraphy of the Potomac River valley bottom near Petersburg and Moorefield, West Virginia: U.S. Geological Survey Open-File Report 89–485, 27 p., 14 pls.

Jacobson, R.B., Miller, A.J., and Smith, J.A., 1989b, The role of catastrophic events in central Appalachian landscape evolution, *in* Gardner, T.W., and Sevon, W.D., eds., Appalachian geomorphology: Geomorphology, v. 2, p. 257–284.

Chapter B

Meteorology of the Storm of November 3–5, 1985, in West Virginia and Virginia

By STEPHEN J. COLUCCI, ROBERT B. JACOBSON, and STEVEN GRECO

U.S. GEOLOGICAL SURVEY BULLETIN 1981

GEOMORPHIC STUDIES OF THE STORM AND FLOOD OF NOVEMBER 3–5, 1985, IN THE UPPER POTOMAC AND CHEAT RIVER BASINS IN WEST VIRGINIA AND VIRGINIA

CONTENTS

FIGURES

TABLES

Meteorology of the Storm of November 3–5, 1985, in West Virginia and Virginia

By Stephen J. Colucci,[1] Robert B. Jacobson,[2] *and* Steven Greco[3]

Abstract

The storm of November 3–5, 1985, in the central Appalachian Mountains of West Virginia and Virginia resulted from a complex sequence of meteorological events. The stage was set by Hurricane Juan, which made landfall in the Gulf Coast on October 31. Juan brought moisture northward up the Mississippi Valley; latent heat released by condensation aloft probably helped to render stationary a high-pressure anticyclone over southeastern Canada. A second low-pressure cyclone, moving north through the Southeastern United States, was blocked by the stationary anticyclone, intensifying a surface-pressure gradient that forced moist air from the Atlantic westward up the slope of the Appalachian Mountains. In the Cheat and Potomac River basins the resulting rainfall was of moderate intensity but of long duration. In Pendleton County, W. Va., the 1985 storm was the largest on record for durations from 24 to 72 h; the highest rainfall recurrence intervals were registered at durations of 24 to 48 h. Estimates of rainfall recurrence intervals from highly skewed records yield values ranging from 80 to 300 yr.

INTRODUCTION

Heavy rainfall during November 3–5, 1985, in West Virginia and Virginia produced extraordinary flooding and triggered thousands of landslides. Most of the damage occurred in the Cheat and Potomac River basins, although substantial damage was also recorded in the James River basin and smaller basins. The meteorological factors leading to the heavy rainfall are of interest in order to evaluate the frequency and spatial distributions of such storms in the Appalachian Mountains. This chapter discusses the meteorology of the storm, antecedent soil moisture conditions, rainfall distribution, and frequency analysis of selected rain gage data in the Cheat and Potomac River basins.

Manuscript approved for publication February 22, 1991.

[1] Department of Soil, Crop and Atmospheric Sciences, Cornell University, Ithaca, NY 14853.

[2] U.S. Geological Survey.

[3] Department of Environmental Sciences, University of Virginia, Charlottesville, VA 22903.

Acknowledgments

We thank F. Richards and J.A. Smith of the National Weather Service for thoughtful reviews of this manuscript. We are grateful to T. Purkey, U.S. Soil Conservation Service, and S. Kite, West Virginia University, for use of their bucket-survey data.

METEOROLOGICAL FACTORS

The heavy rainfall of November 3–5, 1985, was caused by a surface cyclone moving northeastward from the Gulf of Mexico along the southeastern Atlantic coastline toward a nearly stationary anticyclone over southeastern Canada (fig. 1). The surface pressure gradient between the cyclone and anticyclone centers increased from 9.3×10^{-3} millibars per kilometer (mbar/km) at 7 p.m. November 3 to 18.4×10^{-3} mbar/km by 7 p.m. November 5. If the effects of surface friction are not taken into account, the horizontal surface winds are instantaneously proportional in magnitude to the pressure gradient and oriented perpendicular to the line connecting the low- and high-pressure centers, the low pressure occurring to the left. Therefore, the surface wind speed that was perpendicular to this line (which is roughly parallel to the Appalachian Mountains) theoretically doubled during this period.

Precipitation is caused when rising moist air cools sufficiently to condense and form droplets large enough to fall to the surface. During the period under study, the moist, westward-moving air was transported upward over the mountains of Virginia and West Virginia and contributed to the substantial rainfall. Other mechanisms that might have contributed to this heavy rainfall include the ascent of warm moist air from the east over cold air trapped near the surface east of the mountains (typically observed with the arrangement of surface weather systems depicted in fig. 1) and (or) the ascent of air near the surface cyclone due to the ventilation of air aloft during intensification of the cyclone (that is, during the period of pressure fall at the cyclone center).

Many factors may have influenced rainfall; therefore understanding the origin, behavior, and three-dimensional

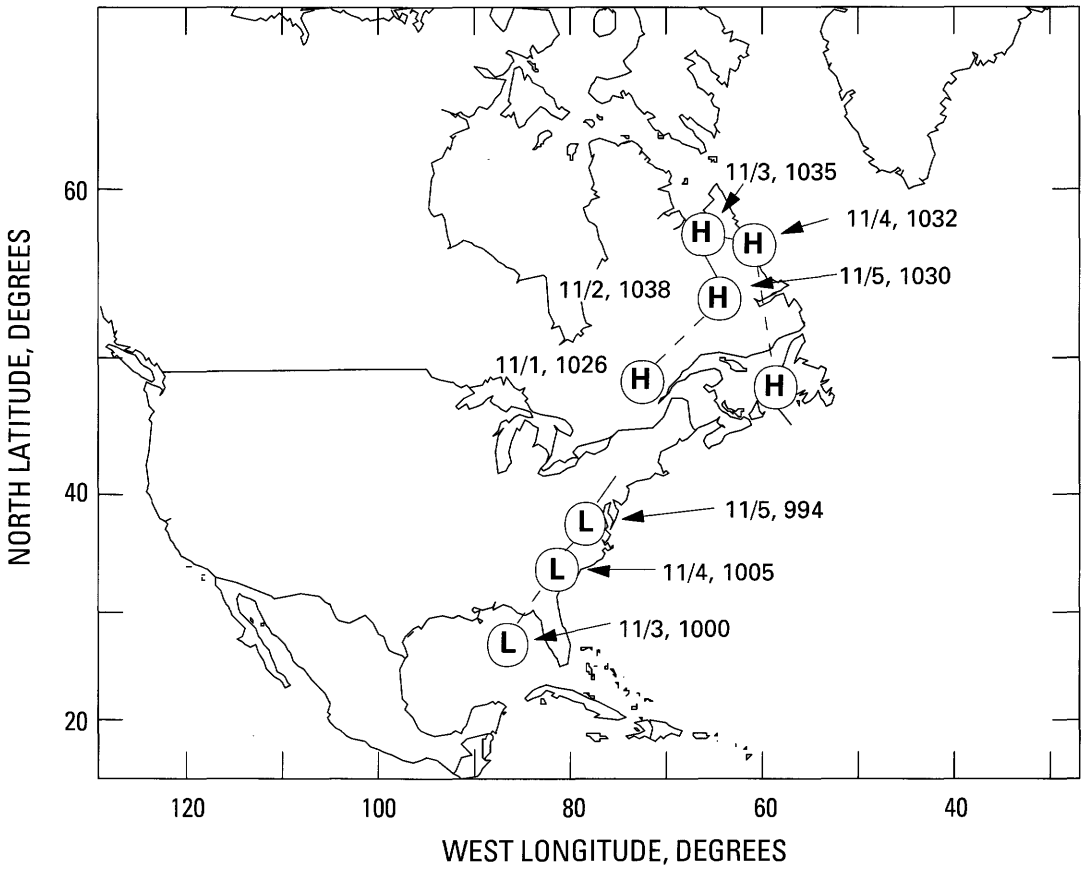

Figure 1. Schematic surface weather map, October 31 to November 5, 1985. Positions of surface cyclone (L) and anticyclone (H), are marked for 7 p.m. EST with date and central pressure in millibars.

structure of both the surface cyclone and the anticyclone will help explain the meteorological conditions that contributed to the flood. In the middle latitudes of the Northern Hemisphere, surface cyclones tend to be observed to the east of troughs aloft (relatively low height of the 500-mbar pressure surface in the middle troposphere), while surface anticyclones are found near ridges aloft (relatively high elevation of the 500-mbar pressure surface). A sequence of 500-mbar maps preceding the event is presented in figure 2. The upper- level trough associated with the surface cyclone is observed at 7 a.m. November 3 over the lower Mississippi River Valley (fig. 2*D*), having moved eastward from western Mexico 24 h earlier (fig. 2*C*). Inspection of the 500-mbar temperature maps for this case (fig. 3) reveals that the trough was a region of cold air relative to its surroundings. The ascent of air east of the trough caused air to expand and cool; hence the trough (and associated surface cyclone) moved generally eastward.

The upper-level ridge associated with the surface anticyclone moved from the mid-Atlantic States at 7 a.m. October 31 (fig. 2*A*) to the Northeastern States 24 h later (fig. 2*B*) and finally merged with an upper-level ridge moving westward from over the Atlantic Ocean (fig. 2*C*). The merged ridge became stationary (compare figs. 2*C* and 2*D*), accounting for the stationarity of the surface anticyclone. The stationarity of the upper-level ridge, a critical meteorological factor in this event, can be explained as follows.

The upper-level ridge was warm relative to the surrounding air (fig. 3). Under ordinary conditions, the sinking (and thus compression and warming) of air parcels found east of the ridge would favor eastward displacement of the ridge and also of the surface anticyclone. Opposing the eastward displacement of the upper-level ridge is its westward drift due to the rotation of the Earth (the Coriolis effect). Also, since the ridge is a warm air mass, any processes that produce local atmospheric warming on the west side of the ridge would favor westward drift of the ridge. Temperatures at 500 mbar increased on the west side of the upper-level ridge during the period October 31 to November 5 (figs. 2, 3). Maximum warming was observed over northwestern Quebec, where 500-mbar temperatures increased from −30 °C on October 31 to −15 °C on November 2 (figs. 3*A*, *C*).

This local warming may have caused the upper-level ridge to become stationary, or it may have been a conse-

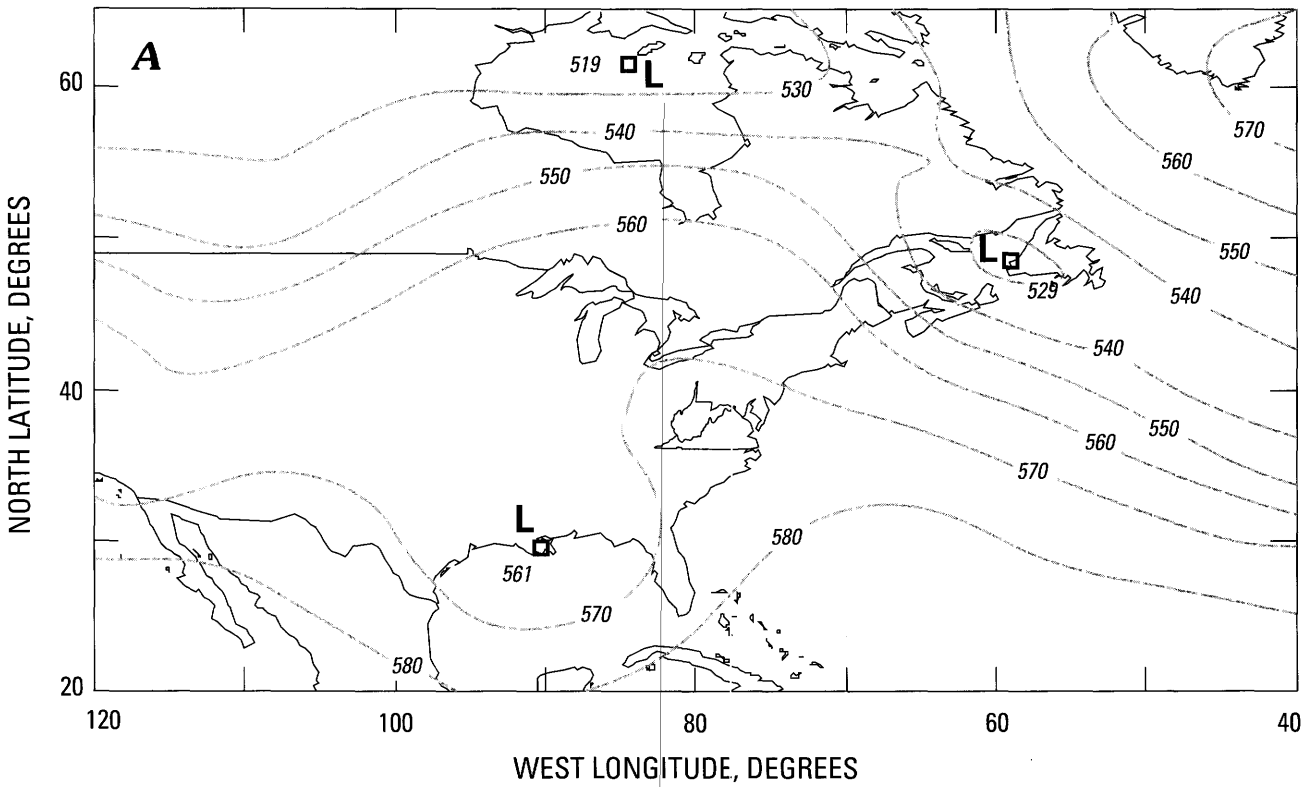

Figure 2. Mid-tropospheric maps, October 31 to November 3, 1985. Shown is the 500-mbar height (tens of meters) at (*A*) 7 a.m. October 31, (*B*) 7 a.m. November 1, (*C*) 7 a.m. November 2, and (*D*) 7 a.m. November 3.

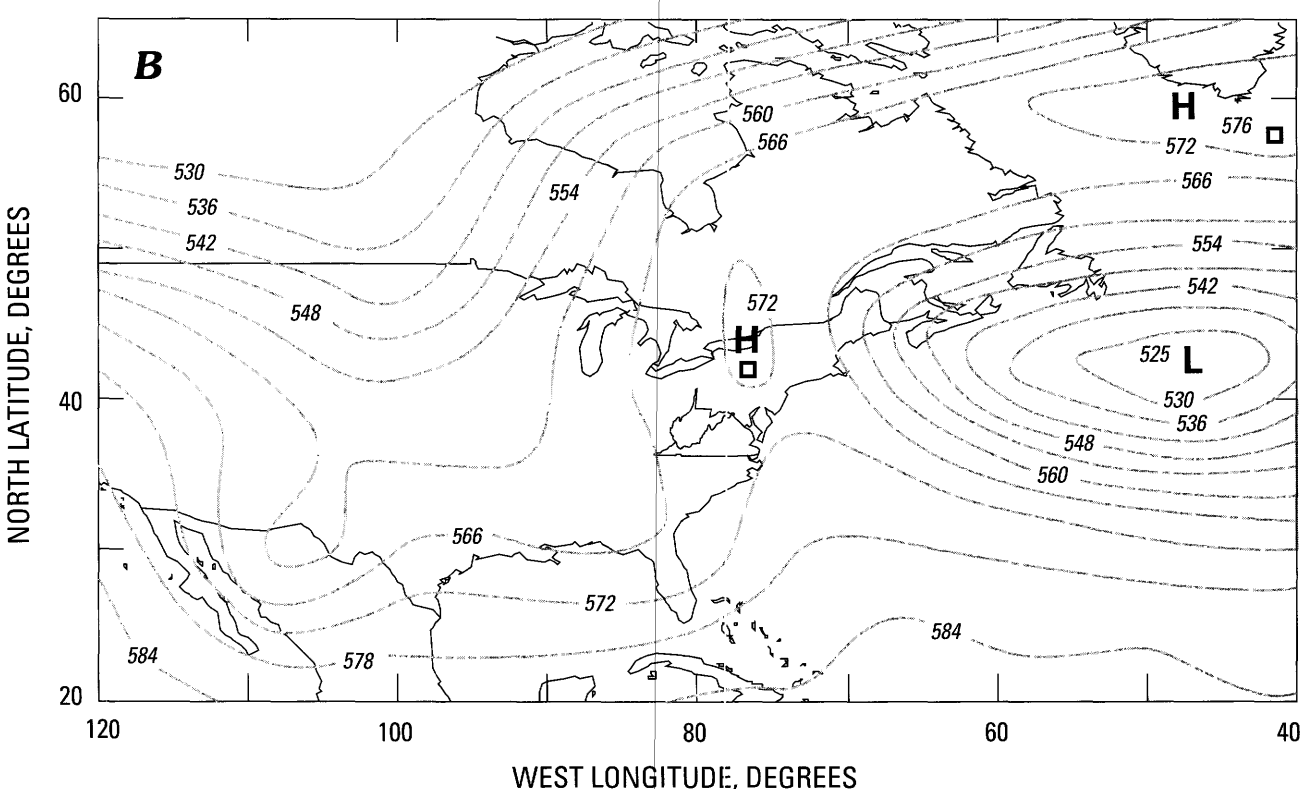

Figure 2. Continued.

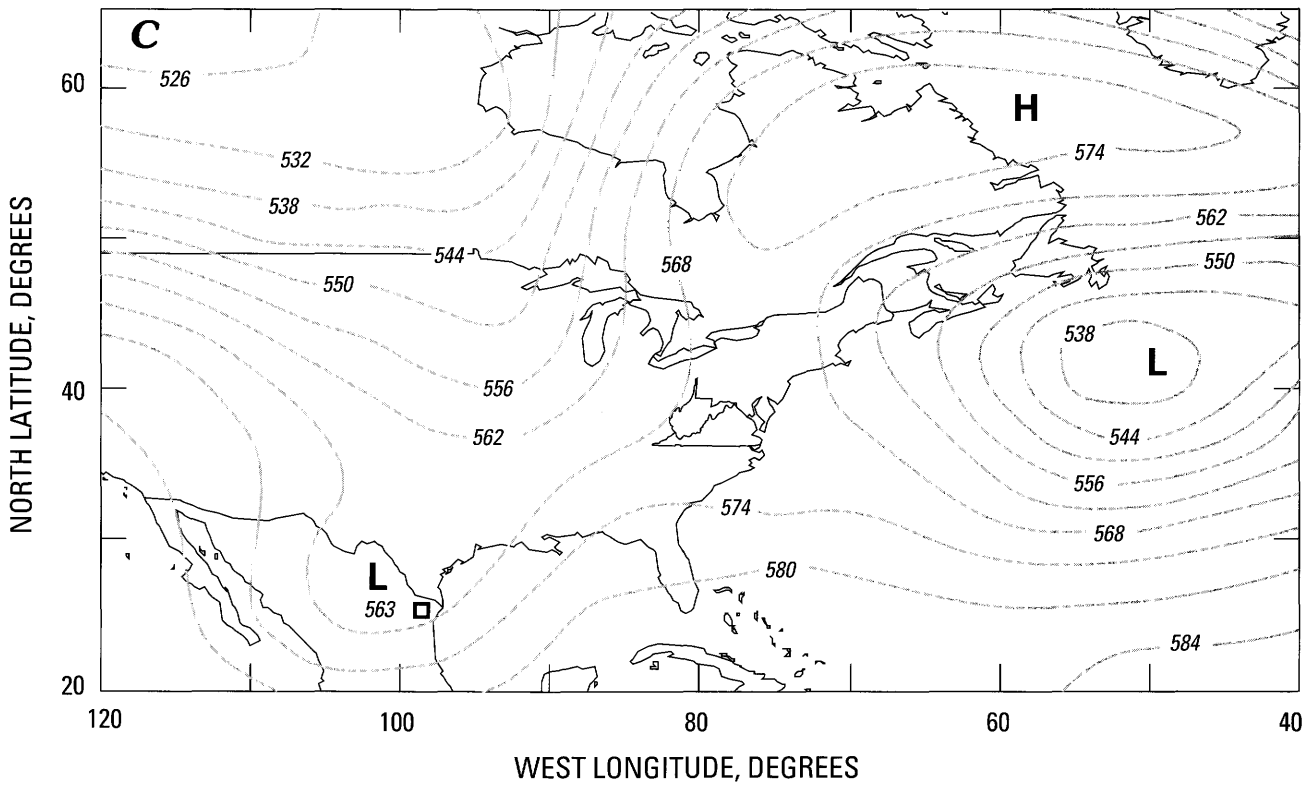

Figure 2. Continued.

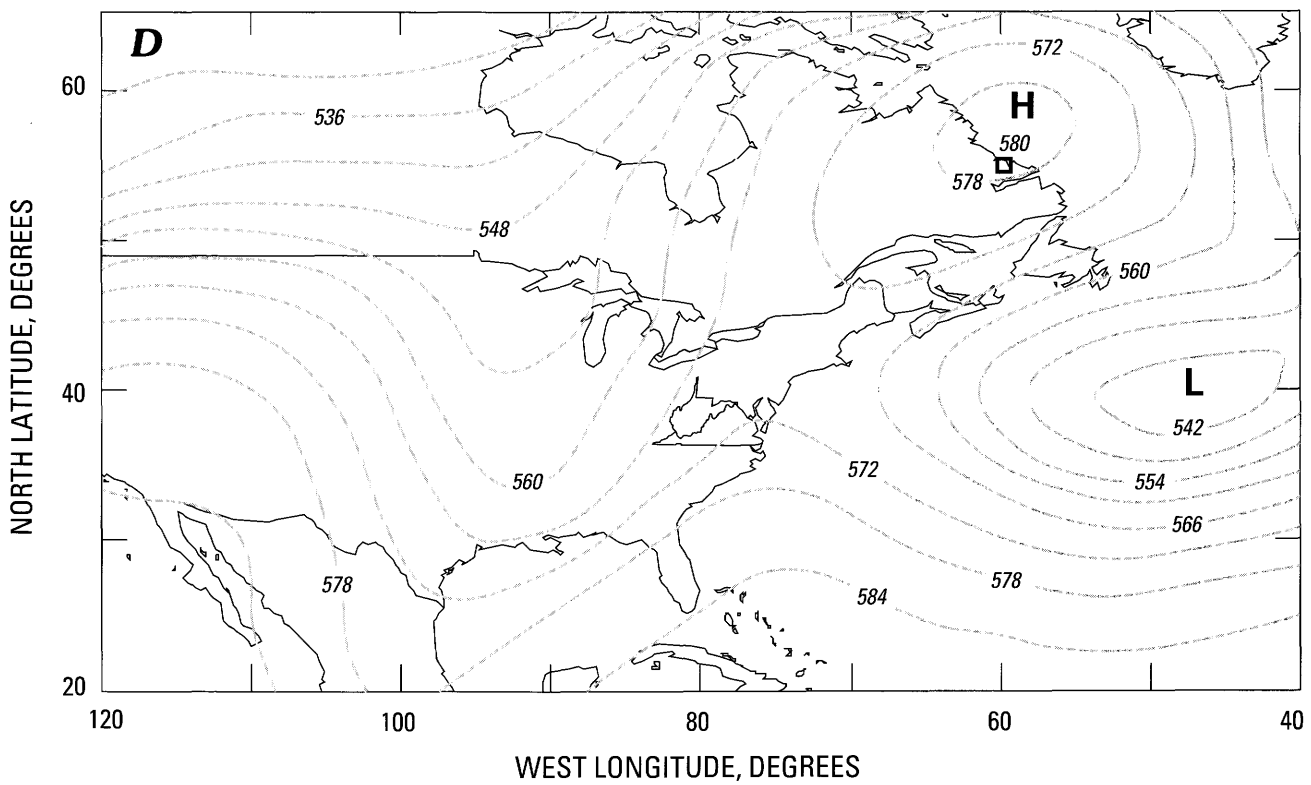

Figure 2. Continued.

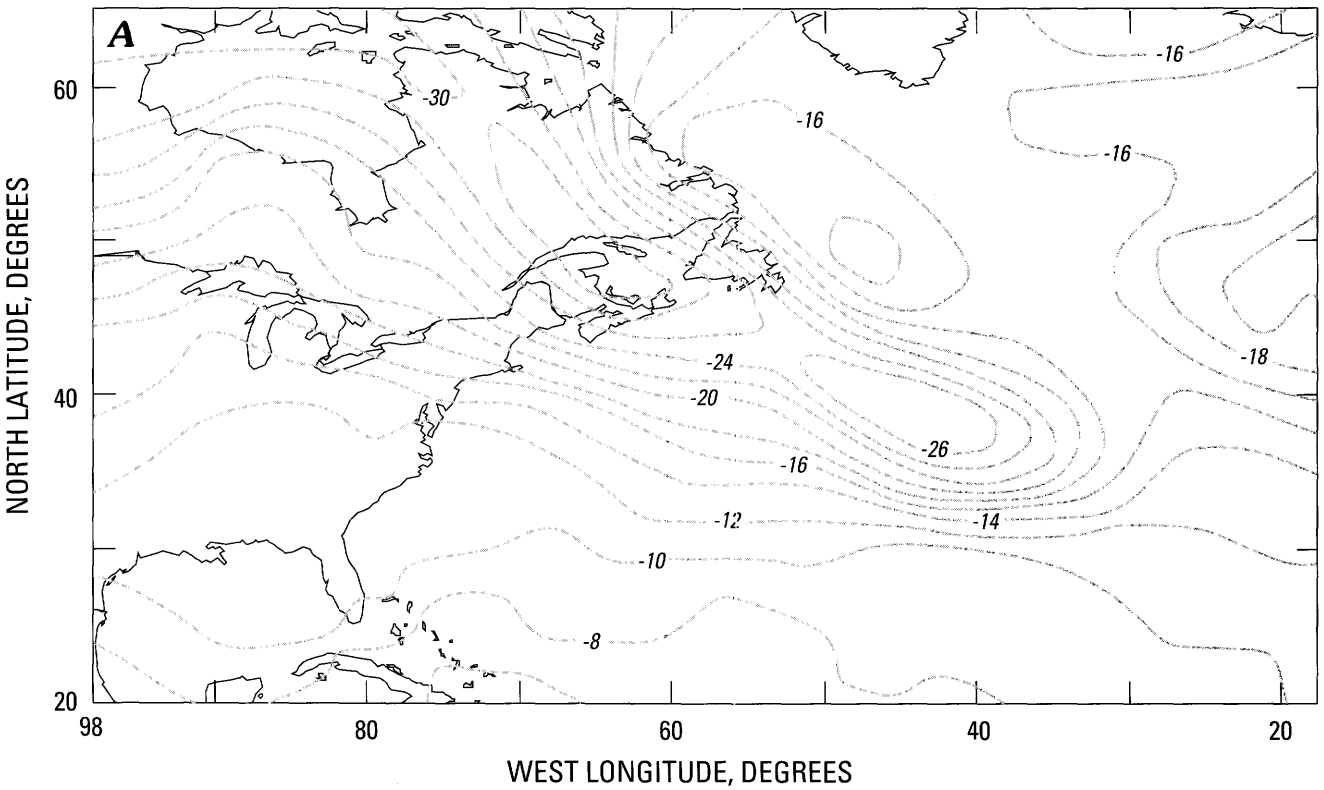

Figure 3. Temperature distribution maps, October 31 to November 3, 1985. Shown are 500-mbar temperatures (degrees Celsius) at (*A*) 7 a.m. October 31, (*B*) 7 a.m. November 1, (*C*) 7 a.m. November 2, and (*D*) 7 a.m. November 3.

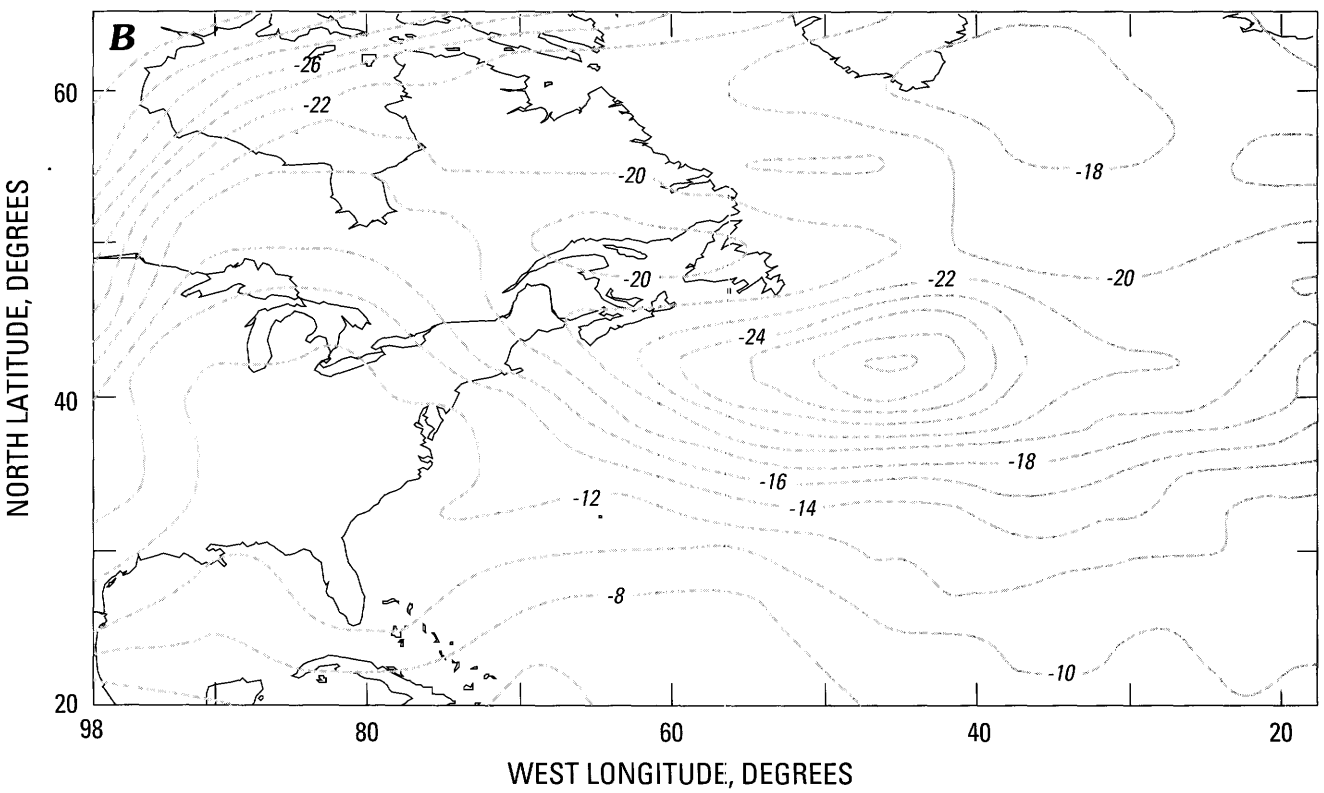

Figure 3. Continued.

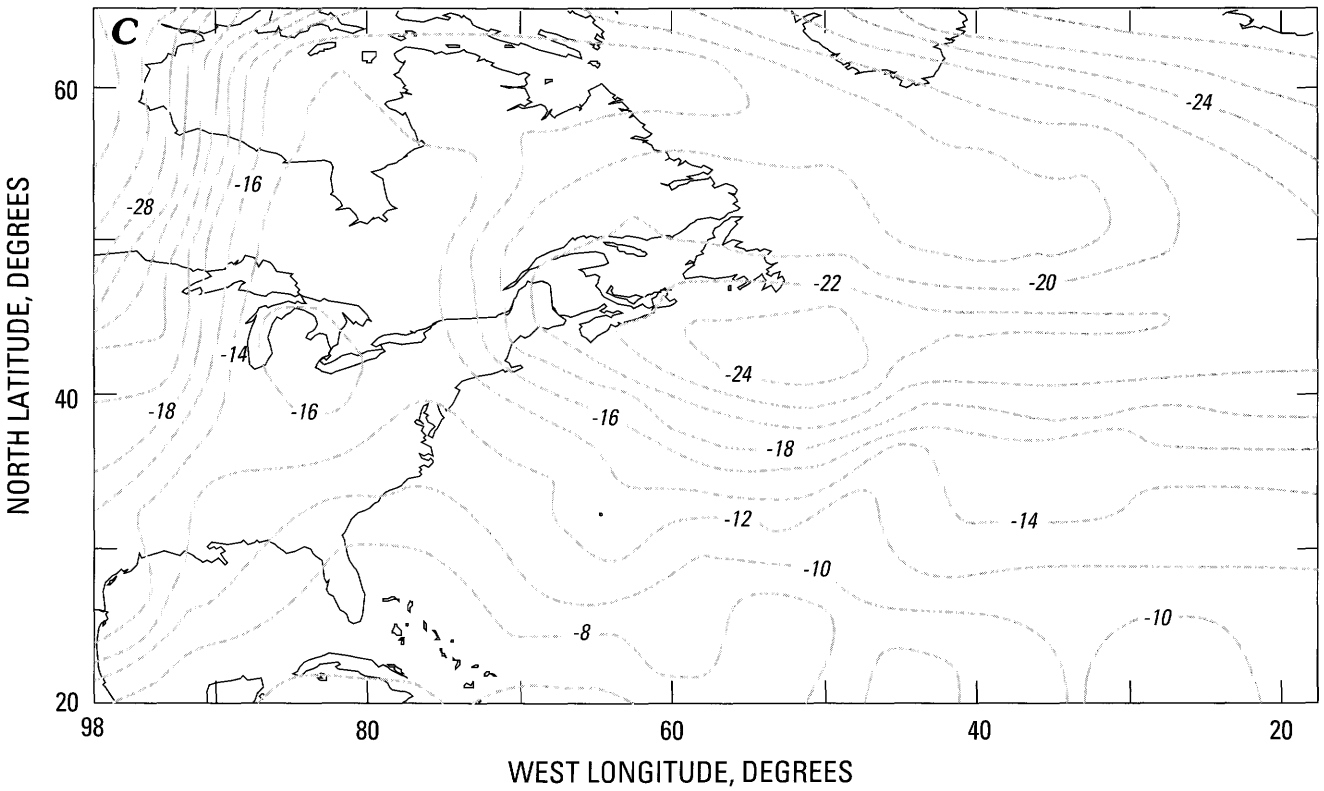

Figure 3. Continued.

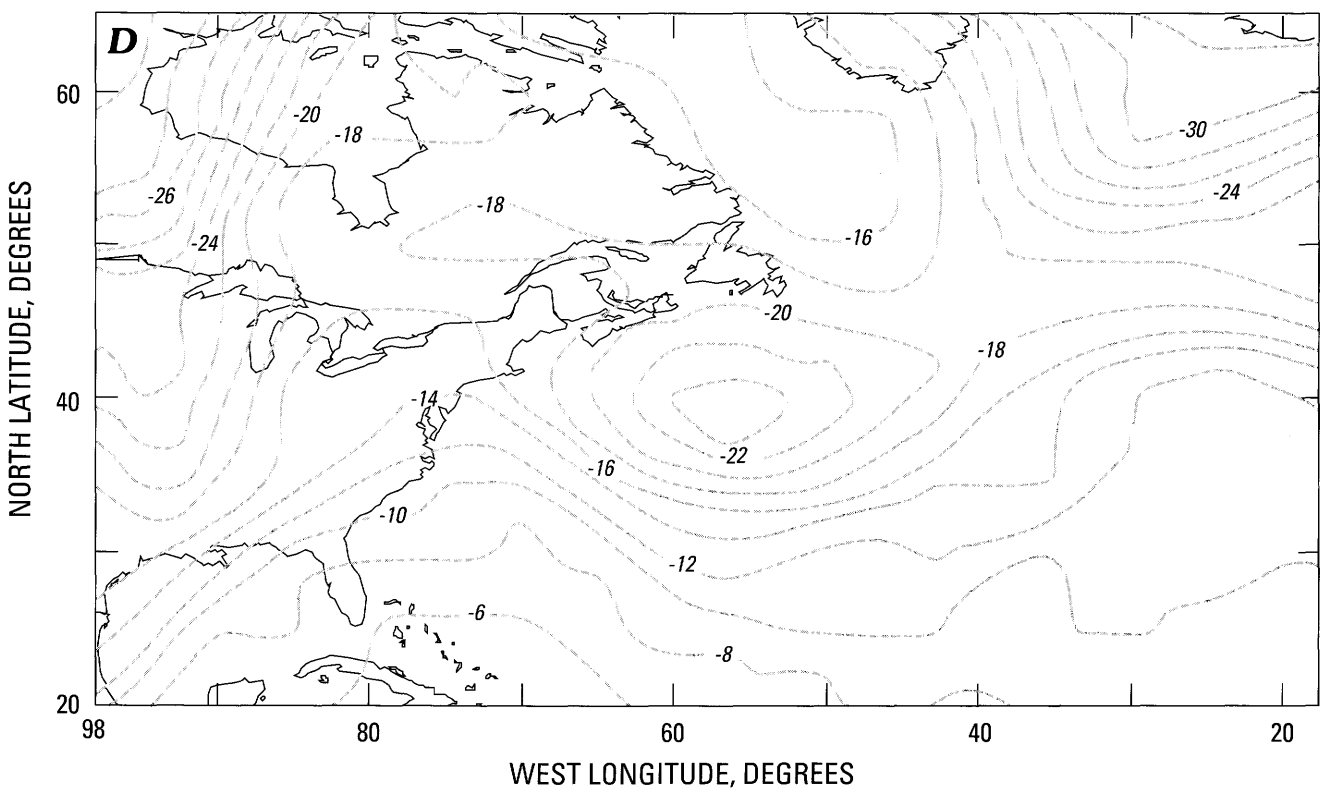

Figure 3. Continued.

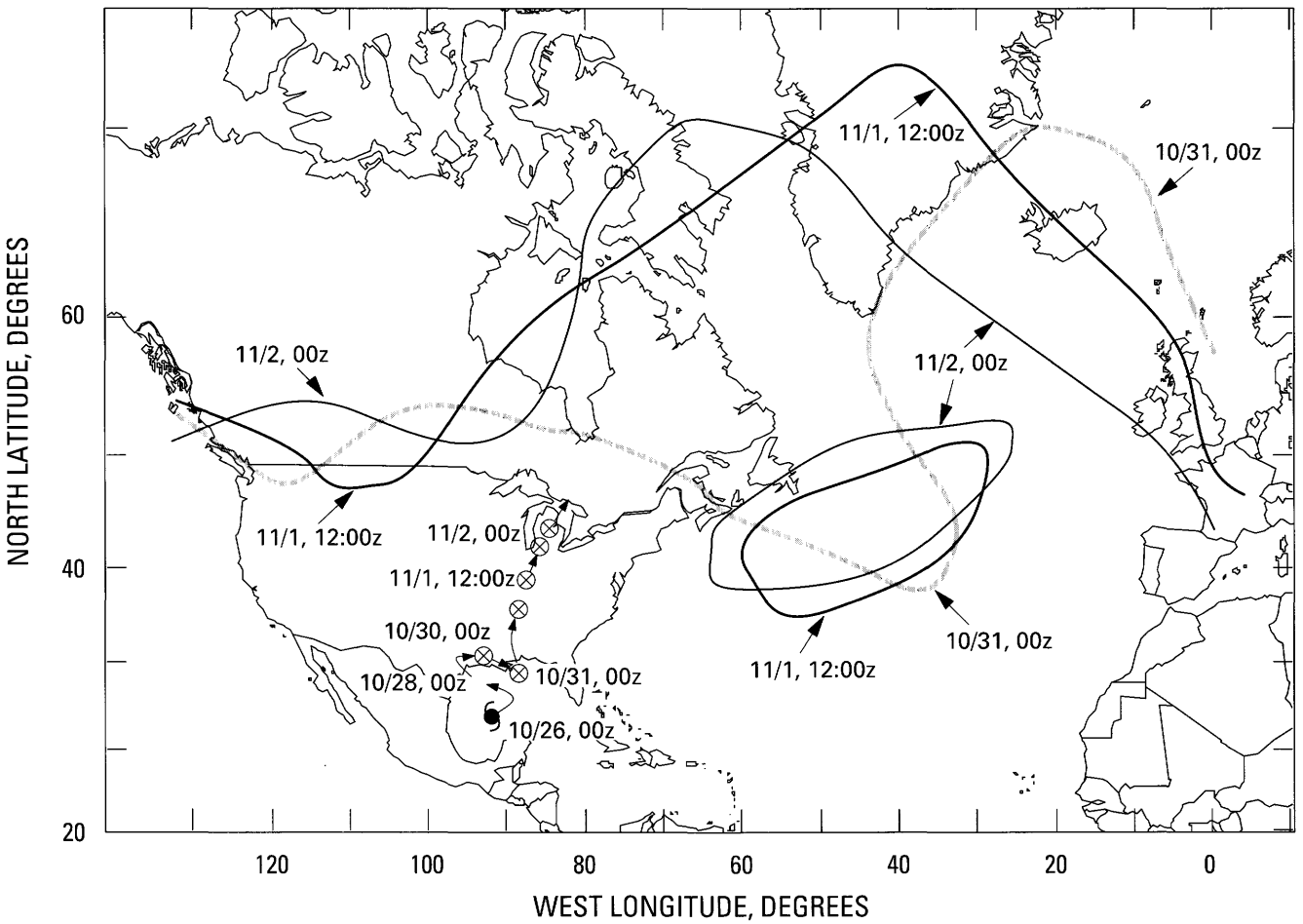

Figure 4. Positions of Hurricane and Tropical Storm Juan (circled crosses) with dates and Greenwich (z) times (5 h before EST) and the position of the 5,460-m height contour at 500 mbar on October 31 and November 1 and 2, 1985.

quence of the tendency for the ridge to drift westward due to the Coriolis effect. The possible impact of the Coriolis effect was evaluated with a diagnostic model that estimates the change in height of the 500-mbar surface (Holton, 1979). Calculations showed that, in the 48-h period centered at 7 a.m. November 1, the Coriolis effect could have contributed approximately +40 m to the height change of the 500-mbar surface. This value is an order of magnitude smaller than the observed height increase of about 400 m between 7 a.m. October 31 and 7 a.m. November 2 (figs. 2*A*, 2*C*). Assuming as a boundary condition that the Coriolis effect produced no change in the pressure or temperature of the surface weather systems, then the model calculation also implies a 2 °C increase over 48 h in the temperature of the 500-mbar surface over northwestern Quebec. This is much smaller than the observed 15 °C warming at 500 mbar during this period. Thus, the Coriolis effect does not appear to have contributed significantly to local warming, suggesting that the warming was primarily a cause, rather than a consequence, of the westward drift and the near stationarity of the upper-level ridge.

The warm air over Quebec could have been produced locally by the release of heat from precipitating clouds, for example, or it could have been imported from a remote location. The northward migration of the −16 °C isotherm at 500 mbar from near the Great Lakes at 7 a.m. October 31 (fig. 3*A*) to northeastern Canada at 7 a.m. November 2 (fig. 3*C*) suggests the latter possibility. Note that 500-mbar winds, being parallel to the height contours, were from the south over this key region at 7 a.m. November 1 (fig. 2*B*) and 7 a.m. November 2 (fig. 2*C*). Farther to the south, a uniformly warm air mass existed within an upper-level trough over Louisiana at 7 a.m. October 31 (figs. 2*A*, 3*A*). Ordinarily, upper-level troughs are cold, but this one was associated with Hurricane Juan, situated on the Louisiana border. This storm, accompanied by substantial rainfall (Case, 1986) and attendant release of latent heat, subsequently moved inland, as illustrated in figure 4. This figure also schematically illustrates concurrent changes in the 500-mbar patterns over North America and the Atlantic Ocean.

A simple estimate of the heat released in the hurricane's precipitation is obtained by assuming that the heat

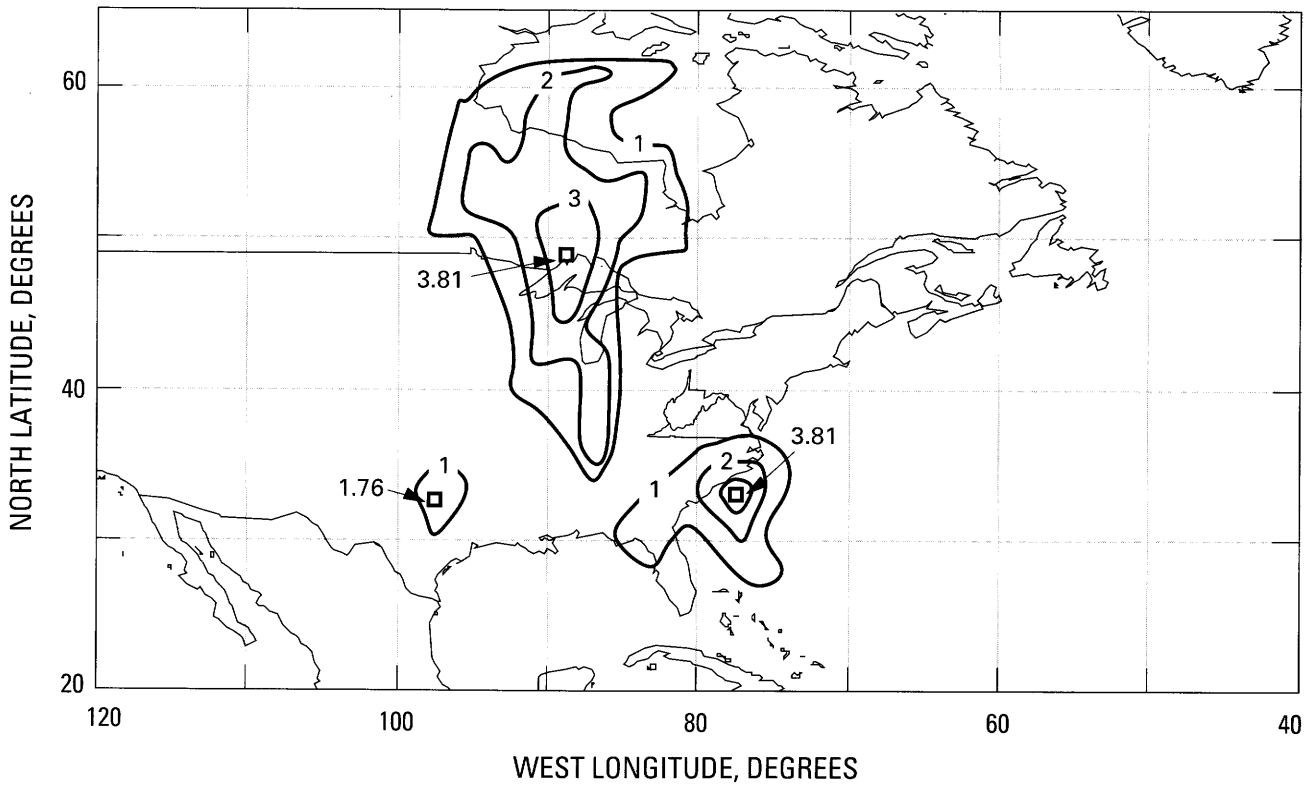

Figure 5. Temperature increase (in degrees Celsius per 12 h) of air at 500 mbar due to precipitation at 7 a.m. on November 1.

release is distributed in the vertical direction in proportion to total heating calculated as a residual in the thermodynamic energy equation (Holton, 1979). Heating from the vertically integrated precipitation is calculated with satellite-derived estimates of ground precipitation (Robertson, 1987). The heating thus obtained at 500 mbar is shown in figure 5 for 7 a.m. November 1. The calculated heating maxima occur far from the region of the maximum 500-mbar temperature increase over Quebec, suggesting that precipitation heating is not directly responsible for warming the Quebec upper-level trough. However, because the heating maximum near the Great Lakes is situated upwind from northwestern Quebec (compare figs. 2*B* and 5), the heat generated by precipitation over the Great Lakes could have been imported to northwestern Quebec. In fact, the maximum calculated heating rate near the Great Lakes (3.81 °C/12 h) corresponds exactly to the 15 °C/48 h warming observed over northwestern Quebec. This analysis suggests that heating from precipitation over the Great Lakes influenced the local warming over Quebec.

The heavy rainfall of November 3–5 in West Virginia and Virginia therefore appears to be an indirect consequence of Hurricane Juan. The heat released in the rainfall was transported northward, thereby favoring westward (rather than eastward) displacement of a warm 500-mbar upper-level ridge. This movement, in turn, favored the stationarity of a surface anticyclone over southeastern Canada. In conjunction with a northward-moving surface cyclone, this stationary anticyclone caused an increase in the surface pressure gradient along the Appalachian Mountains, the flow of surface air up the mountains, and thus the heavy precipitation.

This complex sequence of events was specific to this storm and is unlikely to repeat itself exactly. However, the general situation of a stationary surface anticyclone over southeastern Canada and surface cyclone over the Southeastern United States is a recurring blocking pattern that has been associated with other substantial rainstorms in the Eastern United States (Hirschboeck, 1987).

ANTECEDENT CONDITIONS

The rainfall of November 3–5 occurred at a time of year when leaves had fallen from the trees and ambient air temperatures were relatively low. As a result, evapotranspiration was probably minimally effective in removing antecedent soil moisture.

Usually, October is a month of low soil moisture in the central Appalachians. No direct data exist on soil moisture for the period antecedent to the storm, but rainfall and streamflow data for October 1985 suggest that storage levels of soil moisture were moderate. Figure 6 shows

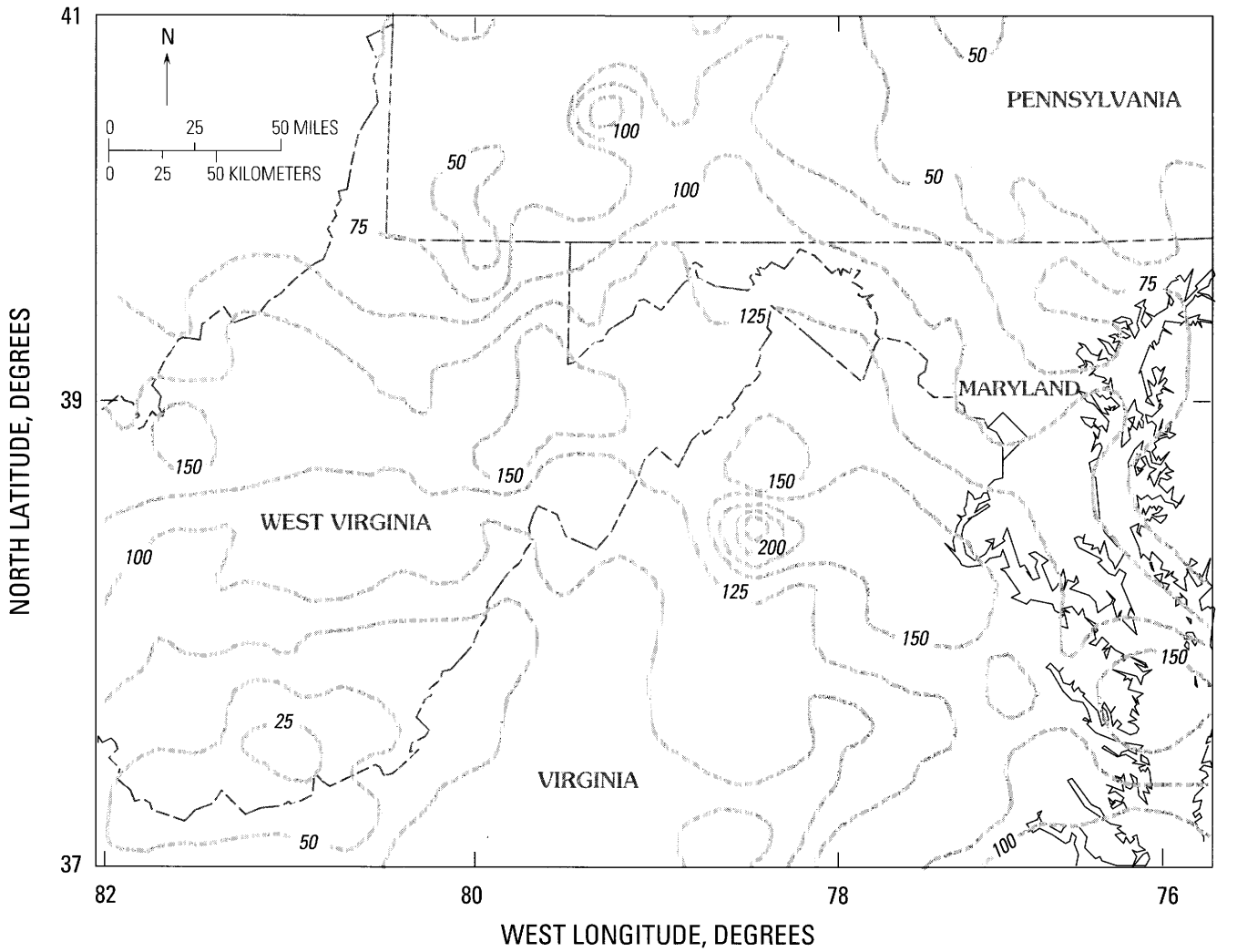

Figure 6. Rainfall map for October 1985 (data from NOAA, 1986).

rainfall during October 1985 for West Virginia and Virginia. In the Cheat and Potomac River basins, October rainfall was as much as 200 percent of normal at isolated rain gages, but most stations were only slightly above normal (normal values are calculated as the average for the years 1951–1980). Thirty-day rainfall totals for September and October at Spruce Knob and Franklin, W. Va., show that the 1985 totals were equaled or exceeded in more than half the years of record (fig. 7). Average streamflow for the month was also slightly above normal. At the South Branch Potomac River gage at Springfield, W. Va., in October 1985 the average streamflow was 125 percent of normal (Embree and others, 1987; S. Runner, personal communication).

RAINFALL DISTRIBUTION

The sequence of meteorological events described above produced large amounts of rainfall at moderate intensity and long duration. The isohyetal map for November 3–5 is shown in figure 8. This map was contoured from the official National Oceanic and Atmospheric Administration (NOAA) rain gage network (table 1) and shows the general spatial distribution and magnitude of the storm. Although the extremes of high and low precipitation from the storm are probably not recorded by the official gage network, data from bucket surveys in West Virginia do not disagree substantially with figure 8 (table 2).

Figure 8 shows a large area of concentrated rainfall (totals exceeding 250 mm) dominating eastern West Virginia and western Virginia. Along the Blue Ridge in central Virginia, local orographic effects appear to have triggered intense convection, and total rainfall for the storm was in excess of 325 mm. Reconnaissance of the central Virginia area shortly after the storm revealed little flood and landslide damage, possibly because of the hydrologic and geomechanical stability of the particular rocks and regoliths under conditions of rainfall intensity and duration of this

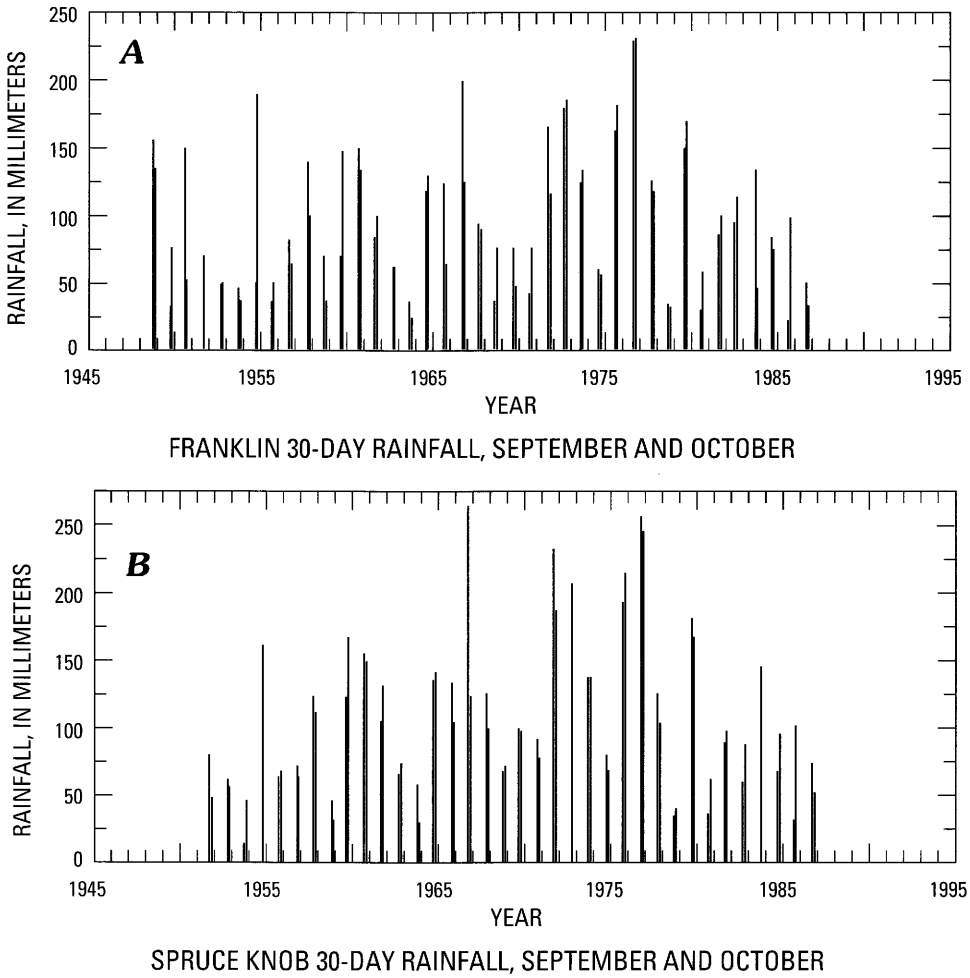

Figure 7. Rainfall records from gages at Franklin and Spruce Knob, W. Va. (*A, B*) Thirty-day duration rainfall during the months of September and October for the years of record. (*C, D*) Thirty-day duration rainfall for all months of the year (100-mm minimum cut off) (data from NOAA, 1986).

storm. Alternatively, slopes and channels in the area may still be adjusted to the intense precipitation from Hurricane Camille in 1969 (Williams and Guy, 1973; Gryta and Bartholomew, 1989).

The most dramatic flood and landslide damage in 1985 was associated with the rainfall maximum located in eastern West Virginia (fig. 8). Rain-gage data recorded hourly illustrate the history of the storm. Rainfall intensities were not exceptional (fig. 9). The most rainfall for 1-h duration was only 38 mm/h, recorded at Hot Springs, Va. According to Hershfield (1961), 1-h rainfall intensities of this magnitude recur on the average approximately every 3 yr in the central Appalachian Mountains. Due to the sparse network of hourly recording rain gages, it is likely that actual hourly intensities were greater than those recorded. Anecdotal accounts by residents, however, did not emphasize extreme intensities.

Although intensities were only moderate, duration of rainfall was long. In eastern West Virginia the storm began late in the morning of November 4, peaked in the early evening, and continued into the morning of November 5. For durations up to 8 h, intensity was near 10 mm/h at many hourly recording gages and probably over much of the area. The main storm event was a little longer than 24 h in duration, ending by evening on November 5. Several rain gages also reported light rainfall preceding the event on November 3 and lasting into the evening of November 5 (table 1).

Rainfall in eastern West Virginia and western Virginia was concentrated in the headwaters of the Cheat and Potomac River basins. An isohyetal map for this area at larger scale is shown in plate 1 of Jacobson (chapter A, this volume). Although most of the rain fell on November 4, this map incorporates gage data over the period November

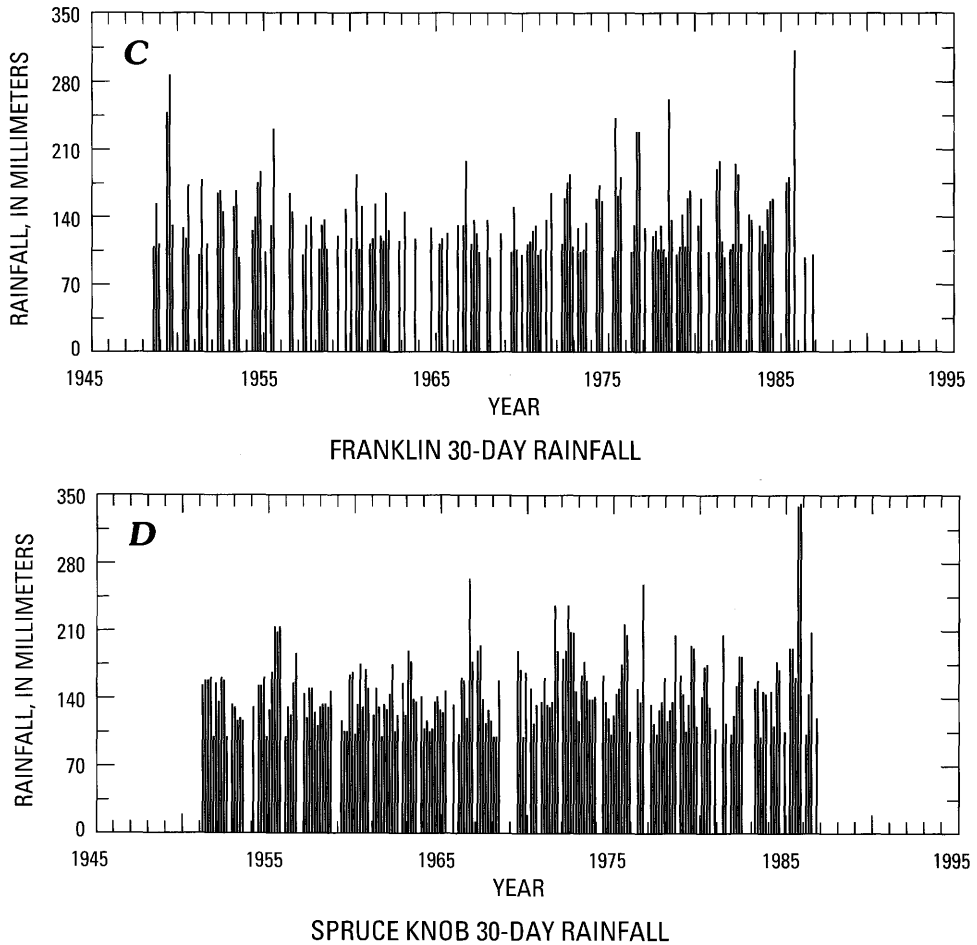

Figure 7. Continued.

3–5 in order to include all rain delivered as the storm moved across the area and to account for different reading times among gages. Peak rainfall recorded in this area for a 24-h period was 191 mm at Franklin, W. Va., and for a 48-h period was 241 mm at Upper Tract, W. Va.

The rainfall was also spread over a large part of the mountainous region; an area in excess of 12,800 km^2 received more than 220 mm (Miller, 1990).

DURATION, INTENSITY, AND FREQUENCY OF RAINFALL

The storm of November 3–5, 1985, was remarkable for its moderate intensity and long duration. Depicted graphically in figure 10 is the ratio of recorded rainfall to rainfall of the 100-yr event for durations ranging from 1 h to 7 days. Total rainfall of the 100-yr event is estimated from Hershfield (1961) and Miller (1964); because these data sources are fairly old, the plotting of the recorded data points with respect to the vertical axis may not be very accurate. However, of more interest is plotting with respect to the horizontal axis, which shows the relative importance of rainfall durations for a single storm. The 1985 storm was important over long time intervals, peaking in the 1- to 2-day durations.

Two representative rain gages in the South Branch Potomac River basin were chosen for frequency analysis because of their long records and locations near the main concentration of rainfall. The Franklin, W. Va., gage began in 1949 and the Spruce Knob, W. Va., gage began in 1952. Histograms of rainfall totals for these gages for 1-, 2-, and 4-day durations are shown in figure 11.

At the Franklin gage the 1985 storm was the largest on record at all durations. The 1985 storm and three others (1949, 1954, and 1972) form a subset of events that are much greater in magnitude than the background events. Similarly, at the Spruce Knob gage, the 1985 and 1972 storms are appreciably larger than the other events in the record. These subsets of large events result in highly skewed populations and suggest the possibility that the record consists of a mixed population of storms; the large events may result from meteorological processes that are quite different from the remainder of the events. Similar

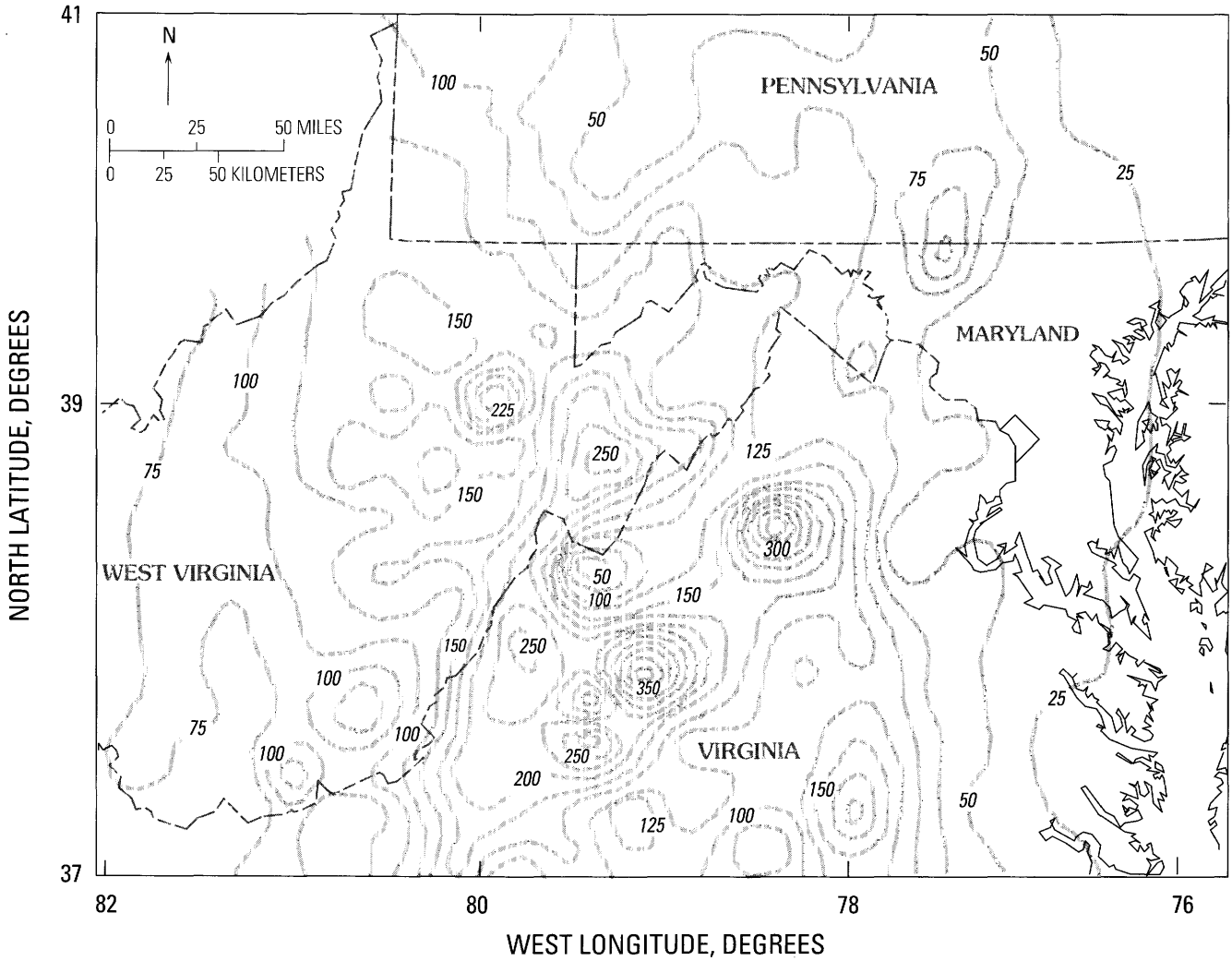

Figure 8. Rainfall map for November 3–5, 1985 (data from NOAA, 1986).

mixed populations of rainfall and runoff events have been noted elsewhere in North America, especially where floods are generated by snowmelt and convective thunderstorms; if sufficient numbers of events exist for the constituent populations, then frequency, duration, and magnitude can be evaluated separately for different types of events, and more accurate models can be made (Waylen, 1985).

With the limited number of large events in the Spruce Knob and Franklin records, an analysis based on mixed populations was not attempted. For this study the population was treated as homogeneous. The annual series of the 1- and 2-day rainfall records were subjected to frequency analysis using log Pearson type III models with regional skew coefficients calculated from four neighboring gages. Frequency plots with the log Pearson type III model fitted with regional skew coefficients are shown in figure 12, and estimates of peak rainfall recurrence intervals are given in table 3. The recurrence intervals of the 2-day rainfall peak recorded at the Upper Tract gage were estimated from the Franklin model.

The highly skewed distributions give a wide range of recurrence intervals for the rare, larger rainfalls, and for both gages the 1985 event falls outside the 95 percent confidence intervals. Using the models as the best available estimates, one would conclude that events of the magnitude of the 1985 storm event would recur on the average approximately every 80–300 yr. This estimate is in general agreement with estimates of the 100- to 500-yr recurrence intervals for flooding from this storm (Miller and Parkinson, chapter E, this volume).

DISCUSSION

The total rainfall, intensity, and duration of the storm are unique in the historical records of this part of the central Appalachians. The sequence of meteorological events

Table 1. Official NOAA rain gage network data, October and November 1–6, 1985

Station	Latitude deg	Latitude arc min	Longitude deg	Longitude arc min	October 1985	November 1985 1	2	3	4	5	5	3–4	4–5	5–6	3–5	4–6	3–6	1–6
Maryland																		
180015	39	28	76	10	80.5	0.0	0.0	0.0	1.5	6.6	5.1	1.5	8.1	11.7	8.1	13.2	13.2	13.2
180193	38	59	76	30	112.5	1.0	0.3	0.5	20.6	7.1	10.9	21.1	27.7	18.0	28.2	38.6	39.1	40.4
180335	38	14	75	8	67.1	4.1	0.8	0.0	0.3	9.4	2.0	0.3	9.7	11.4	9.7	11.7	11.7	16.5
180465	39	11	76	40	63.0	0.0	0.0	2.8	24.1	4.3	0.8	26.9	28.4	5.1	31.2	29.2	32.0	32.0
180470	39	17	76	37	48.5	0.0	0.0	2.5	30.5	8.1	0.3	33.0	38.6	8.4	41.1	38.9	41.4	41.4
180700	39	2	76	53	69.9	0.8	0.5	0.0	23.9	14.5	3.0	23.9	38.4	17.5	38.4	41.4	41.4	42.7
180732	39	30	76	23	71.6	0.0	0.0	2.0	8.1	26.9	9.9	10.2	35.1	36.8	37.1	45.0	47.0	47.0
181032	39	13	77	20	105.9	2.5	0.3	1.8	14.2	19.6	2.3	16.0	33.8	21.8	35.6	36.1	37.8	40.6
181125	39	12	77	1	75.9	0.0	0.0	2.0	33.0	10.2	0.0	35.1	43.2	10.2	45.2	43.2	45.2	45.2
181385	38	34	76	4	45.7	2.3	0.0	0.0	6.6	5.6	6.9	6.6	12.2	12.4	12.2	19.1	19.1	21.3
181530	39	39	77	29	96.0	1.5	0.8	33.0	61.5	38.6	2.5	94.5	100.1	41.1	133.1	102.6	135.6	137.9
181750	39	13	76	4	78.0	0.0	0.5	0.8	3.0	6.6	0.8	3.8	9.7	7.4	10.4	10.4	11.2	11.7
181862	39	15	76	56	76.2	0.0	0.0	0.0	17.0	14.5	2.5	17.0	31.5	17.0	31.5	34.0	34.0	34.0
181995	38	59	76	57	65.3	3.6	0.3	0.3	19.8	15.5	4.1	20.1	35.3	19.6	35.6	39.4	39.6	43.4
182060	39	39	76	10	41.9	0.0	0.0	1.0	0.0	10.9	5.8	1.0	10.9	16.8	11.9	16.8	17.8	17.8
182215	37	59	75	52	110.0	3.3	0.3	0.5	13.5	1.3	5.8	14.0	14.7	7.1	15.2	20.6	21.1	24.6
182282	39	38	78	45	105.9	0.8	2.3	7.9	37.6	31.8	1.3	45.5	69.3	33.0	77.2	70.6	78.5	81.5
182325	38	56	77	7	91.7	7.6	1.0	1.3	29.7	12.2	1.3	31.0	41.9	13.5	43.2	43.2	44.5	53.1
182335	39	16	77	14	85.1	3.3	1.0	2.0	24.1	21.6	2.5	26.2	45.7	24.1	47.8	48.3	50.3	54.6
182523	38	53	75	48	56.1	0.0	0.0	0.8	4.6	4.3	0.0	5.3	8.9	4.3	9.7	8.9	9.7	9.7
182770	39	40	77	33	80.8	0.3	1.3	5.1	34.3	62.2	5.8	39.4	96.5	68.1	101.6	102.4	107.4	109.0
182906	39	41	77	18	77.0	1.3	0.0	17.8	41.1	13.2	2.5	58.9	54.4	15.7	72.1	56.9	74.7	75.9
183348	39	25	77	26	88.9	2.5	0.0	11.4	25.9	20.6	6.4	37.3	46.5	26.9	57.9	52.8	64.3	66.8
183355	39	24	77	22	104.4	1.8	1.3	1.8	17.8	20.3	15.2	19.6	38.1	35.6	39.9	53.3	55.1	58.2
183415	39	40	78	56	142.7	5.1	15.0	14.0	57.9	83.6	3.0	71.9	141.5	86.6	155.4	144.5	158.5	178.6
183675	38	58	76	48	89.9	1.0	0.5	1.5	26.7	12.7	2.8	28.2	39.4	15.5	40.9	42.2	43.7	45.2
183975	39	39	77	44	96.5	4.6	0.5	17.3	25.9	18.5	2.0	43.2	44.5	20.6	61.7	46.5	63.8	68.8
184030	39	42	78	11	102.1	3.0	1.8	30.0	21.8	39.9	0.5	51.8	61.7	40.4	91.7	62.2	92.2	97.0
185080	38	32	77	0	129.8	5.1	2.0	7.1	33.8	6.4	0.3	40.9	40.1	6.6	47.2	40.4	47.5	54.6
185111	39	6	76	54	81.8	0.0	1.3	1.8	36.8	0.0	0.0	38.6	36.8	0.0	38.6	36.8	38.6	39.9
185832	39	35	79	22	112.8	0.5	3.8	8.9	17.8	65.5	15.2	26.7	83.3	80.8	92.2	98.6	107.4	111.8
185865	38	26	76	43	111.8	7.9	5.6	4.6	21.8	4.1	0.0	26.4	25.9	4.1	30.5	25.9	30.5	43.9
185894	39	36	79	5	121.9	2.3	5.1	3.8	40.6	70.1	6.4	44.5	110.7	76.5	114.6	117.1	120.9	128.3
185985	39	16	75	52	63.8	0.0	0.0	0.5	0.5	6.9	4.3	1.0	7.4	11.2	7.9	11.7	12.2	12.2
186350	38	54	76	59	88.4	3.0	12.7	5.1	23.4	30.5	4.3	28.4	53.8	34.8	58.9	58.2	63.2	79.0
186620	39	24	79	24	121.7	3.0	6.6	14.0	39.6	66.5	2.3	53.6	106.2	68.8	120.1	108.5	122.4	132.1
186770	38	41	76	40	105.2	11.4	1.3	16.0	19.0	10.2	1.5	35.1	29.2	11.7	45.2	30.7	46.7	59.4

Table 1. Official NOAA rain gage network data, October and November 1–6, 1985—Continued

Station	Latitude deg	Latitude arc min	Longitude deg	Longitude arc min	October 1985	November 1985 1	2	3	4	5	5	3–4	4–5	5–6	3–5	4–6	3–6	1–6
186844	39	38	76	42	75.7	0.0	0.0	1.3	32.3	7.1	0.0	33.5	39.4	7.1	40.6	39.4	40.6	40.6
186915	38	20	76	25	103.4	2.8	3.0	1.8	14.7	1.0	0.3	16.5	15.7	1.3	17.5	16.0	17.8	23.6
187272	39	2	77	15	91.7	3.0	1.3	2.5	26.7	3.0	0.0	29.2	29.7	3.0	32.3	29.7	32.3	36.6
187330	38	13	75	41	56.6	1.5	0.0	0.8	9.4	3.3	9.9	10.2	12.7	13.2	13.5	22.6	23.4	24.9
187705	39	6	77	6	83.6	3.3	0.8	1.8	44.5	6.9	0.0	46.2	51.3	6.9	53.1	51.3	53.1	57.2
187806	38	43	76	11	52.1	0.0	0.0	0.0	7.9	4.6	8.1	7.9	12.4	12.7	12.4	20.6	20.6	20.6
188000	38	22	75	35	60.7	0.5	0.0	0.0	6.6	3.0	0.8	6.6	9.7	3.8	9.7	10.4	10.4	10.9
188005	38	20	75	31	48.3	0.8	4.3	0.8	11.7	4.3	1.0	12.4	16.0	5.3	16.8	17.0	17.8	22.9
188065	39	31	79	8	140.0	1.0	10.2	7.6	47.5	90.9	5.3	55.1	138.4	96.3	146.1	143.8	151.4	162.6
188380	38	14	75	23	115.3	5.6	0.0	1.3	8.1	7.9	4.3	9.4	16.0	12.2	17.3	20.3	21.6	27.2
188877	39	23	76	34	84.3	0.0	0.0	3.8	17.3	19.6	10.2	21.1	36.8	29.7	40.6	47.0	50.8	50.8
189030	39	27	77	11	77.5	0.0	7.6	5.1	12.7	16.0	0.5	17.8	28.7	16.5	33.8	29.2	34.3	41.9
189070	38	52	76	47	117.1	1.5	0.8	1.3	18.5	16.8	3.0	19.8	35.3	19.8	36.6	38.4	39.6	41.9
189140	38	29	75	50	60.7	0.5	0.3	0.0	6.1	2.8	3.8	6.1	8.9	6.6	8.9	12.7	12.7	13.5
189440	39	33	76	58	72.9	0.0	0.0	2.0	13.5	14.5	4.3	15.5	27.9	18.8	30.0	32.3	34.3	34.3
189750	39	20	76	52	69.6	0.0	0.0	2.5	17.3	20.3	2.8	19.8	37.6	23.1	40.1	40.4	42.9	42.9
Pennsylvania																		
360022	40	32	79	49	69.9	0.0	0.5	11.9	54.6	33.3	1.0	66.5	87.9	34.3	99.8	88.9	100.8	101.3
360106	40	39	75	26	50.0	0.0	0.0	0.0	4.6	20.1	2.5	4.6	24.6	22.6	24.6	27.2	27.2	27.2
360130	40	18	78	19	63.8	1.0	4.1	18.8	21.1	26.9	0.3	39.9	48.0	27.2	66.8	48.3	67.1	72.1
360140	40	30	78	28	95.0	0.0	0.0	10.9	33.0	24.9	4.6	43.9	57.9	29.5	68.8	62.5	73.4	73.4
360355	40	39	79	59	39.4	2.3	13.5	55.9	41.4	2.5	1.0	97.3	43.9	3.6	99.8	45.0	100.8	116.6
360409	41	40	79	2	39.1	24.1	13.5	55.9	38.4	13.0	7.9	94.2	51.3	20.8	107.2	59.2	115.1	152.7
360457	40	50	76	30	47.8	0.0	0.0	0.0	4.3	9.1	6.4	4.3	13.5	15.5	13.5	19.8	19.8	19.8
360475	40	46	80	19	44.5	0.0	0.0	14.2	38.1	50.0	8.1	52.3	88.1	58.2	102.4	96.3	110.5	110.5
360482	40	46	77	9	76.2	0.0	2.8	32.3	11.2	10.7	0.0	43.4	21.8	10.7	54.1	21.8	54.1	56.9
360488	40	23	75	37	63.2	0.0	0.0	0.0	1.3	27.2	2.5	1.3	28.4	29.7	28.4	31.0	31.0	31.0
360560	40	46	75	44	39.1	0.0	0.0	0.0	0.0	13.0	11.9	0.0	13.0	24.9	13.0	24.9	24.9	24.9
360656	39	56	77	15	49.3	0.0	0.0	3.0	48.0	35.1	9.9	51.1	83.1	45.0	86.1	93.0	96.0	96.0
360738	40	26	79	9	84.1	0.0	0.0	11.9	25.9	9.9	9.4	37.8	35.8	19.3	47.8	45.2	57.2	57.2
360763	40	16	77	22	40.6	0.0	0.0	4.6	36.1	20.8	3.3	40.6	56.9	24.1	61.5	60.2	64.8	64.8
360785	40	23	76	2	38.4	0.0	0.0	0.0	0.0	24.1	3.8	0.0	24.1	27.9	24.1	27.9	27.9	27.9
360821	40	9	79	2	80.8	0.0	5.6	8.9	9.7	16.5	6.6	18.5	26.2	23.1	35.1	32.8	41.7	47.2
360861	40	24	79	52	54.9	0.0	0.8	10.9	53.3	30.5	1.3	64.3	83.8	31.8	94.7	85.1	96.0	96.8
360865	41	48	78	38	54.9	0.0	6.1	15.7	7.9	9.9	1.8	23.6	17.8	11.7	33.5	19.6	35.3	41.4
360867	41	57	78	39	82.6	0.0	4.1	5.1	19.0	7.1	7.9	24.1	26.2	15.0	31.2	34.0	39.1	43.2
360868	41	57	78	44	102.9	0.0	10.2	29.2	11.7	6.4	0.5	40.9	18.0	6.9	47.2	18.5	47.8	57.9
361004	41	9	79	5	63.8	0.0	0.3	12.4	33.3	4.3	0.5	45.7	37.6	4.8	50.0	38.1	50.5	50.8

Table 1. Official NOAA rain gage network data, October and November 1–6, 1985—Continued

Station	Latitude deg	Latitude arc min	Longitude deg	Longitude arc min	October 1985	November 1985 1	2	3	4	5	5	3–4	4–5	5–6	3–5	4–6	3–6	1–6
361033	40	18	79	59	67.8	0.0	0.0	0.0	74.9	30.5	0.3	74.9	105.4	30.7	105.4	105.7	105.7	105.7
361080	40	31	75	12	53.3	0.0	0.0	0.0	8.1	14.5	0.5	8.1	22.6	15.0	22.6	23.1	23.1	23.1
361087	39	57	78	39	113.0	2.3	1.8	11.4	34.8	55.4	8.4	46.2	90.2	63.8	101.6	98.6	110.0	114.0
361105	40	23	80	26	75.2	0.0	1.3	15.2	41.4	63.5	3.3	56.6	104.9	66.8	120.1	108.2	123.4	124.7
361139	40	51	79	55	61.0	0.3	1.0	16.3	35.1	42.7	0.8	51.3	77.7	43.4	94.0	78.5	94.7	96.0
361212	41	39	76	51	55.1	0.0	0.0	0.0	14.5	9.7	3.8	14.5	24.1	13.5	24.1	27.9	27.9	27.9
361255	40	35	78	42	51.8	0.0	0.0	7.9	15.7	23.6	7.9	23.6	39.4	31.5	47.2	47.2	55.1	55.1
361301	41	31	77	27	43.2	17.8	0.0	7.9	15.7	23.6	7.9	23.6	39.4	31.5	47.2	47.2	55.1	72.9
361342	39	52	75	37	43.2	17.8	0.0	0.0	0.0	25.9	5.6	0.0	25.9	31.5	25.9	31.5	31.5	49.3
361350	39	51	79	35	83.1	0.0	0.5	11.7	32.8	36.8	11.7	44.4	69.6	48.5	81.3	81.3	93.0	93.5
361354	39	56	77	38	52.8	7.1	0.5	18.8	17.8	30.2	0.5	36.6	48.0	30.7	66.8	48.5	67.3	74.9
361377	40	9	79	54	46.5	0.0	2.8	14.0	53.3	39.4	1.8	67.3	92.7	41.1	106.7	94.5	108.5	111.3
361480	41	3	77	56	40.9	0.0	0.0	0.0	0.0	0.0	0.0	0.0	0.0	0.0	0.0	0.0	0.0	0.0
361485	41	12	79	26	59.9	0.3	0.3	11.4	55.1	19.0	0.5	66.5	74.2	19.6	85.6	74.7	86.1	86.6
361505	40	37	75	39	39.6	0.0	0.0	0.0	0.0	15.5	12.4	0.0	15.5	27.9	15.5	27.9	27.9	27.9
361519	41	1	78	27	48.0	0.3	0.0	5.1	24.9	8.1	2.3	30.0	33.0	10.4	38.1	35.3	40.4	40.6
361534	41	44	78	32	61.5	0.0	0.0	5.3	19.6	8.6	3.8	24.9	28.2	12.4	33.5	32.0	37.3	37.3
361591	39	59	75	52	57.4	0.0	0.0	1.0	14.7	13.5	0.3	15.7	28.2	13.7	29.2	28.4	29.5	29.5
361705	39	48	79	22	77.5	0.0	2.5	11.7	17.8	35.1	10.4	29.5	52.8	45.5	64.5	63.2	74.9	77.5
361719	41	44	80	17	83.8	0.0	0.0	13.2	14.0	99.6	18.0	27.2	113.5	117.6	126.7	131.6	144.8	144.8
361726	39	60	79	36	63.0	0.0	1.3	11.4	25.4	22.9	10.2	36.8	48.3	33.0	59.7	58.4	69.9	71.1
361737	40	4	75	19	44.7	0.0	0.0	0.0	0.0	36.1	2.5	0.0	36.1	38.6	36.1	38.6	38.6	38.6
361749	41	20	79	13	77.5	0.0	0.0	11.4	50.3	10.2	1.8	61.7	60.5	11.9	71.9	62.2	73.7	73.7
361773	40	30	80	5	56.9	0.0	15.2	33.3	32.5	0.5	0.0	65.8	33.0	0.5	66.3	33.0	66.3	81.5
361790	41	55	79	38	89.9	0.0	6.1	8.6	35.6	35.6	2.0	44.2	71.1	37.6	79.8	73.2	81.8	87.9
361806	41	50	78	4	58.4	0.0	0.0	7.1	14.7	6.4	2.5	21.8	21.1	8.9	28.2	23.6	30.7	30.7
361833	41	44	77	7	41.1	0.0	0.0	0.0	10.9	10.2	6.4	10.9	21.1	16.5	21.1	27.4	27.4	27.4
361881	40	41	79	12	56.1	0.0	0.0	7.1	26.9	5.6	4.6	34.0	32.5	10.2	39.6	37.1	44.2	44.2
362013	40	58	76	37	34.8	0.0	0.0	0.0	10.7	7.1	7.1	10.7	17.8	14.2	17.8	24.9	24.9	24.9
362108	40	18	79	20	146.1	0.0	4.6	21.3	33.0	3.0	22.6	54.4	36.1	25.7	57.4	58.7	80.0	84.6
362116	40	5	75	33	47.8	0.0	0.0	1.3	38.1	5.1	0.0	39.4	43.2	5.1	44.4	43.2	44.4	44.4
362183	40	8	79	24	64.8	0.3	2.5	10.4	17.0	16.8	10.2	27.4	33.8	26.9	44.2	43.9	54.4	57.2
362190	40	10	79	52	55.1	2.3	6.6	10.9	49.5	12.7	0.5	60.5	62.2	13.2	73.2	62.7	73.7	82.6
362221	40	18	75	8	61.5	0.0	0.0	0.0	0.0	25.1	0.0	0.0	25.1	25.1	25.1	25.1	25.1	25.1
362260	41	11	78	54	54.4	0.3	2.5	11.9	15.7	0.8	0.0	27.7	16.5	0.8	28.4	16.5	28.4	31.2
362343	41	24	76	35	46.7	0.0	0.0	0.0	3.3	6.4	6.1	3.3	9.7	12.4	9.7	15.7	15.7	15.7

Table 1. Official NOAA rain gage network data, October and November 1–6, 1985—Continued

Station	Latitude deg	Latitude arc min	Longitude deg	Longitude arc min	October 1985	November 1985 1	2	3	4	5	5	3–4	4–5	5–6	3–5	4–6	3–6	1–6
362470	40	28	78	44	75.7	0.0	0.0	8.1	18.8	27.7	6.9	26.9	46.5	34.5	54.6	53.3	61.5	61.5
362537	39	49	77	16	53.8	0.0	0.0	23.9	46.2	15.7	3.8	70.1	62.0	19.6	85.9	65.8	89.7	89.7
362629	41	30	78	14	67.1	0.0	0.0	3.6	21.6	4.6	1.3	25.1	26.2	5.8	29.7	27.4	31.0	31.0
362671	41	52	75	16	52.3	0.0	0.0	0.0	0.0	6.9	11.9	0.0	6.9	18.8	6.9	18.8	18.8	18.8
362682	42	5	80	11	132.1	0.0	16.3	5.8	57.9	49.3	1.5	63.8	107.2	50.8	113.0	108.7	114.6	130.8
362942	40	43	79	30	38.4	0.0	0.3	5.8	48.8	14.7	2.3	54.6	63.5	17.0	69.3	65.8	71.6	71.9
363018	41	7	75	44	69.6	0.0	0.0	0.0	0.0	7.1	11.4	0.0	7.1	18.5	7.1	18.5	18.5	18.5
363028	41	23	79	49	79.0	0.0	0.0	14.5	24.9	53.1	11.4	39.4	78.0	64.5	92.5	89.4	103.9	103.9
363056	41	1	75	54	63.0	0.0	0.0	0.0	0.8	11.9	16.3	0.8	12.7	28.2	12.7	29.0	29.0	29.0
363130	41	44	77	38	48.5	0.0	0.0	7.6	26.7	10.4	3.8	34.3	37.1	14.2	44.7	40.9	48.5	48.5
363158	41	49	79	27	78.5	0.0	0.0	8.6	22.4	29.5	14.7	31.0	51.8	44.2	60.5	66.5	75.2	75.2
363211	41	39	77	40	48.5	0.0	0.0	4.3	33.8	12.2	5.1	38.1	46.0	17.3	50.3	51.1	55.4	55.4
363311	41	34	78	36	60.5	0.0	0.0	4.1	23.1	7.1	2.3	27.2	30.2	9.4	34.3	32.5	36.6	36.6
363321	40	6	75	47	51.1	0.0	0.0	0.0	0.0	34.0	7.6	0.0	34.0	41.7	34.0	41.7	41.7	41.7
363343	40	33	80	13	56.9	0.5	0.5	14.0	39.9	41.9	2.5	53.8	81.8	44.5	95.8	84.3	98.3	99.3
363394	41	15	75	27	32.8	0.0	0.0	0.0	0.0	41.1	6.9	0.0	41.1	48.0	41.1	48.0	48.0	48.0
363437	40	14	75	26	52.8	0.0	0.0	0.0	0.0	27.7	3.0	0.0	27.7	30.7	27.7	30.7	30.7	30.7
363503	39	47	79	55	53.3	0.0	1.5	4.3	44.7	53.3	0.0	49.0	98.0	53.3	102.4	98.0	102.4	103.9
363526	41	25	80	22	82.8	0.0	1.3	17.0	19.3	52.3	11.9	36.3	71.6	64.3	88.6	83.6	100.6	101.9
363632	40	33	75	59	26.4	0.0	0.0	0.0	0.3	15.0	6.6	0.3	15.2	21.6	15.2	21.8	21.8	21.8
363662	39	48	76	59	37.3	0.0	0.0	0.0	11.7	20.8	8.6	11.7	32.5	29.5	32.5	41.1	41.1	41.1
363699	40	13	76	51	34.0	0.0	0.0	5.3	17.5	4.1	0.0	22.9	21.6	4.1	26.9	21.6	26.9	26.9
363758	41	29	75	10	31.0	0.0	0.0	0.0	0.0	11.9	10.7	0.0	11.9	22.6	11.9	22.6	22.6	22.6
364008	41	23	75	26	59.4	0.0	0.0	0.0	0.0	20.3	13.0	0.0	20.3	33.3	20.3	33.3	33.3	33.3
364019	39	50	76	20	27.9	0.0	0.0	0.0	0.5	13.0	7.9	0.5	13.5	20.8	13.5	21.3	21.3	21.3
364043	41	37	75	19	84.1	0.0	0.0	0.0	0.0	9.9	0.0	0.0	9.9	9.9	9.9	9.9	9.9	9.9
364047	40	5	75	50	37.3	0.0	0.0	0.0	0.0	25.4	13.2	0.0	25.4	38.6	25.4	38.6	38.6	38.6
364076	40	12	75	47	59.9	0.0	0.0	0.0	0.3	44.5	7.1	0.3	44.7	51.6	44.7	51.8	51.8	51.8
364166	40	6	77	18	27.9	0.0	0.0	0.0	29.2	31.8	12.7	29.2	61.0	44.5	61.0	73.7	73.7	73.7
364190	39	49	78	44	109.7	3.0	2.8	9.9	30.7	42.7	3.3	40.6	73.4	46.0	83.3	76.7	86.6	92.5
364214	40	36	79	7	68.1	0.0	0.0	10.7	23.4	8.4	6.4	34.0	31.8	14.7	42.4	38.1	48.8	48.8
364325	41	30	80	28	79.5	0.0	5.6	10.4	11.4	96.3	15.0	21.8	107.7	111.3	118.1	122.7	133.1	138.7
364385	40	20	78	55	67.6	0.0	2.0	14.5	8.6	22.4	1.8	23.1	31.0	24.1	45.5	32.8	47.2	49.3
364432	41	41	78	48	72.9	0.0	0.0	8.9	21.3	7.6	3.8	30.2	29.0	11.4	37.8	32.8	41.7	41.7
364481	39	59	78	43	98.8	2.5	7.6	20.3	39.4	34.3	0.0	59.7	73.7	34.3	94.0	73.7	94.0	104.1
364611	40	49	79	32	62.5	0.0	0.0	7.4	55.9	0.0	0.0	63.2	55.9	0.0	63.2	55.9	63.2	63.2
364672	40	54	75	32	39.6	0.0	0.0	0.0	0.0	15.7	5.6	0.0	15.7	21.3	15.7	21.3	21.3	21.3
364727	41	13	75	3	69.9	0.0	0.0	0.3	0.0	19.8	19.0	0.3	19.8	38.9	20.1	38.9	39.1	39.1

Table 1. Official NOAA rain gage network data, October and November 1–6, 1985—Continued

Station	Latitude deg	Latitude arc min	Longitude deg	Longitude arc min	October 1985	November 1985 1	2	3	4	5	5	3–4	4–5	5–6	3–5	4–6	3–6	1–6
364763	40	3	76	17	42.2	0.0	0.0	1.3	0.5	12.2	6.4	1.8	12.7	18.5	14.0	19.1	20.3	20.3
364778	40	7	76	26	30.5	0.0	0.0	0.3	1.3	10.7	4.8	1.5	11.9	15.5	12.2	16.8	17.0	17.0
364853	40	54	77	13	51.1	0.0	0.0	11.7	25.1	22.9	2.8	36.8	48.0	25.7	59.7	50.8	62.5	62.5
364896	40	20	76	28	49.0	0.0	0.0	1.0	1.0	11.4	8.1	2.0	12.4	19.6	13.5	20.6	21.6	21.6
364934	40	50	75	43	39.4	0.0	0.0	0.0	0.0	9.1	16.5	0.0	9.1	25.7	9.1	25.7	25.7	25.7
364972	41	41	76	43	50.5	0.0	0.0	0.0	9.9	12.2	9.7	9.9	22.1	21.8	22.1	31.8	31.8	31.8
364983	41	52	78	39	70.9	0.0	0.0	9.9	17.0	11.2	6.9	26.9	28.2	18.0	38.1	35.1	45.0	45.0
364992	40	35	77	35	39.9	0.0	5.3	33.0	31.2	8.9	0.0	64.3	40.1	8.9	73.2	40.1	73.2	78.5
365050	41	39	80	26	62.2	0.0	0.8	11.7	7.9	95.3	14.0	19.6	103.1	109.2	114.8	117.1	128.8	129.5
365109	41	7	77	27	51.8	0.0	2.3	22.6	12.2	16.5	0.0	34.8	28.7	16.5	51.3	28.7	51.3	53.6
365160	41	3	75	30	63.0	0.0	0.0	0.0	0.0	24.6	8.4	0.0	24.6	33.0	24.6	33.0	33.0	33.0
365212	40	27	79	29	45.7	0.0	1.5	12.4	39.4	6.4	4.6	51.8	45.7	10.9	58.2	50.3	62.7	64.3
365344	40	50	76	8	70.1	0.0	0.0	0.0	0.0	14.0	14.2	0.0	14.0	28.2	14.0	28.2	28.2	28.2
365381	40	24	77	56	63.8	0.0	0.0	6.1	38.9	17.5	12.2	45.0	56.4	29.7	62.5	68.6	74.7	74.7
365390	39	49	75	25	38.6	0.0	0.0	0.0	8.1	27.9	0.0	8.1	36.1	27.9	36.1	36.1	36.1	36.1
365408	40	45	79	2	60.5	0.5	1.8	11.7	24.1	8.4	4.6	35.8	32.5	13.0	44.2	37.1	48.8	51.1
365470	41	22	74	42	47.5	0.0	0.0	0.0	0.0	0.0	0.0	0.0	0.0	0.0	0.0	0.0	0.0	0.0
365606	41	38	80	10	69.6	0.0	0.0	19.3	17.3	75.7	18.5	36.6	93.0	94.2	112.3	111.5	130.8	130.8
365651	41	13	80	14	49.5	0.0	0.8	18.0	24.4	70.4	10.7	42.4	94.7	81.0	112.8	105.4	123.4	124.2
365662	39	50	77	54	92.7	2.5	15.2	43.2	27.9	10.2	0.0	71.1	38.1	10.2	81.3	38.1	81.3	99.1
365686	39	47	79	3	101.9	4.3	9.1	6.1	23.6	80.3	10.2	29.7	103.9	90.4	110.0	114.0	120.1	133.6
365790	40	53	77	29	46.5	1.3	0.0	7.1	19.3	14.5	12.7	26.4	33.8	27.2	40.9	46.5	53.6	54.9
365817	41	6	76	34	37.3	0.0	0.0	0.0	6.9	7.6	8.9	6.9	14.5	16.5	14.5	23.4	23.4	23.4
365902	40	39	80	23	55.4	0.3	0.0	8.1	31.2	49.0	5.6	39.4	80.3	54.6	88.4	85.9	94.0	94.2
365915	41	50	75	52	48.3	0.0	0.0	0.0	0.3	11.7	4.6	0.3	11.9	16.3	11.9	16.5	16.5	16.5
366042	40	8	79	33	62.7	0.0	1.3	20.6	30.2	12.7	6.6	50.8	42.9	19.3	63.5	49.5	70.1	71.4
366126	40	22	76	18	25.4	0.0	0.0	0.0	5.1	11.4	0.0	5.1	16.5	11.4	16.5	16.5	16.5	16.5
366151	40	37	79	43	62.0	0.0	0.3	9.4	52.3	26.7	1.3	61.7	79.0	27.9	88.4	80.3	89.7	89.9
366194	40	9	74	57	43.2	0.0	0.0	0.0	3.0	26.2	0.0	3.0	29.2	26.2	29.2	29.2	29.2	29.2
366233	41	1	80	22	43.4	0.0	0.0	16.3	30.0	33.0	10.4	46.2	63.0	43.4	79.2	73.4	89.7	89.7
366289	39	44	76	30	52.8	0.0	0.0	0.8	5.8	33.8	8.4	6.6	39.6	42.2	40.4	48.0	48.8	48.8
366297	40	29	77	8	49.8	0.0	0.0	13.0	15.5	12.7	2.0	28.4	28.2	14.7	41.1	30.2	43.2	43.2
366310	40	12	79	38	54.4	3.6	14.2	43.2	11.4	3.8	1.0	54.6	15.2	4.8	58.4	16.3	59.4	77.2
366370	40	7	75	21	46.5	0.0	0.0	0.0	0.0	31.0	2.5	0.0	31.0	33.5	31.0	33.5	33.5	33.5
366508	39	48	76	3	57.7	0.0	0.0	0.3	0.3	16.5	3.8	0.5	16.8	20.3	17.0	20.6	20.8	20.8
366622	41	55	76	18	55.6	0.0	0.0	0.0	6.1	17.3	2.0	6.1	23.4	19.3	23.4	25.4	25.4	25.4
366681	40	23	75	30	43.4	0.0	0.0	0.0	1.0	11.9	2.5	1.0	13.0	14.5	13.0	15.5	15.5	15.5
366689	40	48	75	37	55.4	0.0	0.0	0.0	26.4	11.9	2.5	26.4	38.4	14.5	38.4	40.9	40.9	40.9

Table 1. Official NOAA rain gage network data, October and November 1–6, 1985—Continued

Station	Latitude deg	Latitude arc min	Longitude deg	Longitude arc min	October 1985	November 1985 1	2	3	4	5	5	3–4	4–5	5–6	3–5	4–6	3–6	1–6
366721	41	5	79	41	57.9	3.8	3.8	11.4	20.8	31.8	1.8	32.3	52.6	33.5	64.0	54.4	65.8	73.4
366762	41	24	75	14	32.8	0.0	0.0	0.0	0.0	14.7	11.9	0.0	14.7	26.7	14.7	26.7	26.7	26.7
366889	39	53	75	14	39.1	0.0	0.0	0.0	9.7	15.2	0.3	9.7	24.9	15.5	24.9	25.1	25.1	25.1
366916	40	54	78	5	30.2	0.0	0.0	17.8	14.2	5.1	0.0	32.0	19.3	5.1	37.1	19.3	37.1	37.1
366927	40	7	75	30	50.3	0.0	0.0	0.0	9.4	25.1	1.3	9.4	34.5	26.4	34.5	35.8	35.8	35.8
366955	40	2	77	18	54.9	0.0	0.0	4.3	51.6	35.1	18.8	55.9	86.6	53.8	90.9	105.4	109.7	109.7
366993	40	30	80	13	57.7	0.0	13.0	40.1	43.7	1.8	0.0	83.8	45.5	1.8	85.6	45.5	85.6	98.6
367029	41	44	75	27	58.2	0.0	0.0	0.0	0.5	14.2	13.2	0.5	14.7	27.4	14.7	27.9	27.9	27.9
367103	41	49	78	17	51.3	0.0	0.0	5.1	11.2	7.4	4.1	16.3	18.5	11.4	23.6	22.6	27.7	27.7
367167	40	39	78	33	63.5	0.0	0.5	10.4	16.5	10.2	6.1	26.9	26.7	16.3	37.1	32.8	43.2	43.7
367229	40	56	79	17	74.9	0.0	0.0	10.7	41.4	9.1	1.0	52.1	50.5	10.2	61.2	51.6	62.2	62.2
367310	41	52	77	52	50.8	0.0	0.0	0.0	23.6	9.7	3.6	23.6	33.3	13.2	33.3	36.8	36.8	36.8
367312	40	26	78	0	60.2	0.0	0.0	6.4	22.9	21.6	11.9	29.2	44.5	33.5	50.8	56.4	62.7	62.7
367322	40	22	75	56	20.1	0.0	0.0	0.0	0.8	20.6	5.1	0.8	21.3	25.7	21.3	26.4	26.4	26.4
367409	41	20	77	44	36.3	0.5	0.0	8.9	20.8	9.7	6.1	29.7	30.5	15.7	39.4	36.6	45.5	46.0
367477	41	25	78	45	67.1	0.0	0.0	6.4	23.6	3.8	0.8	30.0	27.4	4.6	33.8	28.2	34.5	34.5
367578	40	33	75	43	37.8	0.0	0.0	0.5	1.5	22.9	3.3	2.0	24.4	26.2	24.9	27.7	28.2	28.2
367727	41	47	76	7	39.9	0.0	0.0	0.0	3.0	22.4	2.8	3.0	25.4	25.1	25.4	28.2	28.2	28.2
367728	41	56	79	4	84.6	0.0	0.0	10.2	32.0	17.8	13.7	42.2	49.8	31.5	59.9	63.5	73.7	73.7
367730	41	50	77	28	27.9	0.0	0.0	0.0	27.9	11.4	15.2	27.9	39.4	26.7	39.4	54.6	54.6	54.6
367735	40	47	79	14	58.4	0.0	0.0	8.1	32.3	6.9	2.8	40.4	39.1	9.7	47.2	41.9	50.0	50.0
367782	40	31	79	33	58.7	0.0	8.9	15.7	44.7	8.9	0.0	60.5	53.6	8.9	69.3	53.6	69.3	78.2
367846	40	12	78	15	65.5	0.3	0.0	6.1	24.1	47.8	2.8	30.2	71.9	50.5	78.0	74.7	80.8	81.0
367863	40	41	79	40	54.6	0.0	0.5	10.4	53.3	21.8	1.0	63.8	75.2	22.9	85.6	76.2	86.6	87.1
367931	40	46	76	52	36.8	0.0	0.0	3.8	16.3	3.0	10.4	20.1	19.3	13.5	23.1	29.7	33.5	33.5
367942	40	1	79	18	53.3	0.0	0.0	0.0	0.0	24.6	14.0	0.0	24.6	38.6	24.6	38.6	38.6	38.6
367978	40	48	76	33	35.1	0.0	0.0	0.0	3.3	5.3	9.1	3.3	8.6	14.5	8.6	17.8	17.8	17.8
368057	41	12	76	8	27.7	0.0	0.0	0.0	2.0	5.6	4.8	2.0	7.6	10.4	7.6	12.4	12.4	12.4
368073	40	3	77	31	45.7	0.0	0.8	18.8	32.8	21.8	0.0	51.6	54.6	21.8	73.4	54.6	73.4	74.2
368145	41	19	78	6	81.5	0.0	0.0	5.8	35.1	10.4	5.8	40.9	45.5	16.3	51.3	51.3	57.2	57.2
368184	41	3	80	4	50.5	1.3	16.0	27.9	57.9	10.2	1.3	85.9	68.1	11.4	96.0	69.3	97.3	114.6
368203	41	51	78	29	52.3	0.0	0.0	5.8	16.0	9.7	5.6	21.8	25.7	15.2	31.5	31.2	37.1	37.1
368244	39	60	79	5	80.0	0.8	3.6	6.4	14.7	34.3	3.8	21.1	49.0	38.1	55.4	52.8	59.2	63.5
368308	39	51	77	30	65.5	0.0	0.0	4.3	43.2	61.5	13.7	47.5	104.6	75.2	109.0	118.4	122.7	122.7
368379	39	52	76	52	52.8	0.0	0.0	0.0	10.7	31.2	7.4	10.7	41.9	38.6	41.9	49.3	49.3	49.3
368388	40	13	75	13	54.4	0.0	0.0	0.0	0.0	31.5	0.0	0.0	31.5	31.5	31.5	31.5	31.5	31.5
368449	40	48	77	52	40.9	1.3	0.0	2.5	30.2	20.3	8.6	32.8	50.5	29.0	53.1	59.2	61.7	63.0
368469	41	24	78	1	48.8	0.0	0.0	4.8	32.3	10.2	3.3	37.1	42.4	13.5	47.2	45.7	50.5	50.5

Table 1. Official NOAA rain gage network data, October and November 1–6, 1985—Continued

Station	Latitude deg	Latitude arc min	Longitude deg	Longitude arc min	October 1985	November 1985 1	2	3	4	5	5	3–4	4–5	5–6	3–5	4–6	3–6	1–6
368560	40	6	78	57	78.0	2.3	10.7	14.0	20.8	7.6	0.5	34.8	28.4	8.1	42.4	29.0	42.9	55.9
368570	40	29	76	11	35.8	0.0	0.0	0.0	0.0	13.2	28.7	0.0	13.2	41.9	13.2	41.9	41.9	41.9
368596	41	0	75	11	52.3	0.0	0.0	0.0	0.0	21.1	7.4	0.0	21.1	28.4	21.1	28.4	28.4	28.4
368692	41	57	75	36	57.9	0.0	0.0	0.0	0.0	8.4	5.3	0.0	8.4	13.7	8.4	13.7	13.7	13.7
368758	40	47	75	59	68.3	0.0	0.0	0.0	0.0	13.5	9.7	0.0	13.5	23.1	13.5	23.1	23.1	23.1
368763	40	51	75	59	71.1	0.0	0.0	0.0	0.0	11.9	11.4	0.0	11.9	23.4	11.9	23.4	23.4	23.4
368873	41	29	79	26	89.7	0.0	0.3	11.7	35.3	23.1	6.4	47.0	58.4	29.5	70.1	64.8	76.5	76.7
368888	41	38	79	42	86.6	0.0	0.0	9.7	23.6	41.7	16.8	33.3	65.3	58.4	74.9	82.0	91.7	91.7
368893	41	11	75	25	44.5	0.0	0.0	0.0	0.0	35.6	10.9	0.0	35.6	46.5	35.6	46.5	46.5	46.5
368905	41	45	76	25	36.8	0.0	0.0	0.0	5.3	10.4	8.9	5.3	15.7	19.3	15.7	24.6	24.6	24.6
368959	41	47	76	47	50.8	0.0	0.0	0.0	18.0	10.7	5.1	18.0	28.7	15.7	28.7	33.8	33.8	33.8
369022	40	40	78	13	71.1	0.0	0.0	0.0	0.0	0.0	5.6	0.0	0.0	5.6	0.0	5.6	5.6	5.6
369042	41	54	79	49	75.4	0.0	0.0	9.1	13.7	51.6	20.1	22.9	65.3	71.6	74.4	85.3	94.5	94.5
369050	39	55	79	43	73.2	0.0	0.5	11.9	31.5	33.5	11.2	43.4	65.0	44.7	77.0	76.2	88.1	88.6
369115	41	19	79	39	63.0	0.0	14.2	30.5	36.6	6.4	0.5	67.1	42.9	6.9	73.4	43.4	73.9	88.1
369128	40	36	79	33	52.3	0.3	0.8	7.9	50.5	20.3	3.8	58.4	70.9	24.1	78.7	74.7	82.6	83.6
369298	41	51	79	9	74.7	0.0	0.0	8.4	33.3	12.7	10.4	41.7	46.0	23.1	54.4	56.4	64.8	64.8
369318	40	11	80	11	57.7	0.3	1.3	20.6	43.4	44.7	2.8	64.0	88.1	47.5	108.7	90.9	111.5	113.0
369367	39	54	80	10	45.0	0.0	2.3	11.4	59.4	65.0	2.8	70.9	124.5	67.8	135.9	127.3	138.7	141.0
369385	41	18	78	29	51.8	0.0	0.0	5.8	22.6	7.1	6.6	28.4	29.7	13.7	35.6	36.3	42.2	42.2
369408	41	42	77	16	38.9	0.0	0.0	0.0	16.5	8.1	9.7	16.5	24.6	17.8	24.6	34.3	34.3	34.3
369464	39	58	75	38	51.8	0.0	0.0	0.0	0.0	33.5	3.0	0.0	33.5	36.6	33.5	36.6	36.6	36.6
369490	39	58	75	40	42.4	0.0	0.0	0.0	32.5	10.4	3.3	32.5	42.9	13.7	42.9	46.2	46.2	46.2
369507	41	35	79	24	70.9	0.0	0.0	9.7	31.5	19.6	5.1	41.1	51.1	24.6	60.7	56.1	65.8	65.8
369655	40	44	79	24	53.1	0.0	0.8	7.6	43.2	10.7	3.3	50.8	53.8	14.0	61.5	57.2	64.8	65.5
369702	41	14	75	53	42.2	0.0	0.0	0.0	1.3	3.0	5.1	1.3	4.3	8.1	4.3	9.4	9.4	9.4
369705	41	20	75	44	48.8	0.0	0.0	0.0	0.8	7.9	8.4	0.8	8.6	16.3	8.6	17.0	17.0	17.0
369714	40	28	78	12	60.2	0.0	0.3	5.3	27.9	18.0	7.1	33.3	46.0	25.1	51.3	53.1	58.4	58.7
369728	41	15	76	55	46.5	0.0	0.0	8.9	11.7	14.2	0.0	20.6	25.9	14.2	34.8	25.9	34.8	34.8
369823	40	3	78	32	107.7	1.3	0.0	10.7	32.0	25.4	2.3	42.7	57.4	27.7	68.1	59.7	70.4	71.6
369933	39	55	76	45	39.6	0.0	0.0	1.3	7.1	58.4	7.1	8.4	65.5	65.5	66.8	72.6	73.9	73.9
369950	40	7	76	43	39.6	0.0	0.0	0.0	6.4	10.9	6.9	6.4	17.3	17.8	17.3	24.1	24.1	24.1
369995	40	28	75	27	48.0	0.0	0.0	0.0	0.0	28.4	2.8	0.0	28.4	31.2	28.4	31.2	31.2	31.2
Virginia																		
440021	36	40	81	58	66.8	0.0	22.6	1.3	26.7	36.6	9.7	27.9	63.2	46.2	64.5	72.9	74.2	96.8
440135	36	54	80	44	69.9	0.0	9.4	0.0	5.1	60.5	0.0	5.1	65.5	60.5	65.5	65.5	65.5	74.9
440166	37	6	79	18	94.2	5.3	72.9	29.5	47.5	41.4	0.0	77.0	88.9	41.4	118.4	88.9	118.4	196.6
440187	37	18	78	2	104.9	11.7	38.1	8.1	184.2	15.2	2.8	192.3	199.4	18.0	207.5	202.2	210.3	260.1

Table 1. Official NOAA rain gage network data, October and November 1–6, 1985—Continued

Station	Latitude deg	Latitude arc min	Longitude deg	Longitude arc min	October 1985	November 1985 1	2	3	4	5	5	3–4	4–5	5–6	3–5	4–6	3–6	1–6
440243	37	22	78	50	88.1	15.2	97.0	30.5	85.9	31.8	1.5	116.3	117.6	33.3	148.1	119.1	149.6	261.9
440327	37	45	77	29	122.2	23.4	9.9	5.1	50.8	4.6	0.0	55.9	55.4	4.6	60.5	55.4	60.5	93.7
440385	36	40	75	55	83.8	6.9	7.1	0.5	12.7	19.8	0.0	13.2	32.5	19.8	33.0	32.5	33.0	47.0
440551	37	21	79	31	76.5	3.8	35.8	14.0	33.8	99.1	0.0	47.8	132.8	99.1	146.8	132.8	146.8	186.4
440670	39	9	77	59	151.1	6.9	5.1	5.1	19.6	12.7	5.1	24.6	32.3	17.8	37.3	37.3	42.4	54.4
440720	38	31	78	26	243.1	71.1	67.3	25.4	95.3	191.8	12.2	120.7	287.0	204.0	312.4	299.2	324.6	463.0
440766	37	11	80	25	74.7	2.0	2.5	21.6	5.1	64.8	0.5	26.7	69.9	65.3	91.4	70.4	91.9	96.5
440792	37	6	81	6	59.4	7.6	14.2	5.6	53.3	26.7	1.3	58.9	80.0	27.9	85.6	81.3	86.9	108.7
440993	37	42	78	18	121.9	10.4	36.8	36.1	77.5	0.0	0.0	113.5	77.5	0.0	113.5	77.5	113.5	160.8
441082	37	3	78	56	81.3	3.0	51.6	23.6	47.5	32.3	0.5	71.1	79.8	32.8	103.4	80.3	103.9	158.5
441136	37	33	78	33	121.4	18.8	45.7	20.3	68.6	36.3	0.0	88.9	104.9	36.3	125.2	104.9	125.2	189.7
441209	37	5	81	20	54.6	7.1	6.1	3.6	56.1	13.0	3.6	59.7	69.1	16.5	72.6	72.6	76.2	89.4
441259	36	48	80	59	94.5	8.9	25.4	16.5	48.3	43.2	0.0	64.8	91.4	43.2	108.0	91.4	108.0	142.2
441322	37	2	77	57	160.5	16.8	40.6	3.3	116.1	11.9	0.5	119.4	128.0	12.4	131.3	128.5	131.8	189.2
441585	37	4	78	42	62.5	6.4	71.1	15.5	52.1	23.6	0.5	67.6	75.7	24.1	91.2	76.2	91.7	169.2
441593	38	2	78	31	124.7	28.2	52.1	20.6	78.7	40.9	1.3	99.3	119.6	42.2	140.2	120.9	141.5	221.7
441606	36	50	78	28	106.2	10.2	54.9	21.6	48.3	36.8	0.0	69.9	85.1	36.8	106.7	85.1	106.7	171.7
441614	36	49	79	24	82.0	3.8	20.3	13.0	47.0	86.1	1.0	59.9	133.1	87.1	146.1	134.1	147.1	171.2
441746	36	37	78	34	85.9	4.1	20.8	18.3	55.4	8.1	0.0	73.7	63.5	8.1	81.8	63.5	81.8	106.7
441913	38	15	76	58	89.7	4.1	10.7	18.3	22.6	2.8	1.8	40.9	25.4	4.6	43.7	27.2	45.5	60.2
441929	37	44	78	9	97.8	7.6	25.4	11.4	83.8	24.9	0.8	95.3	108.7	25.7	120.1	109.5	120.9	153.9
441955	37	17	78	58	78.5	6.6	76.5	25.7	77.7	24.1	0.0	103.4	101.9	24.1	127.5	101.9	127.5	210.6
441999	37	6	80	8	100.6	41.9	65.8	17.8	24.4	148.1	0.0	42.2	172.5	148.1	190.2	172.5	190.2	297.9
442009	38	12	77	22	165.9	10.4	16.5	4.6	50.0	4.1	1.3	54.6	54.1	5.3	58.7	55.4	59.9	86.9
442041	37	48	79	60	53.1	5.1	5.1	17.8	17.8	190.5	0.0	35.6	208.3	190.5	226.1	208.3	226.1	236.2
442044	37	48	79	60	64.5	8.1	18.8	14.7	203.2	66.0	0.0	217.9	269.2	66.0	284.0	269.2	284.0	310.9
442064	38	3	79	23	93.0	2.5	6.4	24.6	33.0	122.2	2.0	57.7	155.2	124.2	179.8	157.2	181.9	190.8
442142	37	38	77	48	100.8	8.9	26.2	3.6	87.4	27.7	2.5	90.9	115.1	30.2	118.6	117.6	121.2	156.2
442155	38	28	78	0	167.6	0.0	0.0	0.0	0.0	0.0	0.0	0.0	0.0	0.0	0.0	0.0	0.0	0.0
442160	37	30	78	15	101.3	11.2	33.0	11.4	78.7	30.2	1.5	90.2	109.0	31.8	120.4	110.5	121.9	166.1
442208	38	27	78	56	116.6	19.8	13.5	29.2	47.5	47.5	0.8	76.7	95.0	48.3	124.2	95.8	125.0	158.2
442245	36	35	79	23	65.0	2.8	9.4	5.8	33.0	58.9	1.5	38.9	91.9	60.5	97.8	93.5	99.3	111.5
442504	36	53	76	29	86.9	16.0	12.4	1.8	0.0	0.0	0.0	1.8	0.0	0.0	1.8	0.0	1.8	30.2
442600	37	40	80	14	59.4	11.4	20.8	6.6	20.3	108.2	1.3	26.9	128.5	109.5	135.1	129.8	136.4	168.7
442790	36	41	77	33	75.4	7.6	19.0	1.3	33.0	6.4	0.0	34.3	39.4	6.4	40.6	39.4	40.6	67.3
442941	37	20	78	23	87.6	14.7	36.1	16.5	62.7	28.4	0.8	79.2	91.2	29.2	107.7	91.9	108.5	159.3
443071	36	56	80	18	98.6	0.0	31.2	16.3	10.2	149.1	0.0	26.4	159.3	149.1	175.5	159.3	175.5	206.8
443192	38	19	77	27	159.5	5.1	13.0	3.3	49.3	4.3	2.5	52.6	53.6	6.9	56.9	56.1	59.4	77.5

Table 1. Official NOAA rain gage network data, October and November 1–6, 1985—Continued

Station	Latitude deg	Latitude arc min	Longitude deg	Longitude arc min	October 1985	November 1985 1	2	3	4	5	5	3–4	4–5	5–6	3–5	4–6	3–6	1–6
443213	38	5	76	8	118.1	23.6	50.8	15.7	96.0	51.6	1.3	111.8	147.6	52.8	163.3	148.8	164.6	239.0
443267	36	40	80	55	63.5	7.6	36.1	20.1	52.1	0.0	0.0	72.1	52.1	0.0	72.1	52.1	72.1	115.8
443310	37	57	79	57	57.7	1.0	11.2	9.1	31.0	168.4	0.0	40.1	199.4	168.4	208.5	199.4	208.5	220.7
443375	37	37	79	26	98.3	17.8	49.8	63.5	74.2	141.0	0.0	137.7	215.1	141.0	278.6	215.1	278.6	346.2
443397	37	22	80	52	45.7	2.5	5.6	1.0	14.0	64.8	0.8	15.0	78.7	65.5	79.8	79.5	80.5	88.6
443466	38	5	78	11	120.4	10.7	26.2	9.1	58.7	46.2	4.6	67.8	104.9	50.8	114.0	109.5	118.6	155.4
443470	37	59	79	30	93.5	1.5	21.6	31.8	43.2	130.8	2.5	74.9	174.0	133.3	205.7	176.5	208.3	231.4
443640	37	16	82	5	56.6	0.0	16.8	0.0	31.5	25.1	12.4	31.5	56.6	37.6	56.6	69.1	69.1	85.9
443991	36	44	80	44	97.3	5.3	15.2	21.8	10.7	67.8	1.5	32.5	78.5	69.3	100.3	80.0	101.9	122.4
444039	37	30	79	16	89.7	0.0	0.0	0.0	0.0	0.0	0.0	0.0	0.0	0.0	0.0	0.0	0.0	0.0
444044	36	41	76	47	130.0	16.0	13.2	1.8	29.0	2.8	0.0	30.7	31.8	2.8	33.5	31.8	33.5	62.7
444101	37	18	77	18	158.5	19.8	11.7	1.0	30.7	6.9	0.0	31.8	37.6	6.9	38.6	37.6	38.6	70.1
444128	38	0	79	50	49.5	7.6	24.6	12.2	34.8	209.6	0.0	47.0	244.3	209.6	256.5	244.3	256.5	288.8
444148	37	8	79	32	98.8	9.4	65.0	22.4	32.0	102.1	0.0	54.4	134.1	102.1	156.5	134.1	156.5	230.9
444234	36	39	81	10	84.6	21.3	30.5	14.0	35.6	10.7	0.0	49.5	46.2	10.7	60.2	46.2	60.2	112.0
444410	37	14	82	21	71.6	0.0	10.2	8.9	15.7	29.5	13.7	24.6	45.2	43.2	54.1	58.9	67.8	78.0
444414	36	36	78	17	83.8	5.8	27.9	17.0	37.8	16.3	0.0	54.9	54.1	16.3	71.1	54.1	71.1	104.9
444565	37	51	79	35	100.1	15.2	38.4	35.3	43.2	142.7	0.0	78.5	185.9	142.7	221.2	185.9	221.2	274.8
444568	37	10	78	31	48.3	14.5	27.7	8.9	34.3	0.0	0.0	43.2	34.3	0.0	43.2	34.3	43.2	85.3
444600	37	43	76	23	183.1	23.4	6.6	7.1	11.9	3.0	0.5	19.1	15.0	3.6	22.1	15.5	22.6	52.6
444676	37	14	80	13	78.0	38.4	43.2	12.2	9.4	125.2	0.0	21.6	134.6	125.2	146.8	134.6	146.8	228.3
444720	37	5	76	21	50.3	5.8	6.1	0.5	23.4	0.0	0.0	23.9	23.4	0.0	23.9	23.4	23.9	35.8
444768	36	46	77	56	64.0	43.2	30.5	0.8	135.9	21.8	0.0	136.7	157.7	21.8	158.5	157.7	158.5	232.2
444876	37	47	79	26	78.7	18.0	34.3	27.9	88.6	17.0	0.0	116.6	105.7	17.0	133.6	105.7	133.6	185.9
444909	39	7	77	43	117.3	18.0	0.0	16.3	30.0	18.0	4.1	46.2	48.0	22.1	64.3	52.1	68.3	86.4
445050	38	2	78	0	149.1	21.1	23.1	27.7	53.1	62.5	0.0	80.8	115.6	62.5	143.3	115.6	143.3	187.5
445096	38	40	78	23	102.1	45.7	41.9	50.8	50.8	52.1	54.4	101.6	102.9	106.4	153.7	157.2	208.0	295.7
445120	37	20	79	12	83.8	42.9	39.9	38.4	38.1	1.0	0.0	76.5	39.1	1.0	77.5	39.1	77.5	160.3
445271	36	49	81	31	82.5	3.8	11.7	1.8	33.5	19.8	4.8	35.3	53.3	24.6	55.1	58.2	59.9	75.4
445338	37	27	76	17	138.7	12.2	5.8	2.3	16.5	0.0	0.0	18.8	16.5	0.0	18.8	16.5	18.8	36.8
445416	38	21	79	32	125.7	4.6	11.7	21.1	16.3	11.7	0.0	37.3	27.9	11.7	49.0	27.9	49.0	65.3
445453	36	40	80	27	119.1	11.9	34.5	25.9	16.3	106.9	0.0	42.2	123.2	106.9	149.1	123.2	149.1	195.6
445595	38	21	79	43	83.3	3.8	8.4	10.2	36.1	158.8	5.1	46.2	194.8	163.8	205.0	199.9	210.1	222.3
445685	37	53	79	8	91.7	48.0	82.0	60.5	108.2	201.7	1.5	168.7	309.9	203.2	370.3	311.4	371.9	501.9
445698	38	25	79	35	111.0	8.6	19.8	32.0	100.6	57.9	0.5	132.6	158.5	58.4	190.5	159.0	191.0	219.5
445700	38	1	78	27	116.3	11.7	24.9	9.4	80.5	36.8	2.0	89.9	117.3	38.9	126.7	119.4	128.8	165.4
445756	38	6	79	53	65.5	0.0	0.0	27.2	0.0	210.8	0.0	27.2	210.8	210.8	238.0	210.8	238.0	238.0
445828	37	23	80	32	77.0	9.4	12.4	18.3	63.5	22.1	3.6	81.8	85.6	25.7	103.9	89.2	107.4	129.3

Table 1. Official NOAA rain gage network data, October and November 1–6, 1985—Continued

Station	Latitude deg	Latitude arc min	Longitude deg	Longitude arc min	October 1985	November 1985 1	2	3	4	5	5	3–4	4–5	5–6	3–5	4–6	3–6	1–6
445851	39	4	77	53	149.6	8.4	8.4	5.8	52.1	21.6	11.4	57.9	73.7	33.0	79.5	85.1	90.9	107.7
446012	37	30	80	6	63.2	25.9	22.9	50.8	21.6	142.2	0.0	72.4	163.8	142.2	214.6	163.8	214.6	263.4
446046	37	19	80	31	47.0	5.1	0.0	0.0	15.2	50.8	0.0	15.2	66.0	50.8	66.0	66.0	66.0	71.1
446139	36	54	76	12	99.6	2.5	7.1	1.5	27.7	0.0	0.0	29.2	27.7	0.0	29.2	27.7	29.2	38.9
446173	37	8	82	38	89.7	0.5	2.0	0.5	11.7	33.0	15.2	12.2	44.7	48.3	45.2	59.9	60.5	63.0
446475	37	35	75	49	134.1	25.4	2.0	2.5	16.5	0.3	0.0	19.0	16.8	0.3	19.3	16.8	19.3	46.7
446491	37	52	78	15	103.6	7.6	6.6	21.8	53.8	21.6	3.0	75.7	75.4	24.6	97.3	78.5	100.3	114.6
446593	37	40	79	17	88.9	6.6	23.6	50.3	59.2	95.8	0.0	109.5	154.9	95.8	205.2	154.9	205.2	235.5
446626	36	45	83	3	79.2	1.5	6.1	8.1	13.2	7.9	0.0	21.3	21.1	7.9	29.2	21.1	29.2	36.8
446692	36	47	80	2	189.0	16.8	40.9	14.7	14.0	69.1	0.0	28.7	83.1	69.1	97.8	83.1	97.8	155.4
446712	38	13	78	7	121.9	11.4	30.5	3.8	67.8	74.4	2.8	71.6	142.2	77.2	146.1	145.0	148.8	190.8
446723	37	4	80	21	121.9	11.4	0.0	29.0	49.8	35.1	29.5	78.7	84.8	64.5	113.8	114.3	143.3	154.7
446906	37	33	77	56	101.1	10.4	25.4	5.1	125.7	29.2	1.8	130.8	154.9	31.0	160.0	156.7	161.8	197.6
446955	37	3	80	45	66.5	2.3	11.4	13.2	43.9	0.8	0.0	57.2	44.7	0.8	57.9	44.7	57.9	71.6
446999	37	8	80	33	59.9	2.8	3.6	4.1	8.1	66.5	0.5	12.2	74.7	67.1	78.7	75.2	79.2	85.6
447164	38	24	77	44	159.5	45.2	36.6	8.9	6.4	0.0	0.0	15.2	6.4	0.0	15.2	6.4	15.2	97.0
447201	37	30	77	20	129.3	24.4	6.1	9.7	42.9	0.8	0.0	52.6	43.7	0.8	53.3	43.7	53.3	83.8
447285	37	19	79	58	95.8	35.3	23.6	26.9	167.9	0.3	0.0	194.8	168.1	0.3	195.1	168.1	195.1	254.0
447312	37	48	78	45	124.0	19.3	56.1	27.4	85.3	54.4	1.0	112.8	139.7	55.4	167.1	140.7	168.1	243.6
447338	37	0	79	54	101.3	21.1	43.7	18.3	22.9	50.8	0.0	41.1	73.7	50.8	91.9	73.7	91.9	156.7
447925	36	42	78	53	100.1	4.3	19.8	10.4	41.1	21.8	1.3	51.6	63.0	23.1	73.4	64.3	74.7	98.8
448022	37	16	80	43	81.0	11.2	13.5	5.1	33.5	23.4	1.0	38.6	56.9	24.4	62.0	57.9	63.0	87.6
448062	38	9	79	2	87.9	42.4	33.0	17.8	58.9	83.1	1.5	76.7	142.0	84.6	159.8	143.5	161.3	236.7
448084	38	59	77	28	119.1	3.3	1.8	0.8	22.4	13.7	9.1	23.1	36.1	22.9	36.8	45.2	46.0	51.1
448129	36	55	77	21	86.4	18.8	25.1	0.0	48.5	13.5	0.0	48.5	62.0	13.5	62.0	62.0	62.0	105.9
448170	36	38	80	16	148.8	12.7	26.7	14.0	85.6	2.3	0.0	99.6	87.9	2.3	101.9	87.9	101.9	141.2
448192	36	44	76	36	114.6	9.4	6.6	0.0	31.5	0.0	0.0	31.5	31.5	0.0	31.5	31.5	31.5	47.5
448323	37	50	75	60	217.2	16.0	0.0	10.2	9.4	0.0	0.0	19.6	9.4	0.0	19.6	9.4	19.6	35.6
448396	38	54	77	45	129.3	0.0	5.8	3.8	42.2	19.6	8.6	46.0	61.7	28.2	65.5	70.4	74.2	80.0
448448	38	39	78	43	129.3	5.1	12.2	11.9	43.2	41.7	0.3	55.1	84.8	41.9	96.8	85.1	97.0	114.3
448547	36	40	81	24	128.3	12.7	30.0	9.7	27.2	30.2	0.3	36.8	57.4	30.5	67.1	57.7	67.3	110.0
448600	37	38	78	56	103.9	10.7	11.7	52.3	58.9	6.4	0.0	111.3	65.3	6.4	117.6	65.3	117.6	140.0
448737	38	54	77	13	103.9	2.3	2.0	3.8	36.6	7.4	2.0	40.4	43.9	9.4	47.8	46.0	49.8	54.1
448800	36	59	77	0	64.3	8.4	8.9	1.5	33.0	2.5	0.0	34.5	35.6	2.5	37.1	35.6	37.1	54.4
448829	37	45	77	3	162.8	23.4	7.6	6.4	17.5	5.1	1.8	23.9	22.6	6.9	29.0	24.4	30.7	61.7
448837	36	36	76	26	110.0	22.9	24.9	12.7	27.4	18.8	0.0	40.1	46.2	18.8	58.9	46.2	58.9	106.7
448888	38	41	77	46	153.7	6.6	7.1	5.1	51.6	17.8	8.6	56.6	69.3	26.4	74.4	78.0	83.1	96.8
448894	37	59	76	46	122.7	20.6	8.6	9.7	18.0	1.3	0.5	27.7	19.3	1.8	29.0	19.8	29.5	58.7

Table 1. Official NOAA rain gage network data, October and November 1–6, 1985—Continued

Station	Latitude deg	Latitude arc min	Longitude deg	Longitude arc min	October 1985	November 1985 1	2	3	4	5	5	3–4	4–5	5–6	3–5	4–6	3–6	1–6
448903	38	57	77	27	103.1	4.1	1.0	7.9	34.5	10.4	0.0	42.4	45.0	10.4	52.8	45.0	52.8	57.9
448906	38	51	77	2	97.8	1.5	0.8	0.8	24.6	0.3	0.3	25.4	24.9	0.5	25.7	25.1	25.9	28.2
448975	38	16	79	19	138.4	17.8	35.6	20.3	40.6	0.0	0.0	61.0	40.6	0.0	61.0	40.6	61.0	114.3
449025	37	31	76	50	106.9	20.6	9.1	4.1	10.9	1.5	0.3	15.0	12.4	1.8	16.5	12.7	16.8	46.5
449151	37	18	76	42	115.6	38.1	18.0	7.4	13.5	0.3	0.0	20.8	13.7	0.3	21.1	13.7	21.1	77.2
449169	36	51	80	29	94.2	16.3	18.8	10.2	7.4	108.7	0.0	17.5	116.1	108.7	126.2	116.1	126.2	161.3
449181	39	11	78	9	132.1	5.1	13.5	8.1	39.1	23.4	6.1	47.2	62.5	29.5	70.6	68.6	76.7	95.3
449186	39	11	78	7	139.4	5.3	15.5	9.9	38.6	29.2	7.6	48.5	67.8	36.8	77.7	75.4	85.3	106.2
449213	37	20	77	39	127.0	17.8	22.6	0.8	69.9	15.7	0.5	70.6	85.6	16.3	86.4	86.1	86.9	127.3
449215	36	58	82	34	53.6	3.6	10.9	4.6	18.8	4.6	2.0	23.4	23.4	6.6	27.9	25.4	30.0	44.5
449263	38	54	78	28	124.5	7.4	20.1	6.1	33.0	49.5	6.6	39.1	82.6	56.1	88.6	89.2	95.3	122.7
449272	36	43	80	17	170.4	50.0	50.8	39.4	114.3	14.5	0.0	153.7	128.8	14.5	168.1	128.8	168.1	269.0
449301	36	56	81	5	77.2	12.2	27.2	11.9	40.1	18.8	0.0	52.1	58.9	18.8	70.9	58.9	70.9	110.2
West Virginia																		
460094	39	29	79	38	115.8	0.0	0.5	6.1	23.4	80.0	10.2	29.5	103.4	90.2	109.5	113.5	119.6	120.1
460102	37	44	80	38	46.7	0.0	4.3	3.6	14.7	8.6	0.0	18.3	23.4	8.6	26.9	23.4	26.9	31.2
460355	37	26	81	0	51.1	1.3	30.5	68.6	61.7	12.2	3.8	130.3	73.9	16.0	142.5	77.7	146.3	178.1
460527	39	16	79	22	137.7	1.5	4.8	10.9	14.0	115.6	6.4	24.9	129.5	121.9	140.5	135.9	146.8	153.2
460580	37	47	81	11	39.6	0.0	1.5	0.5	30.0	35.8	5.6	30.5	65.8	41.4	66.3	71.4	71.9	73.4
460582	37	47	81	7	39.9	0.0	1.5	4.6	63.5	7.4	2.5	68.1	70.9	9.9	75.4	73.4	78.0	79.5
460633	39	2	79	57	0.0	0.0	0.0	5.1	3.8	14.0	94.0	8.9	17.8	108.0	22.9	111.8	116.8	116.8
460921	37	18	81	13	40.4	4.6	0.5	2.5	52.1	2.5	1.0	54.6	54.6	3.6	57.2	55.6	58.2	63.2
460939	37	39	80	53	49.0	0.8	2.5	0.8	32.5	40.6	1.5	33.3	73.2	42.2	73.9	74.7	75.4	78.7
461075	38	14	82	12	111.5	0.0	4.8	0.0	23.9	38.1	8.6	23.9	62.0	46.7	62.0	70.6	70.6	75.4
461083	39	40	79	37	85.9	0.0	1.8	12.7	29.0	51.1	7.6	41.7	80.0	58.7	92.7	87.6	100.3	102.1
461215	38	11	80	8	94.2	0.8	5.8	6.9	11.4	93.5	0.8	18.3	104.9	94.2	111.8	105.7	112.5	119.1
461220	39	0	80	16	124.7	0.8	4.3	15.7	82.8	52.1	3.0	98.6	134.9	55.1	150.6	137.9	153.7	158.8
461282	38	51	80	38	152.7	0.0	2.5	9.4	30.5	114.0	6.4	39.9	144.5	120.4	153.9	150.9	160.3	162.8
461324	39	30	78	18	120.7	5.6	10.4	13.2	40.9	48.0	4.1	54.1	88.9	52.1	102.1	93.0	106.2	122.2
461330	39	14	81	11	134.9	0.0	3.0	5.6	25.4	79.2	7.6	31.0	104.6	86.9	110.2	112.3	117.9	120.9
461363	38	22	80	37	116.1	0.0	0.0	10.2	24.4	115.1	24.4	34.5	139.4	139.4	149.6	163.8	174.0	174.0
461393	39	3	79	26	175.3	6.6	8.4	6.6	71.1	134.6	0.8	77.7	205.7	135.4	212.3	206.5	213.1	228.1
461526	38	37	80	35	96.5	8.1	2.5	44.5	81.3	5.6	2.5	125.7	86.9	8.1	131.3	89.4	133.9	144.5
461570	38	22	81	36	92.7	0.0	2.3	13.5	52.6	33.0	0.5	66.0	85.6	33.5	99.1	86.1	99.6	101.9
461677	39	16	80	21	116.6	0.0	4.1	4.8	43.4	127.0	6.4	48.3	170.4	133.4	175.3	176.8	181.6	185.7
461696	38	27	81	5	114.3	0.0	5.6	1.5	35.1	76.5	14.7	36.6	111.5	91.2	113.0	126.2	127.8	133.4
461900	39	41	79	47	108.2	0.0	2.0	15.2	39.6	65.0	23.6	54.9	104.6	88.6	119.9	128.3	143.5	145.5
461959	38	29	81	16	105.7	0.0	6.4	12.7	53.3	4.8	2.5	66.0	58.2	7.4	70.9	60.7	73.4	79.8

Table 1. Official NOAA rain gage network data, October and November 1–6, 1985—Continued

Station	Latitude deg	Latitude arc min	Longitude deg	Longitude arc min	October 1985	November 1985 1	2	3	4	5	5	3–4	4–5	5–6	3–5	4–6	3–6	1–6
462054	38	57	81	17	126.2	0.0	3.8	6.6	26.7	67.1	3.8	33.3	93.7	70.9	100.3	97.5	104.1	108.0
462151	38	48	79	53	166.4	0.0	0.0	9.4	12.7	145.3	8.9	22.1	158.0	154.2	167.4	166.9	176.3	176.3
462358	38	30	80	49	108.0	0.3	3.3	3.3	32.5	67.6	14.5	35.8	100.1	82.0	103.4	114.6	117.9	121.4
462462	37	52	81	28	70.6	0.0	1.5	0.0	41.7	27.2	15.7	41.7	68.8	42.9	68.8	84.6	84.6	86.1
462522	38	1	82	25	136.1	0.0	19.8	0.5	25.4	30.5	12.7	25.9	55.9	43.2	56.4	68.6	69.1	88.9
462718	38	53	79	51	152.4	0.0	11.7	4.6	127.5	19.3	1.8	132.1	146.8	21.1	151.4	148.6	153.2	164.8
462920	39	28	80	8	86.6	3.6	5.8	29.0	93.0	11.2	1.5	121.9	104.1	12.7	133.1	105.7	134.6	144.0
463072	37	35	81	6	56.4	0.8	6.1	1.0	37.6	44.5	10.2	38.6	82.0	54.6	83.1	92.2	93.2	100.1
463215	38	40	79	19	105.4	13.2	11.9	23.9	191.8	0.0	1.0	215.6	191.8	1.0	215.6	192.8	216.7	241.8
463353	37	22	81	33	41.7	0.0	3.6	0.0	26.4	27.9	5.1	26.4	54.4	33.0	54.4	59.4	59.4	63.0
463361	38	40	80	46	112.5	0.0	5.1	7.4	109.2	37.8	3.8	116.6	147.1	41.7	154.4	150.9	158.2	163.3
463464	38	48	79	43	180.1	0.3	1.8	5.6	12.2	110.7	16.0	17.8	122.9	126.7	128.5	138.9	144.5	146.6
463544	38	56	80	49	141.2	0.0	2.5	10.4	43.2	88.1	1.5	53.6	131.3	89.7	141.7	132.8	143.3	145.8
463798	38	39	80	23	118.1	0.0	2.0	0.0	27.9	136.1	17.0	27.9	164.1	153.2	164.1	181.1	181.1	183.1
463846	38	17	82	6	111.5	0.0	5.1	0.5	25.9	37.1	8.9	26.4	63.0	46.0	63.5	71.9	72.4	77.5
464128	38	6	81	0	79.5	0.0	4.8	1.3	23.6	73.9	22.9	24.9	97.5	96.8	98.8	120.4	121.7	126.5
464200	38	41	82	11	157.2	0.5	6.6	14.0	10.7	33.5	2.8	24.6	44.2	36.3	58.2	47.0	61.0	68.1
464372	39	39	80	25	84.3	0.0	1.8	5.8	41.4	90.7	5.6	47.2	132.1	96.3	137.9	137.7	143.5	145.3
464393	38	22	82	33	131.3	23.9	2.3	34.3	14.7	14.2	0.5	49.0	29.0	14.7	63.2	29.5	63.8	89.9
464397	38	25	82	30	133.9	0.3	26.9	27.9	14.7	17.8	2.0	42.7	32.5	19.8	60.5	34.5	62.5	89.7
464408	37	28	81	49	48.0	0.0	25.9	0.8	51.1	48.3	21.6	51.8	99.3	69.9	100.1	120.9	121.7	147.6
464763	39	23	77	53	118.9	2.0	4.3	6.4	37.8	16.5	3.3	44.2	54.4	19.8	60.7	57.7	64.0	70.4
464816	37	50	82	24	100.3	0.0	0.0	0.0	0.0	0.0	0.0	0.0	0.0	0.0	0.0	0.0	0.0	0.0
464956	37	44	81	35	71.9	0.0	4.3	17.8	50.5	37.3	9.1	68.3	87.9	46.5	105.7	97.0	114.8	119.1
465002	39	43	79	51	55.4	0.0	0.8	5.1	29.5	66.0	1.8	34.5	95.5	67.8	100.6	97.3	102.4	103.1
465224	37	46	80	28	55.4	0.0	13.2	0.0	76.2	0.0	0.0	76.2	76.2	0.0	76.2	76.2	76.2	89.4
465353	37	51	82	0	94.2	0.0	8.4	0.0	31.5	34.5	13.0	31.5	66.0	47.5	66.0	79.0	79.0	87.4
465365	38	12	81	22	101.6	0.0	1.3	1.3	22.9	50.8	16.5	24.1	73.7	67.3	74.9	90.2	91.4	92.7
465563	38	3	81	49	78.5	0.0	3.8	0.8	23.9	51.3	16.0	24.6	75.2	67.3	75.9	91.2	91.9	95.8
465600	37	44	81	53	61.0	0.0	8.1	1.0	23.6	37.3	13.2	24.6	61.0	50.5	62.0	74.2	75.2	83.3
465626	39	32	80	30	89.4	4.3	7.9	38.1	109.0	4.3	1.3	147.1	113.3	5.6	151.4	114.6	152.7	164.8
465707	39	24	77	59	121.4	11.4	2.0	30.7	30.0	5.8	0.0	60.7	35.8	5.8	66.5	35.8	66.5	80.0
465739	38	52	78	52	155.7	8.4	9.9	19.6	101.6	72.9	2.5	121.2	174.5	75.4	194.1	177.0	196.6	214.9
465871	37	59	80	45	61.5	0.0	4.8	1.3	22.1	88.9	21.1	23.4	111.0	110.0	112.3	132.1	133.4	138.2
465963	39	29	80	52	103.9	0.0	2.5	5.3	40.6	86.4	5.8	46.0	127.0	92.2	132.3	132.8	138.2	140.7
466163	39	2	78	58	125.7	3.8	4.1	4.8	27.9	71.9	6.6	32.8	99.8	78.5	104.6	106.4	111.3	119.1
466202	39	39	79	55	42.2	0.5	3.3	24.4	88.6	11.4	2.3	113.0	100.1	13.7	124.5	102.4	126.7	130.6
466212	39	37	79	58	52.6	0.0	0.8	2.8	33.0	90.4	8.4	35.8	123.4	98.8	126.2	131.8	134.6	135.4

Table 1. Official NOAA rain gage network data, October and November 1–6, 1985—Continued

Station	Latitude deg	Latitude arc min	Longitude deg	Longitude arc min	October 1985	November 1985 1	2	3	4	5	5	3–4	4–5	5–6	3–5	4–6	3–6	1–6
466248	39	54	80	45	67.3	0.0	3.8	10.7	38.1	95.8	2.8	48.8	133.9	98.6	144.5	136.7	147.3	151.1
466442	40	30	80	36	47.0	3.3	5.6	29.2	67.3	18.3	1.3	96.5	85.6	19.6	114.8	86.9	116.1	125.0
466591	37	58	81	9	71.1	0.0	3.0	0.3	23.4	53.3	14.5	23.6	76.7	67.8	77.0	91.2	91.4	94.5
466849	39	21	81	26	124.2	0.3	10.4	20.6	43.7	12.2	1.8	64.3	55.9	14.0	76.5	57.7	78.2	88.9
466859	39	16	81	34	99.3	0.0	4.6	4.3	24.1	45.0	4.6	28.4	69.1	49.5	73.4	73.7	78.0	82.5
466867	39	6	79	40	153.9	0.0	2.8	7.4	10.4	132.1	7.6	17.8	142.5	139.7	149.9	150.1	157.5	160.3
466900	37	21	81	52	42.2	21.6	0.0	27.9	28.4	9.9	0.0	56.4	38.4	9.9	66.3	38.4	66.3	87.9
466960	38	53	79	12	148.1	7.6	17.8	7.6	41.9	146.1	3.8	49.5	188.0	149.9	195.6	191.8	199.4	224.8
466982	39	9	80	2	126.7	0.0	9.7	2.8	18.8	107.4	14.5	21.6	126.2	121.9	129.0	140.7	143.5	153.2
466991	38	40	80	13	136.9	0.0	4.6	1.8	8.6	173.2	20.8	10.4	181.9	194.1	183.6	202.7	204.5	209.0
467018	40	9	80	42	70.6	0.0	1.8	14.0	27.9	80.0	3.6	41.9	108.0	83.6	121.9	111.5	125.5	127.3
467029	37	35	81	32	54.6	0.3	1.0	1.0	34.3	28.4	12.2	35.3	62.7	40.6	63.8	74.9	75.9	77.2
467207	37	22	81	5	43.4	0.5	7.6	1.3	41.9	54.6	3.3	43.2	96.5	57.9	97.8	99.8	101.1	109.2
467287	38	55	81	55	116.3	0.0	5.1	8.6	16.3	36.6	12.7	24.9	52.8	49.3	61.5	65.5	74.2	79.2
467455	38	0	80	22	121.4	0.0	5.1	8.6	16.3	80.0	1.0	24.9	96.3	81.0	104.9	97.3	105.9	111.0
467552	38	53	81	41	169.7	0.0	7.1	3.0	21.6	53.3	8.1	24.6	74.9	61.5	78.0	83.1	86.1	93.2
467730	39	20	78	46	126.2	0.0	0.0	0.0	0.0	0.0	0.0	0.0	0.0	0.0	0.0	0.0	0.0	0.0
467785	39	20	79	41	163.3	0.0	1.0	7.9	30.7	116.1	12.2	38.6	146.8	128.3	154.7	159.0	166.9	167.9
468051	38	20	79	54	85.1	4.1	11.2	16.0	157.5	14.7	0.5	173.5	172.2	15.2	188.2	172.7	188.7	204.0
468172	38	43	79	38	110.0	2.0	5.1	4.1	20.3	152.4	8.4	24.4	172.7	160.8	176.8	181.1	185.2	192.3
468308	38	24	79	60	115.3	2.5	6.4	11.7	38.1	127.0	5.8	49.8	165.1	132.8	176.8	170.9	182.6	191.5
468384	38	48	81	21	145.8	0.0	5.1	2.8	35.3	66.0	5.6	38.1	101.3	71.6	104.1	106.9	109.7	114.8
468433	38	41	79	31	96.0	8.6	20.6	9.1	41.7	187.2	1.3	50.8	228.9	188.5	238.0	230.1	239.3	268.5
468614	38	14	80	53	115.1	0.0	3.6	1.0	29.7	86.1	23.4	30.7	115.8	109.5	116.8	139.2	140.2	143.8
468662	38	39	80	41	118.4	0.0	1.8	6.9	35.6	111.3	11.2	42.4	146.8	122.4	153.7	158.0	164.8	166.6
468777	39	27	79	33	131.1	0.0	0.8	9.9	22.1	74.9	10.2	32.0	97.0	85.1	106.9	107.2	117.1	117.9
468807	39	9	79	30	157.5	12.7	17.8	7.1	13.7	137.2	11.4	20.8	150.9	148.6	158.0	162.3	169.4	199.9
468844	37	57	81	5	83.1	0.0	1.8	0.5	31.8	51.3	4.1	32.3	83.1	55.4	83.6	87.1	87.6	89.4
469011	37	33	80	32	41.1	0.3	7.4	1.8	10.4	77.5	1.0	12.2	87.9	78.5	89.7	88.9	90.7	98.3
469049	38	47	79	17	113.0	7.1	10.7	27.7	53.1	188.0	0.0	80.8	241.0	188.0	268.7	241.0	268.7	286.5
469086	38	33	80	2	94.2	0.0	6.4	3.8	20.6	78.0	3.8	24.4	98.6	81.8	102.4	102.4	106.2	112.5
469281	39	6	78	35	125.5	7.1	12.2	6.6	33.3	66.5	8.4	39.9	99.8	74.9	106.4	108.2	114.8	134.1
469323	38	14	82	27	169.4	0.0	40.6	6.6	33.3	34.3	12.7	39.9	67.6	47.0	74.2	80.3	86.9	127.5
469333	38	29	80	25	105.7	0.0	1.3	0.0	9.7	120.4	22.9	9.7	130.0	143.3	130.0	152.9	152.9	154.2
469368	40	17	80	37	66.8	0.0	2.8	3.3	50.8	71.1	2.5	54.1	121.9	73.7	125.2	124.5	127.8	130.6
469436	39	3	80	28	126.5	0.0	6.1	6.1	47.8	57.2	3.8	53.8	104.9	61.0	111.0	108.7	114.8	120.9
469522	37	48	80	18	52.3	6.9	13.2	0.5	13.0	90.2	2.0	13.5	103.1	92.2	103.6	105.2	105.7	125.7
469605	37	40	82	17	98.0	0.0	10.2	0.0	15.7	33.3	12.2	15.7	49.0	45.5	49.0	61.2	61.2	71.4
469610	37	42	82	17	95.3	0.0	0.0	0.0	0.0	0.0	0.0	0.0	0.0	0.0	0.0	0.0	0.0	0.0

Table 2. Nonofficial rainfall data from bucket surveys, November 1–6, 1985

[Collected by T. Purkey, Soil Conservation Service, during March 1986, tabulated and checked by S. Kite, West Virginia University. Values in millimeters. Dashes indicate missing values. Asterisks mark estimated values]

Site	UTM coordinates	Date in November						Total	Notes
		1	2	3	4	5	6		
Greenbriar River Basin, Pocahontas County, W.Va.									
Durbin	4267000N 602000E	—	—	—	—	—	—	203.2	
Arborvale	4255000N 603000E	4.6	10.2	17.8	154.9	16.5	—	204.0	Thunder 10:35 a.m., Nov. 4.
Cass	4250000N 594500E	5.3	15.7	22.1	104.6	50.3	2.5	198.1	Usually read 5 p.m.
Clover Lick	4243000N 590000E	—	—	—	>127.0	—	—	>127.0	Ran over 127-mm gage in 7 h.
Dilleys Mill	4234500N 591500E	3.8	14.0	14.0	17.8	109.2	.0	158.8	Usually read at 6:30 a.m.; 58 mm between 6:30 a.m. and 4:30 p.m., Nov. 4.
Tygart Valley River Basin, Randolph County, W.Va.									
Montrose	4325000N 603000E	6.3	6.3	25.4	137.9	6.3	—	184.2	Usually read 7 p.m.; read at 10 p.m., Nov. 3, 11 p.m., Nov. 4.
Elkins	4310500N 592000E	—	10.2	2.5	12.7	139.7*	21.6	186.7*	127-mm gage overflowed Nov. 5.
Cheat River Basin, Randolph County, W.Va.									
Kerens	4319000N 608500E	38.1	50.8	63.5	88.9	—	—	241.3	Usually read 7:30 a.m.
South Branch Potomac River Basin, Pendleton County, W.Va.									
Fort Seybert	4284000N 659000E	15.2	14.0	36.8	196.8	2.5	—	265.4	Usually read 7–8 p.m.; rain ended about 12 a.m., Nov. 4.
Franklin	4284500N 641000E	----------	104.1	----------	175.3	45.7	.0	325.1	Variable reading time: 116.8 mm between 6 p.m., Nov. 3, and 2 p.m., Nov. 4; 58 mm more by 7 p.m., Nov. 4; 46 mm more by 3:00 a.m., Nov. 5; end of rain.
Franklin	4281000N 639000E	—	—	—	—	114.5	—	>267.0	Variable reading times; 152-mm gage overflowed 10 a.m., Nov. 4; 114 more by 7 a.m., Nov. 5; end of rain 10:15 p.m., Nov. 4.
Dahmer	4270000N 638000E	20.3	25.4	38.1	185.1	33.0	—	302.3	Variable reading times; 102 mm 9:30 p.m., Nov. 3, to 3:45 p.m., Nov. 4; 84 mm more by 10:15 p.m., Nov. 4.
Riverton	4290000N 638000E	69.8	114.3	57.2	152.4	—	—	393.7	Usually read in morning.
Circleville	4281000N 631500E	—	29.2	19.0	226.1	55.9	—	>330.2	Usually read at sunset; read at sunset Nov. 4 and 8 a.m., Nov. 5.
North Fork Shenandoah River Basin, Rockingham County, Va.									
Fulks Run	4283500N 678500E	—	127.0	133.4	127.0	—	—	387.4	Unknown reading time.
Fulks Run	4281000N 682000E	15.2	22.9	20.3	91.4	106.7	12.7	265.5	Usually read at 7:00 a.m.
Linville	4265000N 689000E	----------	94.0	----------		85.1	—	179.1	Usually read at 7:00 a.m.
James (Jackson) River Basin, Bath County, Va.									
Mill Gap	4243000N 611500E	3.8	8.4	10.2	36.1	158.8	5.1	222.2	Usually read at 7:00 a.m.
Monterey	4252000N 611500E	8.6	19.8	32.0	100.6	57.9	.5	219.4	Usually read at 5:00 p.m.

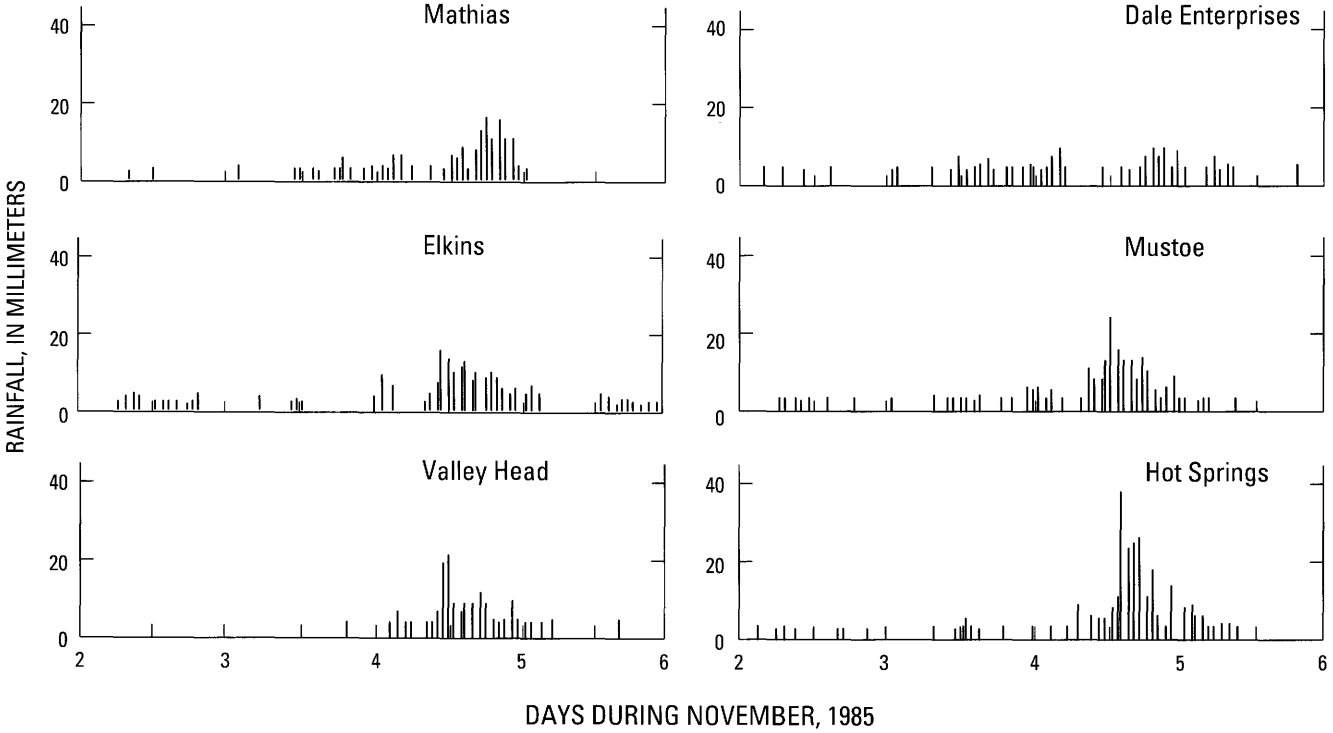

Figure 9. Representative hourly rainfall data for November 2–6 from gages in West Virginia and Virginia (data from NOAA, 1986).

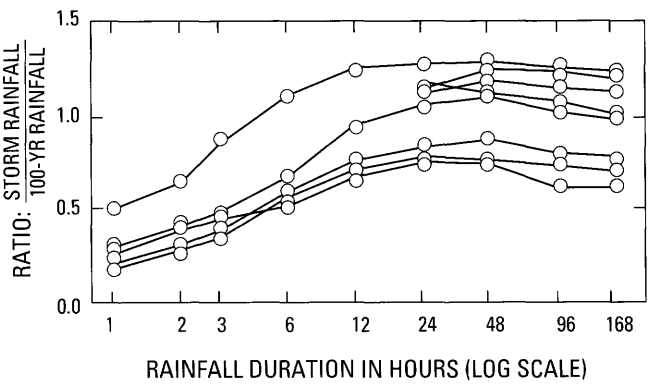

Figure 10. Ratio of storm rainfall to rainfall of the 100-yr event for durations of 1–168 h (7 days). The 100-yr rainfall is estimated from Hershfield (1961) and Miller (1964). Data are from hourly gages in figure 9 plus Franklin and Spruce Knob (data from NOAA, 1986).

responsible for the storm was complex. Especially notable is the role of a late-season tropical storm that brought moisture and latent heat up the Mississippi Valley. Most tropical storms that affect the United States hug the eastern seaboard, and most occur in June-September (Neumann and others, 1981). Jacobson and others (1989) argued that tropical storms produce extreme rainfall and flood events in the Piedmont and Blue Ridge of the central Appalachians more so than in the Valley and Ridge province and Appalachian Plateaus, but stress that extreme rainfall can also arise from frontal and convective storms. While it is unknown whether intensity and duration of rainfall similar to the November 1985 storm could be generated in the same place by different meteorological conditions, it is clear that the specific characteristics of this storm were strongly influenced by an anomalous tropical storm track.

Distinct outliers of some of the highest magnitude events in the rainfall records suggest that different meteorological mechanisms may operate at low frequencies. Identification of the specific meteorological conditions that produce these events would increase our ability to predict extreme rainfall and its geomorphic effects. Synoptic-scale meteorological conditions conducive to extreme floods have been identified elsewhere in the United States (Maddox and others, 1979; Hirschboeck, 1987) but have not been studied in detail in the central Appalachians. It is unclear whether a particular set of conditions is sufficient or necessary to produce extreme rainfall in this area.

In addition to point total rainfall values, the geomorphic effectiveness of a storm is dependent on intensity and duration of rainfall, areal extent of rainfall, position with respect to drainage divides, antecedent moisture conditions, and geology and physiography of the area affected (Jacobson and others, 1989). Different combinations of intensity and duration may produce either similar or different geomorphic effects, depending on where the rain falls. In comparison with other flood- and landslide-triggering storms, the 1985 storm produced rainfall at lower intensities

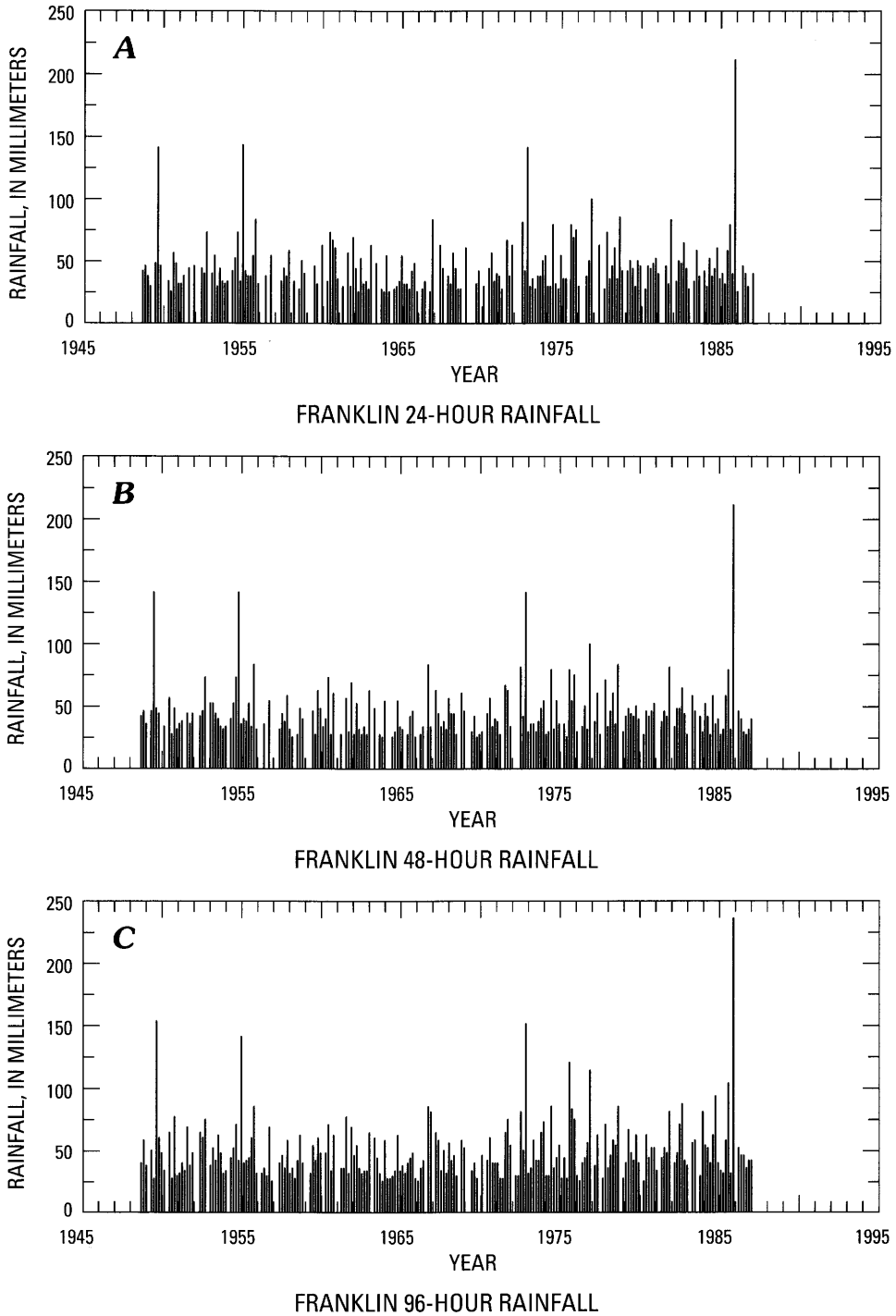

Figure 11. Franklin and Spruce Knob gage records showing (*A*, *D*) 24-h, (*B*, *E*) 48-h, and (*C*, *F*) 96-h duration rainfall (data from NOAA, 1986).

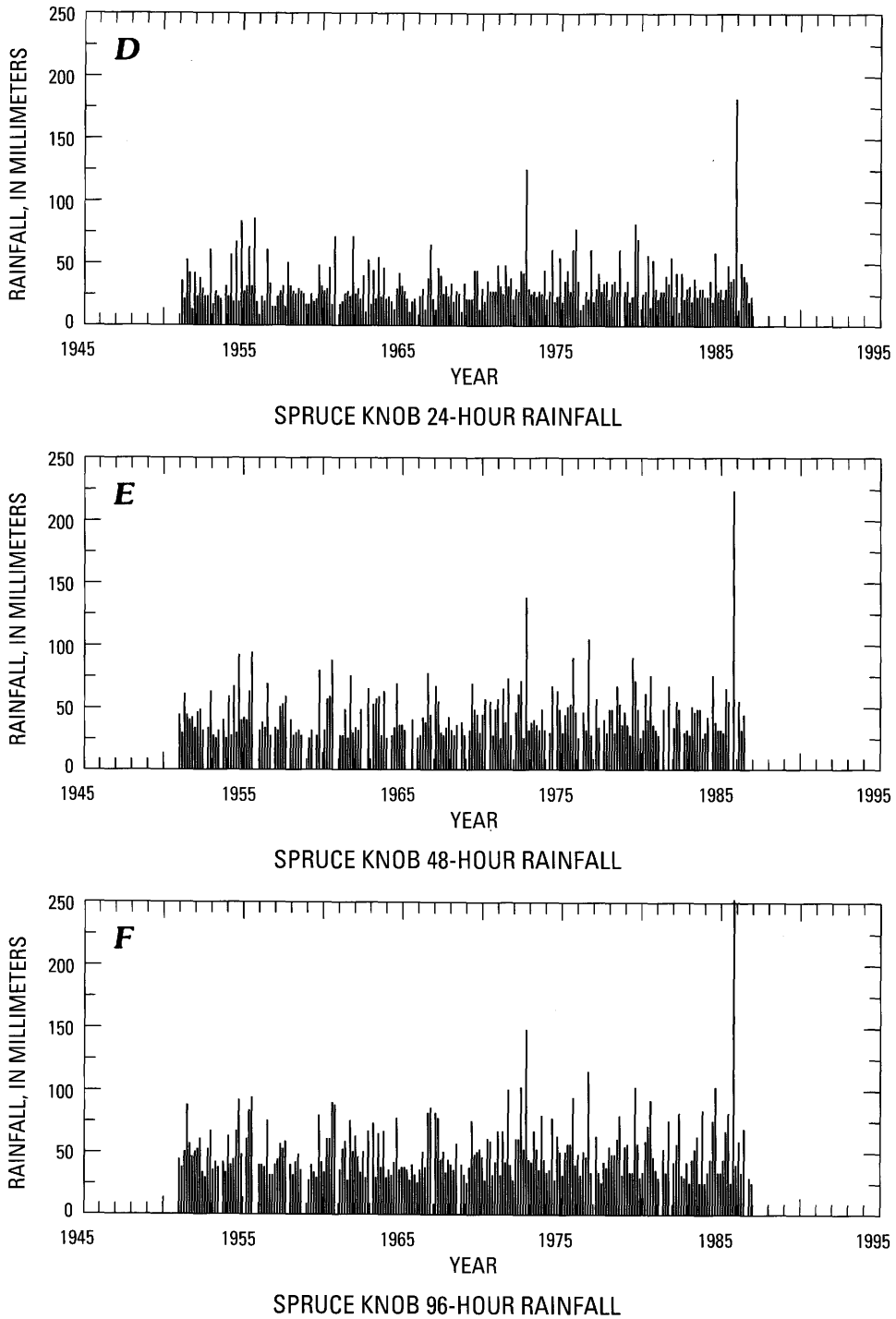

Figure 11. Continued.

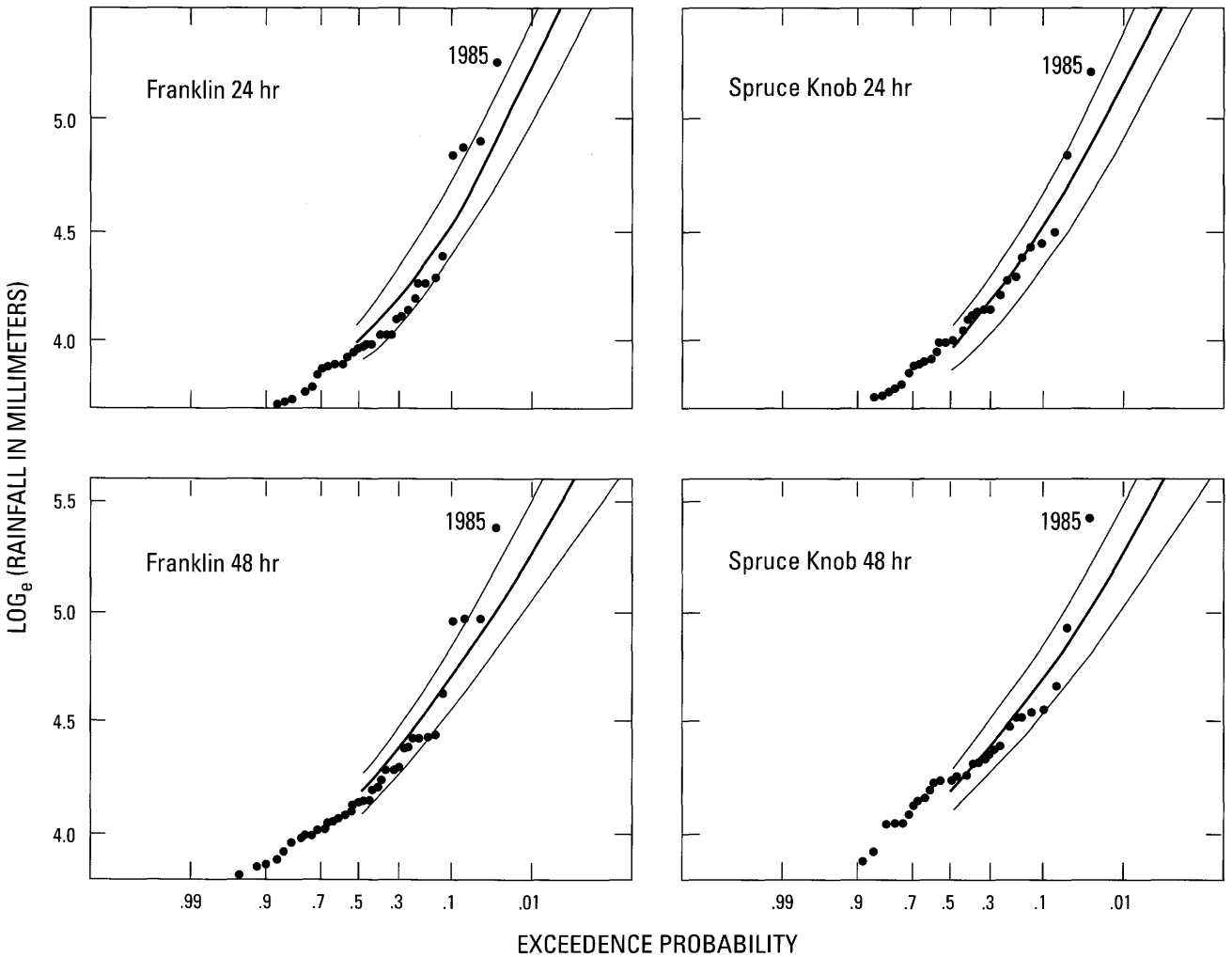

Figure 12. Plots of $\log_e$ (rainfall) against exceedence probability for annual series of 24- and 48-h rainfall at Franklin and Spruce Knob rain gages. Heavy curve is the log Pearson type III distribution fit to each record using a regional skew coefficient. Light curves mark the 95 percent confidence limit.

Table 3. Estimated recurrence intervals of peak rainfall

Gage	Plotting position (Gringorten, 1963)	Log Pearson type III population skew	Log Pearson type III regional skew
Franklin			
1 day	70	71	111
2 day	70	67	166
Spruce Knob			
1 day	68	122	133
2 day	68	263	200
Upper Tract[1]			
2 day	—	83	286

[1]Estimated from Franklin record.

and somewhat longer durations (see discussions by Jacobson and others, chapter C, this volume, and Miller and Parkinson, chapter E, this volume). Other Appalachian storms have had similar rainfall totals, but the 1985 storm covered a larger area (Miller, 1990), had moderate soil moisture levels at the time of the rainfall, and had minimal interception and evapotranspiration. Thus the sequence of meteorological events leading to the November 1985 storm and the suite of geomorphic effects it produced may be sufficiently complex that the event cannot be readily compared with other historical events.

REFERENCES CITED

Case, R.A., 1986, Atlantic hurricane season of 1985: Monthly Weather Review, v. 114, p. 1390–1405.

Embree, W.N., Friel, E.A., and Taylor, F.M, 1987, Water resource data, West Virginia water year 1985: U. S. Geological Survey Water-Data Report WV–85–1, 224 p.

Gringorten, I.I., 1963, A plotting rule for extreme probability paper: Journal of Geophysical Research, v. 69, no. 3, p. 813–814.

Gryta, J.J., and Bartholomew, M.J., 1989, Factors influencing the distribution of debris avalanches associated with the 1969 Hurricane Camille in Nelson County, Virginia, *in* Schultz, A.P., and Jibson, R.W., eds., Landslide processes of the eastern United States and Puerto Rico: Geological Society of America Special Paper 236, p. 15–28.

Hershfield, D.M., 1961, Rainfall frequency atlas of the United States: U.S. Weather Bureau Technical Paper 40, 114 p.

Hirschboeck, K.K., 1987, Catastrophic flooding and atmospheric circulation anomalies, *in* Mayer, L., and Nash, G., eds., Catastrophic flooding: London, Allen and Unwin, p. 25–56.

Holton, J.R., 1979, An introduction to dynamic meteorology: San Diego, Calif., Academic Press, 341 p.

Jacobson, R.B., Miller, A.J., and Smith, J.A., 1989, The role of catastrophic geomorphic events in central Appalachian landscape evolution, *in* Gardner, T.W., and Sevon, W.D., eds. Appalachian geomorphology: Geomorphology, v. 2, p. 257–284.

Maddox, R.A., Chappell, C.F., and Hoxit, L.R., 1979, Synoptic- and meso-scale aspects of flash flood events: Bulletin of the American Meteorological Society, v. 60, p. 115–123.

Miller, A.J., 1990, Flood hydrology and geomorphic effectiveness in the central Appalachians: Earth Surface Processes and Landforms, v. 15, p. 119–134.

Miller, J.F., 1964, Two- to ten-day precipitation for return periods of 2 to 100 years in the contiguous United States: U.S. Weather Bureau Technical Paper 49, 29 p.

National Oceanic and Atmospheric Administration, 1986, Climatic data: Asheville, N.C., National Climatic Data Center, digital media.

Neumann, C.J., Cry, G.W., Caso, E.L., and Jarvinen, B.R., 1981, Tropical cyclones of the North Atlantic Ocean,1871–1980: Asheville, N.C., National Climatic Data Center, 152 p.

Robertson, F.R., 1987, Use of GOES IR data in estimating synoptic-scale rainfall, Algorithm development and transferability: Unpublished manuscript available from author, Mailcode ED42, Space Science Laboratory, Marshall Space Flight Center, AL 35812.

Waylen, P.R., 1985, Stochastic flood analysis in a region of mixed generating processes: Transactions, Institute of British Geographers, v. 10, p. 95–108.

Williams, G.P., and Guy, H.P., 1973, Erosional and depositional aspects of Hurricane Camille in Virginia, 1969: U.S. Geological Survey Professional Paper 804, 80 p.

Chapter C

Landslides Triggered by the Storm of November 3–5, 1985, Wills Mountain Anticline, West Virginia and Virginia

By ROBERT B. JACOBSON, JOHN P. MCGEEHIN, ELIZABETH D. CRON, CAROLYN E. CARR, JOHN M. HARPER, and ALAN D. HOWARD

U.S. GEOLOGICAL SURVEY BULLETIN 1981

GEOMORPHIC STUDIES OF THE STORM AND FLOOD OF NOVEMBER 3–5, 1985, IN THE UPPER POTOMAC AND CHEAT RIVER BASINS IN WEST VIRGINIA AND VIRGINIA

CONTENTS

PLATE

FIGURES

TABLES

Landslides Triggered by the Storm of November 3–5, 1985, Wills Mountain Anticline, West Virginia and Virginia

By Robert B. Jacobson,[1] John P. McGeehin,[1] Elizabeth D. Cron,[1] Carolyn E. Carr,[2] John M. Harper,[3] *and* Alan D. Howard[3]

Abstract

More than 3,000 landslides were triggered by heavy rainfall in the central Appalachian Mountains of West Virginia and Virginia, November 3–5, 1985. These landslides provided the opportunity to study spatial controls on landslides, magnitude and frequency of triggering events, and the effects of landslides on flood-induced geomorphic change. The study area consists of parts of the Wills Mountain anticline, a major NE-trending structure in the central Appalachians, and a portion of the adjacent Appalachian Plateau. Across the anticline and adjacent plateau, bedrock lithologies vary markedly and include pure marine limestone, marine shale, deltaic mudstone/sandstone sequences, and orthoquartzites. Because of the geologic structure, bedrock lithology varies little along strike.

The spatial distribution of landslides triggered by the storm was controlled primarily by rainfall, bedrock lithology, surficial lithology, land cover, and slope morphology. The triggering rainfall was of moderate intensity and long duration. Two-day storm totals varied from 170 mm to more than 240 mm in the study area. Most landslides occurred at the northeast end of the study area, where 48-h rainfall totals were in excess of 200 mm. Different rainfall thresholds are apparent for triggering landslides on different bedrock lithologies. The highest density of landslides occurred in shallow colluvium and residuum of the Reedsville Shale (Ordovician), followed by regolith of the Greenbriar and Mauch Chunk Groups (Mississippian). Most of the landslides in these fine-grained regoliths were shallow slides and slumps, many of which transformed to mudflows and delivered sediment directly to streams; a smaller number of debris avalanches were triggered high on quartzite ridges.

Instability of colluvium and residuum derived from the Reedsville Shale, compared with regolith from four other fine-grained bedrock lithologies, is attributable to its low strength combined with moderate infiltration rates that allowed soil moisture to accumulate under the moderate intensities of the rainfall. Slopes covered by coarse, cobbly debris flow and alluvial deposits, mostly of Pleistocene age, were very stable due to their low slope angles and high frictional strength.

For a particular bedrock lithology, the spatial distribution of landslides appears controlled by interdependent influences of slope morphology and land cover. On the Reedsville Shale, most landslides occurred on north- to northeast-facing slopes, which might have had higher antecedent levels of soil moisture; these slopes have also been preferentially cleared because they produce better pasture forage for livestock. A secondary concentration of landslides on south- to southwest-facing slopes cannot be explained by conventional soil-moisture models. Landslide density was 100–200 percent higher on cleared land than on forested land. On pastured land, most landslides occurred on laterally planar slopes, but on forested land, most landslides occurred in slope positions that were laterally concave (hillslope hollows).

Compared with other documented Appalachian storms that have triggered landslides, the November 1985 storm had lower rainfall intensities over longer durations. Comparison with these other storms suggests that the anomalously high degree of slope instability in 1985 is due to the long duration of low-intensity rainfall on fine-grained regolith derived from shale; the triggering rainfall can be approximated by the 48-h storm total. Landslide density in Reedsville Shale regolith is linearly related to the varying 48-h rainfall along the anticline. These data define a probabilistic model that estimates return intervals of 43 to 300 yr for landslide densities ranging from 1 to 70 landslides/km^2.

Analysis of flood-induced geomorphic changes in 79 small drainage basins that received 210–240 mm of rainfall showed a clear local association between landslides and channel erosion or deposition adjacent to where the landslides delivered sediment to the stream. When chan-

Manuscript approved for publication February 22, 1991.

[1] U.S. Geological Survey.

[2] Geology Department, Carleton College, Northfield, MN 55057.

[3] Department of Environmental Sciences, University of Virginia, Charlottesville, VA 22903.

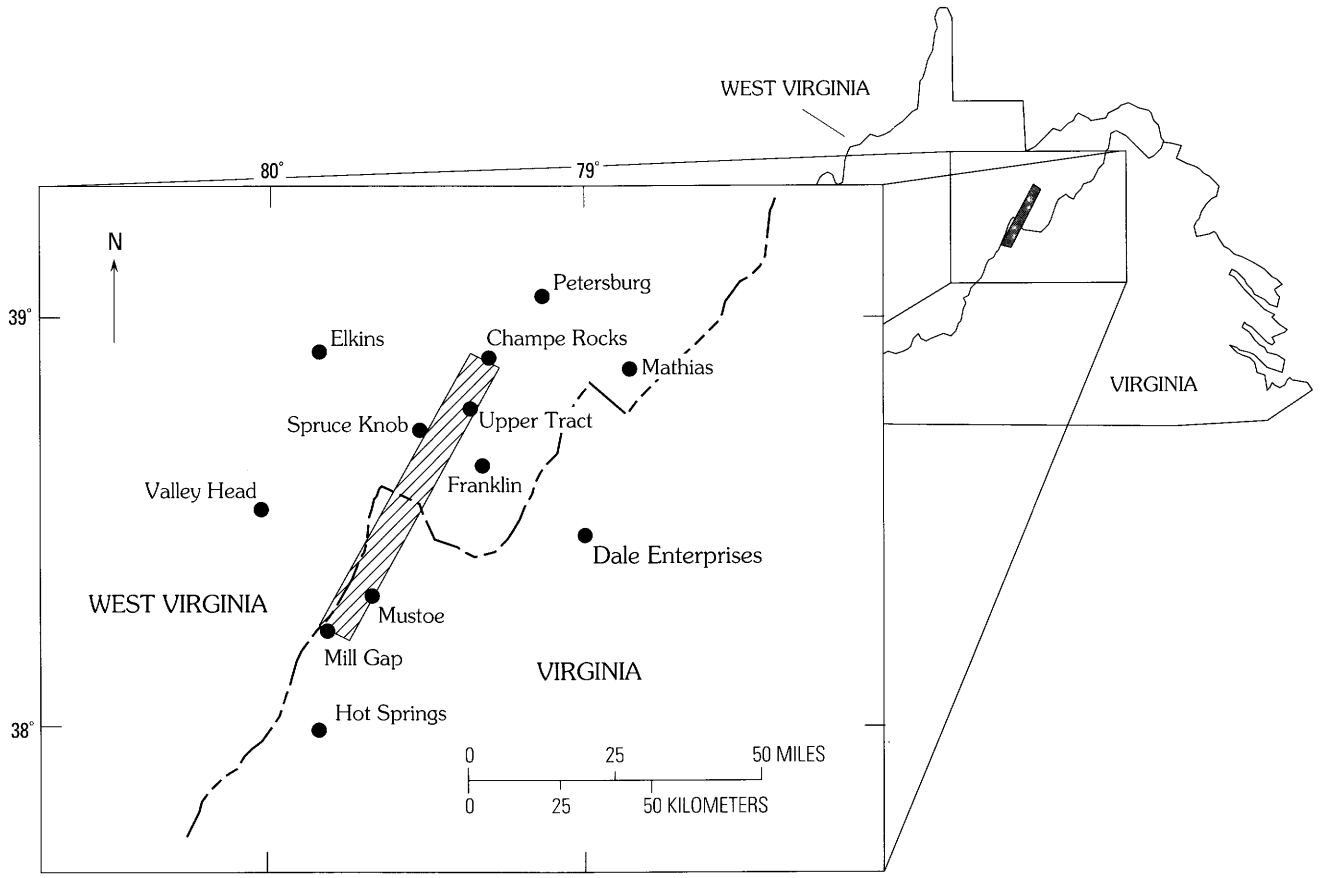

Figure 1. Wills Mountain study area and nearby towns.

nel change was quantified using an index evaluated at each basin mouth, most of the channel change was attributable to the influence of basin morphology on flood discharge. Landslide density in the basins was of secondary, although measurable, importance in explaining flood-induced channel changes at the basin scale.

INTRODUCTION

Heavy rainfall during November 3–5, 1985, triggered more than 3,000 landslides and caused extreme flooding in small drainage basins in Pendleton County, W. Va., and Highland County, Va. One of the main areas receiving high rainfall totals straddled the Wills Mountain anticline, a major Appalachian structure. Rainfall varied from less than 170 mm to more than 240 mm along the anticline (figs. 1, 2; pl. 1), triggering shallow landslides on a variety of bedrock lithologies and in a variety of geomorphic settings. Because of the elongate outcrop pattern, the full range of storm rainfall was applied to all the bedrock lithologies and derived regoliths, thus providing a unique, well-defined geomorphic experiment for evaluating the influences of rainfall, geologic materials, land use, and other factors on slope stability.

Our study of the storm focused on three areas of inquiry: (1) analysis of landslide locations to determine the dominant factors that control landslide susceptibility, (2) analysis of the magnitude and frequency with which landslides occur in this landscape, as reflected by the relationship between rainfall and landslide occurrence along the anticline, and (3) investigation of the extent to which flood-induced geomorphic changes are related to sediment added from upstream landslides.

Factors Controlling Landslide Locations

Empirical studies of landslide distributions in the Appalachian Mountains have attempted to rank the influences of various geologic, geomorphic, land cover, and human factors on slope stability (Pomeroy, 1980, 1982a, 1984, 1987; Lessing and Erwin, 1977; Lessing and others, 1976, 1983; Jacobson, 1985). Because the mechanical equilibrium of a slope site is determined by a complex, and probably nonunique, combination of these variables, empirical studies rarely produce unequivocal results, even with large data sets and rigorous statistical analyses. Furthermore, many studies have been handicapped because they used data sets consisting of landslides recognized on air

A

Period	Stratigraphic Unit	Map Unit (pl. 1A)	Approx. Thickness, ft.
Pennsylvanian	Pottsville Group	Pottsville Group	0
Mississippian	Mauch Chunk Group	Mauch Chunk Group	2000
	Greenbriar Group	Greenbriar Group	
	Pocono Group	Pocono Group	
Devonian	Hampshire Formation	Hampshire Formation	4000
	Chemung Group	Chemung Group	6000
	Brallier Formation	Devonian shales, undifferentiated	8000
	Harrel to Needmore Shales, undivided		
	Oriskany Sandstone and Helderburg Group, undivided	Oriskany Sandstone and Helderburg Group, undivided	
		Undifferentiated Devonian rocks	
Silurian	Tonoloway, Wills Creek, Williamsport Formations, undivided	Tonoloway, Wills Creek, Williamsport Formations, undivided	
	McKenzie Formation, Rochester Shale, and Keefer Sandstone, undivided	McKenzie Formation, Rochester Shale, Keefer Sandstone, and Clinton Group, undivided	10000
	Clinton Group		
	Tuscarora Sandstone	Tuscarora Sandstone	
Ordovician	Juniata Formation	Juniata Formation and Oswego Sandstone	
	Oswego Sandstone		
	Reedsville Shale	Reedsville Shale	12000
	Dolly Ridge Limestone[1] / Nealmont Limestone — Trenton Group	Trenton Group	
	Black River Group	Black River Group	14000
	New Market Limestone	St. Paul Group	

[1] of Perry (1972)

Figure 2. *A*, Generalized stratigraphic column for the study area, with simplified bedrock units used in plate 1. Units are from Cardwell and others (1968) except as noted. *B*, Simplified cross section of the Wills Mountain anticline, modified from Kulander and Dean (1986). Section A–A′ is located in figure 2C. *C*, Locations of study areas.

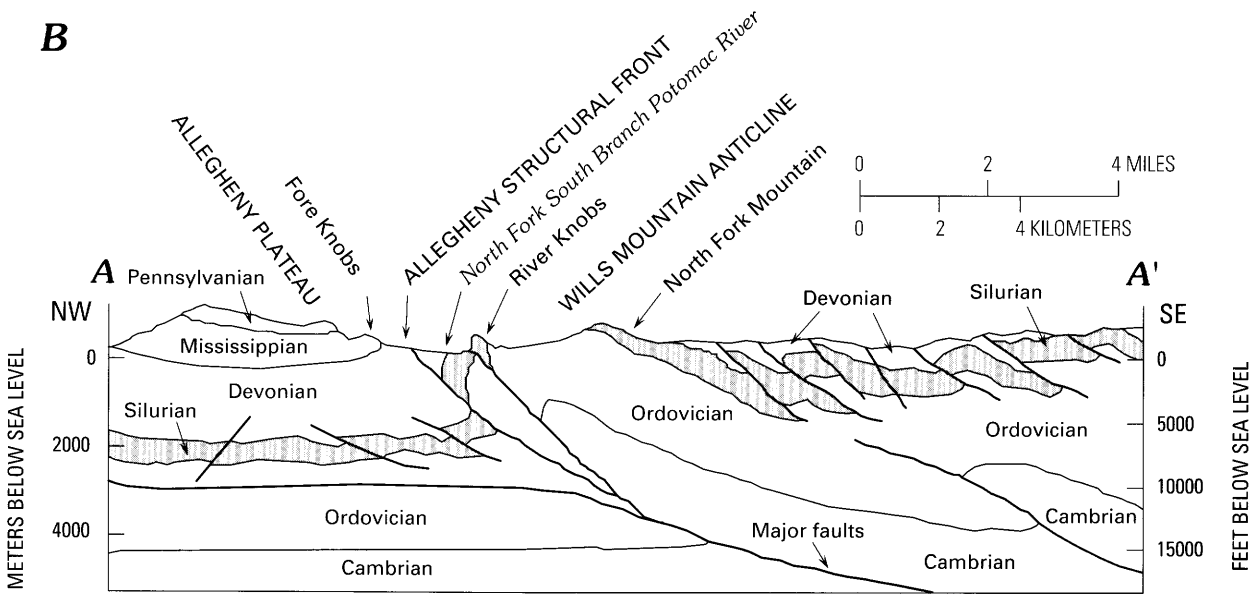

Figure 2. Continued.

photos or in the field, regardless of the age of the landslide. Landslides that heal quickly can be expected to be underrepresented in these data sets, and those that occur where healing processes are slower are probably overrepresented.

Our study of spatial controls on landslides along the Wills Mountain anticline avoids some of these complications first, by including only landslides triggered by the November 1985 storm. Hence, all landslides are equally mappable, except for a small possible bias against the smallest landslides, which might not be identifiable on large-scale air photos. Second, our study is limited to landslides triggered on natural slopes; thus we avoid the biases inherent in including slopes destabilized by man. Third, to the extent possible, our analytical methods characterize the entire landscape, not just the sites of landslides. In this way, we can consider why sites are stable as well as why sites are not.

Magnitude and Frequency of Landslide-Triggering Events

Previous studies of storm-induced landslides in the Appalachians have identified rare rainfall events of high intensity and short duration as triggers (Stringfield and Smith, 1956; Hack and Goodlett, 1960; Williams and Guy, 1973; Schneider, 1973; Bogucki, 1976; Everett, 1979; Pomeroy, 1980, 1984; Clark, 1987; Neary and Swift, 1987). For the most part, these studies documented peak rainfall amounts that were inferred to have triggered landslides. Because they did not measure a range of rainfall bracketing the triggering amount, the studies could only make the limited conclusion that the peak rainfall exceeded stability thresholds for some portion of the slope sites considered; the actual threshold was not determined.

The natural geomorphic experiment produced by the 1985 storm along the Wills Mountain anticline provided the opportunity to investigate slope instability in regolith derived from several bedrock lithologies over a range of rainfall. We were able to define the threshold cumulative rainfall at which the least stable site of a given bedrock lithology failed, and, for the bedrock lithology that experienced the most failures, we were able to document the variation of spatial density of landslides with cumulative storm rainfall. By estimating the recurrence interval for rainfall amounts along the anticline, we were able to estimate the recurrence interval for the associated degree of slope instability.

Landslides, Basin Morphology, and Flood-Induced Geomorphic Changes

Field observations in the study area shortly after the 1985 event indicated that flood-induced erosion and deposition in stream channels were related to landslides on adjacent and upstream slopes. Almost all channel change began where a landslide delivered sediment to the channel, and many channels without upstream landslides showed negligible channel changes compared with channels of comparable drainage area with upstream landslides. These observations suggest that flood effects downstream from tributary drainage basins could be measurably related to sediment supply from landslides upstream in the basins. We

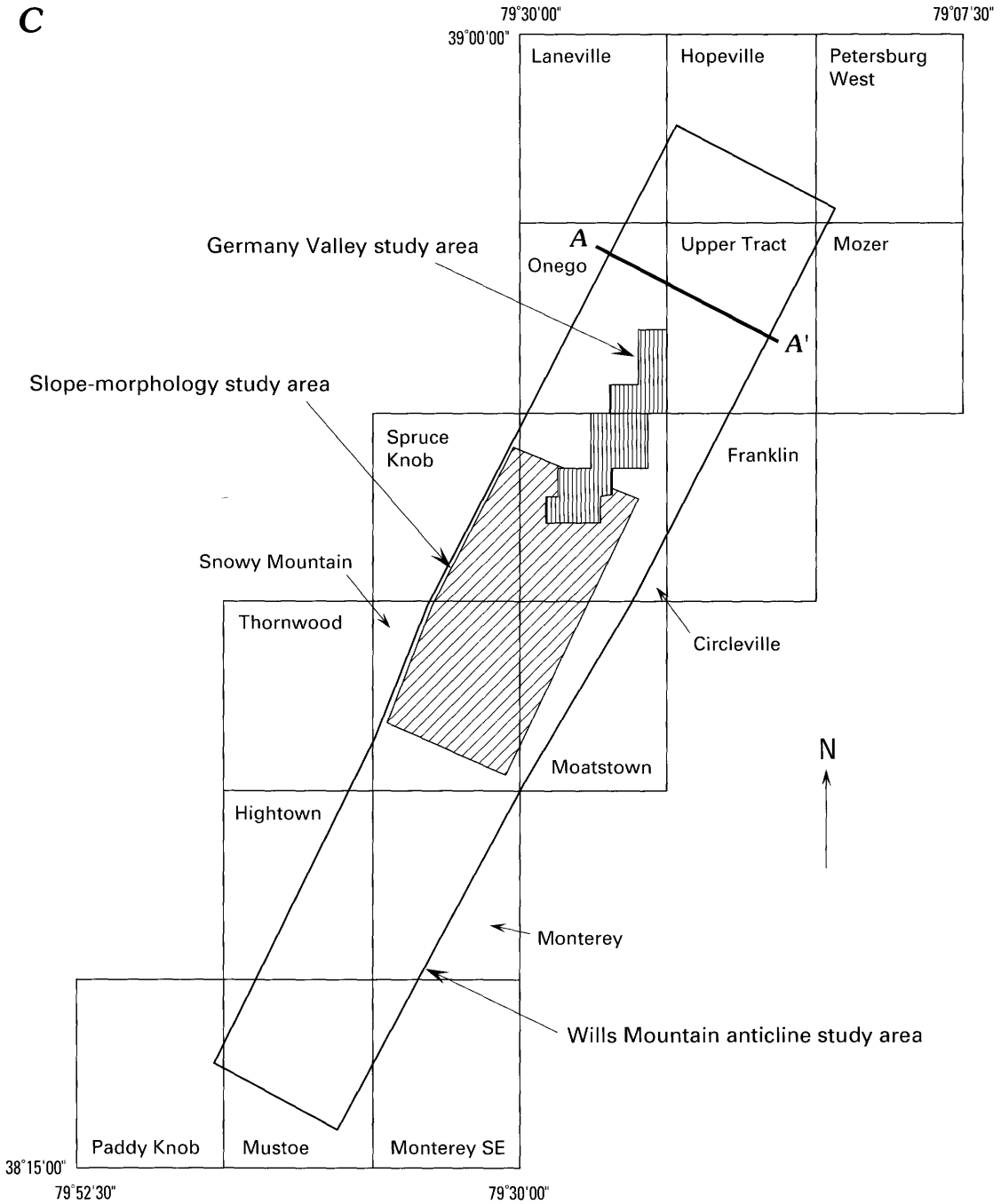

Figure 2. Continued.

have tested this hypothesis by comparing a channel-change index with extent of upstream slope instability, as well as basin morphometric parameters and rainfall amounts.

Methods

Landslides were documented by 1:24,000-scale aerial photographs flown in April 1986. The aerial photography covered the eastern limb of the Wills Mountain anticline to the rim of the Appalachian Plateau, and extended along strike from near Mill Gap, Va., in the southwest to near Ketterman, W. Va., in the northeast (fig. 1; also Jacobson, chapter A, this volume, pl. 1). Landslides triggered during the storm of November 1985 were easily and accurately identified on these photos.

Two separate maps were prepared from the aerial photographs. The first map, outlining the entire photo-coverage area (fig. 2*C*), was prepared by identifying land-

slides with a stereoscope and then transferring the photo data to 1:24,000 bases by zoom-transfer scope. This map was used to relate locations of landslides to bedrock lithology, surficial lithology, land cover, flood-related damage, and rainfall. A version of this map compiled at 1:150,000 scale is shown in plate 1. The entire study area is referred to here as the Wills Mountain anticline study area.

A second map (area shown in fig. 2*C*) for a smaller area of homogeneous rainfall near Circleville, W. Va., was prepared by accurate plotting from the same set of photographs with a PG-2 stereoplotter (Cron, 1990). This map was used for analysis of bedrock lithology, surficial lithology, land cover, and topographic controls on locations of landslides. This study area is referred to here as the Germany Valley study area.

Both maps were extensively evaluated in the field during the spring and fall of 1986, and the spring of 1987 by field mapping of selected test areas. Field checking disclosed accuracy in identification of approximately 95 percent on cleared slopes and 90 percent accuracy in identification under tree cover. The smallest landslide mapped was approximately 15 m^2.

A third nonmapped data base was compiled of landslide data in an area that overlaps the Germany Valley study area and continues to the southwest (area shown in fig. 2*C*). This data base, referred to as the slope morphology data base, was used to evaluate slope morphology controls on locations of 852 landslides in an area of homogeneous rainfall and bedrock lithology.

Channel changes downstream of tributary drainage basins were assessed from low-altitude aerial photography (1:10,000 approximate scale), flown for the West Virginia Department of Highways in November 1985, and compared with preflood aerial photos. These data constitute the data base for tributary flood damage.

Geology was compiled from a variety of sources, including Cardwell and others (1968), Perry (1971), unpublished file maps of the Virginia Division of Mineral Resources, and unpublished mapping by R.B. Jacobson.

Meteorological data were obtained in digital form from the National Climatic Data Center (National Oceanic and Atmospheric Administration, 1986). These data were used to prepare isohyetal maps of the storm using projection, gridding, and contouring programs routinely used by the USGS for contouring geophysical data. The data were also used to graph hourly rainfall intensities and for frequency analysis of rainfall data from representative gages, following the guidelines of the Interagency Advisory Committee on Water Data (1982).

Terminology

The term "landslide" is used in this paper to include all downslope movements of earth materials that are initiated at distinct times, that move over time intervals of seconds to days, and that create distinct scars and (or) deposits that can be identified by eye in the field or in aerial photographs. In general, scars and deposits had to be larger than 15m^2 in area to be included in the data sets used in this study.

The term "regolith" is used for the surficial geologic units that mantle bedrock, including residuum, colluvium, debris, and alluvium. "Residuum" is surficial material that has weathered in place from underlying bedrock. "Colluvium" is poorly sorted surficial material that has been transported and deposited downslope by nonchannelized, diffusive, gravitational processes that include seasonal creep, bioturbation, and landslides. Colluvium is usually very poorly sorted and nonbedded. "Debris" is poorly sorted to well-sorted surficial material transported and deposited by fluid flow but characterized by the presence of diamicton units with matrix-supported clasts, indicative of debris-flow processes. Debris is often characterized by interbedded well-sorted sand, gravel, and cobbles of fluvial origin, and poorly sorted diamicton originating from debris flows. "Alluvium" is moderately sorted to well-sorted fine-to-coarse sediment transported by fluid flow in channels and characterized by the absence of debris flow deposits. The term regolith is used in place of the term "soil" as used by engineers. "Soil" is used in the pedological sense to describe the material resulting from subaerial mineralogical, chemical, biological, and physical changes to regolith from weathering processes.

Acknowledgments

This manuscript benefited from thorough and thoughtful reviews by J.S. Schindler and S.D. Ellen. We are also grateful for advice offered by our colleagues R.H. Campbell, R.W. Jibson, and G.F. Wieczorek and for the continuing support of the U.S. Geological Survey National Center Geographic Information System Laboratory.

GEOLOGY, GEOMORPHOLOGY, AND CLIMATE

A generalized geologic map of the study area and a regional stratigraphic column are provided in plate 1 and figure 2*A*, respectively. Stratigraphic nomenclature is from Cardwell and others (1968) except as noted. For detailed descriptions of bedrock geology, the reader is referred to works by Cardwell and others (1968), Diecchio (1986), and Kulander and Dean (1986). The following description of bedrock geology and geomorphology concentrates on bedrock geologic controls on the landscape.

At a regional scale, the geomorphic form of the study area is controlled by deformed, resistant sandstones of the Paleozoic section (pl. 1, figs. 2*A*, *B*). The Tuscarora

Sandstone underlies the ridges that outline the doubly plunging, asymmetric Wills Mountain anticline. The southeastern limb dips 20°–40° and forms North Fork Mountain. The northwestern limb is nearly vertical to overturned and forms a hogback ridge known as the River Knobs. Streams draining the interior of the anticline pass through constricted gaps in the ridges formed by the anticlinal limbs. Sandstones of the Mississippian Pocono Group form the Fore Knobs, which interrupt the steep slopes ascending westward to the Appalachian Plateau, and buttress a narrow bench underlain by Greenbriar Group and mudstones and sandstones of the Mauch Chunk Group (Cardwell and others, 1968). Pebbly sandstones of the Pottsville Group (Cardwell and others, 1968) of Pennsylvanian age underlie the highest parts of the Appalachian Plateau in this area.

The oldest rocks in the area are pure Ordovician limestones of the St. Paul Group and the Black River Group, exposed in the core of the Wills Mountain anticline (Diecchio, 1986). Overlying the pure limestones are shaley limestones of the Trenton Group. Slopes on these limestones are gentle (0°–12°) except near incised tributaries or the numerous karst depressions. Drainage density in the limestones is very low, and many stream valleys are dry most of the year. Much of the area underlain by limestone is covered with a mantle of coarse debris shed from North Fork Mountain. This debris is composed of large angular cobbles of Tuscarora Sandstone with varying amounts of silty and sandy matrix. Residual soils on limestones vary in thickness from 0 to approximately 1 m.

Above the Trenton Group in the stratigraphic section (fig. 2*A*) is the Reedsville Shale, a calcareous marine shale. This unit forms long, gently sloping spur ridges oriented mainly northwest-southeast, normal to the trend of the anticlinal ridges. Reedsville Shale slopes are embayed by areas of alternating concave- and convex-out contours. Areas of concave-out contours are focal points for studies of slope processes because they serve to converge hillslope sediment and moisture (Hack and Goodlett, 1960; Dietrich and others, 1987). The term "hollow" was originally proposed by Hack and Goodlett to describe areas of concave-out contours. In this paper the term is modified to "hillslope hollow" to avoid confusion with local Appalachian usage of "hollow" to apply to first- and second-order valleys. Side slopes, areas of generally straight contours, on the Reedsville Shale generally range from 12° to 25°, although some areas adjacent to laterally eroding stream channels are much steeper. Like limestone slopes, extensive areas of Reedsville Shale are covered with debris shed from North Fork Mountain. Where debris mantles the Reedsville Shale, the slopes are gentle (1°–12° along the former direction of transport) and hillslope hollows are poorly developed.

Stratigraphically above the Reedsville Shale, the Oswego Sandstone, interbedded mudstone and sandstone of the Juniata Formation, and the Tuscarora Sandstone support steep slopes along North Fork Mountain and the River Knobs. These slopes range from approximately 22° to vertical and overhanging cliffs. North Fork Mountain slopes are corrugated in form and have developed hillslope hollows superimposed on the dominant northwest-facing slope aspects. The hillslope hollows are commonly filled with coarse colluvium and debris.

From the valley of the North Fork River to the Fore Knobs (fig. 2*B*), slopes are cut into shale, limestone, and sandstone of Devonian and Mississippian age. At their bases, these slopes are mantled with debris and are only slightly embayed. Upslope, toward the Fore Knobs, the embayment of hillslope hollows increases in the Devonian Chemung Group and Hampshire Formation. Slopes on the bench protected by the Pocono Group are smooth and gentle on residuum derived from Greenbriar Group and Mauch Chunk Group. Slopes up to the Pottsville Group are mantled with pebbly sandstone debris and are gently corrugated.

Dipslopes on the southeastern limb of the Wills Mountain anticline (North Fork Mountain) are slightly corrugated where mantled by debris in areas where first-order streams have not incised the Tuscarora Sandstone. Interbedded sandstone, shale, shaley limestone, and limestone of the Silurian through Devonian section are rarely exposed on these dipslopes because they are covered by extensive and thick debris accumulations. In areas where the first-order streams have incised the Tuscarora Sandstone, long, steep valleys embay North Fork Mountain.

The climate of the study area is seasonal and sensitive to elevation. In general, the late summer and autumn months are dry, whereas the winter and spring are wet. Mean annual temperature and precipitation vary from 8.4 °C and 1037 mm at 930 m elevation to 10.9 °C and 824 mm at 580 m elevation (National Oceanic and Atmospheric Administration, 1985). Additional climatic data are presented by Colucci and others (chapter B, this volume).

STORM OF NOVEMBER 1985 ALONG THE WILLS MOUNTAIN ANTICLINE

Total rainfall from the November 1985 storm was especially heavy in an area centered over the Wills Mountain anticline, near Upper Tract, W. Va., (pl. 1; also Jacobson, chapter A, this volume, pl. 1). Because of the coarseness of the official National Oceanic and Atmospheric Administration (NOAA) rain gage network, the rainfall depicted on these maps is a general model for the storm; local orographic effects that might be expected to modify the rainfall pattern are not represented, and it is unlikely that the extremes of rainfall were actually measured by the rain gage network. The general form of the distribution of rainfall has been corroborated by residents' observations; bucket survey data of unknown accuracy suggest that local areas of total rainfall in the study area may

have been as high as approximately 225 mm over 24 h and 390 mm over 4 days (Colucci and others, chapter B, this volume, table 2). The highest officially measured 24-h rainfall was 191 cm at Franklin, and the highest 48-h rainfall was 241 cm at Upper Tract.

Only one rain gage, recording hourly, operated within the study area during the storm (Mustoe, fig. 1). Five additional rain gages, recording hourly, range in distance from 22 to 42 km from the study area. Data from the six sites are given by Colucci and others (chapter B, this volume, fig. 9); we assume that these data are representative of conditions in the study area. These gages show that rainfall was continuous for a little more than 24 h, and intensities of 10 mm/h or greater were recorded for more than 12 h at some gages. The peak recorded intensity of 38.1 mm/h at Hot Springs, Va., however, was not extreme for the Appalachian Mountains (Colucci and others, chapter B, this volume).

Although hourly rainfall intensities were not extreme, the rainfall measured over 24- and 48-h durations achieved long recurrence intervals (Colucci and others, chapter B, this volume). The 48-h total at Franklin had an estimated recurrence interval between 67 and 166 yr, while that of Spruce Knob was in excess of 200 yr. The peak 48-h total at Upper Tract had a recurrence estimated at between 83 and 286 yr. As discussed by Colucci and others (chapter B, this volume), estimates of recurrence intervals are necessarily rough because of the highly skewed rainfall records.

DESCRIPTION OF LANDSLIDES

Terminology and Classification

Most of the landslides triggered by the storm are classified as debris slumps, earth slumps, debris slides, earth slides, debris flows, and earth flows, according to accepted landslide terminology (Varnes, 1978); the reader is referred to Varnes (1978) and Campbell and others (1985) for more detailed discussion of landslide classification. The population of landslides is dominated by slides in fine materials (clay to sand with gravel-size clasts) derived from shales, shaley limestones, and interbedded shale, mudstone, and sandstone. Most are shallow, planar slides with depths rarely exceeding 2 m and minor rotational movement at the head of the sliding mass (fig. 3). In this paper, the term "slides" is used in cases where most of the slide mass remained coherent, and "slide flows" are used in cases where the slide mass showed signs of flowing earth or debris at the toe or lateral margins.

A smaller number of landslides occurred in thick (greater than 2 m) colluvial aprons at the bases of slopes and were presumably triggered by lateral stream erosion of the toeslopes (fig. 4). Rotational movement dominates in these landslides; in this paper they are referred to as slumps and slump flows.

Eight large landslides on North Fork Mountain began as sliding masses of sandstone residuum and colluvium. The masses avalanched down steep slopes and flowed long distances, up to 2 km, with varying amounts of erosion and deposition. These complex landslides are best classified as complex debris slide-avalanche flows (Campbell and others, 1985). For simplicity, they are referred to here as debris avalanches.

Slides and Slide Flows

Ninety-five percent of the landslides triggered by the November storm were slides, slide flows, slumps, or slump flows; the remaining 5 percent can be classified as debris avalanches and slide flows transitional to avalanches. Among all landslides, approximately 90 percent were shallow planar slides on thin residuum and colluvium. Typically, the failure plane of these slides was parallel to the surface slope and occurred at depths of 0.5–2 m. Commonly, the failure plane occurred at the transition between pedogenic B horizon and weathered, saprolitic bedrock, or at the contact between thin colluvium and weathered bedrock. Very shallow planar slides, less than 50 cm deep, were common on 50°–70° side slopes along stream margins. These slides usually completely stripped off a thin carpet of roots, organic matter, and residual soil to expose hard bedrock beneath. The deeper planar slides tended to occur in hillslope hollows where thick colluvium had accumulated. Slides in hillslope hollows often eroded down to weathered bedrock in the axes of the hillslope hollows, but, in most cases, significant volumes of colluvium remained intact around the margins of the slide scar.

Rotational failures were less common, approximately 10 percent of the total, and occurred in two specific situations. Many rotational failures occurred as deep-seated slumps in thick toeslope colluvium along streams. Presumably these landslides were triggered by lateral erosion and undercutting of colluvial deposits by floodwaters. Projection of failure planes suggests maximum depths as much as 5 m. Benches of nearly flat lying, interbedded mudstone and limestone high above stream channels were also affected by rotational sliding (fig. 5). In these cases, rotation occurred as sliding masses of weathered bedrock were forced to toe out above underlying competent layers.

Many landslides mobilized as muddy debris flows. Of the 583 landslides mapped in the Germany Valley study area, 89 percent showed some evidence of flow (Cron, 1990). Among the 3,562 landslides mapped over the entire study area, 30 percent delivered some fraction of sediment to streams (table 1). Flows from slides on Reedsville Shale were very fluid, some flowing for tens of meters on 0°–8° slopes over intact turf (fig. 6). On forested slopes, some

Figure 3. Shallow slides and slide flows in residuum derived from the Reedsville Shale. (Photograph taken June 1987. Note sheep for scale.)

Figure 4. Large slump in toeslope colluvium derived from Reedsville Shale. Slump dammed stream at base of slope, causing several cubic meters of deposition upstream. Slump is approximately 5 m across.

Figure 5. Typical landslide on a Greenbriar Group slope. Large solution-bounded blocks of limestone slid out on red shale interbeds.

Table 1. Distribution of slope movements in study area by bedrock stratigraphic unit

[Units are from Cardwell and others except as noted]

Bedrock unit	Predominant lithology	Number	Area, km^2	Density, landslides/km^2	Percent of total
Greenbriar Group	Limestone/shale	10	27.3	4.03	3.09
Pocono Group	Sandstone	40	31.8	1.26	1.12
Mauch Chunk Group	Sandstone/shale	54	38.7	1.40	1.52
Hampshire Formation	Sandstone/shale	9	65.3	.14	.25
Chemung Group	Sandstone(siltstone)	10	76.4	.13	.28
Devonian shales,[1] undifferentiated	Shale	2	9.3	.22	.06
Oriskany Sandstone	Sandstone	21	48.3	.43	.59
Helderberg Group	Limestone	20	37.5	.53	.56
Devonian rocks, undifferentiated	Limestone/shale	31	73.6	.42	.87
Tonoloway, Wills Creek, and Williamsport Formations, undivided	Limestone/shale	54	62.1	.87	1.52
McKenzie Formation and Clinton Group, undivided	Limestone/shale	47	100.8	.47	1.32
Tuscarora Sandstone	Sandstone	7	56.3	.12	.20
Juniata Formation and and Oswego Sandstone, undivided	Sandstone/shale	177	80.9	2.19	4.97
Reedsville Shale	Shale	2812	135.7	20.72	78.94
Trenton Group	Limestone/shale	156	36.0	4.33	4.38
Black River Group	Limestone	11	27.8	.40	.31
St. Paul Group	Limestone	1	22.7	.04	.03
Total		3562	930.5		100

[1] Undifferentiated Devonian shales include thin shales of the Brallier Formation, Harrell Shale, Mahantango Formation, Marcellus Formation, and Needmore Shale, all of Cardwell and others (1968).

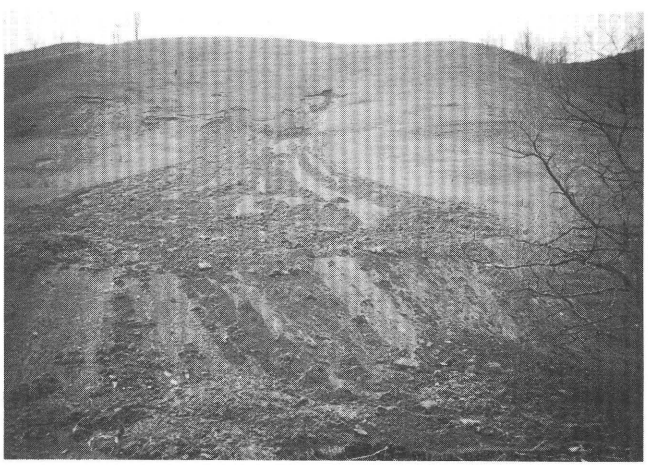

Figure 6. Typical slide flow on Reedsville Shale. Slide flow initiated in thin colluvium and residuum and flowed over turf on toeslope colluvium. Part of the flow was delivered to the stream channel at the base of slope. Flow track is 6 m across.

muddy debris flows passed over the forest floor without disturbing leaf litter. Splash marks 1–1.5 m high on tree trunks on 30°–40° slopes indicate that flows were able to achieve high velocities.

Slopes underlain by residuum and colluvium of the Reedsville Shale had the greatest percentage of mapped landslides (79 percent, table 1). The remaining 21 percent were distributed dominantly among other fine lithologies: colluvium and residuum derived from interbedded sandstone and mudstone of the Juniata Formation (5.0 percent), clayey residuum derived from Trenton Group shaley limestone (4.0 percent), clayey residuum derived from interbedded mudstone and limestone of the Greenbriar Group (3.1 percent), and residuum and colluvium derived from shaley limestone of the Tonoloway Limestone and Wills Creek Formation and shale and mudstone of the Mauch Chunk Group (1.5 percent each).

Slides and slide flows on the Reedsville Shale were approximately 90 percent shallow, planar failures in thin colluvium and residuum and 10 percent rotational failures in toeslope colluvium. Landslides in clayey residuum and thin colluvium of the Tonoloway, Wills Creek, and Williamsport Formations, Trenton Group shaley limestone, and the Mauch Chunk Group were all shallow, planar slides, most of which transformed into muddy debris flows. Regolith on these bedrock units is generally thin (less than 1 m), and slopes are relatively steep (20°–40°).

In contrast to the landslides described above, landslides on slopes underlain by interbedded mudstone and limestone of the Greenbriar Group often involved large fracture- and solution-bounded blocks of intact limestone bedrock sliding on thin red shale interbeds (fig. 5). Many of the limestone blocks were transported tens of meters, and mudflows that mobilized from the landslides flowed hundreds of meters.

Figure 7. Debris avalanche scar at Twin Run. From 25 to 100 cm of fractured sandstone slid along bedding planes at left; diamicton colluvium at right was mostly stable.

Figure 8. Track of debris flow from Twin Run debris avalanche. Note superelevation around curve.

Debris Avalanches and Transitional Slide Flows

Landslides of thin residuum and colluvium derived from interbedded mudstone and sandstone of the Juniata Formation accounted for 5 percent of the total number of landslides (table 1). Almost all of these landslides occurred on steep forested slopes on North Fork Mountain on planar side slopes or subtle hillslope hollows. Most landslides initiated as planar slides generally less than 50 m^2 in area and transformed into flows that delivered sediment to steep first-order channels. In classification, these slide flows are transitional to debris-avalanche flows, in that they began as shallow slides and changed to flows. However, evidence for a rapid avalanching phase was generally absent.

The most dramatic landslides triggered by the November 1985 storm were eight debris avalanches that started at the contact between the Juniata Formation and Tuscarora Sandstone or on dipslopes underlain entirely by Tuscarora Sandstone (figs. 2, 7, 8). Two of these features are documented in detail by Kite and others (1987). Of the eight large debris avalanches triggered by the storm, five occurred on dipslopes on the southeast side of North Fork Mountain. (Dipslopes are slopes with aspects within 90° of the bedrock dip direction; aspect is azimuth the slope faces.) Of the five landslides on dipslopes, three were initiated in fractured Tuscarora Sandstone bedrock on slopes parallel to bedding planes dipping 30°–35° (fig. 8). The other two were initiated in thin colluvium and weathered rock at the contact between the Juniata and the Tuscarora. The three debris avalanches that started on antidipslopes also occurred in thin colluvium and weathered rock at the contact. At all eight sites, the landslides occurred adjacent to thick masses of colluvium that were not mobilized or were only partially mobilized.

Runout tracks of debris flows below the slide and avalanche scars were as long as 2 km (fig. 8). The runout tracks were characterized by variable scour and deposition, common formation of lateral levees, superelevated flow around bends (fig. 8), and large snoutlike deposits of debris and logs (fig. 9). Substantial fluvial reworking of the original deposits took place subsequent to debris flow deposition.

Figure 9. Snout of deposit of debris flow at Hartman's farm, southeast of North Fork Mountain. Snout is approximately 4 m wide, and deposit is about 1.5 m thick.

CONTROLS ON THE SPATIAL DISTRIBUTION OF LANDSLIDES

Examination of the distribution of landslides on plate 1A reveals some obvious controls on landslide location, notably rainfall and bedrock. Landslide density generally increases with increasing rainfall along the anticline except for local gaps in the distribution and a large gap in the northeastern quarter of the study area. Most of the landslides occurred on regolith derived from Reedsville Shale in

the center of the Wills Mountain anticline, with smaller numbers of landslides originating in regolith derived from other fine-grained bedrock lithologies (table 1). Coarser grained bedrock lithologies produced many fewer landslides. Gaps in the distribution that apparently are not related to rainfall or bedrock lithology suggest that other controls are important influences at a more detailed scale of resolution. Comparisons of landslide locations with surficial geologic maps of the study area (pl. 1*B*) indicate that surficial geology is an important determinant of where landslides occurred in 1985. At more detailed scales of resolution, land use, slope morphology, and slope aspect also are apparent controls on landslide locations.

Surficial Geology

Gaps in the distribution of landslides occurring on Reedsville Shale slopes are controlled largely by preexisting debris deposits (pl. 1*B*). In the study area, the thickness of the debris varies from negligible to greater than 5 m. The deposits are arranged on the landscape as gently sloping terrace treads separated by riser slopes underlain by bedrock. Similar deposits have been described in southwestern Virginia (Mills, 1981, 1988). Debris deposits owe their origin to debris-avalanche flow events similar to the eight events triggered in 1985. However, because areas of debris are so extensive on the present-day landscape, it is unlikely that all of the debris could have been produced during the Holocene. Cross-cutting relationships, qualitative evaluation of weathering, and geomorphic positions on the landscape suggest that debris has been deposited during at least four or five discrete episodes dating as far back as 500,000 yr B.P. (Jacobson and others, 1987, 1989). Presumably, debris has accumulated episodically as a response to climatically induced changes in regolith production and (or) transport rates.

In the Germany Valley study area, only 6 percent of 583 landslides occurred on debris deposits; most of these were caused by sliding in underlying Reedsville Shale rather than the overlying debris deposit. Debris covers almost the entire outcrop area of Reedsville Shale and underlying shaley limestones in the northeast quarter of the study area. Gentle slopes (generally less than 8°), presumed high frictional strength imparted by the interlocking structure of the poorly sorted diamicton, and the armoring effect of coarse material have served to stabilize these deposits.

Physical properties, thickness, and stratigraphy of colluvium vary with many other factors on the landscape, including source bedrock lithology, underlying bedrock lithology, mode of deposition, age, and slope morphology. Because of this variability, colluvium may be either weaker or stronger, and more permeable or less permeable, than adjacent and underlying residuum and bedrock. Hence, colluvium is often an important factor influencing slope instability by producing zones of strength or weakness and sites of subsurface moisture accumulation (Dietrich and others, 1987; Fleming and others, 1981; Royster, 1973). Because of the variety of bedrock lithologies in the study area, colluvial properties are also highly variable, and it is difficult to generalize about the importance of accumulations of colluvium at the resolution of this study. In the Germany Valley study area, only 17 percent of the 583 landslides triggered in 1985 occurred on colluvium (that is, in areas where colluvium is greater than 1–2 m thick). On the other hand, field observations indicate that landslides in colluvium tended to be deeper and larger, suggesting that colluvial landslides may have contributed more than 17 percent of the landslide volume. It was beyond the scope of this study to collect sufficiently detailed data to test that hypothesis.

Bedrock Geology

Bedrock controls on slope instability can be divided into those factors that influence the hydrologic properties and strength of regolith, structural factors that influence flow of ground water along bedding planes and provide zones of weakness for preferential sliding, and factors that influence slope morphology and hence influence redistribution of shallow ground water.

Physical Properties of Unstable Regolith

Several regoliths within the study area were chosen for detailed analyses to relate landslide susceptibility to physical properties. Residuum derived from interbedded sandstone and mudstone of the Mauch Chunk Group, interbedded mudstone and limestone of the Greenbriar Group, interbedded sandstone and mudstone of the Juniata Formation, marine shale of the Reedsville Shale, and shaley limestone from the Trenton Group, along with debris derived from Tuscarora Sandstone mixed with components from the Juniata Formation and Reedsville Shale, were sampled for general characterization. The residuum samples were chosen to represent a selection of clayey to sandy regoliths that varied markedly in the spatial density of landslides triggered in 1985 (fig. 10); debris was sampled to characterize materials that were extremely stable during the 1985 event.

Representative sites were chosen for sampling and for performing falling-head, double-ring infiltrometer tests to measure infiltration and drainage characteristics of the regolith. Each site was sampled for bulk density, particle size, Atterberg limits, and clay mineralogy. Because all the regolith types failed dominantly by shallow slides, samples were taken from depths of 10–50 cm. Infiltration rates were recorded during application of 250–750 mm of water in 100-mm falling-head cycles. Final infiltration rates under fully saturated conditions and zero head were used as

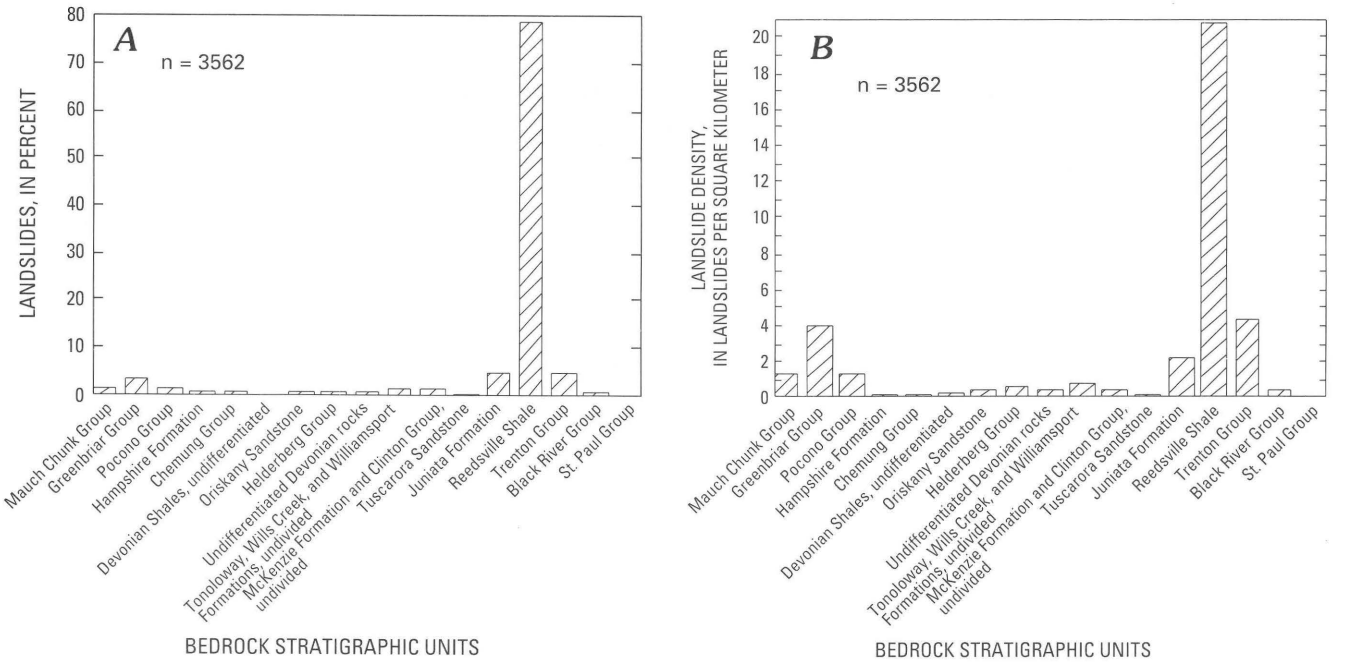

Figure 10. *A*, Histogram of percentages of landslides by bedrock stratigraphic units. *B*, Histogram of density of landslides (landslides/km^2) by bedrock stratigraphic units. Characteristic regoliths on these units are discussed in text; lithologies are given in table 1.

indicative of saturated infiltration and drainage rates for the 0.5–1 m of regolith.

Residuum derived from the Reedsville Shale is much richer in clay than the residuum from the Juniata Formation and Greenbriar Group (fig. 11, table 2). The Reedsville Shale residuum is also richer in clay than residuum of the Mauch Chunk Group and debris, although the differences in sample means are not statistically significant. Residuum from the Trenton Group has the highest clay content among those tested, and residuum from the Juniata Formation is significantly sandier than all other regoliths except for debris.

Atterberg limits of the samples show that all samples are of medium plasticity (fig. 12, table 3). The highest liquid limits (water contents at which the samples begin to act like liquids) and plasticity indices (range of water contents over which the samples deform plastically) are from samples of Reedsville Shale residuum and Trenton Group residuum. Activities (plasticity index divided by percent clay) are about equal for all regolith types, although the range in the Reedsville Shale sample set is greater (table 4).

Infiltration rate and porosity may also influence slope stability by regulating the rate and amount of rainfall that the regolith can soak up, store, and drain during a storm event. Porosities were calculated from measured bulk densities of fist-sized soil aggregates that were representative of peds of the A and B horizons of the soils at each site (table 4, fig. 13). The Juniata Formation regolith has a significantly higher porosity than all other regoliths, presumably because of its high sand content. Conversely, the Reedsville Shale regolith has porosity that is significantly lower than all but the Trenton Group and debris. In general, ped-scale porosity of these residua increases with sand content and decreases with clay content.

Although limiting infiltration rates are highly variable among these regoliths (fig. 14), most are much higher than the measured rainfall intensities of 38 mm/h (Colucci and others, chapter B, this volume). In general, low infiltration rates were measured on debris and Greenbriar limestone residuum, and the highest were measured on Trenton Group shaley-limestone residuum. Only the very lowest limiting infiltration rates measured on the Mauch Chunk and Greenbriar residua were comparable with the highest measured rainfall intensity; most of the saturated infiltration rates are much greater than rainfall intensities. Samples from the tests on infiltration rates had water contents ranging from 79 to 100 percent of fully saturated conditions, indicating that most were fully saturated during the infiltrometer tests. Water contents less than 100 percent of saturation are attributed to areas in the soil that were bypassed by infiltrating water flowing in macropores.

The data on physical properties of the fine-grained regoliths do not indicate a single variable that might be responsible for the differences in observed instability of regoliths that received virtually identical rainfall. However, the data can help to constrain which variables were most influential in causing the relative instability during this storm.

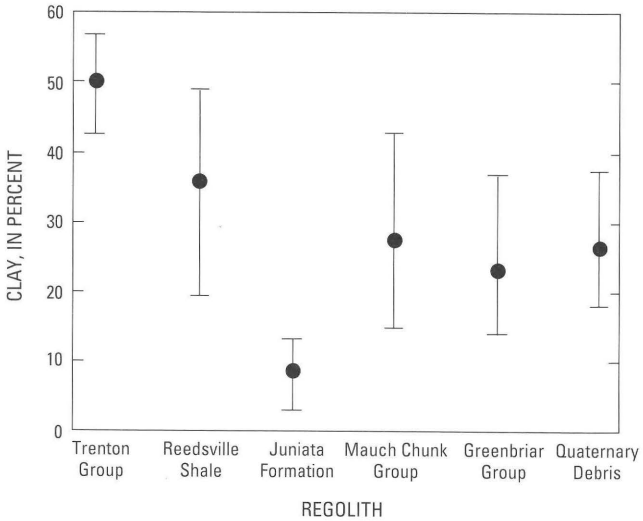

Figure 11. Range diagram of clay content (percent less than 2 microns) for six regoliths. Vertical line marks range of sample values, solid circle marks mean value.

Table 2. Particle-size distributions for sampled regoliths

[Std Dev, standard deviation. All values in weight percent. *N*, number in sample. Particle-size data exclude coarse fragments greater than 2 mm. Sand is 0.065–2 mm, silt is 0.002–0.065 mm, and clay is less than 0.002 mm]

Size class	Minimum	Maximum	Mean	Std Dev
Quaternary debris, *N*=5				
Sand	14.8	42.3	28.8	11.0
Silt	28.2	63.8	44.0	13.4
Clay	19.0	38.4	27.2	7.6
Mauch Chunk Group, mudstone/sandstone residuum, *N*=8				
Sand	5.7	53.7	21.8	16.4
Silt	31.1	64.4	50.1	11.4
Clay	15.2	43.0	28.0	9.3
Greenbriar Group, limestone/mudstone residuum, *N*=7				
Sand	7.6	38.9	24.7	11.7
Silt	38.4	67.5	52.3	9.5
Clay	14.2	37.6	23.0	8.2
Juniata Formation, mudstone/sandstone residuum, *N*=3				
Sand	29.9	58.2	47.6	15.4
Silt	33.4	57.7	43.0	13.0
Clay	4.0	12.4	9.4	4.7
Reedsville Shale, shale residuum and colluvium, *N*=19				
Sand	4.8	50.8	17.3	12.2
Silt	29.8	60.1	46.6	7.0
Clay	19.4	49.0	36.1	9.7
Trenton Group, limestone residuum, *N*=4				
Sand	3.7	22.2	11.7	8.8
Silt	34.6	43.6	37.9	4.1
Clay	43.2	56.8	50.4	5.8

Theoretically, failure at a slope site occurs when pore-water pressures reduce normal stress on a failure plane sufficiently to allow failure in response to applied shear stress, assuming that site geometry is not altered during the event. Hence, at sites of equal slope, failure susceptibility is controlled mainly by factors that determine inherent shear strength of the material and factors that influence buildup of pore-water pressure. These two groups of factors may have different degrees of importance, depending on the storm characteristics and regolith involved.

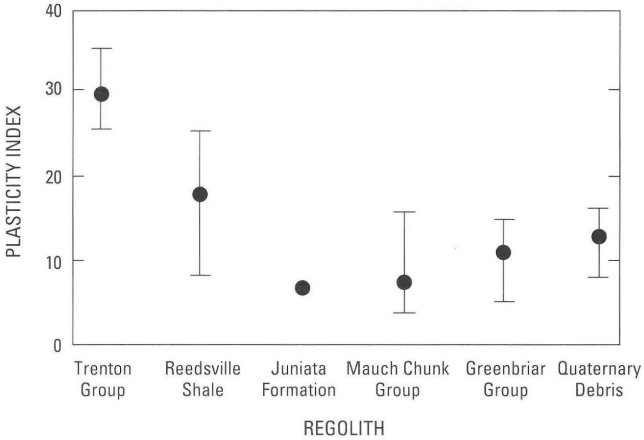

Figure 12. Range diagram of plasticity index (liquid limit−plastic limit) for six regoliths. Vertical line marks range of sample values, solid circle marks mean value.

Table 3. Atterberg limits, plasticity indexes, activities, and dominant clay minerals of regolith samples

[Std Dev, standard deviation. *N*, number in sample. Atterberg limits are expressed as water contents, weight percent. Activity is the plasticity index divided by percent clay]

Parameter	Minimum	Maximum	Mean	Std Dev
Quaternary debris, *N*=3, dominant clay minerals are illite and kaolinite				
Liquid limit	32.0	55.8	46.7	12.8
Plasticity limit	23.7	40.0	34.4	9.2
Plasticity index	8.3	15.8	12.3	3.8
Activity	.44	.83	.61	.12
Mauch Chunk Group, *N*=9, dominant clay mineral is vermiculite				
Liquid limit	23.8	42.1	37.3	6.0
Plasticity limit	17.9	32.1	26.5	4.4
Plasticity index	5.9	14.5	10.8	3.1
Activity	.36	.51	.42	.05
Greenbriar Group, *N*=4, dominant clay mineral is vermiculite				
Liquid limit	33.7	43.7	38.5	4.7
Plasticity limit	26.9	31.3	29.4	1.8
Plasticity index	4.1	13.9	9.1	4.0
Activity	.21	.56	.41	.18
Juniata Formation, *N*=2, dominant clay mineral is vermiculite				
Liquid limit	33.4	38.0	35.7	3.2
Plasticity limit	27.4	30.8	29.1	2.4
Plasticity index	6.0	7.2	6.6	0.8
Activity	.50	.56	.54	.04
Reedsville Shale, *N*=5, dominant clay mineral is illite				
Liquid limit	28.6	59.6	40.1	12.4
Plasticity limit	19.7	33.2	26.1	5.8
Plasticity index	4.2	26.4	14.0	10.2
Activity	.12	1.24	.53	.42
Trenton Group, *N*=4, dominant clay mineral is illite				
Liquid limit	59.2	67.0	62.6	3.2
Plasticity limit	32.5	34.7	33.4	0.9
Plasticity index	25.9	32.3	29.1	2.6
Activity	.49	.81	.60	.14

Table 4. Bulk density, void ratio, and porosity for selected regoliths

[Bulk density in g/cm^3; void ratio and porosity in decimal fraction. Std Dev, standard deviation. *N*, number in sample. Void ratio is the ratio of volume of voids to volume of solids; porosity is the ratio of the volume of voids to the total volume of the sample]

Parameter	Minimum	Maximum	Mean	Std Dev
Quaternary debris, *N*=8				
Bulk density	1.30	2.02	1.69	0.26
Void ratio	.31	1.04	0.61	.27
Porosity	.24	.51	.36	.10
Mauch Chunk Group, mudstone/sandstone residuum, *N*=16				
Bulk density	1.40	1.77	1.57	.10
Void ratio	.50	.89	.70	.10
Porosity	.33	.47	.41	.04
Greenbriar Group, limestone/mudstone residuum, *N*=10				
Bulk density	1.39	1.78	1.52	.11
Void ratio	.49	.91	.75	.12
Porosity	.33	.48	.43	.04
Juniata Formation, mudstone/sandstone residuum, *N*=4				
Bulk density	1.24	1.43	1.32	.08
Void ratio	.85	1.15	1.02	.12
Porosity	.46	.53	.50	.03
Reedsville Shale, shale residuum and colluvium, *N*=29				
Bulk density	1.45	1.80	1.63	.08
Void ratio	.47	.83	.63	.08
Porosity	.32	.45	.39	.03
Trenton Group, limestone residuum, *N*=5				
Bulk density	1.53	1.68	1.64	.06
Void ratio	.58	.73	.62	.07
Porosity	.37	.42	.38	.02

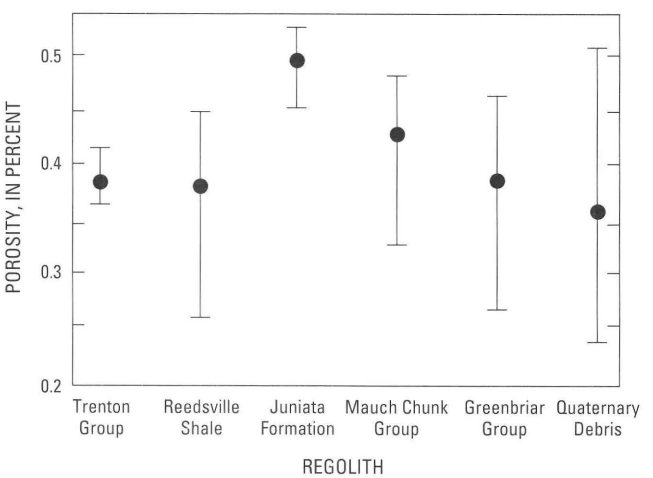

Figure 13. Range diagram of porosity for six regoliths. Vertical line marks range of sample values; solid circle marks mean value.

Consistent with their high clay contents, the regoliths of the Reedsville Shale and the Trenton Group have the highest plasticity indexes and liquid limits among those tested. As illustrated by Mitchell (1976), residual friction angles of engineering soils generally decline with both

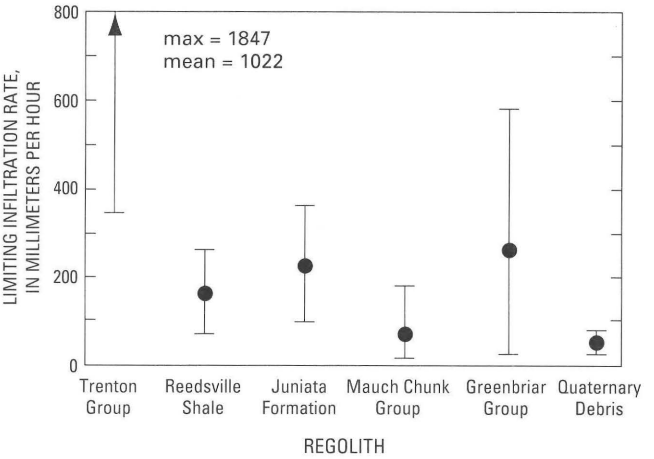

Figure 14. Range diagram of limiting infiltration rates for six regoliths. Vertical line marks range of sample values, solid circle marks mean value.

increased plasticity index and liquid limit, although additional frictional strength may be added by the presence of interlocking clasts. Except for Quaternary debris, the clast content (greater than 2-mm diameter) of tested regoliths was uniformly low, ranging up to approximately 5 percent. Hence, the plasticity index data suggest that residuum from the Reedsville Shale and Trenton Group shaley limestones should have the lowest frictional strengths. Low strength may explain why the Reedsville Shale was much more susceptible to failure than regolith of the Quaternary debris, Greenbriar Group, Mauch Chunk Group, and Juniata Formation, but comparable low strength of the Trenton Group regolith suggests that hydrologic factors that influence buildup of pore-water pressure were also important.

Buildup of pore-water pressure occurs where soil moisture accumulates because of vertical drainage rates that are less than rainfall intensity (where infiltration rate is not a limiting factor) or because of convergence of throughflow of shallow ground water. Accumulation and convergence are controlled by the complex interactions of rainfall intensity, infiltration rate, lateral and vertical permeabilities of regolith and bedrock, porosity and thickness of regolith, and topographic concavity or convexity (Wieczorek, 1987). Stability of a given regolith unit during a rainfall event will be determined by these hydrologic factors and the ranges and spatial distributions of the shearing resistance.

Because stratigraphic and topographic controls on net inflow and outflow of water in regolith at slope sites are highly variable across the landscape, they could not be considered in detail in this study. As an approximation, it can be assumed that, for the thin regolith that constituted most of the landslides, drainage rates are roughly proportional to infiltration rates, although they certainly will vary. Other factors not measured in this study, such as regolith thickness and topographic convergence, also influence sta-

bility and probably should be considered in subsequent studies. For this analysis, it is assumed that the relative drainage characteristics of the studied regoliths were measured by the infiltration tests.

The lowest infiltration rates measured were for the debris and Greenbriar Group residuum. Low rates in debris are probably due to its relative lack of intrapedal secondary permeability; development of soil structure in debris is presumably limited by the high clast content. Low infiltration rates measured on Greenbriar Group residuum are partly misleading because the only sites with slopes gentle enough for infiltration tests were benches underlain by shale. Fracture permeability in limestone layers (fig. 5) could produce much greater infiltration rates locally.

The highest infiltration rates measured were on residuum of the shaley limestones of the Trenton Group. The A and B horizons of these soils were extremely well structured (fig. 15), and we assume that the high infiltration rates resulted from flow in intrapedal macropores; drainage may have been augmented by flow into dissolution features in the underlying limestone. Infiltration rates on the Reedsville Shale were moderate, although still substantially higher than the maximum rainfall intensity.

We interpret the differences in slope stability between regoliths over Reedsville Shale and Trenton Group shaley limestone to reflect primarily the trade-off between shear strength and accumulation of soil moisture. Infiltration rates of Reedsville Shale regolith were sufficient to allow moisture to infiltrate and accumulate but low enough to bring many sites to failure conditions during this long storm. In contrast, because of higher drainage rates, few sites on Trenton Group slopes could accumulate sufficient moisture to achieve failure despite comparably low strength. Higher infiltration rates and (or) greater strength similarly made other regoliths more stable than Reedsville Shale residuum during this storm event.

Geologic Structure

Ground-water seepage from bedding planes exposed in road cuts is commonly observed in the study area. Although ground-water flow along bedding planes has not been evaluated directly for natural slopes, these observations suggest that bedding planes may provide important pathways for downdip flow of ground water. If ground water flows significantly down bedding planes, we would expect greater numbers of landslides on dipslopes (those slopes with dip directions within 90° of slope aspect) than on antidipslopes. However, downdip flow of ground water may trade off with topographic concentrations of shallow ground water, regolith properties, and land cover to determine slope stability.

Steep forested slopes on the northwest side of North Fork Mountain, underlain by the Juniata Formation and the Tuscarora Sandstone, had a moderate number of small debris avalanches and slides. These slopes are inclined 20°–40° away from the dip of bedrock bedding planes (that is, they are antidipslopes), which should cause them to be relatively dry to the extent that shallow ground-water flow will follow the bedding planes. Landslides on the Juniata Formation antidipslope occurred mainly in hillslope hollows (table 5*A*), where convergence of shallow ground water may have compensated for lack of downdip drainage.

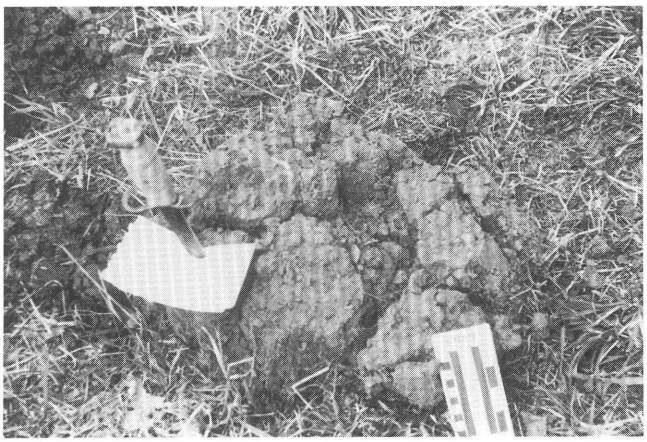

Figure 15. Well-developed, blocky soil structure at 15-cm depth (transition between lower A horizon and upper B horizon) in residual soil derived from Trenton Group shaley limestone.

Slopes on the southeastern side of North Fork Mountain generally dip with the direction of bedding planes and are underlain by the Tuscarora Sandstone and interbedded sandstone, shale, and limestone rocks of Silurian and Devonian age (pl. 1, fig. 2). The lower portions of these slopes are mantled extensively with debris. The upper parts of the slope show little development of hillside hollows, except where first-order streams have incised through the Tuscarora Sandstone into less resistant units of the Juniata Formation. Three of the four largest debris avalanches originated in areas of straight to convex-out contours on the upper slopes in thin (generally less than 1 m) colluvium over fractured sandstone bedrock. Most of the failure sites were adjacent to thicker deposits of colluvium that were stable or only partly involved with failure. The combination of low frictional strength on bedding planes and, perhaps, accumulation of shallow ground water by flow along bedding planes may have made these sites less stable during this rainfall event than areas of hillslope hollows with thick accumulations of colluvium.

In the Germany Valley area, the 583 landslides studied by Cron (1990) showed no influence of geologic structure on locations. These landslides were mainly shallow slides and slide flows in shaley regolith that may have been less sensitive to downdip redistribution of ground water because most of the infiltrating moisture was stored in the slowly permeable regolith.

Table 5. Effects of slope morphology and land cover on landslide location

A. Percent of 852 landslides in topographic convergence classes for wooded and cleared slopes[1]

Topographic convergence class	Percent on cleared slopes	Percent on wooded slopes	Total
Nose	5.9	0.2	6.1
Planar	60.4	4.1	64.5
Subtle hillslope hollow	11.5	4.0	15.5
Distinct hillslope hollow	5.3	8.6	13.9
All hillslope hollow	16.8	12.6	29.4
Total	83.1	16.9	100.0

B. GIS data for cells with and without landslides, for slope aspect and land cover controls on landslide locations[2]

Slope-aspect class	Percent of cells in class			Percent of cells with landslides		
	Overall	Wooded	Cleared	Overall	Wooded	Cleared
North-facing	58	50	50	6	2	10
South-facing	42	60	40	5	3	7

[1] Area of sample is approximately 100 km^2; it is underlain by Reedsville Shale, Oswego Sandstone, and Juniata Formation; approximately 220–240 mm of rainfall fell November 4–5, 1985.

[2] Area of sample is 75 km^2; it is underlain by Trenton Group, Reedsville Shale, Oswego Sandstone, Juniata Formation, and Tuscarora Sandstone; it received 220–240 mm rainfall November 3–5, 1985. Data from Cron (1990).

Slope Morphology and Land Cover

Slope morphology and land cover may also contribute to the stability of slope sites. Slope steepness, which is commonly assumed to be an important variable in landslide location, is not considered explicitly in this study because most of the variation in slope steepness is related directly to bedrock lithology. Cron (1990) found that 85 percent of the landslides in her data set in the Germany Valley area occurred on the most gentle slopes (0°–14°) because gentle slopes are characteristic of the Reedsville Shale. Steeper slopes occur on the more competent sandstones and sandstone/mudstone slopes, but these were more stable during this storm event because factors other than slope steepness were also operating. Slope steepness could be an important predictor of landslide locations among slopes underlain entirely by one bedrock lithology if the resolution of the topographic data base was sufficient to resolve the range of slope inclinations for that lithology. Presumably, landslides would occur preferentially on the steeper slopes of that bedrock lithology if other factors did not vary. Topographic data available for this study were not sufficiently detailed to resolve the ranges of slope steepness for the different bedrock lithologies.

In an area of homogeneous regolith, slopes with concave-out contours (hillslope hollows) will be sites of convergence of soil moisture (Dietrich and others, 1987). Over a time interval of years to millenia, hillslope hollows also accumulate colluvium (Reneau and others, 1986). Theoretically, convergence of moisture and colluvium should make hillslope hollows preferred sites for initiation of landslides (Reneau and Dietrich, 1987), and areas of convex-out contours (noses) should be relatively stable. As pointed out by Wieczorek (1987), however, topographic convergence can be less important on steeper slopes and where depth to bedrock is very shallow (0.2–0.5 m deep).

Slides and Slide Flows

The importance of topographic convergence in determining landslide location during the 1985 storm was investigated from a data base of landslides that occurred in a homogeneous area of approximately 100 km^2 underlain by Reedsville Shale, Oswego Sandstone, and the Juniata Formation (slope morphology study area, pl. 1., fig. 2, table 5). Land cover in the sample area is approximately equally divided between cleared grassland (48.9 percent) and woodland (51.1 percent). Using aerial photographs, each of 852 landslides was classified according to land cover (wooded or cleared) and topographic convergence.

Topographic convergence classes are defined according to convergence angle, approximated here as the angle between the medial axis of the hillslope hollow and a line perpendicular to contours at the inflection point where the contour changes from concave-out to convex-out. The topographic convergence classes were noses (areas of convex-out contours), planar side slopes (areas of nearly straight contours, convergence angles less than approximately 10°), subtle hillslope hollows (areas of concave-out contours with convergence angles approximately 10°–30°), and distinct hillslope hollows (areas of concave-out contours with convergence angles greater than approximately 30°).

Most of the 852 landslides (70.6 percent) were initiated on planar slopes or noses rather than in hillslope hollows. Among landslides that occurred on planar slopes, 94 percent occurred on cleared slopes. In contrast, among landslides that occurred in distinct hillslope hollows, 62 percent were in forested areas. For all landslides in this

sample, 83 percent occurred on cleared slopes. Because landslides on cleared, planar side slopes in the sample area tended to be smaller and shallower than those in hillslope hollows, the smaller volume of landslide material may somewhat diminish the dominance implied by the large percentages of these landslides.

These data suggest that on sites where trees contributed root strength, topographic convergence of moisture or thickened accumulations of colluvium determined the slope instability during this event. On sites where tree root strength was lacking, topographic convergence was less important in determining instability.

Debris Avalanches

As noted earlier, all eight of the debris avalanches occurred on forested slopes. Five of the eight were on dipslopes, where failure took place along bedding planes in fractured sandstone under residuum or thin colluvium, or at sites that may have received a component of ground-water flow along bedding planes. Of these five sites, the largest was on a topographic nose, three were on planar side slopes, and one was in a subtle hillslope hollow. In contrast, all three debris avalanches occurring on antidipslopes were in distinct hillslope hollows. These observations suggest that on dipslopes, low strength along bedding planes and (or) downdip flow of ground water can lower stability as much as or more than topographic convergence of moisture or presence of thick colluvium.

Slope Aspect and Land Cover

At a broader scale of resolution, landslide location is influenced by both slope aspect and land cover. Observations from field and aerial photographs indicate a clear tendency for landslides to occur on north- to northeast-facing slopes (fig. 16). Land use practices, however, are not independent of slope aspect (table 5*B*). The north- to northeast-facing slopes, being wetter, are preferentially cleared for pasture, while the drier, south- to southwest-facing slopes are preferentially wooded.

The interrelations among slope aspect, land cover, and landslide occurrence were investigated in the Germany Valley study area (Cron, 1990). Cron used a computer-assisted geographic information system (GIS) with 100-m by 100-m grid cells over 75 km^2 to compare topography, land cover, bedrock geology, and surficial geology for both stable and unstable slopes. She concluded the following:

- North-facing (northwest through east) and south-facing (southeast through west) slopes are about equally represented (58 and 42 percent, respectively) among the entire population of slope prospects.
- Due to land-use practices, 50 percent of the area of north-facing slopes is cleared for pasture and hay, while only 40 percent of the south-facing slopes is cleared.

Figure 16. Aerial photograph showing association of landslides with cleared, northeast-facing slopes on Reedsville Shale in the center of the Wills Mountain anticline.

- For all slopes, 9 percent of cleared cells had one or more landslides, whereas only 3 percent of the forested cells had one or more landslides.
- For north-facing slope cells, 6 percent had one or more landslides, and for south-facing slope cells, 5 percent had one or more landslides.
- For north-facing cleared slopes 10 percent of the cells had one or more landslides, compared with 2 percent for wooded cells; for south-facing cleared slopes, 7 percent had one or more landslides compared with 3 percent for wooded cells (table 5).

These data indicate that, over areas of homogeneous bedrock and surficial geology, tree cover was an important factor in determining slope stability. Because this storm occurred at a time of year when leaves had fallen from the trees and evapotranspiration by trees was negligible, the influence of tree cover was probably through additions of root strength rather than from reductions in soil moisture.

Slope aspect alone had a more subtle influence on slope stability, accounting for a relative increase of stability on south-facing slopes of only 17 percent. Slope aspect and land cover data together show that cleared land on north-facing slopes is 5 times as unstable as woodland, whereas cleared land on south-facing slopes is only 2.3 times as unstable as woodland. The increased stability of south-facing cleared slopes is probably due to lower soil moisture, relative to north-facing cleared slopes antecedent to the storm.

Hence, these data indicate that the spatial distribution of slope instability triggered by the November 1985 storm was controlled by a combination of slope aspect and land cover factors in addition to meteorologic, lithologic, structural, and topographic convergence factors. Meteorologic and geologic controls on landslide locations are apparent at the scale of the entire Wills Mountain anticline study area (approximately 800 km^2). Competing influences of topographic convergence, slope aspect, and land cover become apparent over smaller areas (tens of km^2), where meteorologic and geologic factors do not vary. The quantitative importance of these factors and their operating mechanisms remains to be determined.

MAGNITUDE AND FREQUENCY OF LANDSLIDE EVENTS

Cumulative Rainfall Thresholds for Landslides

The spatial distribution of landslides along the Wills Mountain anticline can be used to estimate the 48-h rainfall totals that triggered landslides on different lithologies in November 1985. Instability in regolith derived from the Reedsville Shale and Juniata Formation required approximately 180 mm or more cumulative rainfall; in regolith derived from the Greenbriar Group and Mauch Chunk Group, instability required 220 mm or more, but these rocks are not present in areas that received less than about 200 mm; and large debris avalanches on dipslopes of the Tuscarora Sandstone required more than 220 mm.

These observations provide crude rainfall thresholds for landsliding in these units, but the thresholds may be misleading because, while they illustrate conditions that were *sufficient* for failure, they may not resolve the combination of conditions *necessary* for failure. For example, the failures may have been triggered by a high-intensity rainfall interval during the storm, or they might have been dependent on antecedent soil moisture conditions.

Unfortunately, data on rainfall intensity and observations of the times that individual landslides were triggered are insufficient to determine confidently whether high-intensity periods within the storm may have been responsible for triggering some of the landslides or for the observed differences in thresholds. The available data and reports of residents, however, suggest that high-intensity periods were not immediate triggers of landslides. According to the most reliable hourly rainfall data (Colucci and others, chapter B, this volume, fig. 8), the highest rainfall intensities were recorded in the afternoon of November 4. Residents of the area agree that landslides in the Reedsville Shale started during the night of November 4–5 and continued with slow movement and occasional flow events during the morning of November 5. A resident at the base of North Fork Mountain at Judy Gap placed the time of the large debris avalanche there at approximately 9:00 p.m. on November 4, and a resident near the Twin Run debris avalanche reported that the avalanche occurred sometime during the night of November 4–5 (Kite and Linton, 1987, p. 23, 36).

The role of antecedent soil moisture cannot be evaluated directly without detailed soil moisture data. Rainfall and runoff during October 1985 suggest that antecedent soil moisture conditions were only slightly wetter than normal for what is usually the driest season of the year (Colucci and others, chapter B, this volume).

Rainfall Intensity and Duration Thresholds for Landslides

Compared with other documented landslide events in the Appalachian Mountains, the November 1985 storm was characterized by an extremely large number of small slides and slide flows triggered on shaley lithologies by moderate-intensity rainfall. Events similar in failure style and magnitude have not been reported elsewhere in the Appalachian Mountains. Instead, most other documented events have been characterized by large, destructive debris slides and debris avalanches triggered by high-intensity rainfall on steep slopes (Stringfield and Smith, 1956; Hack and Goodlett, 1960; Schneider, 1973; Bogucki, 1976; Everett, 1979; Pomeroy, 1980, 1982b; Neary and Swift, 1987). Debris slides and avalanches constituted only a small portion of the landslides triggered during the 1985 storm. This comparison illustrates how unusual the 1985 event was and, by implication, identifies the most probable rainfall duration responsible for triggering these landslides.

For durations from 1 to 48 h, mean intensities of measured rainfall in the 1985 storm are comparable to or above the threshold curve of Caine (1980) for shallow landslide and debris-flow (fig. 17). This curve defines a minimum threshold estimated from 73 cases of landslides worldwide, collected from a variety of physiographic, geologic, and antecedent moisture conditions. Many of the data points Caine used to define the relation lie substantially above the minimum curve. As discussed by Sidle and others (1985, p. 90–93), the Caine curve describes the minimum intensity that is necessary to trigger failure under saturated antecedent conditions at the least stable sites. Also, as with our data from the 1985 storm, many of the data in Caine's

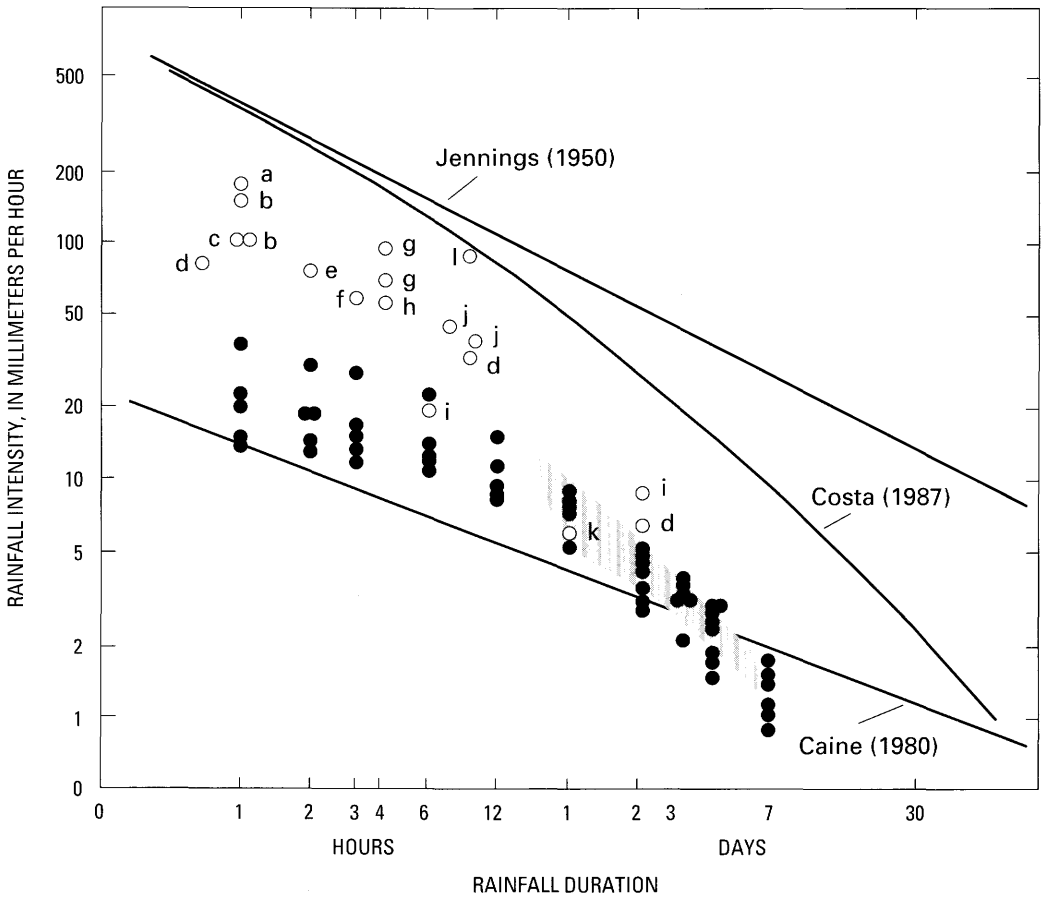

Figure 17. Intensity and duration of rainfall of some storms responsible for triggering landslides in the central Appalachian Mountains: (a) Smethport, Pa., July 1942 (Eisenlohr, 1952); (b) Great Smoky Mountains, Tenn., September 1951 (Bogucki, 1976); (c) Asheville, N.C., November 1977 (Neary and Swift, 1987); (d) Johnstown, Pa., July 1977 (Pomeroy, 1980); (e) Shickshinny Mountain, Pa., 1947 (Braun and others, 1989); (f) Bens Creek, W. Va., August 1972 (Everett, 1979); (g) Greenbriar, Tenn., August 1938 (Moneymaker, 1939); (h) Reddish Knob, Va., June 1949 (Hack and Goodlett, 1960); (i) Petersburg, W. Va., June 1949 (Stringfield and Smith, 1956); (j) Spring Creek, W. Va., August 1969 (Schneider, 1973); (k) East Brady, Pa., August 1984 (Pomeroy, 1984); (l) Nelson County, Va., August 1969 (Camp and Miller, 1970). Solid circles are values measured in or near the Wills Mountain anticline study area November 3–5, 1985. Shaded area shows range of intensity and duration known to have occurred in study area.

curve are not peak intensities but, rather, mean intensities averaged over a given duration and empirically associated with landslide initiation. Unmeasured peak intensities may have been the actual triggers. These factors in the Caine curve tend to underestimate triggering intensities. However, in a study of storm-triggered debris flows in the California Coast Range, Wieczorek (1987) found thresholds considerably below the Caine curve when the occurrence of individual debris flows could be confidently associated with a specific intensity and duration of rainfall. Hence, the Caine curve is also sensitive to spatial scale and is most appropriately applied to events where extensive slope instability indicates that more slope sites failed than just the least stable.

That points from the 1985 storm lie above the Caine threshold curve (fig. 17) is interpreted as evidence that the 1985 storm had the potential to trigger landslides under some undefined combination of geologic, physiographic, and antecedent conditions, and not that particular durations were instrumental in actually triggering landslides in the Wills Mountain anticline area. Several Appalachian storms noted for triggering large debris avalanches are also plotted in figure 17. In general, these plot higher and at shorter durations than the 1985 data. Because these data are mean intensities averaged over longer durations, they tend to underestimate the maximum storm intensities. This is especially true for older data in areas where hourly recording rain gages were not available, for example, the June 1949

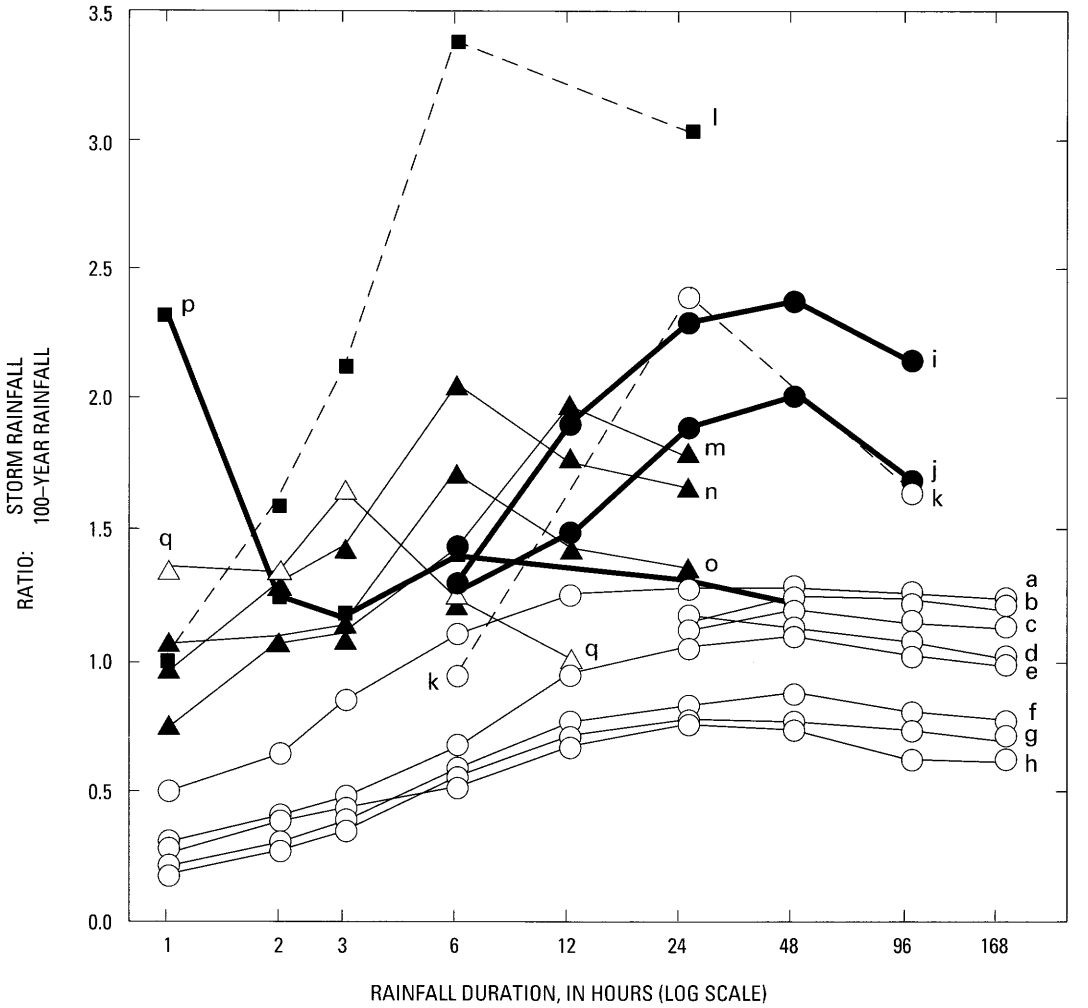

Figure 18. Duration spectra for some storms that have triggered landslides in the central Appalachian Mountains. Graph shows ratio of storm rainfall to rainfall of the 100-yr event for durations of 1 to 168 h (7 days). The 100-yr rainfall is estimated from Hershfield (1961) and Miller (1964). Curves represent the following storms: (a–h) November 3–5, 1985 (NOAA, 1986); (i, j) Hurricane Agnes, June 1972 (Bailey and others, 1975); (k) June 1949, near Petersburg, W. Va. (Stringfield and Smith, 1956); (l) Hurricane Camille, August 1969 (Camp and Miller, 1970); (m, n, o) Johnstown, Pa., July 1977 (Hoxit and others, 1982); (p) Smethport, Pa., July 1942 (Eisenlohr, 1952); (q) Burnsville, W. Va., August 1943 (Erskine, 1952).

storm near Petersburg, W. Va. (Stringfield and Smith, 1956).

Another useful measure is duration spectra of the individual storms (fig. 18). Unfortunately, the data needed to prepare duration spectra are available for only a few storms, and estimates from early studies are crude. Compared with other Appalachian storms, the November 1985 storm has a distinctive duration spectrum that shows high relative recurrence intervals at long durations (fig. 18). The 1985 storm never reached the recurrence intervals of the other storms, but the moderate-intensity rainfall in the 12- to 48-h range was very effective in destabilizing slopes.

Hurricane Agnes in 1972 produced rainfall with greater amounts but over durations similar to the 1985 storm. Few landslides were triggered by Agnes (Pomeroy, 1980; Costa, 1974), probably because the heaviest rainfall occurred over relatively stable lithologies in gently sloping areas of the Blue Ridge and Piedmont in Pennsylvania, Maryland, and Virginia. Based on the effects of the 1985 storm, one would expect rainfall from Agnes to produce disastrous slope instability if it had fallen on the steeper slopes and shaley lithologies of the Wills Mountain anticline study area.

Data for the 1949 storm that occurred just north of the Wills Mountain anticline study area are not very reliable but are included as a minimum description of that important storm. Studies of the effects of the 1949 storm by Hack and Goodlett (1960) and Stringfield and Smith (1956) cite

evidence that peak intensities were not recorded by the official or unofficial rain gages. The Stringfield and Smith study is particularly germane to our study because the large debris avalanches that they described are similar in location, process, and size to those triggered in 1985; however, many more were triggered during the 1949 event (Clark, 1987, fig. 3). In contrast, no landslides on shaley lithologies were documented in the Petersburg area (Stringfield and Smith, 1956), and air photos of the Wills Mountain anticline study area from 1952 reveal only a few fresh landslides. We suspect that the rainfall in 1949 was effective in triggering the large debris avalanches on sandstone lithologies because it was more intense than actual measurements showed (compare fig. 18, curves a–h and k). The rainfall intensity may have been sufficient to overwhelm infiltration rates on shaley lithologies. Alternatively, the triggering rainfall may have been confined to a very localized convective cell over sandstone. Large debris avalanches on sandstone and shaley sandstone slopes in the Little River area of Virginia were triggered by the same storm (Hack and Goodlett, 1960), but precipitation data are insufficient to adequately characterize intensity and duration of rainfall at that location.

Two other storms depicted in fig. 18 are noteworthy. The rainfall in central Virginia from Hurricane Camille in 1969 was the largest in magnitude among all the storms, and the duration spectrum peaked at 6 h. This storm was noted for the many large debris avalanches it triggered along the Blue Ridge (Williams and Guy, 1973; Gryta and Bartholomew, 1989). The Smethport, Pa., storm of July 1942 has one of the highest 1-h intensities ever recorded. Some small slides, debris flows, and "blowouts" were triggered by the storm, but they were not studied systematically (Eisenlohr, 1952), presumably because the effects were not that dramatic.

Rainfall and Spatial Density of Landslides

As more rainfall infiltrates during a storm event, pore pressures will rise to failure levels for sites of successively greater mechanical stability. Conceptually, the stability of each slope site is characterized by its factor of safety (FS), the ratio of summed resisting forces to summed driving forces. The frequency distribution of FS on the landscape, categorized by site and varying with moisture content, if it could be ascertained, would be a fundamental descriptor of aggregate landscape sensitivity to slope instability. Subjected to a storm delivering uniform rainfall, a landscape with many sites at low FS would have many failures triggered after the initial threshold was reached, and then fewer as the sites of lower stability are cleaned out. Conversely, a landscape with the FS distribution skewed toward many sites at high stability would have few failures in the initial stages of rainfall, but as storm rainfall mounted, more and more sites would be brought to failure. Depending on the shape of the frequency distribution, the number of sites destabilized may suddenly increase or decrease. Furthermore, secondary thresholds may be encountered as landslides or sediment-laden floodwaters erode and unload toe support of neighboring slope sites. A landslide response curve of this type is important for evaluating whether denudation and hazards are related to frequent, low-magnitude events or rare, high-magnitude events (Wolman and Miller, 1960; Wolman and Gerson, 1978).

The relation between rainfall and landslide density (number of landslides per unit area) reflects the FS frequency distribution and will indicate whether sudden thresholds are met with increasing rainfall totals. If the triggering intensity and duration of rainfall can be estimated, then frequency analysis of the triggering rainfall would yield an estimate of the recurrence intervals of associated slope instability.

To construct a relation between rainfall and landslide density for the 1985 storm in the study area, we assumed that the peak of the duration spectrum for the storm (fig. 18) at 48 h is indicative of the triggering duration for Reedsville Shale regolith. The spatial density of landslides at various 48-h precipitation totals on Reedsville Shale was estimated along the Wills Mountain anticline by counting landslides in a 4 km^2 grid cell. Along the southwest two-thirds of the anticline, 48-h rainfall totals and landslide spatial density vary directly with one another (fig. 19). The relation seems to deteriorate near kilometers 45–50, approximately where the southwesternmost large debris avalanches were triggered. Comparison with plate 1*B* shows that almost all of the outcrop belt of Reedsville Shale in the northwestern part of the anticline is covered with a blanket of debris that was shed from North Fork Mountain. Presence of debris, which served to protect the Reedsville Shale slopes from failure, was ignored in the procedure used here to measure the landslide spatial density. When the sampling cells known to be covered by debris are eliminated from the data set, a linear relation between landslide spatial density and 48-h rainfall is evident (fig. 20). The linear relation suggests that no substantial secondary thresholds occurred during the storm.

By using the best fit model of rainfall frequency from the Franklin, W. Va., rain gage, the recurrence intervals for landslides triggered by 48-h rainfall along the valley are estimated to range from 43 to 286 yr. These recurrence intervals can be converted to model the relationship between landslide spatial density and probability of occurrence in any year (fig. 21). Since this frequency analysis does not consider antecedent moisture conditions, it may substantially underestimate or overestimate recurrence intervals for landslide densities. To the extent that other combinations of intensity and duration could be equally or more effective in destabilizing these slopes, this frequency analysis may overestimate recurrence intervals. Evaluations

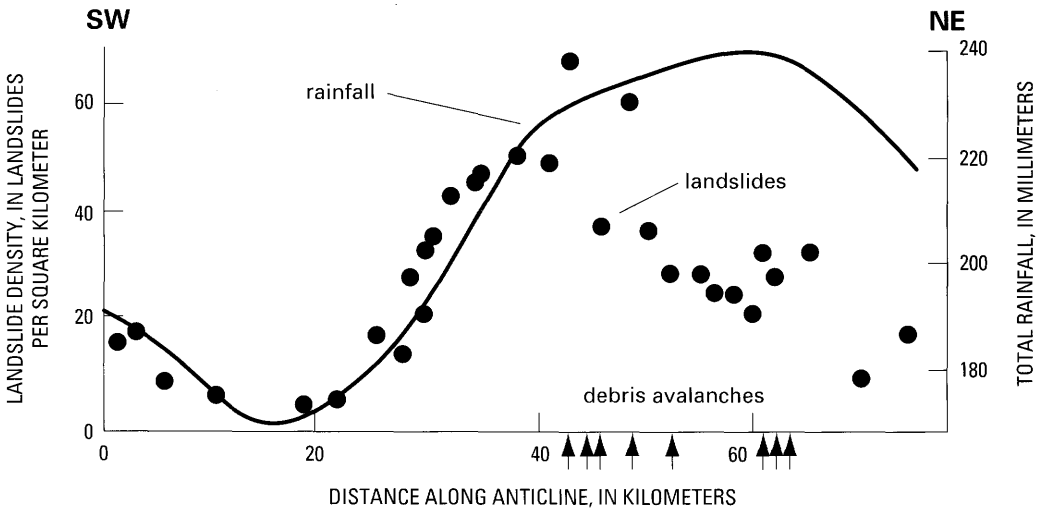

Figure 19. Plot of landslide areal density (landslides/km^2) on Reedsville Shale regolith against distance along SW-NE longitudinal transect of Wills Mountain anticline (solid circles) and 48-h rainfall (solid line) along same transect. Arrows mark locations along transect of large debris avalanches. Northeast of kilometer 45, much of the outcrop area of Reedsville Shale is covered by debris.

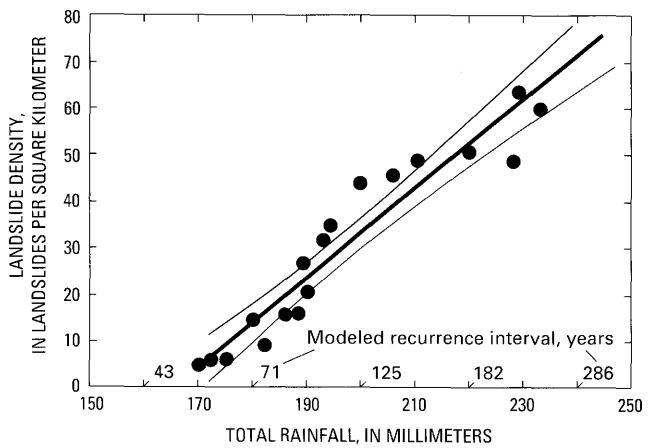

Figure 20. Landslide density on Reedsville Shale (with debris soil removed) plotted against 48-h rainfall totals with estimated recurrence intervals. Thin lines are 90 percent confidence intervals. Equation of the line is landslide density=−169+1.0 (48-h rainfall). R^2=0.90.

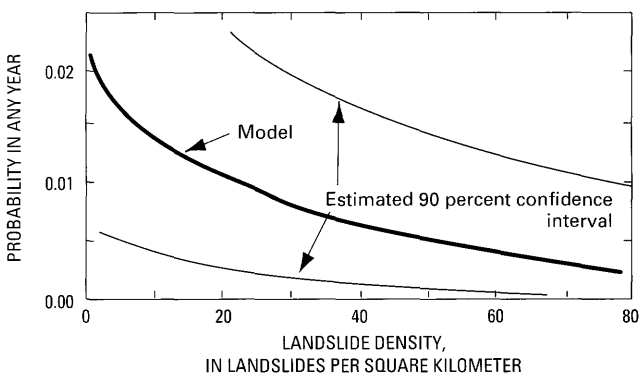

Figure 21. Probability model for landslide density on Reedsville Shale regolith, assuming that 48-h rainfall is the triggering rainfall and that frequency model for 48-h rainfall is accurate. Thin lines are approximate 90 percent confidence intervals estimated from rainfall frequency model (Colucci and others, chapter B, this volume, fig. 12) and landslide density regression.

of these complications and improvements in rainfall measurement will require additional study.

LANDSLIDES AND FLOOD-INDUCED GEOMORPHIC CHANGE

Both the geomorphology of the drainage basin and the sediment delivery from landslides influenced flood damage in the main valley of the North Fork of the South Branch Potomac River. Two methods of analysis were applied to determine the extent of this influence. In the first, the association between presence or absence of landslides and presence or absence of channel erosion or deposition was evaluated for 79 small draining basins. In the second method, the influence of water and sediment discharges from each of the tributary basins was evaluated by an index of flood-induced geomorphic change in the channel and flood plain at the tributary's junction with the North Fork flood plain and compared with basin geomorphology and landslide density.

Channel Changes and Landslides

The study area encompasses parts of the North Fork drainage area (see plate 1 in Jacobson, chapter A, this volume). The river flows through a relatively narrow, structurally controlled valley bordered on the west by the Allegheny Structural Front and on the east by the River Knobs, formed by the northwest limb of the Wills Mountain anticline. Tributary basins drain to the North Fork from the center of the Wills Mountain anticline, through narrow gaps in the River Knobs, and from the Appalachian Plateau. Seventy-nine perennial and intermittent tributary basins as identified on 1:24,000 topographic maps (except Seneca Creek, which was not covered by aerial photography used in the landslide mapping) were selected for the study. These basins ranged in size from 0.13 to 22.41 km^2.

The tributary basins were grouped according to their dominant bedrock geology into the following classes:

- ORV is the interior of Wills Mountain anticline where underlain primarily by Reedsville Shale (19 basins).
- HV is high valley underlain by limestone of the Greenbrier Group and interbedded mudstone and sandstone of the Mauch Chunk Group (16 basins).
- DCH is underlain by sandstone and interbedded mudstone and sandstone of the Devonian Chemung Group and Hampshire Formation (36 basins).
- SD is underlain by Tuscarora Sandstone and limestone, sandstone, and shale in the stratigraphic interval up to the Helderberg Group (8 basins).

For each of the 79 tributary basins in the data set, the association between channel changes and landslides was evaluated by noting the presence or absence of both landslides and fresh erosional and depositional features that were identifiable on air photos and attributable to the 1985 event (table 6). Erosional features were reaches of streams that were newly entrenched, steep and freshly eroded banks, and anomalously widened reaches. Depositional features were cobble and gravel channel deposits, levee and splay deposits, and fans. For the data set, 97 percent of the changed stream channels are associated with landslides, and only 7 percent of nonchanged stream channels are associated with landslides. A chi-square test of the association between channel change and landslides is significant at the 0.005 level.

Although this evidence for association is overwhelming, it does not consider the causal link between landslides and channel change. For basins underlain predominantly by Reedsville Shale (ORV basins), field observations confirmed that, in the majority of cases, channel change began abruptly at the point where landslide sediment was delivered to the channel. This relation was not as clear in basins underlain by other lithologies, where channel damage generally increased in proportion to increasing drainage area.

Table 6. Association between slope movement and damage to stream channel for 79 drainage basins

Category	Slope movement	No slope movement	Total
Channel damage	36	1	37
No channel damage	3	39	42
Total	39	40	79

Tributary Channel-Change Index, Analytical Methods, and Results

Geomorphic effects from flooding in tributary basins were widespread and locally intense. The semiquantitative channel-change index was developed to characterize the geomorphic effects at the mouths of the 79 tributaries where they meet the North Fork River, and to evaluate how the addition of sediment from landslides into the basins contributed to flood damage. The index was based on the presence of the following features: channel widening and scour, channel avulsion, deposition along the channel and at the mouth, braided-channel development, and damage to roads, vegetation, and structures. Aerial photographs (both preflood and postflood) were utilized to evaluate these criteria (see Miller and Parkinson, chapter E, this volume, figs. 22–28, for examples). Most of the observations were made from postflood photographs, which were taken for the West Virginia Department of Highways within several days after the flood (scale approximately 1:10,000). Pre-1985 photographs from the U.S. Soil Conservation Service (scale approximately 1:20,000) were used as a reference for preflood conditions. Many of the tributaries were also visited in the field in 1987 to substantiate the classification.

The effects most commonly seen on the tributaries were channel widening combined with deposition or exposure of a lag deposit of coarse sediment near the mouth and along the lower reaches of the stream. Many of the tributaries had well-imbricated deposits of cobbles across the entire channel and along the margins, a condition indicative of bed mobilization during the flood. Several stream channels that carried large amounts of coarse sediment and organic debris had logjams that trapped substantial amounts of sediment upstream. In these cases, morphologic changes at the tributary junction are presumably smaller than would be expected if all the sediment was delivered from the basins. Most of the tributaries had a "gutted" appearance due to channel widening, cobble levees, and removal of fine sediment and vegetation. Fans that existed at the mouths of tributaries prior to the 1985 event showed renewed sedimentation of gravel and cobbles and (or) erosion.

The following classes of change were used to evaluate the tributary channel-change index:

1. No apparent change
2. Very slight change; small amount of channel scouring or sediment deposited at mouth

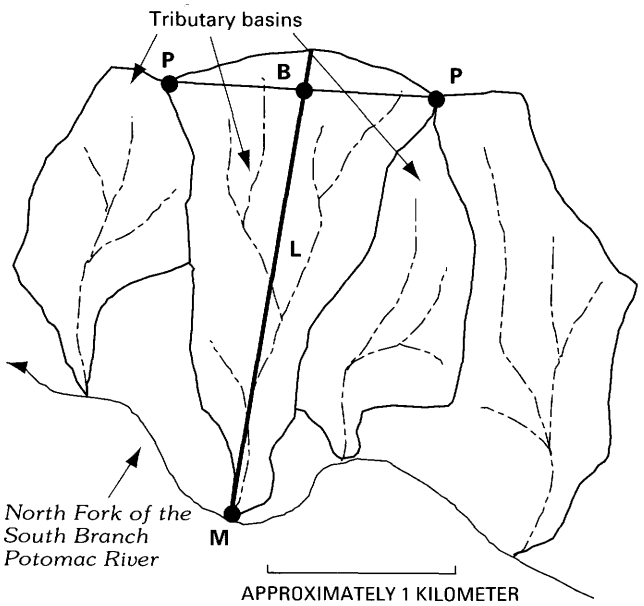

Figure 22. Measurement parameters for basin morphology. Points P are the highest points along the side divides. Basin length, L, is the length of the line that bisects PP, at point B, and connects the basin mouth M and the basin divide.

3. Transition
4. Slight change; sediment deposited at mouth and/or some disruption of preflood channel
5. Transition
6. Moderate change; some channel widening and/or substantial amount of sediment at mouth and/or erosion or deposition along portions of tributary channel; may have some deposition on alluvial fan (if present) at the mouth of the tributary
7. Transition
8. Major change; large deposit on fan at mouth (if flow does not enter directly into main flood channel) and disruption of major portion of preflood channel
9. Transition
10. Extreme change; large, well-developed deposit on fan at mouth or creation of new fan and modification of entire preflood channel

Basin length, relief, and area were measured from USGS 1:24,000 topographic maps to characterize morphometry of the basins that might be related to hydrologic responses. Basin length was measured along the basin axis as defined in figure 22. The basin axis was determined by drawing a straight line between the mouth and the bisector of a line between the highest elevation points on the side divides of the adjacent basins. Basin length and relief were measured between the mouth and the point where this "basin axis" intersected the basin divide. In many basins, this point was also the highest or farthest from the mouth. Although this method will not work in very irregular and dogleg-shaped basins, it did work well to characterize these basins.

Relief ratio, defined as the ratio of basin relief to basin length, was used as a parameter for relative steepness of the basins. Among basins of uniform geology, basins with high relief ratios should have faster, and presumably more erosive, runoff than those with low relief ratios.

The change index is highly correlated with the morphometric parameters of basin length, relief, and area as well as with landslide density (table 7, fig. 23). For all basins, and for most subsets by dominant bedrock geology, correlations are highest with basin length. Landslide density is generally significantly correlated with the channel-change index, although it commonly ranks second or third behind basin length. In most cases, also, the morphometric parameters are highly correlated among themselves, reflecting the tendency for larger basins to encompass greater relief. Correlations with rainfall, which varied from 190 to 240 mm over the study basins, are relatively poor.

All correlation coefficients are higher for analyses limited to ORV basins. In ORV basins, the correlation between landslide spatial density and channel-change index is much higher than that for all basins, and precipitation is of minor importance. Correlation coefficients for DCH, SD, and HV basins are all extremely low (<0.10), possibly because of the low numbers of samples, uncertainties in evaluation of the change index for the smaller DCH basins, or insensitivity of the change index to measured parameters.

The same independent variables were used in stepwise multivariate regression in order to rank their importance in influencing channel-change index. Because high collinearity exists among basin length and basin area, only basin length was used in the analysis. Although basin length and basin relief also vary collinearly, basin relief was retained as an independent variable.

The results of the multivariate regression (table 8) show that basin length explains most of the variance for all basins and is important for most subsets of basins. For DCH basins, none of the variables provides significant explanation, and for SD basins the sample size is too small to resolve adequately the importance of individual variables. Landslide density, relief, and rainfall are of secondary importance. Landslide density makes substantial contributions to model R^2 values when all basins are combined and when only ORV basins are considered.

Landslide Spatial Density, Basin Morphology, and Flood Effects

Among the subsets of basins sorted by dominant bedrock geology, ORV basins had the highest landslide densities. The weak but significant relation between channel-change index and landslide spatial density for ORV basins suggests that landslide activity in these basins was

Table 7. Correlation coefficients between basin variables

[The top number is the correlation coefficient (R) and the bottom is the probability that R=0. Density is landslide spatial density in basin; other variables and basin groups are explained in text. *N*, number of basins in sample]

Variable	Damage	Density	Length	Area	Relief ratio	Rain
			All basins, *N*=76			
Damage	1.00000	0.42904	0.59807	0.50973	0.36831	0.00640
	.0000	.0001	.0001	.0001	.0009	.9556
Density		1.00000	.34867	.19194	.16724	− .09960
		.0000	.0018	.0923	.1433	.3856
Length			1.00000	.74599	.85356	− .25484
			.0000	.0001	.0001	.0243
Area				1.00000	.49495	− .01819
				.0000	.0001	.8744
Relief ratio					1.00000	− .30151
					.0000	.0073
Rain						1.00000
						.0000
			DCH, *N*=36			
Damage	1.00000	0.29626	0.14406	0.08082	0.12716	− .07820
	.0000	.0794	.4019	.6394	.4599	.6503
Density		1.00000	.00191	− .07397	− .03379	.03188
		.0000	.9912	.6681	.8449	.8535
Length			1.00000	.71575	.34664	− .59515
			.0000	.0001	.0383	.0001
Area				1.00000	.37693	− .47677
				.0000	.0234	.0033
Relief ratio					1.00000	− .13282
					.0000	.4400
Rain						1.00000
						.0000
			HV, *N*=16			
Damage	1.00000	0.01821	0.23714	−0.02366	−0.04921	−0.02948
	.0000	.9466	.3765	.9307	.8564	.9137
Density		1.00000	− .27066	− .60215	− .30535	.26928
		.0000	.3106	.0136	.2501	.3132
Length			1.00000	.61884	.90013	− .47865
			.0000	.0106	.0001	.0607
Area				1.00000	.55999	− .26166
				.0000	.0241	.3276
Relief ratio					1.00000	− .47419
					.0000	.0635
Rain						1.00000
						.0000
			ORV, *N*=19			
Damage	1.00000	0.72059	0.77477	0.58383	−0.04282	0.47009
	.0000	.0007	.0002	.0110	.8660	.0490
Density		1.00000	.59643	.22411	− .11531	.30348
		.0000	.0090	.3713	.6487	.2209
Length			1.00000	.72060	.50006	.62499
			.0000	.0007	.0346	.0055
Area				1.00000	.26213	.63119
				.0000	.2934	.0050
Relief ratio					1.00000	.31692
					.0000	.2001
Rain						1.00000
						.0000

Table 7. Correlation coefficients between basin variables—Continued

Variable	Damage	Density	Length	Area	Relief ratio	Rain
			SD, N=6			
Damage	1.00000	0.70141	0.46805	0.39806	0.28242	0.55391
	.0000	.1204	.3492	.4345	.5876	.2541
Density		1.00000	.22357	.20915	.13413	.42333
		.0000	.6702	.6908	.8000	.4029
Length			1.00000	.96408	.92117	− .46892
			.0000	.0019	.0091	.3482
Area				1.00000	.98855	− .49060
				.0000	.0002	.3231
Relief ratio					1.00000	− .56052
					.0000	.2473
Rain						1.00000
						.0000

sufficient to influence geomorphic changes in the flood plain and channel during the flood. Apparently, the spatial densities of landslides in basins dominated by other types of bedrock geology did not contribute enough sediment to the tributary channels to exceed channel erosion thresholds.

The channel-change index correlates poorly with relief ratio (R^2=0.002−0.14), a result that is contrary to our initial expectations that steeper topography would be associated with faster runoff and more erosive flows. Instead, the channel-change index correlates better with basin length (R^2=0.02−0.60). The direct relation between channel-change index and basin length does not reflect simply the effect of greater basin area because in all cases the correlation between the index and basin area is weaker than that between the index and basin length (table 7).

The process responsible for the importance of basin length is unknown, but a variety of possibilities exist. Longer ORV basins appear to have a greater percentage of the basin underlain by the Reedsville Shale, in which there is a greater spatial density of landslides; this condition would promote greater relative sediment supply in the longer ORV basins. Also, the lower reaches of the longer streams are generally wider, have lower channel gradients, and have better developed flood plains than the shorter ones. Hence, the longer streams provide a better environment for channel erosion and deposition, whereas sediment may be flushed through the shorter basins without producing the kinds of changes detected in this study. Also, the longer basins may have greater drainage densities than the shorter basins, and greater lengths of high-order channels; this would increase the efficiency of routing sediment and water to the lower reaches. The relative importance of each of these factors is unknown; further study and an expanded data base are needed to evaluate and rank the factors.

DISCUSSION AND CONCLUSIONS

Our analysis of landslides triggered by the November 1985 storm indicates that landslide locations in this landscape are determined by a complex combination of factors: stability of slope sites related to rainfall, antecedent moisture of regolith, bedrock lithology, bedrock structure, surficial geology, slope morphology, and land cover. Among these variables, only rainfall, bedrock lithology, and bedrock structure can be considered independent. Slope morphology and surficial geology are strongly related to the bedrock; land cover and antecedent moisture of regolith are interdependent with slope morphology and the geologic factors.

At the scale of the entire study area, the primary control on the spatial distribution of landslides is the distribution of rainfall. Second in importance is the bedrock lithology, which, through its control on regolith properties, determined the extent of slope stability for the rainfall intensity and duration of this particular storm. Third, but superimposed on bedrock lithology, the distribution of Quaternary debris had an important role in determining where landslides were located in a given bedrock unit. Land cover and slope morphology become important factors in slope stability for areas where the rainfall, bedrock, and surficial geology do not vary.

Study of the physical properties of several of the materials that were more susceptible to failure during the 1985 storm suggests that landslide susceptibility was due to particular combinations of infiltration rate and strength. The most unstable lithology, residuum derived from the Reedsville Shale, had intermediate infiltration rates and low strength, as indicated by its high plasticity index. However, regolith of the Trenton Group, which had higher plasticity and hence probably lower strength, had very few failures, probably because of its extremely high infiltration and drainage rates. Relative stability of other regoliths is attributable to higher infiltration and drainage rates, or other factors imparting higher strength. Other documented storm events that have been effective in triggering landslides in the Appalachian Mountains have involved more intense rainfall on coarser grained regolith that presumably would have relatively high infiltration and drainage rates.

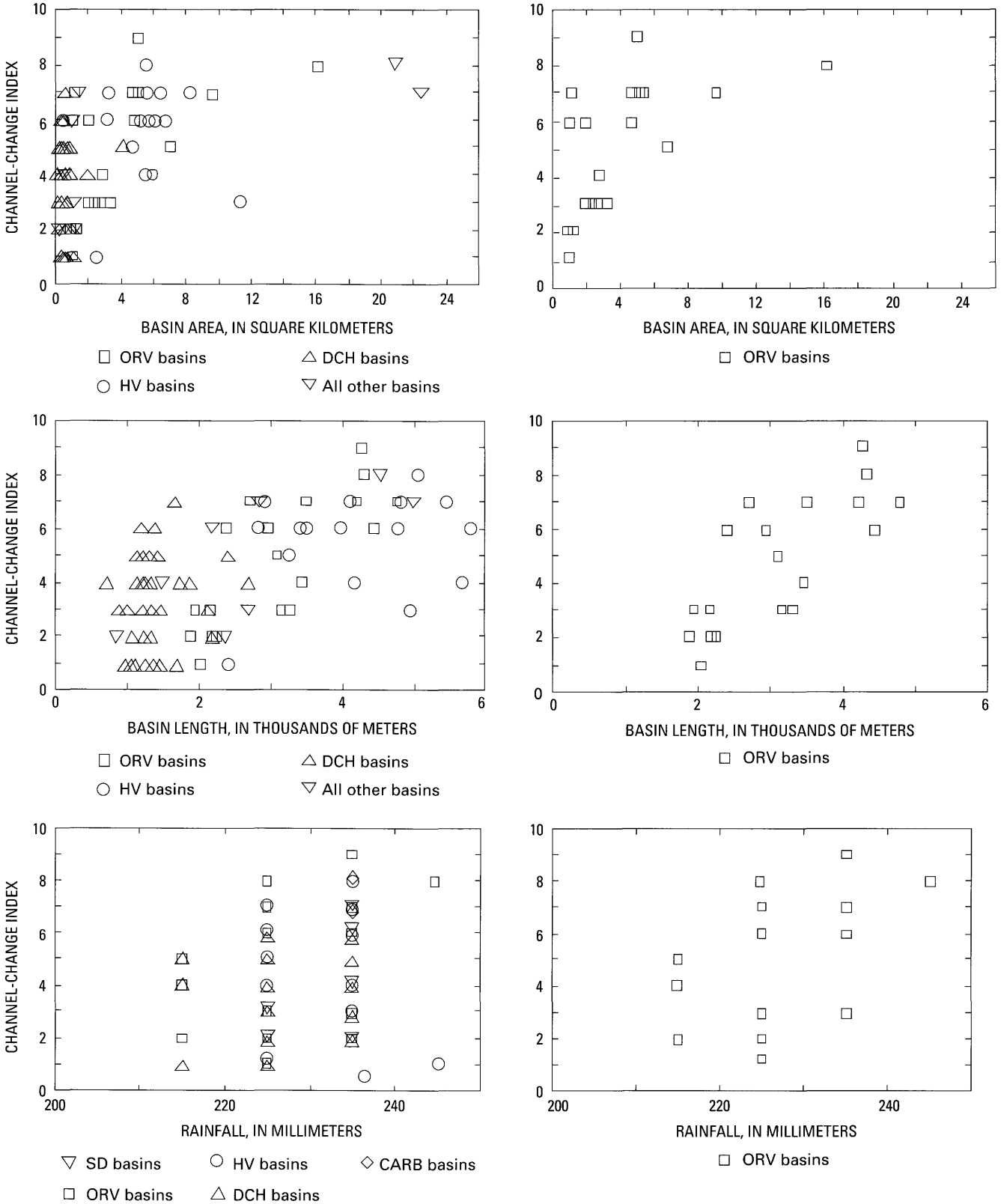

Figure 23. Scatter plots of the channel-change index and basin parameters, by basin types according to dominant lithology. Points labeled NTH are Noah Teter Hollow, where a large amount of sediment supplied from upstream was trapped behind a slump dam on the side of the stream. Separate plots of ORV, which were the basins experiencing the greatest landslide density, show influence of basin length and landslide density.

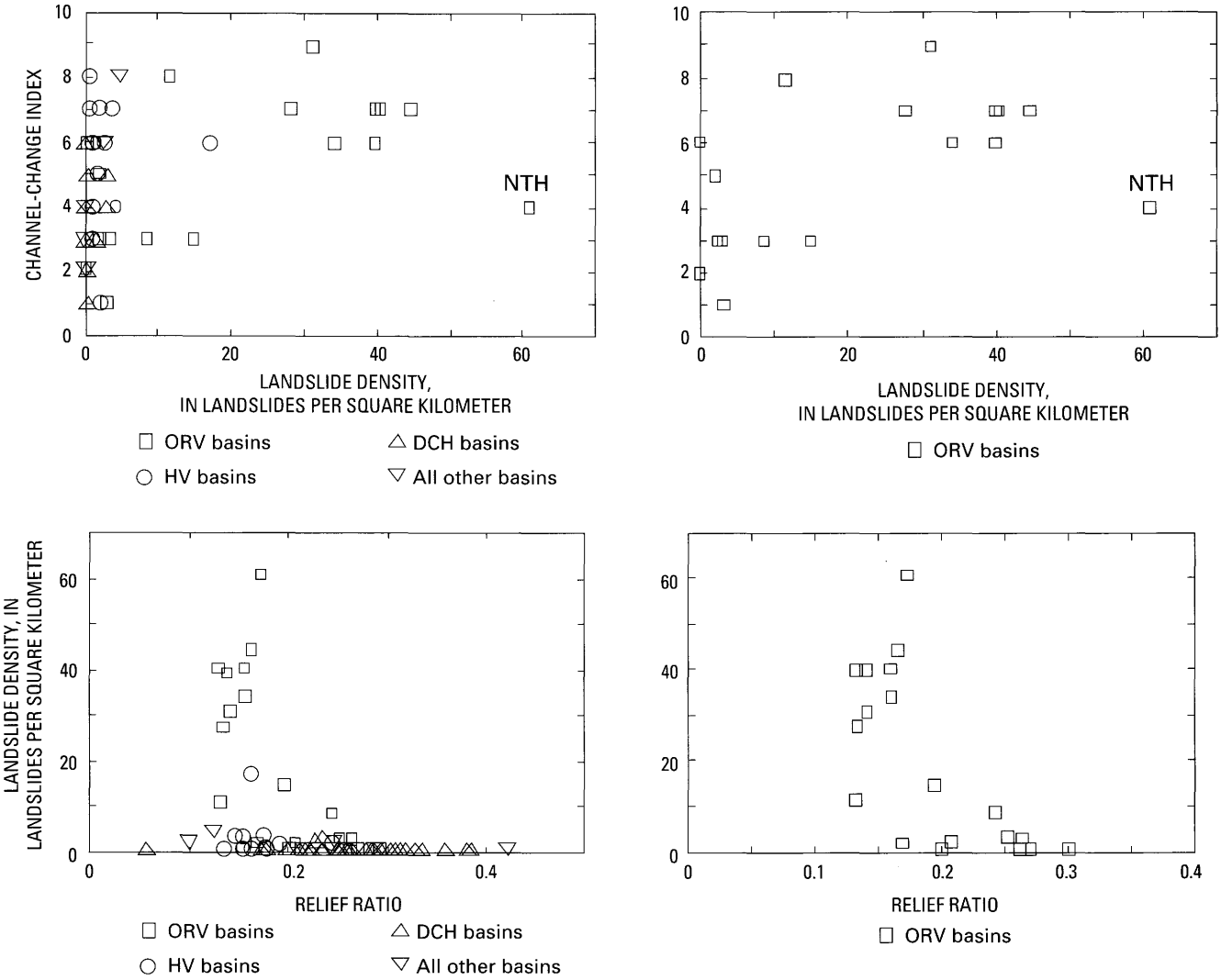

Figure 23. Continued.

Over areas underlain only by regolith derived from Reedsville Shale, the slope morphology and land cover type become additional factors in determining the distribution of slope instability. Interdependence of these factors is further complicated by trade-offs among them in determination of stability of individual sites. For example, the tendency for landslides under forest to occur in hillslope hollows, whereas those under pasture cover tend to occur on other parts of the landscape as well, suggests that strength imparted by tree roots is compensated by increased moisture and (or) thicker colluvium in hillslope hollows. Similarly, for sandy regolith derived from sandstone bedrock, both ground-water flow and low strength on bedding plane surfaces tend to make dipslopes relatively insensitive to topographic convergence, whereas on antidipslopes, topographic convergence in hillslope hollows assumes greater importance in determining slope stability.

Our observations on the controlling factors for landslide location may hold only for the particular intensity and duration of the November 1985 triggering event. Storms of different intensity and duration will probably destabilize sites with different characteristics. In particular, our observation that the high-intensity 1949 storm destabilized large areas of North Fork Mountain underlain by Tuscarora Sandstone, and that similar areas were relatively stable in 1985, suggests that rainfall intensity and duration are important determinants of what types of lithologies are destabilized.

The highly selective destabilization of regoliths during this storm and comparisons with other storms suggest that, in the Appalachian Mountain landscape, different rainfall characteristics are effective in destabilizing slopes, depending primarily on the underlying bedrock lithology. Bedrock lithology, in turn, strongly determines regolith

Table 8. R^2 values for multivariate models explaining the channel-damage index

[Basin groups are explained in text. *N*, number of basins]

Number of variables in model	R^2	Variables in model
All basins, *N*=76		
1	0.32753208	Length
1	.19937544	Density
1	.13641939	Relief ratio
1	.00017394	Rain
2	.40251798	Length, relief ratio
2	.39205539	Length, density
2	.35243367	Length, rain
2	.28856567	Relief ratio, density
2	.20033295	Density, rain
2	.14741423	Relief ratio, rain
3	.43152481	Length, relief ratio, density
3	.41850116	Length, relief ratio, rain
3	.41633221	Length, density, rain
3	.30409283	Relief ratio, density, rain
4	.44907037	Length, relief ratio, density, rain
DCH basins, *N*=36		
1	0.08777079	Density
1	.02075444	Length
1	.01617088	Relief ratio
1	.00611482	Rain
2	.10836223	Length, density
2	.10660956	Relief ratio, density
2	.09545999	Density, rain
2	.02753288	Length, relief ratio
2	.02084254	Length, rain
2	.01999700	Relief ratio, rain
3	.11706091	Length, relief ratio, density
3	.11153759	Relief ratio, density, rain
3	.10836996	Length, density, rain
3	.02753475	Length, relief ratio, rain
4	.11720699	Length, relief ratio, density, rain
HV basins, *N*=16		
1	0.05623464	Length
1	.00242114	Relief ratio
1	.00086919	Rain
1	.00033150	Density
2	.41980936	Length, relief ratio
2	.06539307	Length, rain
2	.06355956	Length, density
2	.00601965	Relief ratio, rain
2	.00243231	Relief ratio, density
2	.00160626	Density, rain
3	.42056862	Length, relief ratio, rain
3	.41981953	Length, relief ratio, density
3	.07039695	Length, density, rain
3	.00617309	Relief ratio, density rain
4	.42062404	Length, relief ratio, density, rain

Table 8. R^2 values for multivariate models explaining the channel-damage index—Continued

Number of variables in model	R^2	Variables in model
ORV basins, *N*=18		
1	0.60027558	Length
1	.51925368	Density
1	.22098481	Rain
1	.00183317	Relief ratio
2	.84711837	Length, relief ratio
2	.70398994	Length, density
2	.58887082	Density, rain
2	.52089756	Relief ratio, density
2	.26187869	Relief ratio, raid
3	.84820140	Length, relief ratio, density
3	.84733988	Length, relief ratio, rain
3	.70430002	Length, density, rain
3	.59271532	Relief ratio, density, rain
4	.84831393	Length, relief ratio, density, rain
SD basins, *N*=6		
1	0.49197952	Density
1	.30681818	Rain
1	.21906862	Length
1	.07976379	Relief ratio
2	.98579687	Length, rain
2	.81939800	Relief ratio, rain
2	.59394197	Length, density
2	.57243706	Density, rain
2	.52810288	Relief ratio, density
2	.36511838	Length, relief ratio
3	.99482908	Length, density, rain
3	.98926965	Length, relief ratio, rain
3	.85371516	Relief ratio, density, rain
3	.66746404	Length, relief ratio, density
4	.99895547	Length, relief ratio, density, rain

properties and slope morphology. High-intensity, short-duration storms would be more effective in destabilizing regolith with high infiltration and drainage rates, such as regolith derived from sandstones and coarse-grained igneous rocks. High-intensity, short-duration storms may be too short to allow concentration of sufficient moisture in regolith with slower infiltration rates, and rainfall intensities may be high enough to promote direct runoff. Low-intensity, long-duration storms, like the 1985 storm, would be slow enough to allow moisture to drain from most slopes on coarse-grained regolith but would allow moisture to accumulate on fine-grained regolith.

One implication of this model is that predicted locations of landslide hazards should be determined from rock type and rainfall intensity and duration characteristics of particular storms, rather than just total rainfall. Another implication for general geomorphic models is that the magnitude and frequency of meteorologic events that are geomorphically effective on slopes will vary across the landscape, depending primarily on rock type. Hence, in the Appalachian Valley and Ridge, where bedrock lithologies are highly variable, different slopes can be said to be equilibrated to different types of storms.

The 1985 storm produced long, slow rainfall with storm totals that were rare over durations from 24 to 72 h. Landslide density on Reedsville Shale has a linear relation with measured 48-h rainfall along the Wills Mountain anticline. Available evidence does not indicate any signif-

icant secondary thresholds or sudden increases in landslide density with increasing rainfall. Comparison of landslide density to recurrence frequency of the apparent triggering rainfall shows that the recurrence of slope instability experienced in 1985 varied from 43 yr for 1 landslide/km^2 to nearly 300 yr for 70 landslides/km^2. However, error limits on these frequencies are large, and further refinement will require more well-documented landslide events, calibration with data from instrumented slopes, longer rainfall records, and refined frequency analysis techniques.

Analysis of the relation between landslides and flood-induced geomorphic effects in stream channels shows a strong correlation between the presence of landslides and the presence of substantial channel changes. In shaley lithologies, individual landslides had the most influence on stream channels that were directly adjacent. Erosion and deposition attributable to individual landslides decreased downstream as opportunities occurred for sediment retention behind temporary dams and as water discharge increased and diluted the sediment concentrations. As a result, the direct effects of these landslides usually were not apparent at distances of 50–100 m downstream. In contrast, local effects of single landslides triggered in sandy, bouldery regolith associated with the Tuscarora Sandstone were obvious and dramatic up to 2 km downstream (Kite and Linton, 1987; Jacobson and others, 1989).

Channel changes at tributary-main stem junctions measured the indirect, cumulative influences of landslides and other morphometric variables on geomorphic changes induced by the flooding. This analysis showed that channel change is correlated best with basin length, a morphometric parameter that may be related to volume or rate of runoff from the basins. Landslide density in the basins is of secondary importance, being more significant in basins underlain by the geologic unit that is most susceptible to failure: the Reedsville Shale. Linkage of the magnitude of flood damage to landslide influences suggests that in the steep Appalachian landscape, flood hazards are augmented by upstream sediment supply from landslides.

REFERENCES CITED

Bailey, J.F., Patterson, J.L., and Paulhus, J.L.H., 1975, Hurricane Agnes rainfall and floods, June–July 1972: U.S. Geological Survey Professional Paper 924, 403 p.

Bogucki, D.J., 1976, Debris slides in the Mt. Le Conte area, Great Smoky Mountains National Park, U.S.A.: Geografiska Annaler, v. 58A, p. 179–191.

Braun, D.D., Gilmeister, N.M., and Inners, J.D., 1989, Postglacial to historic dip-slope block slides in the Valley and Ridge province of northeastern Pennsylvania, *in* Schultz, A.P., and Jibson, R.W., eds., Landslide processes of the Eastern United States and Puerto Rico: Geological Society of America Special Paper 236, p. 75–88.

Caine, N., 1980, The rainfall intensity-duration control of shallow landslides and debris flows: Geografiska Annaler, v. 62A, p. 23–27.

Camp, J.D., and Miller, E.M., 1970, Flood of August 1969 in Virginia: U.S. Geological Survey Open-File Report, 120 p.

Campbell, R.H., Varnes, D.J., Fleming, R.W., Hampton, M.H., Prior, D.B., Sangrey, D.A., Nichols, D.R., and Brabb, E.E., 1985, Landslide classification for identification of mud flows and other landslides, *in* Campbell, R.H., ed., Feasibility of a nationwide program for the identification and delineation of hazards from mud flows and other landslides: U.S. Geological Survey Open-File Report 85–276, p. A1–A24.

Cardwell, D.H., Erwin, R.B., and Woodward, H.P., 1968, Geologic map of West Virginia: West Virginia Geological and Economic Survey, scale 1:250,000, 2 sheets.

Clark, G.M., 1987, Debris slide and debris flow historical events in the Appalachians south of the glacial border, *in* Costa, J.E., and Wieczorek, G.E., eds., Reviews in engineering geology, v. vii: Boulder, Colo., Geological Society of America, p. 125–138.

Costa, J.E., 1974, Response and recovery of a Piedmont watershed from tropical storm Agnes, June 1972: Water Resources Research, v. 10, p. 106–112.

———1987, A comparison of the largest rainfall-runoff floods in the United States with those of the People's Republic of China and the world: Journal of Hydrology, v. 96, p. 101–115.

Cron, E.D., 1990, Analysis of landslides resulting from a severe storm; a geographic information system application: Fairfax, Va., George Mason University, unpublished Masters thesis, 30 p.

Diecchio, R.J., 1986, Taconian clastic sequence and general geology in the vicinity of the Allegheny Front in Pendleton County, West Virginia, *in* Neathery, T.L., ed., Centennial field guide, v. 6: Southeastern Section of the Geological Society of America, p. 85–90

Dietrich, W.E., Reneau, S.L., and Wilson, C.J., 1987, Overview: "Zero-order basins" and problems of drainage density, sediment transport and hillslope morphology: Erosion and sedimentation in the Pacific rim (Proceedings of the Corvallis Symposium, August 1987): International Association of Hydrological Sciences Publication 165, p. 27–37.

Eisenlohr, W.S., Jr., 1952, Floods of July 18, 1942 in north-central Pennsylvania: U.S. Geological Survey Water Supply Paper 1134–B, 98 p.

Erskine, H.M., 1952, Flood of August 4–5, 1943 in central West Virginia: U.S. Geological Survey Water Supply Paper 1134–A, 57 p.

Everett, A.G., 1979, Secondary permeability as a possible factor in the origin of debris avalanches associated with heavy rainfall: Journal of Hydrology, v. 43, p. 347–354.

Fleming, R.W., Johnson, A.M., Hough, J.E., Gokce, A.O., and Lion, T., 1981, Engineering geology of the Cincinnati area, *in* Roberts, T.G., ed., Cincinnati 1981 field trip guidebook, v. 3: Boulder, Colo., Geological Society of America, p. 543–570.

Gryta, J.J., and Bartholomew, M.J., 1989, Factors influencing the distribution of debris avalanches associated with the 1969 Hurricane Camille in Nelson County, Virginia, *in* Schultz,

A.P., and Jibson, R.W., eds., Landslide processes of the Eastern United States and Puerto Rico: Geological Society of America Special Paper 236, p. 15–28.

Hack, J.T., and Goodlett, J.C., 1960, Geomorphology and forest ecology of a mountain region in the central Appalachians: U.S. Geological Survey Professional Paper 347, 66 p.

Hershfield, D.M., 1961, Rainfall frequency atlas of the United States: U.S. Weather Bureau Technical Paper 40, 114 p.

Hoxit, L.R., Maddox, R.A., Chappell, C.F., and Brua, S.A., 1982, Johnstown–western Pennsylvania storm and floods of July 19–20, 1977: U.S. Geological Survey Professional Paper 1211, 68 p.

Interagency Advisory Committee on Water Data, 1982, Guidelines for determining flood flow frequency: U.S. Geological Survey, Bulletin 17B of the Hydrology Subcommittee, 27 p. + app.

Jacobson, R.B., 1985, Spatial and temporal distributions of slope processes in the upper Buffalo Creek drainage basin, Marion County, West Virginia: Baltimore, Md., Johns Hopkins University, unpublished Ph.D. dissertation, 485 p.

Jacobson, R.B., Cron, E.D., and McGeehin, J.P., 1989, Slope movements triggered by heavy rainfall, November 3–5, 1985, in Virginia and West Virginia, U.S.A., *in* Schultz, A.P., and Jibson, R.W., eds., Landslide processes of the Eastern United States and Puerto Rico: Geological Society of America Special Paper 236, p. 1–14.

Jacobson, R.B., McGeehin, J.P., and Cron, E.D., 1987, Hillslope processes and surficial geology, Wills Mountain anticline, West Virginia and Virginia, *in* Kite, J.S., ed., Research on the Late Cenozoic of the Potomac highlands, Southeastern Friends of the Pleistocene, v. 1: West Virginia Geologic and Economic Survey Open-File Report OF 88–02, p. 31–50.

Jennings, A.H., 1950, World's greatest observed point rainfall: Monthly Weather Review, v. 78, p. 4–5.

Kite, J.S., and Linton, R.C., 1987, Judy Run debris avalanche-debris flow, *in* Kite, J.S., ed., SEFOP 1987 Field guide for the first annual meeting of the Southeastern Friends of the Pleistocene: Southeastern Friends of the Pleistocene, v. 2: West Virginia Geologic and Economic Survey Open-File Report, OF 88–02, p. 23–24, 36.

Kite, J.S., Linton, R.C., and Gerritsen, S., 1987, The Twin Run debris avalanche-debris flow, *in* Kite, J.S., ed., SEFOP 1987 Field guide for the first annual meeting of the Southeastern Friends of the Pleistocene: Southeastern Friends of the Pleistocene, v. 2: West Virginia Geologic and Economic Survey Open-File Report, OF 88–02, p. 34–52.

Kulander, B.R., and Dean, S.L., 1986, Structure and tectonics of central and southern Appalachian Valley and Ridge and Plateau provinces, West Virginia and Virginia: American Association of Petroleum Geologists Bulletin, v. 70, p. 1674–1684.

Lessing, Peter, and Erwin, R.B., 1977, Landslides in West Virginia, *in* Coates, D.R., ed., Landslides, Reviews in engineering geology series, v. III: Boulder, Colo., Geological Society of America, p. 245–254.

Lessing, Peter, Kulander, B.R., Wilson, B.D., Dean, S.L., and Woodring, S.M., 1976, West Virginia landslides and slide-prone areas: West Virginia Geological and Economic Survey, Environmental Geology Bulletin 15, 64 p., 35 pls.

Lessing, Peter, Messina, C.P., and Fonner, R.F., 1983, Landslide risk assessment: Environmental Geology, v. 5, p. 93–99.

Miller, J.F., 1964, Two- to ten-day precipitation for return periods of 2 to 100 years in the contiguous United States: U.S. Weather Bureau Technical Paper 49, 29 p.

Mills, H.H., 1981, Boulder deposits and the retreat of mountain slopes, or "gully gravure" revisited: Journal of Geology, v. 89, p. 649–660.

———1988, Surficial geology and geomorphology of the Mountain Lake area, Giles County, Virginia, including sedimentological studies of colluvium and boulder streams: U.S. Geological Survey Professional Paper 1469, 57 p.

Mitchell, J.K., 1976, Fundamentals of soil behavior: New York, Wiley and Sons, 422 p.

Moneymaker, B.C., 1939, Erosional effects of the Webb Mountain (Tennessee) cloudburst of August 5, 1938: Journal of the Tennessee Academy of Science, v. 14, p. 190–196.

National Oceanic and Atmospheric Administration, 1985, Climatological data, West Virginia, v. 93, no. 11: Asheville, N.C., National Climatic Data Center, 19 p.

———1986, Climatic data: Asheville, N.C., National Climatic Data Center, digital media.

Neary, D.G., and Swift, L.W., Jr., 1987, Rainfall thresholds for triggering a debris avalanching event in the southern Appalachian Mountains, *in* Costa, J.E., and Wieczorek, G.E., eds., Reviews in engineering geology, v. vii: Boulder, Colo., Geological Society of America, p. 81–92.

Perry, W.J., Jr., 1971, Structural development of the Nittany Anticlinorium, Pendleton County, West Virginia: New Haven, Conn., Yale University, unpublished Ph.D. dissertation, 227 p. and maps.

Pomeroy, J.S., 1980, Storm-induced debris avalanching and related phenomena in the Johnstown area, Pennsylvania, with reference to other studies in the Appalachians: U.S. Geological Survey Professional Paper 1191, 23 p.

———1982a, Mass movement in two selected areas of Washington County, Pennsylvania: U.S. Geological Survey Professional Paper 1170–B, 17 p.

———1982b, Landslides in the greater Pittsburgh region, Pennsylvania: U.S. Geological Survey Professional Paper 1229, 48 p.

———1984, Storm-induced landslides at East Brady, northwestern Pennsylvania: U.S. Geological Survey Bulletin 1618, 16 p.

———1987, Slope stability in the Marietta area, Washington County, southeastern Ohio: U.S. Geological Survey Bulletin 1695, 47 p.

Reneau, S.L., and Dietrich, W.E., 1987, Size and location of colluvial landslides in a steep forested landscape: Erosion and sedimentation in the Pacific rim (Proceedings of the Corvallis Symposium, August 1987): International Association of Hydrological Sciences Publication 165, p. 39–48.

Reneau, S.L., Dorn, R.I., Berger, C.R., and Rubin, Meyer, 1986, Geomorphic and paleoclimatic implication of latest Pleistocene radiocarbon dates from colluvium-mantled hollows, California: Geology, v. 14, p. 655–658.

Royster, D.L., 1973, Highway landslide problems along the Cumberland plateau in Tennessee: Association of Engineering Geologists Bulletin, v. 10, p. 255–287.

Schneider, R.H., 1973, Debris slides and related flood damage resulting from Hurricane Camille, 19–20 August, and subsequent storm, 5–6 September, 1969, in the Spring Creek drainage basin, Greenbriar County, West Virginia: Knoxville, Tenn., University of Tennessee, unpublished Ph.D. dissertation, 131 p.

Sidle, R.C., Pearce, A.J., and O'Loughlin, C.L., 1985, Hillslope stability and land use, Water Resources Monograph 11: Washington, D.C., American Geophysical Union, 140 p.

Stringfield, V.T., and Smith, R.C., 1956, Relation of geology to drainage, floods, and landslides in the Petersburg area, West Virginia: West Virginia Geological and Economic Survey, Report of Investigation 13, 19 p.

Varnes, D.J., 1978, Landslides, types and processes, *in* Schuster, R.L., and Krizek, R.J., eds., Landslides—analysis and control: National Academy of Sciences, Transportation Research Board Special Report 176, p. 11–33.

Wieczorek, G.E., 1987, Effect of rainfall intensity and duration on debris flows in central Santa Cruz Mountains, California, *in* Costa, J.E., and Wieczorek, G.E., eds., Reviews in engineering geology, v. vii: Boulder, Colo., Geological Society of America, p. 125–138.

Williams, G.P., and Guy, H.P., 1973, Erosional and depositional aspects of Hurricane Camille in Virginia, 1969: U.S. Geological Survey Professional Paper 804, 80 p.

Wolman, M.G., and Gerson, Ran, 1978, Relative scales of time and effectiveness of climate in watershed geomorphology: Earth Surface Processes, v. 3, p. 189–208.

Wolman, M.G., and Miller, J.P., 1960, Magnitude and frequency of forces in geomorphic processes: Journal of Geology, v. 68, p. 54–74.

Chapter D

Depositional Aspects of the November 1985 Flood on Cheat River and Black Fork, West Virginia

By J. STEVEN KITE and RON C. LINTON

U.S. GEOLOGICAL SURVEY BULLETIN 1981

GEOMORPHIC STUDIES OF THE STORM AND FLOOD OF NOVEMBER 3–5, 1985, IN THE UPPER POTOMAC AND CHEAT RIVER BASINS IN WEST VIRGINIA AND VIRGINIA

CONTENTS

FIGURES

TABLES

Depositional Aspects of the November 1985 Flood on Cheat River and Black Fork, West Virginia

By J. Steven Kite *and* Ron C. Linton[1]

Abstract

Widespread, intense rainfall in November 1985 produced floods that exceeded all historic events on Cheat River and most of its tributaries. Official discharge estimates for Cheat River ranged from 4,800 to 5,380 m^3/s (170,000–190,000 ft^3/s) with a recurrence interval of >100 yr. In addition to considerable property damage and the loss of five lives, the November 1985 flood left a variety of deposits, many of which differ from those produced by moderate floods.

Clay or silt deposits were uncommon after the flood; most were restricted to slack-water deposits at the mouths of hydraulically dammed or back-flooded tributaries. These slack-water deposits were composed of four different sedimentary units: basal gravel and sand (unit A), sandy loam (unit B), silt loam (unit C), and upper fine sandy loam (unit D). The four units always occurred in the same stratigraphic order, but low-gradient tributaries lacked the top and bottom units. The silt loam unit was deposited by water from Cheat River, but the other three were derived from the tributaries. Simple one-unit sandy slack-water deposits formed near very large boulders and bridges. Neither type of slack-water deposit proved to be an accurate indicator of flood stage, so these deposits may be imprecise paleohydraulic indicators for central Appalachian streams.

Sand dunes and arcuate splays of cobbles and small boulders developed on flood-plain sites downstream from isolated scours or erosional ramps attached to the river channel. Gravel deposits commonly were juxtaposed on top of sandy preflood alluvium, providing evidence of considerable tractive force in what is normally a low-energy overbank environment. The flood transported large volumes of cobbles and boulders from the channel margin to sites hundreds of meters from the channel. Most of the mobilized sediment originated on the flood plain.

Extremely large boulders (>2.75-m intermediate axes) were transported in two of the steeper reaches of Cheat River. Published empirical equations relating stream competence to mean flow velocity, tractive force, and unit stream power suggest these boulders approached the largest size that a flood of this magnitude could transport.

Trees and trash appeared to be the most voluminous sediments left by the November 1985 flood. These nonclastic deposits commonly were scattered widely about the flood plain, but they also occurred as clusters of dunelike forms on unforested surfaces or as thick lobate forms on forested bottomlands.

Postflood mitigation has destroyed most of the November 1985 flood deposits, precluding detailed study of some effects of the flood. If the extensive mitigation had not occurred, some of the morphologic and stratigraphic effects of this extreme flood would have persisted in the Cheat River and Black Fork fluvial systems for centuries.

INTRODUCTION

Learning From Catastrophe

The November 1985 flood left more than a legacy of death and property damage. It created deposits and landforms that revealed much about the geomorphology of extremely large floods in the Appalachian region. Many of these deposits and landforms differ from those formed by more moderate floods. Some are important to the long-term development of the flood plain, and others have potential to reveal the risk from future catastrophic flooding.

Extreme floods are serious hazards in mountainous landscapes that cannot store storm runoff. Unfortunately, gage records in the United States usually are too short to determine the likelihood of floods with recurrence intervals exceeding 50–200 yr (Thomas, 1987). Sediments and landforms on or near flood plains can be used to extend flood records far beyond historic gage data. Two promising approaches to extending flood records are reconstruction of floodwater levels from slack-water deposits (Kochel and Ritter, 1987; Baker and Kochel, 1988; Kochel and Baker, 1988) and estimation of various indices of flow strength, such as flow velocity, based on the size of the clasts that

Manuscript approved for publication February 22, 1991.

[1] Department of Geology and Geography, West Virginia University, Morgantown, WV 26506.

were transported by the flood (Costa, 1983; Williams, 1984; Komar, 1988). These and other geomorphologic methods can be powerful flood-plain management tools, if users thoroughly understand their accuracy and limitations. The November 1985 flood in the Cheat River basin provides a test of how well these methods reconstruct a catastrophic flood of known discharge.

Scope of Research

This paper is a general survey of a wide variety of deposits formed along Cheat River and its largest tributary, Black Fork, during the November 1985 flood. Much of this paper is based on initial field reconnaissance conducted in late 1985 and early 1986, supplemented by interpretation of aerial photographs taken before and after the flood. Later field work was directed at testing various methods of paleohydraulic reconstruction (Linton and Kite, 1987). In this pursuit, most of our detailed work has been devoted to fine-grained slack-water deposits and to the largest boulders transported during the flood. Preliminary findings concerning paleohydraulic aspects are described briefly. Other types of deposits were studied only at a reconnaissance level.

Postflood mitigation by man included extensive removal or relocation of flood deposits by heavy equipment. The mitigation efforts destroyed or modified most of the features studied at reconnaissance level within a few months of the flood, including many of the larger and more unusual deposits and landforms. Only the study of aerial photographs taken right after the flood can sustain research on these features. We repeat the warnings of Williams and Guy (1973) and Williams and Costa (1988) that many geomorphologic aspects of major floods must be studied immediately after the event, before mitigation begins.

Study Area

Cheat River begins at the confluence of Black Fork and Shavers Fork at Parsons, W. Va. (fig. 1; Jacobson, chapter A, this volume, pl. 1). The Cheat flows 125 km (78 mi) northward from Parsons to Point Marion, Pa., where it flows into the Monongahela River. From an altitude of 497 m (1,630 ft) at Parsons, Cheat River descends to 238 m (780 ft) at Point Marion, giving an average gradient of 0.00207. The total drainage area is 3,688 km^2 (1,424 mi^2; U.S. Army Corps of Engineers, 1963).

Black Fork begins at Hendricks, W. Va., at the confluence of Dry Fork and Blackwater River. Only 6.5 km (4 mi) long, Black Fork descends 21 m (70 ft), giving a gradient of 0.00324. Drainage area of Black Fork is 1,295 km^2 (500 mi^2), nearly 70 percent of which is in the Dry Fork basin (U.S. Army Corps of Engineers, 1963). Shavers Fork has a drainage area of 560 km^2 (216 mi^2; U.S. Army Corps of Engineers, 1963). Slightly more than half of the Cheat River basin lies upstream from Parsons. The only large tributary that enters Cheat River downstream from Parsons is Big Sandy Creek, which drains 539 km^2 (208 mi^2).

Bedrock Geology and Topography

The entire drainage basin lies in the rugged eastern Appalachian Plateau. The bedrock geology of the basin is dominated by clastic sedimentary rocks, ranging from Upper Devonian to Upper Pennsylvanian (Cardwell and others, 1968). Most formations include thick, resistant sandstone lenses. Weak rocks, such as limestone or shale, are relatively minor. The bedrock is deformed by gently plunging, open folds that produce relatively wide northeast-southwest trending strike belts.

Although influence of bedrock lithology and structure on topography is less striking in the Cheat River basin than in some parts of the central Appalachians, one lithostratigraphic unit, the Lower and Middle Pennsylvanian Pottsville Group, produces distinctive effects on the landscape. Sandstones and conglomerates of the Pottsville are the most resistant bedrock lithologies in the Cheat basin. The Pottsville Group caps most of the prominent ridges in the basin. Pottsville outcroppings support steep valley walls where the unit has been incised deeply, especially in the Cheat Canyon and Cheat Narrows. Extremely large boulders occur in streams wherever the Pottsville crops out in or near the channel. The steepest gradients on Cheat River occur in two of these bouldery reaches: Cheat Narrows (0.0044) and Cheat Canyon (0.0067).

Upper Devonian Chemung Group and Hampshire Formation or Lower Mississippian Pocono (Price) Sandstone form some ridges in the basin (Cardwell and others, 1968). However, unlike the Pottsville Group, these units produce neither steep canyons nor extremely large boulders.

The Cheat River's headwaters are steep, with many small flashy streams, although there are a few subbasins with considerable runoff storage (see Jacobson, chapter A, this volume, pl. 1). Blackwater River has storage in the wetlands of Canaan Valley and adjacent uplands, but between Davis and Hendricks (fig. 1) this tributary flows through steep, scenic Blackwater Canyon. Shavers Fork drains the highest point in the basin (1,478 m, or 4,850 ft) in Pocahontas County, but Shavers Fork has an elongate drainage basin and a relatively wide flood plain; flood crests attenuate upstream from the Cheat at Parsons. Dry Fork is the flashiest of the Cheat's large tributaries because of its dendritic drainage pattern and steep headwater slopes.

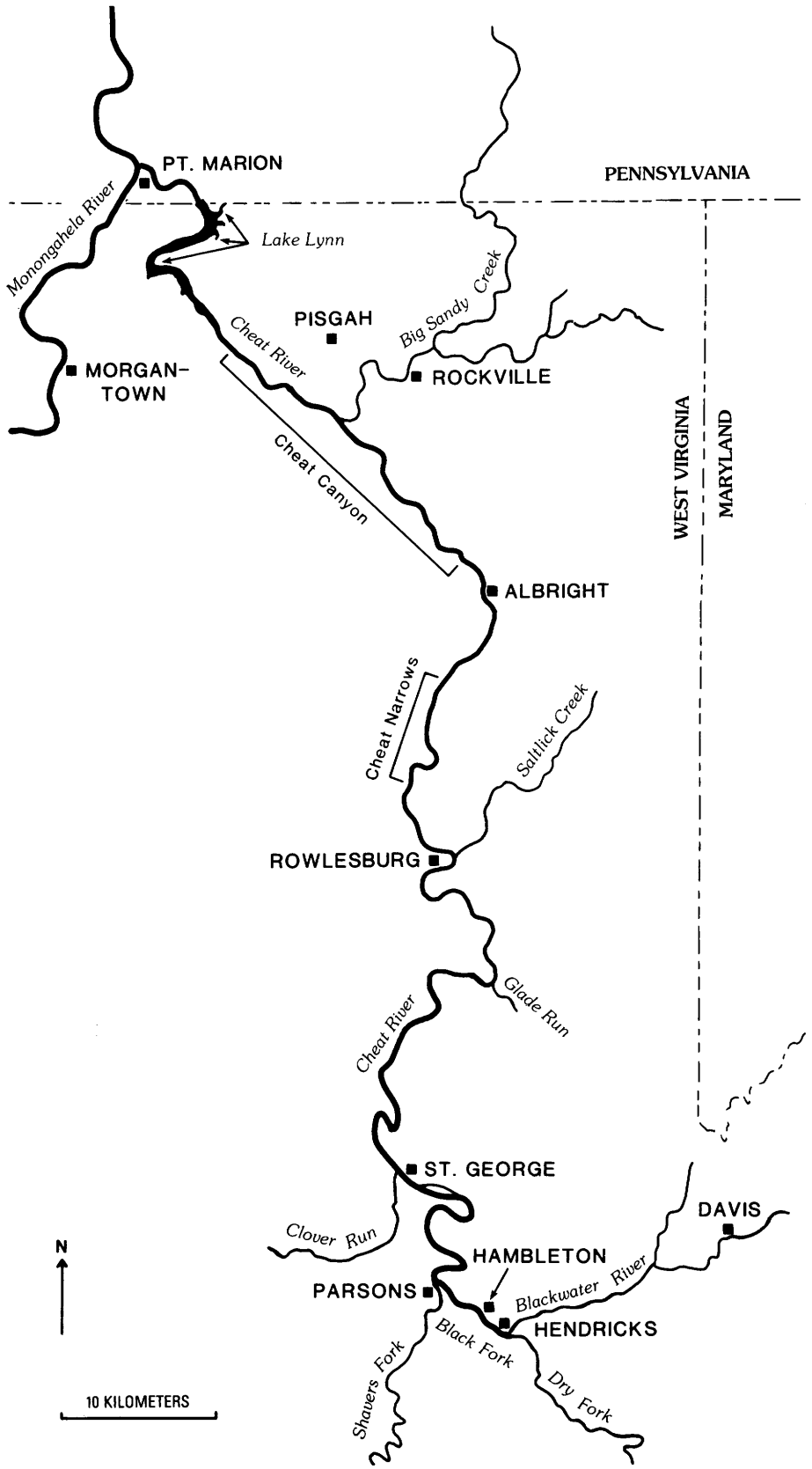

Figure 1. Map showing Cheat River, Black Fork, and selected tributaries. The extent of Cheat Narrows and Cheat Canyon is shown by bracketlike symbols. Refer to Jacobson, (chapter A, this volume, pl. 1) for topography.

Land Use in the Cheat River Basin

Most of the basin is forested, although cropland and pastures are common along the bottomlands and terraces adjacent to Cheat River and its larger tributaries. Most agricultural land on slopes is pasture. Total farmland in Tucker and Preston Counties decreased from 62.4 percent in 1900 to less than 24.8 percent in 1987; total cropland decreased from 31.3 percent to 9.9 percent (U.S. Bureau of the Census, 1913; 1989a, b).

Coal strip mining is important in areas underlain by Pennsylvanian rocks, particularly the northwestern third of the basin. The rest of the basin has no useful coal resource and no coal mines (West Virginia Geological and Economic Survey, no date).

Nearly the entire basin was clear-cut for timber between 1850 and 1930 (Fansler, 1962; Preston County Historical Society, 1979). Poor logging practices led to fires that burned surface organic horizons in soils over much of the basin (Fansler, 1962; Venable, 1990). Loss of forest cover and organic horizons has been shown to decrease runoff storage and contribute to accelerated runoff (Dunne and Leopold, 1978). Forest cover has increased over most of the Cheat River basin since 1920 (Fansler, 1962; North, 1985), although surface organic horizons have not recovered completely from the disturbance caused by logging and burning (Venable, 1990). Land use probably contributes to less rapid runoff today than it did at the turn of the century, but there may be somewhat less runoff storage today than prior to 1850.

A few communities occur on flood plains in the Cheat River basin, including Hendricks, Hambleton, Parsons, and St. George in Tucker County and Rowlesburg and Albright in Preston County (pl. 1). All of these communities have experienced repeated historic flooding, and all were badly damaged by the flood of November 1985. Point Marion, in Fayette County, Pa., is prone to flooding from both the Cheat and Monongahela Rivers.

Acknowledgments

This work was supported by the West Virginia Water Research Institute, the Southeastern Section of the Geological Society of America, and Sigma Xi, the Scientific Research Society. This research has benefited from discussions with R. Jacobson, A. Miller, D. Parkinson, J. Harper, and R. Behling and from reviews of an earlier draft by J. Grimm and J. Schmidt. Commissioner W. Ritchie and M. Christianson facilitated procurement of aerial photographs from the West Virginia Department of Highways.

THE FLOOD OF NOVEMBER 1985

Meteorology and Hydrology

The meteorologic events that produced the flood of November 1985 are described elsewhere (Clark and others, 1987; Colucci and others, chapter B, this volume) and are not repeated here. Most of the Cheat River basin received between 125 and 175 mm of precipitation in October 1985 (Colucci and others, chapter B, this volume, fig. 6), somewhat above the monthly means of 83 mm at Parsons and 110 mm at Rowlesburg (U.S. Army Corps of Engineers, 1963). High flows produced by October rains subsided by November 1, when flows at Parsons (14.5 m^3/s, or 513 ft^3/s) and Rowlesburg (21 m^3/s, or 743 ft^3/s) were only one-third of the daily average discharges and more than 3 m below flood stages at both gage stations (USGS-WRD, unpublished gage data; Embree and others, 1985). Rainfall was recorded on the first three days of November, but flow of the Cheat River increased only gradually until the afternoon of November 4.

The primary flood-producing event occurred during the 48-h period ending on the morning of November 5. The headwaters of Dry Fork and Blackwater River were under the western end of a heart-shaped cell of precipitation that exceeded 150 mm (Jacobson, chapter A, this volume, pl. 1; Colucci and others, chapter B, this volume, fig. 6). Canaan Valley received 238 mm during the 48-h period ending on the morning of November 5 (GAI Consultants, 1985). On November 4, flood stage was reached at Parsons at 5:40 p.m., following a 1.5-m rise in 100 min, and flood stage was reached at Rowlesburg between 8 and 9 p.m. during a 1-m rise in 60 min (USGS-WRD, unpublished gage data).

Flow at Parsons crested 3.3 m above flood stage between 3 and 5 a.m. on November 5 (GAI Consultants, 1985; Charleston Gazette, 1985; Teats and Young, 1985). The flood crest moved downstream at an average velocity of 15–20 km/h, reaching Rowlesburg around 6–7 a.m., Albright at 9:30 a.m., and Lake Lynn about 11 a.m. that same day (GAI Consultants, 1985; Charleston Gazette, 1985; Plum, 1985; Teats and Young, 1985). Peak runoff was 2.59 $m^3/s/km^2$ (237 $ft^3/s/mi^2$) on the Cheat at Parsons and 2.14 $m^3/s/km^2$ (195 $ft^3/s/mi^2$) at Rowlesburg.

Damage and Fatalities

Receding waters in the next few days revealed the worst damage in the written history of the Cheat River. Discharge far exceeded previous historic floods except for tributaries in the northern end of the basin. Five people drowned in the Cheat River basin (R.E. O'Dell, West Virginia State Police, telephone communication, 1988). All communities adjacent to the Cheat River and most of its major tributaries were severely damaged, particularly those located inside meander bends, such as Albright (fig. 2),

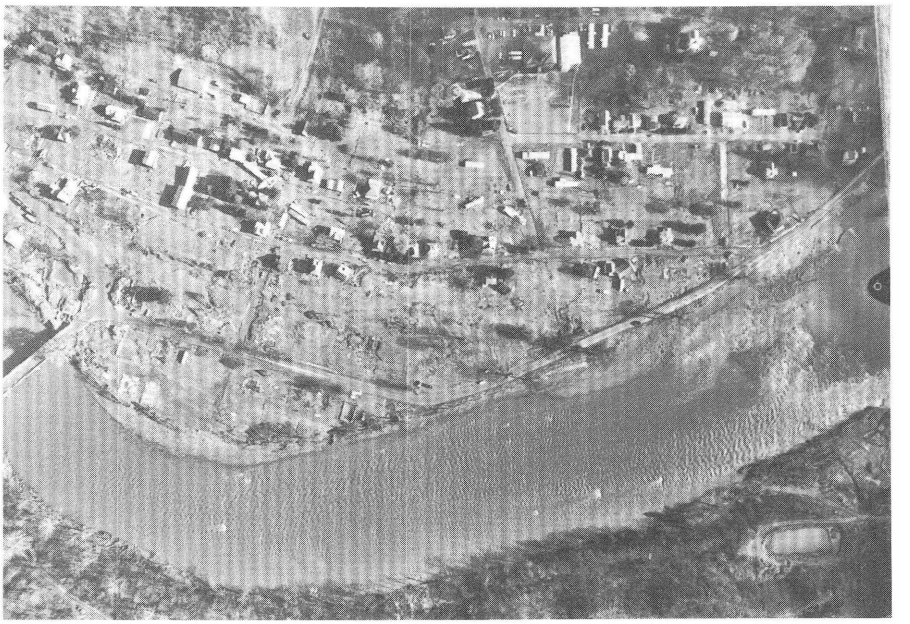

Figure 2. Aerial photograph of destruction at Albright, W. Va., taken a few days after the November 1985 flood. Note numerous foundations where buildings were washed away. Cheat River flow is from right to left (northward) (West Virginia Department of Highways photograph).

Rowlesburg, and Parsons. Half or more of the buildings in each community were destroyed or damaged. Property damage in the basin may have exceeded $100 million. Initial estimates of damages were more than $30 million in Preston County and more than $66 million in Tucker County (Region III Interagency Flood Hazard Mitigation Team, 1985). A total of 479 private homes were destroyed and another 162 condemned because of flood damage in these two counties, which are mostly within the Cheat drainage basin (Teats and Young, 1985). These estimates do not include considerable destruction from Cheat River tributaries in Randolph County, W. Va., or damage near the mouth of the Cheat in Fayette County, Pa. Runoff from the Cheat River basin contributed to flooding by the Monongahela River, which caused damage to 2,784 homes and created losses in excess of $11 million to commercial and industrial establishments downstream from Point Marion (Murphy, 1986).

The fundamental cause of the unique severity of the 1985 floods in the Cheat River basin is the extraordinary amount of rain that fell over most of the drainage basin in a short amount of time. Much of the rainfall was delivered rapidly to streams because antecedent rainfall and minimal plant transpiration produced partially saturated soils. The estimated average rainfall for the week ending November 5, 1985, was 164 mm (6.45 in) for the Cheat River basin upstream from Parsons and 152 mm (6.00 in) for the basin upstream from Rowlesburg (R. Jacobson and J. McGeehin, unpublished data). Total runoff from the Cheat River basin was approximately 125 mm (4.93 in) at the outlet to Lake Lynn (GAI Consultants, 1985).

Historic Floods and the Recurrence Interval of the 1985 Flood

Discharge during the November 1985 flood was unprecedented for most of the Cheat River basin (tables 1 and 2). Five of six active U.S. Geological Survey (USGS) gaging stations in the basin experienced record floods, exceeding previous maximum discharges by 72–231 percent. Only the gage on Big Sandy Creek recorded an event that was relatively minor in comparison with previous floods. These are no USGS gages on Cheat River downstream from Big Sandy Creek, but estimates of the flow into Lake Lynn (GAI Consultants, 1985) indicate that discharge decreased downstream from Rowlesburg (table 1). The flood attenuated because of runoff storage on the flood plain and because downstream tributaries were outside the area of maximum precipitation and had crested well before the peak flood on Cheat River reached their confluence. The 1985 flood had approximately 25 percent greater discharge than the greatest previously recorded floods near the mouth of the Cheat (table 1).

The oldest gage record in the Cheat River basin has been maintained at Rowlesburg since 1884 (Embree and others, 1985). The Rowlesburg record (table 2) includes historic accounts of two substantial mid-19th century floods that were not recorded at other stations. The flood of July 6,

Table 1. Comparison of selected large floods in the Cheat River basin

[Unit of measure is cubic meters per second. Equivalent values in cubic feet per second are given in parentheses. Rowlesburg data are based on most recent rating curve (see discussion in table 2). The 1844 and 1888 floods predate USGS discharge gage stations; discharges were estimated from historical accounts or National Weather Service gage data. Sources: Speer and Gamble (1965), U.S. Geological Survey (1976), Embree and others (1985), Lescinsky (1986), Robert Eli, Department of Civil Engineering, West Virginia University (personal commun., 1988), R.S. Runner, U.S. Geological Survey, Charleston, W. Va. (personal commun., 1988). "?" denotes no record known]

Measure	Stream						
	Dry Fork	Shavers Fork	Blackwater River	Cheat River	Cheat River	Big Sandy Creek	Cheat River
Locality	Hendricks	Parsons	Davis	Parsons	Rowlesburg	Rockville	Three stations (see notes below)
Area, ha	89,400 (345 mi^2)	55,400 (214 mi^2)	22,300 (86.2 mi^2)	186,000 (718 mi^2)	252,000 (972 mi^2)	1,800 (200 mi^2)	ca. 357,000 (ca. 1,380 mi^2)
Gage record	1940–present	1910–1926, 1940–present	1921–present	1913–present	1923–present	1909–1918, 1921–present	
Date of flood							
July 6, 1884	?	?	?	?	2,520 (89,000)	?	?
July 10, 1888	?	708 (25,000)	?	1,450 (51,300)	2,380 (84,000)	850 (30,000)	[1]4,530 (160,000)
October 16, 1954	1,330 (47,000)	453 (16,000)	193 (6,800)	1,475 (52,100)	1,880 (66,300)	447 (15,800)	[2]4,160 147,000)
November 5, 1985	2,830 (100,000)	1,230 (43,500)	354 (12,500)	4,810 (170,000)	5,380 (190,000)	202 (7,140)	[3]5,660 (200,000)

[1] Near Morgantown, drainage area is 357,000 ha (1,380 mi^2); gaged in 1903–1905, 1909–1917, and 1923–1926; station inundated by Lake Lynn in 1926.

[2] Near Pisgah, drainage area is 351,000 ha (1,354 mi^2); gaged in 1927–1958; upstream from Lake Lynn.

[3] Estimated flow into Lake Lynn (Cheat Lake), from calculations by R. Eli, who calculated discharge at Lake Lynn spillway was 4,960 m^3/s (175,000 ft^3/s), somewhat more than the GAI Consultants (1985) preliminary estimate of 4,250 m^3/s (150,000 ft^3/s). Drainage area at the spillway is 366,000 ha (1,413 mi^2).

1844, was the greatest recorded at Rowlesburg prior to 1985. Four of the seven largest floods at Rowlesburg occurred between 1888 and 1907, roughly coincident with peak logging activity in the basin. The October 1954 flood on the Cheat came in the aftermath of Hurricane Hazel. However, if the northern end of the Cheat River basin is excluded, none of the earlier gaged floods exceeded 60 percent of the 1985 flood discharge. Log Pearson type III analysis of the flood frequencies for the Dry Fork, Blackwater River, Shavers Fork, and two stations on Cheat River estimated recurrence intervals of >100 yr (Lescinsky, 1986; Carpenter, 1990) to >500 yr for the 1985 flood (E.A. Friel, unpublished data). The flood at the two gages on Cheat River was particularly impressive, being 2.1–2.3 times the calculated 100-yr flood at Rowlesburg and 2.3–3.0 times the calculated 100-yr flood at Parsons (based on data from U.S. Army Corps of Engineers, 1963; U.S. Geological Survey, 1985; R.S. Runner, personal communication, 1988).

Historic accounts, summarized in table 3, have been of limited use in estimating the recurrence interval of the 1985 flood. The bottomlands along the Cheat have been settled continuously since 1773 (Wiley and Frederick, 1882), but no floods were recorded before 1834 (Maxwell, 1884; Fansler, 1962). In fact, the earliest history written about Preston County (Wiley and Frederick, 1882) makes no specific mention of floods, despite at least nine references to bridge construction and discussion of one bridge that was destroyed by wind and another by an act of war. Fansler (1962) discussed floods in length in his history of Tucker County. He described the July 1888 flood as the worst in the history of Cheat River, but this assessment may reflect flood damage, not stream discharge. The 1844 flood, the greatest known at Rowlesburg prior to 1985, is not discussed by Fansler (1962) or any other published history of Preston or Tucker Counties. Communities on the flood plains remained quite small until after 1850 (Wiley and Frederick, 1882; Fansler, 1962), so the lack of an early flood record may reflect sparse settlement, rather than a lack of flooding. The historic accounts indicate that the 1985 event exceeded any recorded on Cheat River, a conclusion consistent with recurrence-interval estimates of >100 yr.

DEPOSITS FORMED DURING THE NOVEMBER 1985 FLOOD

General

The 1985 flood deposited a complex array of sediments. Clay and silt were not abundant on the flood plain and generally were deposited only in silt loam and sandy loam units in slack-water settings. Sand was deposited in many different facies, including slack-water environments,

Table 2. Comparison of discharges reported for historic floods on the Cheat River at Rowlesburg

[Discharge measured downstream from Saltlick Creek, except as noted. Unit of measure is cubic meters per second; equivalent values in cubic feet per second are given in parentheses]

Date of flood	U.S. Army Corps of Engineers (1963)[1]	Wells (1957); Paulson (1953)[2]	U.S. Geological Survey (1971, 1976); Hendricks (1964); Embree and others (1985); Lescinsky (1986)
Nov. 5, 1985[3]	—	—	5,380 (190,000)
July 6, 1844	3,310 (117,000)	3,540 (125,000)	2,520 (89,000)
July 10, 1888	2,970 (105,000)	3,340 (118,000)	2,380 (84,000)
April 18, 1852	2,605 (92,000)	—	—
July 22, 1896	2,270 (80,000)	—	—
Feb. 22, 1897	2,210 (78,000)	—	—
July 17, 1907	2,100 (74,000)	—	—
Oct. 16, 1954	2,010 (71,000)	—	1,880 (66,300)

[1] Data for the proposed Rowlesburg Dam site, upstream from Saltlick Creek. Data appear to be derived from an obsolete rating curve, with a reduction for discharge from Saltlick Creek. (This reduction may be inappropriate; in the 1985 flood, lower Saltlick Creek was hydraulically dammed and did not contribute to peak flow on Cheat River.)

[2] Data are based on obsolete rating curve.

[3] Discharge for 1985 flood reflects revisions of preliminary data published by Lescinsky (1986).

thin veneers in low-to-moderate energy overbank environments, and dunes in high-energy overbank environments. Gravel was deposited at the base of slack-water sequences, in high-energy overbank environments, and near all stream channels. Extremely large boulders were transported and deposited along the steepest reaches of Cheat River.

Organic and manmade sediments appeared to be more voluminous than clastic sediments. Accumulations of large trees and branches were widespread in high-energy environments, whereas smaller organic sediments were deposited in low-energy environments, including the high-water limit. Manmade materials were the dominant sediments in and immediately downstream from towns.

Methods Used to Study 1985 Flood Deposits

Deposits in the study area were examined between November 1985 and December 1987. Most field work was conducted along Cheat River between Parsons and Albright. Field work was supplemented by examination of 1:3000-scale aerial photographs that were taken by the West Virginia Department of Highways a few days after the November 1985 flood. The 1:3000-scale photography covers all of the Black Fork flood plain and most of the Cheat River flood plain between Parsons and Albright. Length and width dimensions for most deposits were determined from the aerial photographs, but slack-water deposits were measured in the field.

Particle-size distributions for fine gravel, sand, silt, and clay were determined in the Quaternary Geology Laboratory at West Virginia University. Standard dry-sieving was used for sand or fine gravel; pipette analysis was used for silt and clay (Bell, 1986; Linton, 1992).

Long, short, and intermediate axes of at least ten boulders were measured at each site where boulder deposition was studied, although only the five largest intermediate axes were used in paleohydraulic equations (Costa, 1983). Aerial photographs of various scales were used to identify boulders to be examined in the field or to confirm movement of clasts that was suggested by field criteria. Aerial photographs were not used for particle-size determinations, although some of the transported boulders could be measured from the photographs with error of less than 10 percent.

In general, paleohydraulic and hydraulic reconstruction followed the methods of Costa (1983). Detailed discussion of methods used in the study of slack-water deposits, and of methods used to determine discharge, mean flow velocity, tractive force, and unit stream power, are given by Linton (1992).

Physical Characteristics of Slack-Water Deposits

Distinct slack-water deposits formed in two different settings during the 1985 flood, namely, near large obstructions on the flood plain and at sheltered mouths of tributaries to Cheat River. Slack-water deposits were poorly developed at flood-plain expansions and contractions, and the few slack-water deposits in these sites commonly were disturbed by mitigation efforts soon after the flood. Slack-water deposits less than 2 cm thick were not studied in detail because these thin deposits have little chance of long-term preservation as a recognizable stratigraphic unit and are unlikely to be of use in paleohydraulic reconstructions of prehistoric floods. Bioturbation and surface runoff in the first 2 yr after the flood have supported this interpretation.

Slack-water deposits near flood-plain obstructions such as bridges or large boulders are relatively simple lenses or pockets of laminated sand, up to 25 cm thick and interbedded with thin layers of transported coal, fly ash, or leaf detritus. Except where sheltered from precipitation and surface runoff, the sand was eroded and severely gullied soon after the flood peak.

Slack-water deposits were not equally developed at all tributary mouths. The most important prerequisite for development of slack-water deposits was that the tributary mouths be sheltered from direct flow of Cheat River

Table 3. Historic floods in the Cheat River basin through 1985

[Except as noted, discharge values for Cheat River at Rowlesburg are from U.S. Army Corps of Engineers (1963), which is based on an older rating curve, briefly discussed in footnote 1 to table 2]

Date	Reference	Comment
1773	Wiley and Frederick (1882); Fansler (1962)	First permanent settlement on Cheat River (Preston County).
1834	Maxwell (1884); Auvil (1977)	Timbers to be used for covered bridge at the Northwest Turnpike were washed away by a flood before construction. Discharge unknown, but flood may have been minor. Oldest flood recorded on Cheat. Completed bridge withstood all floods until it burned in 1964.
July 6, 1844	Embree and others, (1985); U.S. Army Corps of Engineers (1963)	Cited as highest flood known at Rowlesburg before the November 1985 flood. See table 2. Not recorded at other stations. Not discussed in other historical references given here, including several written in 1880s.
1851 or 1852	Morton (1914); Wiley and Frederick (1882)	B&O Railroad bridge constructed at Rowlesburg. Later upgraded for heavier traffic, but never destroyed until 1985 flood. Prior to onset of work on B&O, there was only one house in Rowlesburg.
April 18, 1852	U.S. Army Corps of Engineers (1963)	Fourth largest peak discharge recorded at Rowlesburg: 2,605 m^3/s (92,000 ft^3/s). Not discussed in other historical references cited here.
July 1855	Preston County Journal (1888a)	Worst flood known at Albright before 1888. Stage 0.6 m lower than 1888.
1857	Fansler (1962)	Destroyed a mill in Parsons built after 1844; rebuilt mill survived until after 1920. Only three families lived in Parsons, all on higher ground.
July 10, 1888	Embree and others (1985); Fansler (1962); Preston County Historical Society (1979); U.S. Army Corps of Engineers (1963); Preston County Journal (1888a,b)	Worst flood damage on Cheat and Black Fork (Fansler, 1962) prior to 1985. Discharge on Cheat at Parsons was greater in 1954 (Embree and others, 1985), but apparently damage was greater in 1888. Black Fork and Dry Fork flooded at same time. Large slope failures (debris flows?) on Backbone Mtn. near Hendricks. Erosion of new WVC&P railroad grade between Parsons and Hendricks. The 1844 flood was higher at Rowlesburg, but a mill that survived 1844 flood was destroyed on Black Fork. Third greatest flood at Rowlesburg since 1844 (table 2), $150,000 damage; B&O bridge badly damaged, but water was 1 m below floor of bridge; scour up to 2 m deep, sand deposition up to 1 m thick at Rowlesburg. Albright streets navigable only by boat. Flood of record on Big Sandy Creek (850 m^3/s). Discharge on Cheat downstream from Big Sandy Creek, 4,530 m^3/s, nearly that of 1985. Many buildings and much livestock lost throughout basin.
July 21, 1896	Fansler (1962); U.S. Army Corps of Engineers (1963)	Fifth greatest flood on Cheat at Rowlesburg since 1844: 2,270 m^3/s (80,000 ft^3/s). Shavers Fork flooded business district of Parsons.
Feb. 22–23, 1897	Fansler (1962); U.S. Army Corps of Engineers (1963)	Snowmelt event; washed out railroads on Dry Fork and Black Fork. Lumber mill and other logging structures severely damaged on Black Fork. Most flow came from Dry Fork. Rebel Run in Hendricks was roaring cataract. Sixth greatest flood on Cheat at Rowlesburg since 1844: 2,210 m^3/s (78,000 ft^3/s).
July 17, 1907	Embree and others (1985); U.S. Army Corps of Engineers (1963); Preston County Journal (1907)	Equaled 1888 flood on Shavers Fork (second greatest on record: 708 m^3/s (25,000 ft^3/s)). Seventh greatest recorded flood on Cheat at Rowlesburg: 2,100 m^3/s (74,000 ft^3/s). Shavers Fork flooded Parsons business district.
July 24–25, 1912	U.S. Army Corps of Engineers (1963); Fansler (1962)	Twelfth worst recorded flood on Cheat at Rowlesburg: 1,620 m^3/s (57,200 ft^3/s). One of 12 worst floods on Black Fork from 1888 to 1962 (Fansler, 1962). Highest flow since 1888 on Big Sandy Creek at Rockville: 603 m^3/s (21,300 ft^3/s).
March 29, 1924	Lescinsky (1986); U.S. Army Corps of Engineers (1963)	Highest gaged flood on Blackwater River at Davis between 1921 and 1985. Relatively minor flood on Cheat at Rowlesburg: 1,170 m^3/s (41,300 ft^3/s).
Oct. 15–16, 1954	Fansler (1962); U.S. Army Corps of Engineers (1963); Preston County Historical Society (1979)	Hurricane Hazel. Worst gaged flood prior to 1985 at many stations. USGS discharge estimate greater on Cheat at Parsons than during 1888 flood, but Fansler stated 1888 flood was worse on Black Fork. Eighth worst flood since 1844 on Cheat at Rowlesburg (table 2). Black Fork and Shavers Fork flooded at same time. Damage to streets, tannery ($100,000) and railroad ($60,000) in Hendricks. Cheat well below 1985 level at St. George. Basements flooded in Hendricks and Albright for first time since 1888.
Aug. 17, 1955	Fansler (1962)	Hurricane Diane. Dry Fork and its tributaries hit hard. One of 12 worst floods on Black Fork from 1888 to 1962 (Fansler, 1962). Not listed in Corps of Engineers (1963) table of floods.
March 20, 1982	Embree and others (1985)	Discharge of 476 m^3/s (16,800 ft^3/s) on Shavers Fork at Parsons slightly exceeded pre-1985 flood of record (1954). Little flow on Dry Fork and no significant flood on Cheat River.

Table 3. Historic floods in the Cheat River basin through 1985—Continued

Date	Reference	Comment
Nov. 5, 1985	Lescinsky (1986); Region III Interagency Flood Hazard Mitigation Team (1985); Carpenter (1990)	Greatest recorded floor on Cheat River at Parsons and Rowlesburg, on Dry Fork at Hendricks, on Blackwater River at Davis, and on Shavers Fork at Parsons. Apparently worse than 1888 flood at Albright, but there are no published gage records. Floods of 1888 and 1954 may have approached the same discharge near mouth of the Cheat (table 2). Unlike 1888 and 1954 floods, Big Sandy Creek contributed little to this flood. Much destruction in all towns along Cheat. Point Marion flooded by Monongahela and Cheat Rivers. Damage in Cheat basin may have exceeded $100 million. Five deaths in basin.

floodwaters. Wherever adjacent terraces or valley walls were high enough to block overbank currents of the Cheat River, hydraulic damming by the swollen river back-flooded the lower reaches of these tributaries. Deposits with various morphologies and a wide range of particle sizes formed in the back-flooded areas.

The slack-water deposits at tributary mouths ranged from thin mantles conformable to preexisting surfaces on low-gradient tributaries, to relatively flat-topped surfaces resembling Gilbert-type deltas (Elliot, 1986) at the mouths of steep tributaries. Deposits in the deltalike landforms lack sedimentary structures typically associated with Gilbert-type deltas, specifically fine-grained bottomset beds and steeply dipping foreset beds. Tributaries incised new channels during the falling stage of the November 1985 flood or very soon after flood recession. Most slack-water deposits are exposed along the banks of these 0.4- to 1.2-m-deep channels.

The sedimentology of slack-water deposits at sheltered tributary mouths is complicated (fig. 3). Each depositional package contains up to four distinct sedimentary units (Linton and Kite, 1987). The units always occur in the same stratigraphic sequence, but low-gradient tributaries typically lack the first and fourth units. Gravel and sand make up the lowest unit (unit A), which underlies a sandy loam (unit B) and a silt loam (unit C). The uppermost unit is fine sandy loam (unit D), which was severely eroded soon after the November 1985 flood.

The basal gravel and sand unit A occurs at the mouths of tributaries with relatively steep gradients, in excess of 0.050. In general, thickness and particle size in unit A are proportional to tributary gradients. The unit is up to 1.0 m thick at the mouth of the steepest ($\geq$0.127) tributaries; cobbles are the largest clasts. Commonly, unit A is clast-supported, but a few exposures reveal matrix support. The upper 5–10 cm is finer grained than the rest of the unit. The unit occurs only within, or adjacent to, the tributary channels and has imbrication showing down-tributary flow. Upstream from the slack-water sites, reconnaissance study of tributaries with steep gradients indicated that gravel beds of these streams were mobilized during the 1985 flood. Unit A represents tractive-load deposition in, or adjacent to, the preflood tributary channel near its confluence with Cheat River during the early rising stages of the flood.

Light olive-brown (7.5Y 5/4) sandy loam dominates unit B in the slack-water strata. Portions of this unit range in texture to loamy sand. The sandy loam unit attains 20 cm in thickness and forms nearly continuous mantles over either unit A or over pre-1985 flood-plain surfaces. The unit has fine laminations and abundant organic matter. A gradational contact occurs where unit B caps unit A. The unit is thickest near the tributary channel and thinnest near the tributary valley walls. It appears to have been derived from the tributary, probably when high waters on the Cheat River began to impede tributary flow.

Unit C is mostly silt loam, although loam is locally important. Organic matter, typically leaves or twigs, is abundant in unit C. Color varies from dark brown (10Y 3/3) to black (5Y 2.5/2). The unit generally shows a sharp contact with underlying sandy loam of unit B. Unit C was the uppermost sediment on many slack-water surfaces, and it commonly displayed desiccation cracks when examined after the flood. It is thickest (up to 25 cm) near Cheat River and forms a mantle over slack-water sites that is more extensive than any other unit in the slack-water sediment package.

Unit C is typically massive to weakly laminated, but one locality showed cross-bedding that was dipping up-tributary. It is the only unit in the slack-water package that was derived largely from waters of Cheat River. Unit C thins abruptly at the mouth of one large tributary, Clover Run, where thickness decreases from more than 10 cm to zero within a few meters. This abrupt thinning occurs about 110 m from Cheat River and has little relationship to flood-plain topography.

The uppermost slack-water unit (unit D) is olive-brown (7.5Y 4/4) fine sandy loam that occurs near the channels of steep tributaries. Unit D is easily eroded and forms a discontinuous mantle, best developed where the surface is sheltered from direct precipitation and surface runoff. Maximum thicknesses of 5 cm occur near tributary channels. Most of this unit was eroded away before the

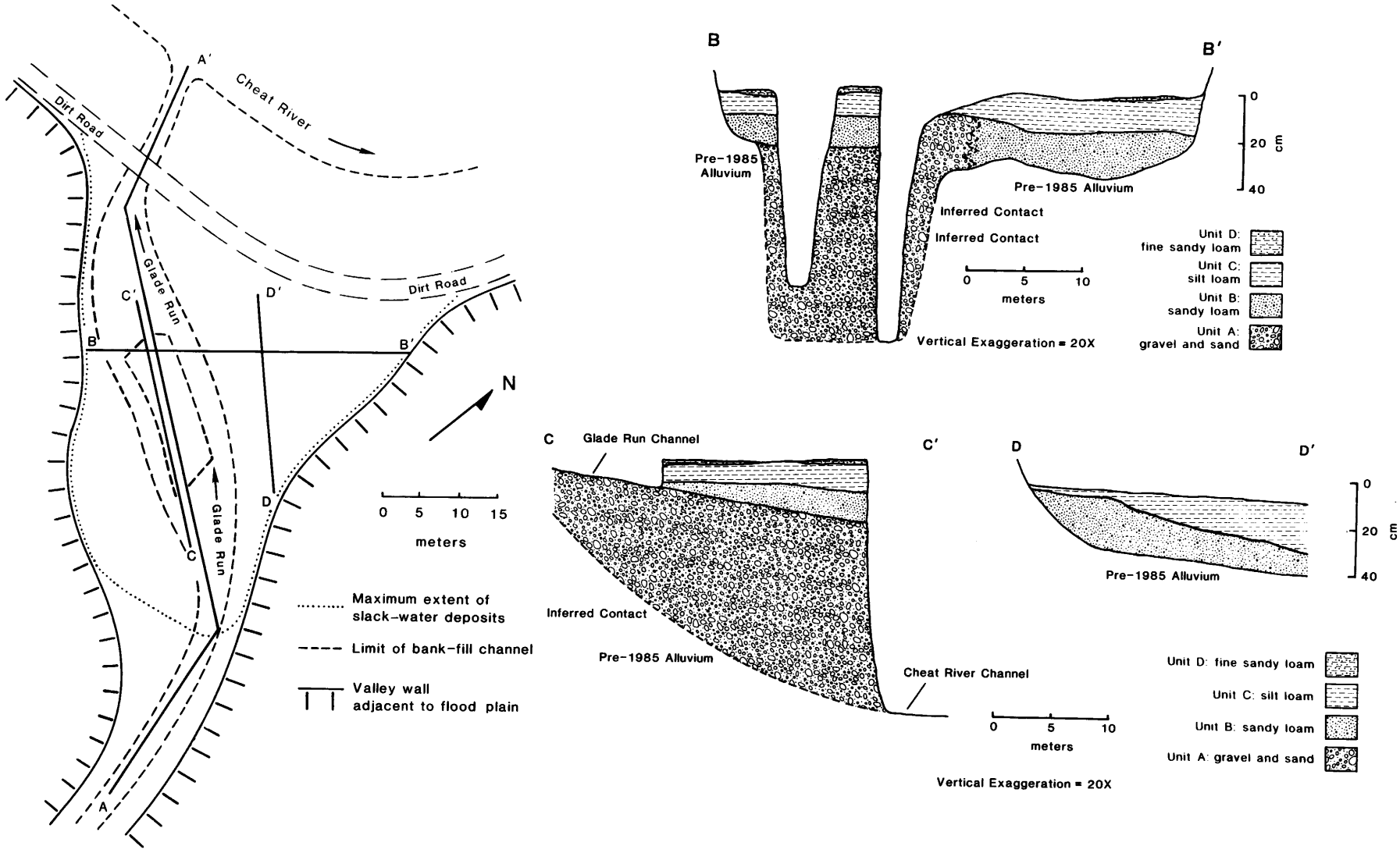

Figure 3. Map and cross section of slack-water deposit formed at the mouth of Glade Run during the 1985 flood.

summer of 1986. Much of the eroded sediment was either deposited within mud cracks in the underlying silt loam or washed into nearby topographic lows. Current indicators have not been identified, but its geometry indicates that unit D was derived from the tributary, probably after peak flow on Cheat River.

Locally, unit D is capped with scattered pebbles, granules, or wood fragments. The pebbles and granules are always adjacent to the tributary channel, but are too few and too scattered to be considered a separate unit. These coarse-grained clasts may have been eroded from unit A when the slack-water deposit was incised, either during the waning stages of the November 1985 flood or soon after.

Discontinuous, thin (<2 cm) sand lenses, covering up to 2 m^2, exist in some tributaries that experienced slack-water sedimentation. These sand lenses are not attached to the main slack-water sedimentary package and may occur well up the tributaries, many meters above 1985 flood levels on Cheat River. Although some of the sand lenses may be related to back-flooding of the tributary mouth, these minor deposits cannot be considered useful for the purpose of paleohydraulic reconstructions. Even if they could be assigned to true slack-water sedimentation, they are too thin to have much potential for long-term preservation as a distinct unit.

The lower three units in the slack-water sediment present a sequence of gradually finer deposits, from bottom to top, reflecting a decrease in flow velocity at the tributary mouth as Cheat River rose to its flood peak. Cross beds and deposit geometry show that the lower two units were derived from tributary flow, but unit C was deposited from turbid Cheat River water ponded in the mouth of the tributary. Unit D and associated gravels were deposited during the resumption of flow by the tributary, as the slack-water conditions abated.

Cheat River slack-water sediments exhibit some attributes in common with sediments formed in similar settings during extreme floods in other basins. Moss and Kochel (1978) described two units in slack-water sediments formed at mouths of tributaries to the Susquehanna River during Hurricane Agnes in 1972. Their basal unit consisted of coarse silt, sand, and gravel derived from the tributaries, comparable to units A and B in the Cheat River basin. The upper unit was made up of fine sand, silt, and clay deposited by water from the Susquehanna River, comparable to unit C along Cheat River. Moss and Kochel (1978) did not describe sediments comparable to the fine sandy loam of unit D and associated gravel. Baker (1973) and Baker and Bunker (1985) have suggested that slack-water rhythmites may be formed by multiple flow surges during one flood. There is little repetition of beds in slack-water deposits at tributary mouths along the Cheat, but surge phenomena may have caused the stratification in deposits associated with flood-plain obstructions.

Slack-Water Deposits as Indicators of Flood Stage

Slack-water deposits have been used in many different environments as indicators of flood stage (Patton and others, 1979; Baker and others, 1985; Baker and Kochel, 1988; Kochel and Baker, 1988). Many of these stage reconstructions have successfully extended flood records, but the accuracy and precision of slack-water deposits as stage indicators remains poorly known for the temperate humid climate of the Eastern United States. Slack-water deposits created on Cheat River in 1985 provide an excellent opportunity to evaluate the utility of these methods in the central Appalachians. If the highest slack-water deposits on the 1985 flood correspond with maximum flood stage, then an incentive exists to use prehistoric slack-water deposits to study recurrence intervals of extreme floods for rivers in the region.

We conclude that slack-water deposits in the study area are not good indicators of 1985 flood levels compared to high-water marks, such as rounded wood debris and other flotsam deposited on the ground or in large trees (Linton, 1992). This conclusion is reached in spite of the many hours spent searching for deposits that would correspond well with high-water marks up the back-flooded tributaries. Particular emphasis was put on the elevation of the maximum stage. The upper limit of significant (≥2 cm thick) slack-water deposits ranged from 2.9 to 5.6 m below high-water marks at sites of detailed study (fig. 4). The mean difference between slack-water deposits and high-water marks was 3.8 m, a significant fraction of the 6- to 11-m mean water depths at these localities during the 1985 flood. Accordingly, slope-area method reconstructions of the flood based on the levels of slack-water deposits underestimated discharge by 51–67 percent (table 4).

The conspicuous differences between high-water marks and the upper limit of slack-water deposits are difficult to explain. Individually or collectively, three factors may contribute to the lack of slack-water sediments at higher levels:

1. The tributaries were contributing water to the flood, so perfect slack-water conditions probably did not develop. Nonflooding tributaries are a prerequisite for a good match between high-water levels and the limit of slack-water deposition (Kochel and Baker, 1988).
2. Tributary inflow may not have mixed readily with Cheat River water; waters from the two different sources may have interacted as two distinct, partly stratified water masses, separated by a pycnocline. Most of the tributaries in the study area experienced less severe flooding than those farther upstream and reached peak flow earlier than the Cheat River. These factors suggest that the sediment load on the tributaries was less than that of the main stream during maximum flood flows on the Cheat. This contrast in sediment load would have

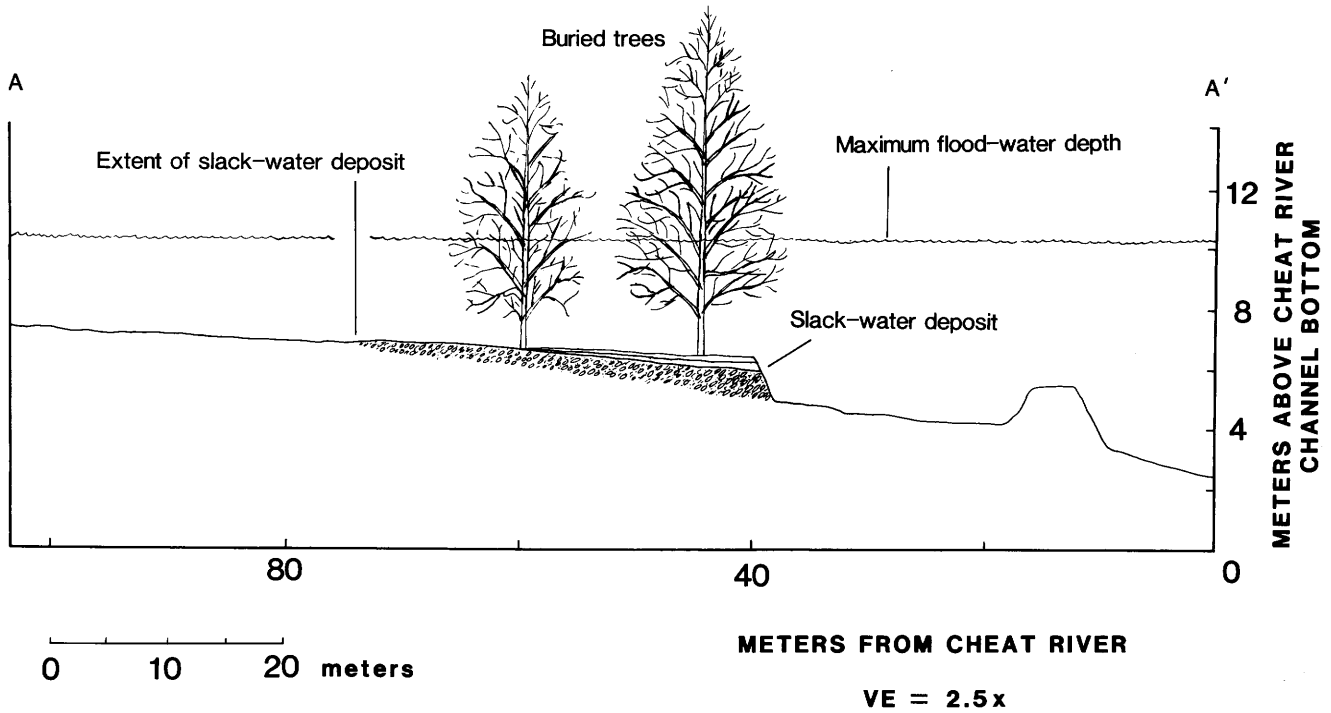

Figure 4. Diagram showing upper limit of slack-water sediments compared with the high-water mark at the mouth of Glade Run. Profile follows line A–A′ on figure 3.

Table 4. Slope-area discharge calculations based on high-water levels versus those based on slack-water deposits

[Locations, methods, and discharge estimates at additional localities are given by Linton (1991). Slope-area discharge values based on high-water indicators are greater than published discharge estimates for the Cheat River (table 1)]

Locality and profile criteria	Stream gradient	Manning's *n*	Mean depth (m)	Mean velocity (m)	Discharge (m^3/s)
Glade Run I					
High-water marks	0.00117	0.025	4.78	3.89	6,027
Slack-water deposits	.00117	.025	3.72	3.29	2,084
Glade Run II					
High-water marks	.00117	.025	5.34	4.19	6,540
Slack-water deposits	.00117	.025	3.17	2.96	2,189
Cheat Narrows I					
High-water marks	.00441	.050	8.79	5.67	5,392
Slack-water deposits	.00441	.050	6.38	4.58	2,611
Cheat Narrows II	.00441	.050	9.66	6.04	6,281
High-water marks					
Slack-water deposits	.00441	.050	6.26	5.03	2,857

produced a relatively clear, low-density water mass from the tributary, overlapping a sediment-laden high-density water mass from Cheat River. The abrupt thinning of unit C at Clover Run supports the existence of distinct water masses. The zone in which the unit thins does not coincide with any change in flood-plain topography, suggesting that a sediment-laden water mass was unable to migrate up the tributary flood plain beyond this zone. Relatively clear tributary inflow would have ponded upstream of the turbid Cheat River water, but left little evidence of high-water levels except for flotsam strewn over the Clover Run flood plain and thin, discontinuous sandy deposits farther upstream.

3. Maximum water discharge may have occurred before or after the maximum sediment load had been transported. If either of these conditions occurred, then slack-water deposits may accurately mark high water at the time of deposition, but not at peak flood stage.

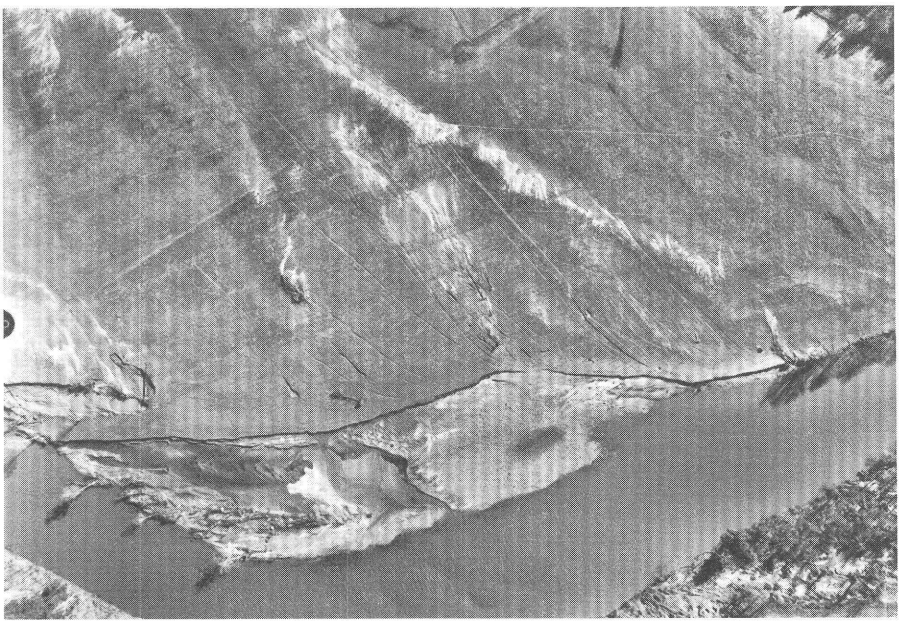

Figure 5. Aerial photograph of Cheat River flood plain near St. George, W. Va. Note evidence of bank retreat (bottom), incision of long narrow grooves (right and center), and deep scour around a standing tree (left). Deposits include sand dunes, sand ribbons, and flood-rafted trees. Normal flow in the river is from right to left (northwestward), but the grooves and tree alignment show flow was diverted northward across the flood plain during the flood (West Virginia Department of Highways photograph).

The low estimates of discharge for the 1985 flood evoke questions about the accuracy and precision of paleohydraulic reconstructions based on slack-water deposits, at least for this type of flood in the Cheat River basin. Reconnaissance study of slack-water deposits left by the 1985 flood along the South Branch Potomac River (Jacobson, chapter A, this volume, pl. 1) suggests that the deposits have better correlation to other high-water indicators than do similar deposits on the Cheat River (J.S. Kite and S.J. Tharp, unpublished data). However, we lack adequate data to determine whether slack-water methods can be applied accurately and precisely to floods on other rivers in the Appalachian region.

Other Fine-Grained Deposits

Thin veneers of sand or sandy loam were deposited at many sites. In general, sand and silty sand veneers ranged in thickness from 0.2 to 10 cm. Thicker, blanketlike sand deposits occurred only in slack-water areas. In open, wide flood plains, fine-grained veneers tend to be transitional to dune forms, suggesting that the 1985 flood produced currents over most of the flood plain that were capable of transporting sand. The same flood-plain sites experience low-energy overbank deposition of sand and silt during less extreme floods.

Mitigation and natural postflood modification make it impossible to quantify how much of the flood plain was covered by veneers. However, veneers could not be seen on most flood-plain surfaces during reconnaissance field work undertaken soon after the flood. It is likely that some undetected sites experienced minor deposition and that these sediments quickly washed in between the leaves of plants on the flood plain, but many surfaces received no sediments except for flotsam and a few isolated starved ripples. A terrace in St. George provided a good example. The terrace has a well-developed soil profile and was not inundated during the October 1954 flood (Fansler, 1962). Floodwaters, 1.8 m deep, flowed over the terrace in 1985. Considerable flotsam, including home appliances, was strewn over the surface, but no fresh alluvium could be discerned on the terrace in December 1985. Lower flood-plain surfaces at St. George showed some sand veneer and shallow dune development, but much of the flood plain either was eroded or experienced little deposition or erosion. Throughout the basin, plowed fields tended to experience severe surface scour, whereas pastures were more typically damaged by bank retreat or incision of long narrow grooves (fig. 5).

Sand dunes formed at many sites in the study area. The best developed dune fields occurred at the Parsons Tree Nursery (fig. 6) and the Preston County Country Club, 4 km south of Albright (fig. 7). Dunes are composed of sand and a minor amount of granules. The largest dunes occurred at Parsons and were up to 1.3 m high, 40 m wide, and 70 m long. Dune shape varied. Larger dunes tended to have

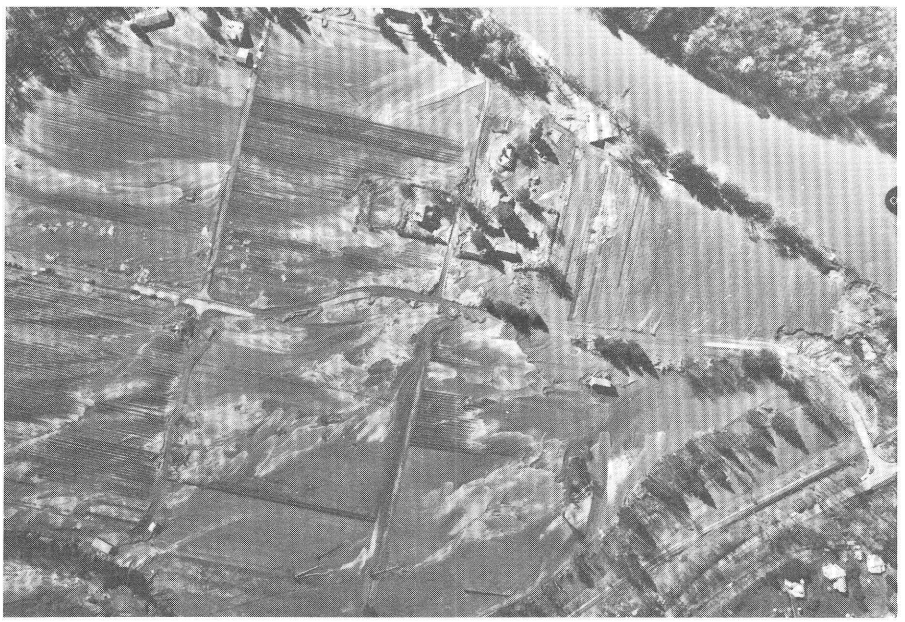

Figure 6. Aerial photograph showing parabolic and complex dunes on Black Fork flood plain at the Parsons Tree Nursery. Note buildings and automobiles for scale. Dunes occur just downstream from gravel splay and gravel stripes shown in figure 9. Transported asphalt slabs occur at left (south); dune sediments have been bulldozed from the roads (center) (West Virginia Department of Highways photograph).

Figure 7. Aerial photograph showing sand deposits at the Preston County Country Club, south of Albright. Normal streamflow is from right to left (northward). Complex and parabolic dunes near Cheat River indicate flow at a 45° angle to the channel. Barchan-shaped dunes and sand "shadows" in the lee of trees near the top of the photograph indicate that flow over the flood plain was nearly parallel to the channel. Much of the sand at this site was derived from sand traps on the golf course. Tree shadows are more obvious than trees in this vertical aerial photograph (West Virginia Department of Highways photograph).

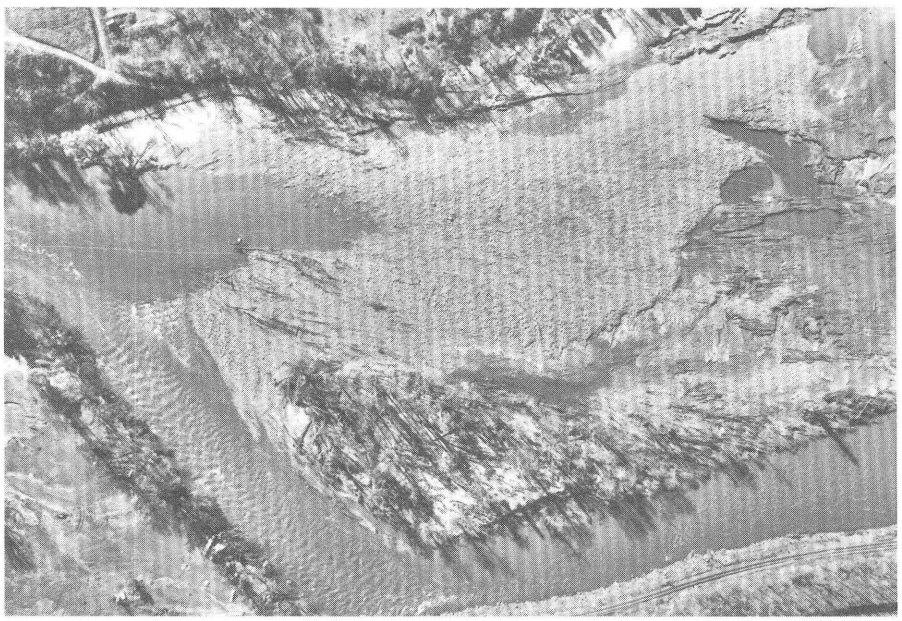

Figure 8. Aerial photograph showing cobble-boulder splay on the Black Fork flood plain near Hendricks. Flow was from left to right across meander. The channel bank and adjacent flood plain were severely eroded during the creation of an elliptical ramp at the upstream (left) end of the meander. The gravel splay (center) overlies eroded pre-1985 alluvium (which also occurs at right). Complex sand deposits occur among standing trees (bottom) (West Virginia Department of Highways photograph).

parabolic forms, whereas smaller ones displayed transverse or barchan forms. Many dunes had irregular plan geometry and appeared to be composite forms modified during waning flows. Where dunes were not disturbed during flood mitigation, establishment of vegetation has been slow. Wind has modified unmitigated dune surfaces, leaving granule lags and subduing some of the dune topography.

All of the major dune fields were associated with sediment from source areas less than 1 km upstream. Most of these source areas were zones of intense scour of preexisting flood-plain sands, but much of the dune sand at the Preston County Country Club was derived from sand traps on the golf course (fig. 7).

Deposits of Small Boulders and Cobbles

Cobbles and small boulders were transported in the channel along most reaches of Cheat River and Black Fork during the 1985 flood. These coarse-grained sediments were commonly deposited on top of alluvial sand or sandy loam in environments that receive relatively low-energy overbank deposition during less severe floods. Most coarse-grained sediments deposited in overbank environments were scoured from preexisting flood-plain deposits within a few hundred meters. Some scour sites were isolated holes or clusters of holes in the middle of the flood plain, commonly where flow around a large tree caused turbulence (fig. 5). Many of these isolated scour holes exceeded 3-m depth. Typical maximum widths were 15–20 m, and at least two exceeded 100 m in length. Virtually all deep scours were filled in and graded during mitigation efforts soon after the flood.

Scouring of ramps along channel margins produced most of the cobbles and small boulders deposited on top of the flood-plain sands. Ramps developed at the downstream end of cutbanks on many meanders, where floodwaters had jumped the meander and flowed nearly straight down the valley. Most of the ramps were obliterated during flood mitigation, but aerial photographs and reconnaissance field work done soon after the flood show that individual ramps were up to 100 m long, 50 m wide, and at least 3–4 m deep (figs. 7, 8). Thousands of cubic meters of alluvium were eroded from the larger ramps, and much of this material was deposited in splays on the flood plain just downstream from the site of erosion.

A typical ramp had an elliptical form, rising from the channel onto the flood plain (figs. 8, 9). At many sites, cobbles and small boulders were washed from the channel, up the ramp, and onto the flood plain. Knox (1987) has suggested that ramps extending from the channel onto the flood plain are important avenues for large clasts to be juxtaposed on top of fine-grained overbank alluvium. However, it is not clear whether most of the large clasts transported onto the flood plain were in the river channel or

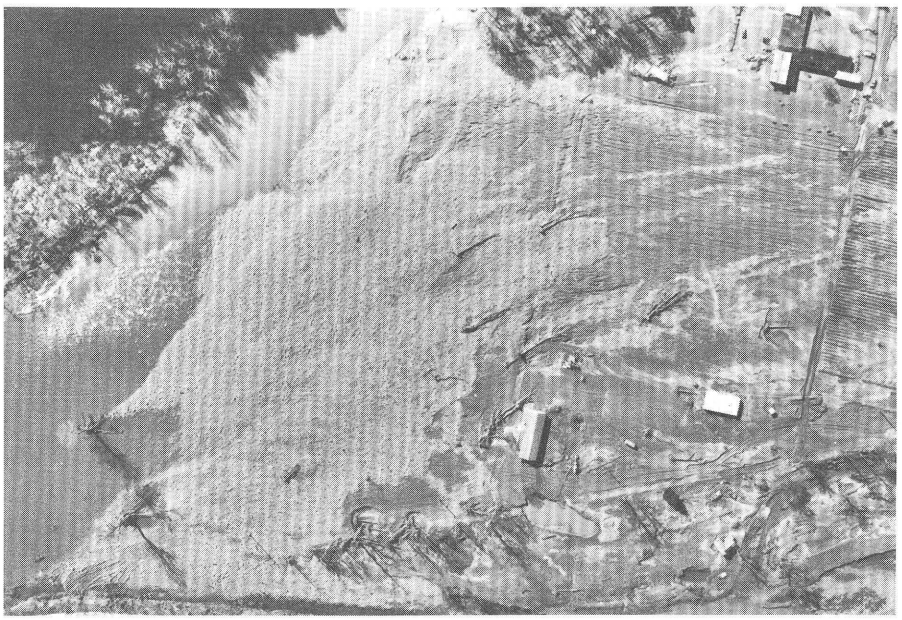

Figure 9. Cobble-boulder splay (left) on the Black Fork flood plain near the Parsons Tree Nursery. Splay is associated with semi-elliptical ramp (lower left). Cobble-boulder stripes occur downstream of (right of) splay. Figure 6 shows sand deposits farther downstream on same meander (West Virginia Department of Highways photograph).

had been buried in flood-plain deposits prior to the 1985 flood.

The large ramps can be traced into broad arcuate cobble-boulder splays on the downstream end of the ramp. The splays commonly have a shape similar to parabolic dunes, with steep downstream faces and "horns" on each side projecting upstream to the point of attachment to the channel bank. These arcuate splays are typically 100 m wide by 140 m long. Gravel thickness in the arcuate splays locally exceeded 1 m. Typically, cobbles and boulders at the steep downstream ends of the splays were deposited over fine-grained preflood deposits. Unfortunately, few of these splays were visited before they were destroyed during mitigation.

The ramps and associated boulder-cobble splays were the surface expression of high-velocity currents over the flood plain, as in the upper Potomac River basin (Miller and Parkinson, chapter E, this volume). High-velocity currents developed over the flood plain where the river temporarily increased its gradient by short-cutting preflood meanders. We presume that these erosional forms developed at or near peak flow. Unlike less extreme floods, erosion was much more common on the inside of meander bends than on the outside. In several reaches, the least damage to flood-plain vegetation was on the outside of meanders, where flow must have had much less energy than at the ramps and splays. However, the duration of these high-velocity currents was insufficient to erode new low-flow channels on Cheat River.

Sand dunes were abundant on flood-plain surfaces that were downstream from splays. Longitudinal cobble-boulder stripes developed downstream from the splays at the Parsons Tree Nursery (fig. 9) but were rare elsewhere. The stripes were composed of large cobbles and small boulders with minor amounts of high-density manmade trash. Stripes typically were one clast thick, 0.5–5 m wide, and 100 m long. The stripes probably represent portions of the arcuate cobble-boulder splays that were detached by extremely fast currents during or near peak flow.

Flood mitigation efforts have modified most of the ramp-and-splay associations beyond recognition and may destroy evidence that sites are susceptible to repeated flood damage. Old newspaper accounts of the July 1888 flood describe a "new channel" eroded nearly 2 m deep across the inside of a large meander at Rowlesburg (Preston County Journal, 1888a). Between 0.6 and 1.0 m of sand was deposited just downstream from the new (1888) channel (Preston County Journal, 1888b). The site of erosion in Rowlesburg was later filled in, but similar scour took place at the same site in 1985. Many buildings were destroyed at the site during both floods.

Extremely Large Boulders

Extremely large boulders transported during the 1985 flood occur in several reaches of Cheat River. So many boulders in Cheat Canyon were reworked during the flood

that white-water raft guides had to relearn almost all of the major falls along this popular waterway. Photographs and personal accounts by white-water raft guides indicate that clasts with intermediate axes up to 2.75 m long were moved. Reconnaissance field work in Cheat Canyon has confirmed transportation of clasts with intermediate axes in excess of 1.5 m.

Our study of large clasts transported during the 1985 flood has concentrated on Cheat Narrows, near the Cheat Narrows slack-water deposit. Various criteria were used to determine which clasts were moved by the flood. Some clasts were large enough to be identified on preflood and postflood aerial photographs, but utility of the photographs was limited by the resolution of preflood photography, by a tree canopy that obscured most of the boulders prior to the 1985 flood, and by high water levels that obscured most of the channel-bottom clasts on postflood photographs. Because of these limitations, aerial photography was used only to identify boulders to be examined in the field or to confirm movement suggested by field criteria, such as the location of impact marks and oxide staining, or fragments of fresh wood or manmade materials trapped under boulders.

Two types of impact marks were common on boulders in Cheat Narrows: flakes and bruises. Boulder-boulder or boulder-bedrock collisions were sufficient to spall off flakes. Flake scars as large as 35 cm by 25 cm were readily discerned from undisturbed surfaces because they lacked lichen growth or weathering rinds. Intact flakes were rarely found; most were possibly crushed during subsequent collisions.

Bruises, created by surface compression during clast collisions, were the most common impact features on boulders in Cheat Narrows. Where bruised, a boulder surface was crushed and lacked vegetation, oxide straining, or a well-developed weathering rind. Bruises commonly occurred at the point of impact where a flake scar was created. A typical bruise was 5–10 cm in diameter and had a very irregular shape. Some bruises either were elongate or occurred in association with chatter marks, both conditions suggesting scraping and shearing of large boulders during transportation.

Although impact marks show that a collision between large clasts occurred, they are not sufficient to determine that a clast has moved. However, the position of impact marks may be used to document clast transportation. Some of the transported boulders showed impact marks on all sides, including those that would be sheltered from impact in their present orientation. A few of the boulders had tens of fresh impact marks on many different faces, indicating that the clast experienced many collisions and was probably transported many meters.

Well-developed impact marks were observed on boulder or bedrock surfaces that were beneath a large boulder. The overlying boulder could not have been at that location when the impact marks were created, unless it had been the colliding clast. In either case, fresh impact marks on a surface under a boulder show that the overlying boulder was transported in the 1985 flood.

A weathering varnish, presumably composed of iron or manganese oxides, coats many clasts exposed at the surface to a level 1–1.5 m above typical low flows in the Cheat Narrows. This varnish gives way to lichen- and moss-covered surfaces farther above the low-water levels. Boulders exhumed from preflood deposits do not show this varnish. The varnish can be identified on clasts that were transported from positions in the channel to positions on the flood plain above the varnish limit. In one case, the orientation of the varnish allowed reconstruction of the amount of rotation that an extremely large clast experienced during the 1985 flood (fig. 10). We have not used the distribution of varnish on boulders as the sole criterion to determine which clasts were transported, but we have found it helpful in finding boulders that show other evidence of recent transportation.

The most convincing field evidence of transportation occurs where the full weight of a clast had trapped something demonstrably young. Boulders pinning automobile frames, tires, sheet metal, and other common artifacts had clearly moved since those artificial materials were introduced to the river. The 1985 flood was so much larger than any other flood in the past few decades that it was considered reasonable to attribute deposition of the largest of these boulders to the 1985 flood. A relatively young age also could be assigned to boulders that overlie cut lumber, uprooted trees, or broken branches. To confidently determine that a boulder has been transported, the wood beneath it had to be partly crushed by the weight of the boulder. Lumber fragments beneath boulders were examined carefully; many looked convincing but could be extracted with some effort. It is likely that some of these weakly lodged pieces of lumber were washed in by floodwaters but then expanded as they became water-saturated with prolonged exposure.

The largest transported clast identified in the field at Cheat Narrows measured 2.4 m by 4.0 m by 10.0 m (fig. 10). The mass of this clast is estimated to be 160,000–200,000 kg, somewhat larger than the largest clasts transported by either floodwaters or debris flow in the upper Potomac River basin (Kite and others, 1987; Miller, 1987). Most clasts of this size in the Cheat channel were not transported in 1985.

Many boulders with diameters greater than 1 m were moved in 1985, but many smaller boulders were not. Orientation relative to other clasts and position within the flood channel are just as important as clast size in determining susceptibility to movement. Local hydraulic effects, such as macroturbulence, were also important, but these are difficult to reconstruct after the flood (Baker, 1973).

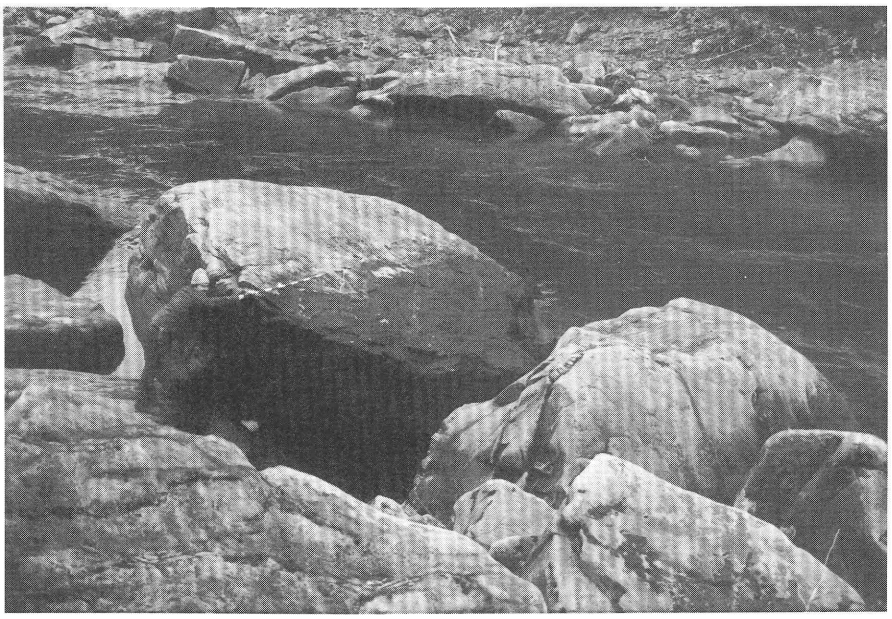

Figure 10. Photograph of the largest clast (intermediate axis of 4.0 m) documented to have moved during the 1985 flood in Cheat Narrows. The clast rotated about 70°, and its center of gravity was moved less than 5 m by flow from right to left. Many clasts with intermediate axes in excess of 2.0 m were transported much farther in Cheat Narrows. The boulders have numerous fresh impact marks on all surfaces; some were deposited on 1985 trash or the stumps of freshly killed trees.

The mean of the intermediate axes of the five largest transported clasts was used in paleohydraulic reconstructions; that value for Cheat Narrows was 2.76 m.

Paleohydraulic Reconstructions From Large Boulders

Various empirical equations have been used to relate the competence of floods with hydraulic variables, including mean flow velocity, tractive force, and unit stream power (Costa, 1983; Williams, 1984). Unfortunately, these empirical equations are derived from very few data on the transportation of clasts with intermediate axes greater than 1 m (Costa, 1983). The November 1985 flood in bouldery Cheat Narrows presents an opportunity to examine which of these equations best describe the relationship between the transportation of very large boulders and hydraulic variables.

Obviously, paleohydraulic reconstructions based on competence require that the largest clast that a flow could transport be present in the channel (Baker and Ritter, 1975). This is a particular problem because it appears that the most accurate paleohydraulic curves are those indicating that relatively low flows can move very large clasts (Williams, 1984). Field observations in Cheat Narrows showed that clasts of the maximum size should be abundant, because some clasts the same size or smaller than the largest transported clast were not moved because of sheltering by other clasts, close packing, or other local considerations.

The only practical way to determine if a reach contains clasts that were large enough to test the competence of a stream during a given flood is to identify reaches with numerous clasts that were too large to be transported during that flood. Only two reaches of Cheat River meet this criterion: Cheat Narrows and Cheat Canyon. Both of these reaches contain very large boulders derived from sandstones of the Pottsville Group.

Table 5 shows predicted values (P) of velocity, tractive force, and unit stream power determined by substituting Cheat Narrows boulder data into published paleohydraulic equations (Linton, 1992). For comparison, table 5 also shows values of the same indices of flow strength determined from slope-area (Manning equation) calculations and field measurements. Slope-area calculations are sensitive to the selection of roughness coefficients (Manning's n). The 0.050 roughness coefficient used for these calculations gave good match to discharge values reported for Cheat River at Rowlesburg and Parsons (Lescinsky, 1986; R.S. Runner, unpublished data). Selection of different roughness coefficients would affect the calculated values, but we believe this source of error is less than the 25–100 percent likely error that is reported for this type of prediction (Williams and Costa, 1988).

Most of the published equations for flow strength overestimate velocity, tractive force, and unit stream power

Table 5. Comparison of hydraulic variables predicted from empirical equations with calculations based on slope-area determinations of discharge and velocity

[Field measurements made at Cheat Narrows after the 1985 flood. Calculated values are averaged from two cross sections (table 4) by Linton (1992)]

Equation	Reference	Value predicted from equations and particle size (*P*)	Value calculated by slope-area method (*C*)	P/C×100
Mean velocity v				
$v=0.20d^{0.455}$ m/s	Costa (1983, eq. 10)	8.53	5.86	146
$v=0.18d^{0.487}$ m/s	Costa (1983, eq. 8)	7.36	5.86	126
$v=0.27d^{0.4}$ m/s	Costa (1983, eq. 8)[1]	6.42	5.86	110
$v=0.216d^{0.44}$ m/s	Modified from Williams (1984) after Koster (1978)[2]	7.05	5.86	120
$v=0.065d^{0.5}$ m/s	Williams (1984)	3.41	5.86	58
Tractive force (τ):				
$\tau=0.056d^{1.213}$ N/m^2	Costa (1983)	836	397	210
$\tau=0.030d^{1.49}$ N/m^2	Williams (1984) after Baker and Ritter (1975)	4,019	397	1,012
$\tau=0.17d$ N/m^2	Williams (1984)	469	397	118
Unit stream power ω				
$\omega=0.009d^{1.686}$ N/m/s	Costa (1983)	5,697	2,567	222
$\omega=0.079d^{1.29}$ N/m/s	Williams (1984)	2,170	2,567	85

[1] Equation modified to fit only clasts with intermediate axes measuring 500–3,200 mm (Costa, 1983).

[2] Based on equation for critical velocity ($v_c = 0.18d^{0.44}$), assuming that $v = 1.2v_c$ (Williams, 1984).

(table 5). Although most of these overestimates are within the likely error of the method, they suggest that the boulders transported by the Cheat River do approach the upper limit of sizes that could have been transported by a flood of this magnitude.

Field observations in Cheat Narrows showed important aspects of using large boulders to reconstruct flood flows. Extremely large clasts were deposited only in or adjacent to the channel in Cheat Narrows, where flow velocity and depth were greatest during the flood. It is likely that more useful empirical equations could be constructed by regression of clast size with maximum values of velocity, tractive force, or unit stream power, rather than with mean values of these variables. Mean values in most reaches of Cheat River were inappropriately lowered by inclusion of parts of the flood plain that experienced little flow and no boulder movement.

Miscellaneous Deposits

A number of curious, yet somber, deposits of manmade articles were strewn about the flood plain after the 1985 flood. Many low-density items were scattered across the flood-plain surface, stranded when floodwater receded. Clothing, plastic items, and foam rubber tended to be trapped in trees or shrubs. Most of the lumber, refrigerators, propane tanks, trash dumpsters, and other manmade debris that clogged the Lake Lynn floodgates was entrained at Albright, 40 km away, or even farther upstream. Heavier manmade objects, such as automobiles and hot-water heaters, traveled shorter distances, apparently as bedload. A few residential buildings and mobile homes remained relatively intact after being swept from their foundations, but most disintegrated into smaller fragments carried in flotation, suspension, or traction.

Large slabs of asphalt were eroded from roads and parking lots on the flood plain. The largest slabs were 4 m wide by 6 m long, but only 10–15 cm thick (fig. 6). Some of the asphalt slabs were transported more than 100 m without being broken into small fragments. Their survival suggests transportation by flows of relatively high velocity but little turbulence, near the bottom of flow over the flood plain.

Trees and trash appeared to make up most of the volume of deposits left by the 1985 flood. Uprooted trees and broken branches were the most obvious sediment in these deposits, although great volumes of trash were deposited immediately downstream from towns. It appears that virtually all of the trees grew on the flood plain before the flood. Many were quite large and presumed to be over 100 yr old. Some of the transported tree trunks, particularly *Platanus* (sycamore), sprouted new growth barely 6 months after the flood.

Many flood-plain surfaces lacked forest cover before the 1985 flood. Hundreds of individual trees, transported as flotation load, were stranded on unforested surfaces during waning stages. Most were stripped of much of their bark and smaller branches, and were deposited with root masses pointing upstream. Long narrow grooves incised into flood-plain pastures may have been initiated by trees dragged across the surface (fig. 5).

Trash and trees were deposited in dunelike forms on several reaches with wide flood plains (Kite, 1986). These dunelike forms may have formed during the waning stage, as larger trees lodged on the flood plain and served as a nucleus for deposition of other trees and trash.

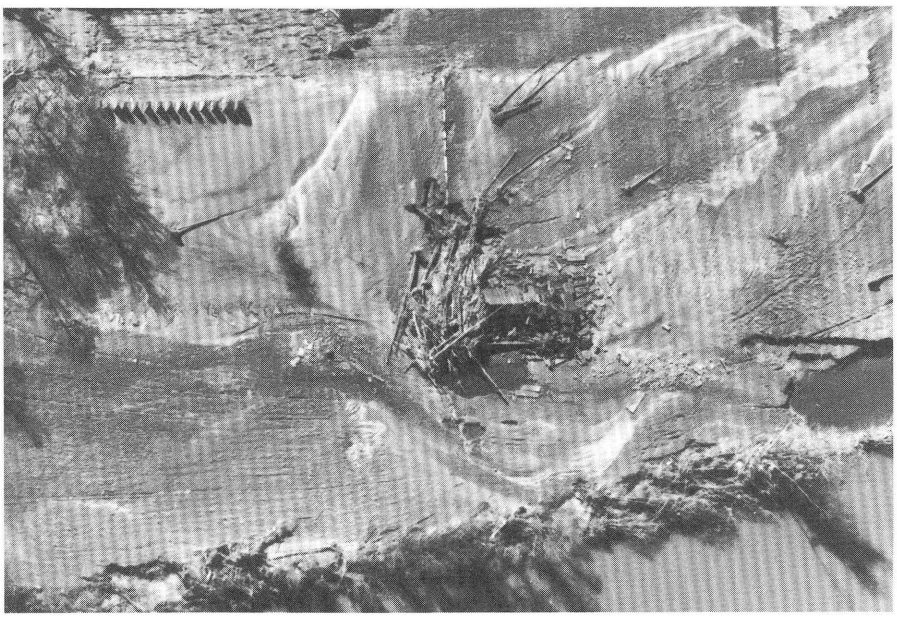

Figure 11. Aerial photograph of building that served as nucleus for tree jam, Black Fork flood plain near Hendricks. Flow is from left to right (northward) (West Virginia Department of Highways photograph).

Trees and trash were deposited more commonly in logjams than in dunelike forms. The nuclei of most logjams were one or more substantial trees not toppled by the flood. Some buildings also served as logjam nuclei (fig. 11). These buildings suffered severe damage from the impact of large trees floating in high-velocity currents, but the trees provided armoring that deflected currents from the buildings and kept them from being swept away (Fonner, 1987).

Logjams were widespread on forested bottomlands. Tree-and-trash accumulations were thickest along fronts that separated upstream surfaces (from which most trees were swept away) and downstream surfaces (on which most trees remained standing). Logjams developed lobate morphology where high-velocity currents swept forested bottomlands. Several meanders were nearly cleared of forest cover, particularly those that experienced high-velocity flows and development of ramps and cobble-boulder splays. Log-dammed pseudo-terraces, like those formed during the same flood in the Little River basin of Virginia (Kochel and others, 1987), were rare on Cheat River and Black Fork, possibly because the width of these rivers allowed toppled trees to float more freely than did the narrower Little River.

Deposits of mineral sediments were not well developed along valley sidewalls or on many other low-energy, low-terrace, and upper flood-plain environments, but floating wood fragments and trash were widespread, and the most easily observed indicators of high water. The trash component was quite varied; clothing, bottles, and objects made of styrofoam, foam rubber, or lightweight plastics were abundant. Most of the wood consisted of well-rounded sticks, less than 15 cm long, but slightly larger pieces of lumber were common. Painted surfaces and nails in many of these boards suggest they were derived from structures destroyed during the flood.

It is difficult to assess the significance of tree-and-trash deposits to the long-term flood-plain stratigraphy of Cheat River and Black Fork. Obviously, much of the trash, such as styrofoam and lightweight plastics, would not have been deposited by floods before the 20th century. Trees and shrubs would have been the only significant source of low-density sediments during prehistoric floods. Even if landforms were made from these sediments during earlier floods, these landforms would have collapsed almost completely as the organic matter decayed. Large, coarse organic deposits may have a significant indirect effect on flood-plain geomorphology before they decay; they may either block or deflect flow, setting up extreme turbulence and erosion at some sites and backwater effects and deposition at others.

SOURCES OF FLOOD-PLAIN SEDIMENTS

Slope failures during the 1985 flood are beyond the scope of this report, but our reconnaissance field work and our examination of aerial photographs show that slope failures were much less common here than in the upper Potomac River basin, where thousands of failures have been mapped (Jacobson and others, 1987a, b; chapter C, this volume). Two large landslides occurred adjacent to Cheat River between Macomber and Rowlesburg, and tens of

small failures were triggered along channel margins, presumably the result of scour at the base of slopes and of high pore pressures in the failed colluvial deposits. Debris-flow and debris-avalanche deposits have not been identified in our study area.

Gully erosion and piping of coarse-grained colluvium appear to have been important slope phenomena during the flood. Surface A horizons in typical colluvial soils of the Cheat basin are composed of loose, organic-rich channery loam (Pyle and others, 1982). After the flood, these soils showed steep, shallow gullies, tens of meters long and less than a meter wide, in which organic-rich surface horizons had been washed away. Angular coarse-grained clasts exposed in the shallow gullies were totally clast-supported, lacking the loose loam matrix found in adjacent soils. On rainy days after the flood, surface runoff was observed infiltrating into the coarse-grained clasts and continuing downslope through subsurface piping. If piping occurred during the 1985 flood, it may have facilitated runoff on colluvial slopes, thereby reducing the number of localities where pore-water pressure reached the level necessary for slope failures. Moreover, the scarcity of slope failures may help explain why silt and clay deposits were uncommon and poorly developed on flood plains in the Cheat River basin.

The distribution of flood deposits shows that most sediments transported by Cheat River and Black Fork during the flood were on the flood plain prior to 1985. In effect, flood-plain sediments were traded from preflood deposits to new deposits downstream. The close proximity of gravel bars and sand dunes to areas of intense flood-plain scour suggests that the average distance of transport was much less than a kilometer. Flood-plain surfaces that were not near sites of scour generally received little sedimentation.

The route of clast transport during the 1985 flood was not typical of sediment trading, where sediment is eroded from a cut bank on the outside of one meander and deposited on a point bar at the inside of the next meander downstream. The high-velocity turbulent flows across the Cheat River and Black Fork flood plains eroded clasts from the channel margin at the downstream end of a cut bank and deposited them on the flood-plain surface well away from the normal channel of the river.

CONCLUSIONS AND IMPLICATIONS

Summary of Flood Geomorphology

Many landforms and deposits created by the 1985 flood are unlike those formed by more frequent flows in the Cheat River basin. Extremes of sediments ranged from silty loam slack-water deposits to boulders more than 2 m in diameter. Well-developed slack-water deposits formed at back-flooded tributary mouths but were far below high-water levels indicated by flotsam. The creation of large ramps and arcuate gravel splays juxtaposed coarse tractive-load sediments and sand dunes on top of low-energy overbank deposits. This juxtaposition extended hundreds of meters away from the preflood channel. The boulders transported on steep reaches of Cheat River appear to be nearly the largest clasts that can be moved by a flow of this magnitude. Organic and artificial deposits were quite voluminous and probably warrant considerably more attention by fluvial geomorphologists. All of these deposits have long-term significance to fluvial geomorphology.

Effectiveness of Large Floods in Long-Term Flood-Plain Evolution

The 1985 floods on Cheat River and Black Fork have implications about how flood plains evolve in the central Appalachians. These implications are clearer when post-flood changes in vegetation, morphology, and stratigraphy are considered separately. Recovery periods for these types of changes are quite different, so the significance of extreme floods depends on which type of change is under consideration and on the nature of the flood plain. Disregarding the artificial influences of postflood mitigation, the 1985 flood shows that high-magnitude, low-frequency floods can have significant long-term influence on the geomorphology and stratigraphy of Appalachian flood plains.

Extreme floods probably are not particularly effective controls of bottomland vegetation (Wolman and Gerson, 1978; Hupp, 1988). Many trees in the age range of 50–100 yr (or older) were destroyed by the November 1985 flood, but the recovery of flood-plain vegetation is relatively short (decades for most trees, less for most nontree species). Bottomland plant ecology is more affected by frequency of inundation than by age of flood-plain surface, so more frequent floods play a larger role than extreme floods (Hupp, 1988).

Channels floored with cobbles and small boulders recover their preflood morphology rapidly. These clasts can be moved by moderate events on Cheat River and Black Fork, so the channel will soon approach a hydraulic geometry adjusted to these flows. Rapid morphologic recovery has been documented after extreme floods elsewhere in the Eastern United States (Costa, 1974; Moss and Kochel, 1978); new point-bar deposits on the Cheat River flood plain show that morphologic recovery is occurring in cobble and small-boulder channels in the aftermath of 1985. If no other extremely large floods occur before the "adjustment" landforms are vegetated, then the cobble and small-boulder channels will recover morphologically in less time than the >100-yr recurrence interval of the flood.

Morphologic recovery of the channel takes much longer where moderate flows cannot transport bedload clasts (Baker, 1977; Kochel, 1988). The easiest places to

demonstrate dominance by high-magnitude, low-frequency events are steep, bouldery reaches like Cheat Narrows and Cheat Canyon. The November 1985 flood has been the only event during this century capable of transporting the large boulders in these two reaches. These boulders are the main control on valley-bottom morphology and flood hydraulics in these reaches, so deposition during moderate and frequent flows is indirectly determined by boulder movement during much larger floods.

Although most discussions of morphologic recovery in fluvial systems (e.g., Wolman and Gerson, 1978; Kochel, 1988) focus on channel morphology, we should remember that moderate flows are probably less effective at recovery of flood-plain morphology. River channels are much higher energy environments than flood plains during moderate floods in humid landscapes. This situation reversed on parts of the flood plain during the 1985 flood, creating erosional and deposition landforms at many sites that are unlikely to experience other high-velocity flows until the next catastrophic flood. Bioturbation, local colluviation or slope wash, and the periodic draping of fine-grained sediment are the main natural processes of recovery between extreme floods. Many of the 1985 landforms had relief of a meter or more, so morphologic recovery may have taken centuries if postflood mitigation by humans had not obliterated most of the new landforms.

Events like the November 1985 flood have long-lasting effects on flood-plain stratigraphy, too. Widespread juxtaposition of cobbles and small boulders on top of fine-grained overbank alluvium only occurs when deep, high-velocity flows develop on the flood plain. In a natural system the cobble and boulder deposits would persist until destroyed by lateral channel migration or subsequent extreme floods. In either case, these deposits could last a long time.

The stratigraphic framework of the flood plain may reflect a catastrophic event long after the channel and flood plain return to their preflood morphology. Waning stages of a catastrophic flood and later moderate floods leave deposits that fill many of the erosional features created during the large flood. Much of the deposition is in direct response to the scour and channel widening by the catastrophic flood. Postflood filling is part of morphologic recovery to preflood hydraulic geometry, but the flood plain may never recover its preflood stratigraphy. Many stratigraphic units formed as a result of a catastrophic flood will last until either another extreme flood erodes them away or lateral channel migration completely reworks the flood plain.

There is one major unresolved question concerning the effectiveness of floods like the 1985 event on controlling morphology and stratigraphy: Is this flood representative of floods that have occurred in the past? The 20th century drainage basin is not analogous to the prehistoric basin, so there is a natural tendency to attribute some of the radical flood-plain and channel changes to artificial influences acting on runoff, flood-plain cover, and resistance to overbank flow. Yet, as was stated previously, the unique severity of the 1985 flood in the Cheat River basin can be attributed to the extraordinary amount of rain that fell over most of the drainage basin in a short amount of time. We believe that if similar meteorologic events occurred in the drainage basin before the local historic record began, a similar flood would have resulted, producing deposits and landforms like those formed on Cheat River and Black Fork in 1985.

Implications for Flood-Plain Management

Our research suggests that it is feasible to extend the Cheat flood record with paleohydraulic reconstructions from slack-water deposits and large transported boulders. However, the ability of slack-water deposits to serve as precise indicators of prehistoric water levels may be poor. More work in other basins affected by catastrophic flooding is essential before we can evaluate the applicability of these methods to practical flood-plain management in the region.

Extreme floods in the Appalachians present many flood hazards that can be avoided by flood-plain management based on geomorphology. Much of the damage in 1985 was caused by high-velocity flows over flood-plain surfaces, presenting a much greater problem than simple inundation. Buildings experienced serious structural damage or were swept completely away. These high-velocity flows also created diagnostic landforms such as ramps and arcuate gravel splays. Sites that exhibit either of these features should not be developed without considering whether development entails unnecessary risk to lives or property. Although the merits of costly postflood mitigation are far beyond the scope of this research, it does bear notice that postflood disturbance may obliterate geomorphologic and sedimentologic evidence that may be of great use to sound flood-plain management.

REFERENCES CITED

Auvil, Myrtle, 1977, Covered bridges of West Virginia, past and present, third ed.: Parsons, W. Va., McClain Printing, 249 p.

Baker, V. R., 1973, Paleohydrology and sedimentology of Lake Missoula flooding in eastern Washington: Geological Society of America Special Paper 144, 79 p.

———1977, Stream response to floods, with examples from central Texas: Geological Society of America Bulletin, v. 88, p. 1057–1071.

Baker, V.R., and Bunker, R.C., 1985, Cataclysmic late Pleistocene flooding from glacial Lake Missoula: Quaternary Science Reviews, v. 4, p. 1–41.

Baker, V.R., and Kochel, R.C., 1988, Flood sedimentation in bedrock fluvial systems, *in* Baker, V.R., Kochel, R.C., and Patton, P.C., eds., Flood geomorphology: New York, John Wiley and Sons, p. 123–137.

Baker, V.R., Pickup, G., and Polach, H.A., 1985, Radiocarbon dating of flood events, Katherine Gorge, Northern Territory, Australia: Geology, v. 13, p. 344–347.

Baker, V.R., and Ritter, D.F., 1975, Competence of rivers to transport coarse bedload material: Geological Society of America Bulletin, v. 86, p. 975–978.

Bell, A.M., 1986, Morphology and stratigraphy of terraces in the upper Shenandoah Valley, Virginia: Morgantown, West Virginia University, M.S. thesis, 161 p.

Cardwell, D.H., Erwin, R.B., and Woodward, H.P., 1968, Geologic map of West Virginia: Morgantown, W. Va., West Virginia Geological and Economic Survey, 2 sheets.

Carpenter, D.H., 1990, Floods in West Virginia, Virginia, Pennsylvania, and Maryland, November 1985: U.S. Geological Survey Water-Resources Investigations Report 88–4213, 86 p.

Charleston Gazette, 1985, Rivers' crests in flooded areas: Charleston [W. Va.] Gazette, Nov. 6, p. 3A.

Clark, G.M., Jacobson, R.B., Kite, J.S., and Linton, R.C., 1987, Storm-induced catastrophic flooding and related phenomena in Virginia and West Virginia, November 1985, *in* Mayer, Larry, and Nash, David, eds., Catastrophic flooding: London, Allen and Unwin, p. 355–380.

Costa, J.E., 1974, Response and recovery of a Piedmont watershed from Tropical Storm Agnes, June 1972: Water Resources Research, v. 10, p. 106–112.

———1983, Paleohydraulic reconstruction of flash-flood peaks from boulder deposits in the Colorado Front Range: Geological Society of America Bulletin, v. 94, p. 986–1004.

Dunne, T., and Leopold, L.B., 1978, Water in environmental planning: San Francisco, Calif., W.H. Freeman and Company, 818 p.

Elliott, T., 1986, Deltas, *in* Reading, H.G., ed., Sedimentary environments and facies, second ed.: Oxford, Blackwell Scientific Publications, p. 113–154.

Embree, W.N., Friel, E.A., and Taylor, F.M., 1985, Water resources data, West Virginia water year 1984: U.S. Geological Survey Water-Data Report WV–84–1, 323 p.

Fansler, H.F., 1962, History of Tucker County, West Virginia: Parsons, W. Va., McClain Printing, 702 p.

Fonner, R.F., 1987, Homeowner's guide to geologic hazards: Mountain State Geology: Morgantown, W. Va., West Virginia Geological and Economic Survey, p. 1–9.

GAI Consultants, Inc., 1985, West Penn Power Company, Greensburg, Pennsylvania, Cheat River basin flood of 4–5 November 1985, Postflood inspection report Lake Lynn Dam, FERC Project 2459—W. Va.: Monroeville, Pa., GAI Consultants, Inc., 20 p. and app.

Hendricks, E.L., 1964, Compilation of records of surface waters of the United States, October 1950 to September 1960, part A, Ohio River basin except Cumberland and Tennessee River basins: U.S. Geological Survey Water-Supply Paper 1725, 560 p.

Hupp, C.R., 1988, Plant ecological aspects of flood geomorphology and paleoflood history, *in* Baker, V.R., Kochel, R.C., and Patton, P.C., eds., Flood geomorphology: New York, John Wiley and Sons, p. 335–356.

Jacobson, R.B., Cron, E.D., and McGeehin, J.P., 1987a, Preliminary results from a study of natural slope failures triggered by the storm of November 3–5, 1985, Germany Valley, West Virginia and Virginia, *in* Schultz, A.P., and Southworth, C.S., eds., Landslides of eastern North America: U.S. Geological Survey Circular 1008, p. 11–16.

Jacobson, R.B., McGeehin, J.P., and Cron, E.D., 1987b, Hillslope processes and surficial geology, Wills Mountain anticline, West Virginia and Virginia, *in* Kite, J.S., ed., Research on the late Cenozoic of the Potomac Highlands, Southeastern Friends of the Pleistocene, vol. 1: Morgantown, W. Va., West Virginia Geological and Economic Survey Open-File Report 88–2, p. 31–55.

Kite, J.S., 1986, Erosion and deposition in the Monongahela and Potomac drainage basins during the floods of November 1985: Geological Society of America Abstracts with Programs (North-Central sectional meeting), v. 18, p. 313.

Kite, J.S., Linton, R.C., and Gerritsen, S., 1987, The Twin Run debris avalanche-debris flow, *in* Kite, J.S., and Linton, R.C., eds., SEFOP 1987, Field guide to the first annual meeting of the Southeastern Friends of the Pleistocene: Morgantown, W. Va., West Virginia Geological and Economic Survey Open-File Report 88–1, p. 34–52.

Knox, J.C., 1987, Stratigraphic evidence of large floods in the upper Mississippi Valley, *in* Mayer, Larry, and Nash, David, eds., Catastrophic flooding: London, Allen and Unwin, p. 155–180.

Kochel, R.C., 1988, Geomorphic impact of large floods, review and new perspectives on magnitude and frequency, *in* Baker, V.R., Kochel, R.C., and Patton, P.C., eds., Flood geomorphology: New York, John Wiley and Sons, p. 169–187.

Kochel, R.C., and Baker, V.R., 1988, Paleoflood analysis using slackwater deposits, *in* Baker, V.R., Kochel, R.C., and Patton, P.C., eds., Flood geomorphology: New York, John Wiley and Sons, p. 357–376.

Kochel, R.C., and Ritter, D.F., 1987, Implications of flume experiments on the interpretation of slackwater paleoflood sediments, *in* Singh, V.J., ed., Regional flood frequency analysis: Boston, Mass., D. Reidel, p. 365–384.

Kochel, R.C., Ritter, D.F., and Miller, J., 1987, Role of tree dams in the construction of pseudo-terraces and variable geomorphic responses to floods in Little River valley, Virginia: Geology, v. 15, p. 718–721.

Komar, P.D., 1988, Sediment transport by floods, *in* Baker, V.R., Kochel, R.C., and Patton, P.C., eds., Flood geomorphology: New York, John Wiley and Sons, p. 97–111.

Koster, E.H., 1978, Transverse ribs: their characteristics, origin and paleohydraulic significance, *in* Miall, A.D., ed., Fluvial sedimentology: Calgary, Alberta, Canadian Society of Petroleum Geologists, p. 161–186.

Lescinsky, J.B., 1986, Flood of November 1985 in West Virginia, Pennsylvania, Maryland and Virginia: U.S. Geological Survey Open-File Report 86–486, 33 p.

Linton, R.C., 1992, Slackwater deposits along the Cheat River in east-central West Virginia: Morgantown, West Virginia University, M.S. thesis, 173 p.

Linton, R.C., and Kite, J.S., 1987, Slack-water deposits along the Cheat River in east-central West Virginia: Geological Society of America Abstracts with Programs (Southeast sectional meeting), v. 19, p. 95.

Maxwell, H., 1884, History of Tucker County, West Virginia: Kingwood, W. Va., Preston Publishing, 531 p.

Miller, A.J., 1987, Stop 1, Hopeville Canyon overlook, *in* Kite, J.S., and Linton, R.C., eds., SEFOP 1987, Field guide to the first annual meeting of the Southeastern Friends of the Pleistocene: Morgantown, W. Va., West Virginia Geological and Economic Survey Open-File Report 88–1, p. 57.

Morton, O.F., 1914, A history of Preston County, West Virginia: Kingwood, W. Va., The Journal Publishing, 564 p.

Moss, J.H., and Kochel, R.C., 1978, Unexpected geomorphic effects of the Hurricane Agnes storm and flood, Conestoga drainage basin, southeastern Pennsylvania: Journal of Geology, v. 86, p. 1–11.

Murphy, A.J., 1986, Testimony of Hon. Austin J. Murphy, a Representative in Congress of the State of Pennsylvania, Flood damages along the Monongahela and Cheat Rivers in Pennsylvania and West Virginia as the result of severe flooding in November 1985, (99–41) hearing before the Subcommittee on Water Resources of the Committee on Public Works and Transportation, House of Representatives, 99th Cong., 2nd sess., p. 2–8.

North, E.L., 1985, The 55 West Virginias, a guide to the State's counties: Morgantown, W. Va., West Virginia University Press, 118 p.

Patton, P.C., Baker, V.R., and Kochel, R.C., 1979, Slack-water deposits, a geomorphic technique for the interpretation of fluvial paleohydrology, *in* Rhodes, D.P., and Williams, G.P., eds., Adjustments of the fluvial system: Dubuque, Iowa, Kendall/Hunt Publishing, p. 225–253.

Paulson, C.G., 1953, Surface water supply of the United States 1950, part 3, Ohio River basin: U.S. Geological Survey Water-Supply Paper 1173, 730 p.

Plum, K., 1985, Albright, Rowlesburg devastated by flood: The Morgantown Dominion Post, Nov. 6, p. 14A–15A.

Preston County Historical Society, 1979, Preston County West Virginia history: Dallas, Texas, Taylor Publishing, 514 p.

Preston County Journal, 1888a, A great flood, destruction along Cheat, the highest waters ever known, bridges, houses, lumber, and all kinds of property swept away: Kingwood, W. Va., Preston County Journal, no. 1143, July 12, p. 1.

———1888b, More about the great flood of '88: Kingwood, W. Va., Preston County Journal, no. 1144, July 19, p. 1.

———1907, Cloudburst—Preston County suffered many dollars damage: Kingwood, W. Va., Preston County Journal, July 18, vol. 46, no. 46, p. 3.

Pyle, R.E., Beverage, W.W., Yoakum, T., Amick, D.P., Hatfield, W.F., and McKinney, D.E., 1982, Soil survey of Randolph County area main part, West Virginia: U.S. Department of Agriculture Soil Conservation Service and Forest Service, 167 p., 59 maps.

Region III Interagency Flood Hazard Mitigation Team, 1985, Interagency flood hazard mitigation report in response to the November 7, 1985, disaster declaration: Federal Emergency Management Agency, Report FEMA–753–DR–WV, 56 p., 9 app.

Speer, P.R., and Gamble, C.R., 1965, Magnitude and frequency of floods in the United States, part 3-A, Ohio River basin except Cumberland and Tennessee River basins: U.S. Geological Survey Water-Supply Paper 1675, 630 p.

Teats, B., and Young, S., 1985, Killing waters, the great West Virginia flood of 1985: Terra Alta, W. Va., Cheat River Publishing, 112 p.

Thomas, W.O., Jr., 1987, Techniques used by the U.S. Geological Survey in estimating the magnitude and frequency of floods, *in* Mayer, Larry, and Nash, David, eds., Catastrophic flooding: London, Allen and Unwin, p. 267–288.

U.S. Army Corps of Engineers, 1963, Review of reports (House Document 645, of 78th Cong., 2nd sess.) Rowlesburg Reservoir, app. I, Hydrology: Pittsburgh, Pa., 26 p. and 20 pls.

U.S. Bureau of Census, 1913, Thirteenth census of the United States taken in 1910, vol. II, Agriculture 1909 and 1910, Nebraska-Wyoming: Washington, D.C., U.S. Department of Commerce, 1013 p.

———1989a, 1987 Census of agriculture advance copy report, Preston County, W. Va.: Washington, D.C., U.S. Department of Commerce, 2 p.

———1989b, 1987 Census of agriculture advance copy report, Tucker County, W. Va.: Washington, D.C., U.S. Department of Commerce, 2 p.

U.S. Geological Survey, 1971, Surface water supply of the United States 1961–1965, part 3, Ohio River basin, vol. 1, Ohio River basin above Kanawha River: U.S. Geological Survey Water-Supply Paper 1907, 621 p.

———1976, Surface water supply of the United States 1965–1970, part 3, Ohio River basin, vol. 1, Ohio River basin above Kanawha River: U.S. Geological Survey Water-Supply Paper 2107, 668 p.

———1985, National water conditions, November 1985, Streamflow during November: U.S. Geological Survey, 7 p.

Venable, N.J., 1990, Canaan Valley: West Virginia Renewable Resources Unique areas series 812, West Virginia University Extension Service, 32 p.

Wells, J.V.B., 1957, Compilation of records of surface waters of the United States through September 1950, part 3-A, Ohio River basin except Cumberland and Tennessee River basins: U.S. Geological Survey Water-Supply Paper 1305, 652 p.

West Virginia Geological and Economic Survey, no date, Generalized geologic map of the coal fields of West Virginia: Morgantown, W. Va., West Virginia Geological and Economic Survey, 1 sheet.

Wiley, S.T., and Frederick, A.W., 1882, History of Preston County (West Virginia): Kingwood, W. Va., The Journal Printing House, 529 p.

Williams, G.P., 1984, Paleohydrologic equations for rivers, *in* Costa, J.E., and Fleisher, P.J., eds., Developments and applications of geomorphology: Berlin, Springer-Verlag, p. 343–367.

Williams, G.P., and Costa, J.E., 1988, Geomorphic measurements after floods, *in* Baker, V.R., Kochel, R.C., and Patton, P.C., eds., Flood geomorphology: New York, John Wiley and Sons, p. 65–77.

Williams, G.P., and Guy, H.P., 1973, Erosional and depositional aspects of Hurricane Camille in Virginia, 1969, U.S. Geological Survey Professional Paper 804, 80 p.

Wolman, M.G., and Gerson, R., 1978, Relative scales of time and effectiveness of climate in geomorphology in watershed geomorphology: Earth Surface Processes, v. 3, p. 189–208.

Chapter E

Flood Hydrology and Geomorphic Effects on River Channels and Flood Plains: The Flood of November 4–5, 1985, in the South Branch Potomac River Basin of West Virginia

By ANDREW J. MILLER and DOUGLAS J. PARKINSON

U.S. GEOLOGICAL SURVEY BULLETIN 1981

GEOMORPHIC STUDIES OF THE STORM AND FLOOD OF NOVEMBER 3–5, 1985, IN THE UPPER POTOMAC AND CHEAT RIVER BASINS IN WEST VIRGINIA AND VIRGINIA

CONTENTS

PLATE

FIGURES

Unless otherwise indicated, all postflood aerial photographs are from a set of flight lines flown for the West Virginia Department of Highways within 3 days after the flood. Preflood aerial photographs are from a project flown in 1980 for the Army Corps of Engineers.

TABLES

Flood Hydrology and Geomorphic Effects on River Channels and Flood Plains: The Flood of November 4–5, 1985, in the South Branch Potomac River Basin of West Virginia

By Andrew J. Miller[1] *and* Douglas J. Parkinson[2]

Abstract

The November 1985 flood was the largest recorded in the South Branch Potomac River basin. Discharges exceeded values estimated for a recurrence interval of 500 yr at four of six stations in the basin. Flow velocities in the channel were as high as 4.6 m/s and may have exceeded 6 m/s at some locations; estimated values of unit stream power at U.S. Geological Survey gage locations were as high as 988 W/m^2 and may have exceeded 2,500 W/m^2 at some locations. Along the three forks of the South Branch Potomac River, discharges of 1,000–7,000 m^3/s flowed through valley cross sections that ranged in width from less than 70 m to 1,700 m, and, as a result, hydraulic conditions were extremely variable. Valley constrictions and expansions were important determinants of erosion and deposition patterns.

Geomorphic impacts on valley floors along the three forks of the South Branch Potomac River included formation of a wide array of erosion and deposition features. Flood-generated erosion features included longitudinal grooves, scour marks, widened channels, stripped flood plains, chutes, anastomosing erosion channels, and jet-shaped erosion forms. Deposition features were generally adjacent to eroded areas and included channel gravel bars, gravel splays, gravel and sand sheets, isolated gravel bars and sand dunes on flood plains, wake deposits, and backwater deposits.

Mapping of erosion damage classes along 384 km of channel and valley floor revealed that 82.8 percent of the valley length experienced at least incipient erosion, 30.2 percent experienced severe erosion, and 5.7 percent experienced catastrophic erosion of the valley floor. Reach-average values of unit stream power were positively correlated with the percent of the valley reach that experienced severe erosion; percentages of 50 percent or more were associated with average values of 200–500 W/m^2. These results suggest that, with further research, it should be possible to define threshold conditions for bottomland erosion.

INTRODUCTION

The flood of November 4–5, 1985, was the largest recorded in the South Branch Potomac River basin. Peak discharges exceeded previous records at five of six gaging stations and exceeded the estimated 500-yr discharge at four of those gage sites (tables 1, 2). Crest stage exceeded the 1949 record flood crest by amounts ranging from 0.79 to 3.41 m at five gages and equaled the 1949 record at the sixth gage.

The three major forks of the South Branch Potomac River (pl. 1, fig. 1) began to overflow their banks on the afternoon of November 4. The actual time of the flood crest was recorded at only one gage, and there are few eyewitness reports available for other locations. From these reports, we project that the upper reaches reached crest stage between 6 p.m. and 9 p.m., the middle reaches between 10 p.m. and 2 a.m. the next morning, and the South Branch below the confluence of the forks after 4 a.m. on November 5. Reports from some locations along the middle reaches indicate that the flood receded rapidly and the rivers were only slightly above flood stage by midmorning; thus, the most extreme flow conditions occurred under cover of darkness. The only complete stage record from the South Branch basin was collected on the South Fork South Branch Potomac River at Brandywine, W. Va., and shows that the South Fork exceeded bankfull stage for 27–28 h; however, the stage was more than 1 m above bankfull for only 14 h. During the daylight period of November 5, the flood crest continued moving down the main stem of the South Branch;

Manuscript approved for publication February 22, 1991.

[1] Department of Geography, University of Maryland Baltimore County, Baltimore, MD 21228.

[2] Department of Geography and Environmental Engineering, The Johns Hopkins University, Baltimore, MD 21218.

Table 1. Hydrologic data compiled for U.S. Geological Survey gage sites: November 1985 flood, South Branch Potomac River basin

Station	Drainage area		Peak discharge		Peak unit discharge		Ratio of peak discharge to previous record discharge	Average precipitation upstream of gage (mm)
	km^2	mi^2	m^3/s	ft^3/s	$m^3/s/km^2$	$ft^3/s/mi^2$		
South Branch Potomac River at Franklin, W.Va.	471	182	1,246	44,000	2.65	242	2.93	191
North Fork South Branch Potomac River at Cabins, W.Va.	813	314	2,549	90,000	3.14	287	1.80	221
South Branch Potomac River near Petersburg, W.Va.	1,663	642	3,681	130,000	2.21	202	2.10	220
South Fork South Branch Potomac River near Brandywine, W.Va.	264	102	1,147	40,500	4.34	397	.98	158
South Fork South Branch Potomac River near Moorefield, W.Va.	733	283	3,115	110,000	4.25	389	2.82	171
South Branch Potomac River near Springfield, W.Va.	3,810	1,471	6,796	240,000	1.78	163	1.68	176

Table 2. Comparison of 1985 peak (Q_{pk}) discharge with estimated 100-yr (Q_{100}) and 500-yr (Q_{500}) peak discharge

Station	P=0.01 (Q_{100})		P=0.002 (Q_{500})		November 1985 (Q_{pk}) (m^3/s)	Q_{pk}/Q_{100}	
	Bulletin 17B[1] (m^3/s)	Regional curves[2] (m^3/s)	Bulletin 17B[1] (m^3/s)	Regional curves[2] (m^3/s)		[3]	[4]
South Branch Potomac River at Franklin, W.Va.	595	736	883	1,199	1,246	2.09	1.69
North Fork South Branch Potomac River at Cabins, W.Va.	1,371	1,209	2,330	1,992	2,549	1.86	2.11
South Branch Potomac River near Petersburg, W.Va.	2,071	2,316	3,440	3,873	3,681	1.78	1.59
South Fork South Branch Potomac River near Brandywine, W.Va.	818	445	1,361	735	1,147	1.40	2.58
South Fork South Branch Potomac River near Moorefield, W.Va.	1,453	1,099	2,748	1,808	3,115	2.14	2.83
South Branch Potomac River near Springfield, W.Va.	4,305	4,927	7,404	8,374	6,796	1.58	1.38

[1] Estimates based on individual station records, supplemented by data on historic floods (Interagency Advisory Committee on Water Data, 1982). Results furnished by W.O. Thomas, U.S. Geological Survey.

[2] Regional flood-frequency curves for West Virginia region 3 (Runner, 1980).

[3] Ratio of November 1985 peak to estimated 100-yr peak as computed using Bulletin 17B (see footnote 1).

[4] Ratio of November 1985 peak to estimated 100-yr peak as computed using West Virginia regional flood-frequency curves.

crest stage was recorded at about 10:15 p.m. at Paw Paw, W. Va., downstream of the confluence with the North Branch (fig. 2).

No direct observations of current velocity were made during the flood. Estimates based on slope-area measurements of peak discharge indicate cross-section average velocities up to 4.6 m/s in constricted canyon reaches and average velocities in the range 2–2.5 m/s in broader reaches. The force of the flow was sufficient to cause widespread erosion of valley floors and transportation of enormous amounts of debris, with the largest boulders transported exceeding 2 m along the intermediate axis. Property damage in some areas was reminiscent of the effects of a tornado (figs. 3, 4). Groves of trees were uprooted or broken off above ground level, and many trees came to rest in debris jams accumulating around flow obstructions on the valley floor. Buildings were lifted off their foundations or torn apart where they stood; debris jams often contained fragments of houses or their contents. In several cases, people trapped by the rising water took refuge in houses and later drowned when those buildings were overturned or destroyed (West Virginia Advocate, 1986). Mobile homes and motor vehicles at some sites were entrained in the flow and transported tens to hundreds of

Figure 1. Major streams, drainage divides, and gaging stations in the South Branch Potomac River basin. Drainage divides within the basin are represented by dashed lines.

meters along the valley floor. Railroad tracks in at least two areas were lifted off their beds, carried downvalley, and twisted into spiral patterns.

Where erosion was most intense, particularly along the North Fork South Branch Potomac River downstream of Circleville, W. Va., roads and bridges were swept away. News reports following the flood suggested that many farms in prime agricultural bottomland would never grow crops again, owing either to total removal of topsoil or to deposition of sheets of gravel on the flood plain (West Virginia Advocate, 1986). Only a massive relief effort, in some cases including the use of imported fill material, permitted reestablishment of agriculture at these sites. Channel rehabilitation efforts generally restored the river

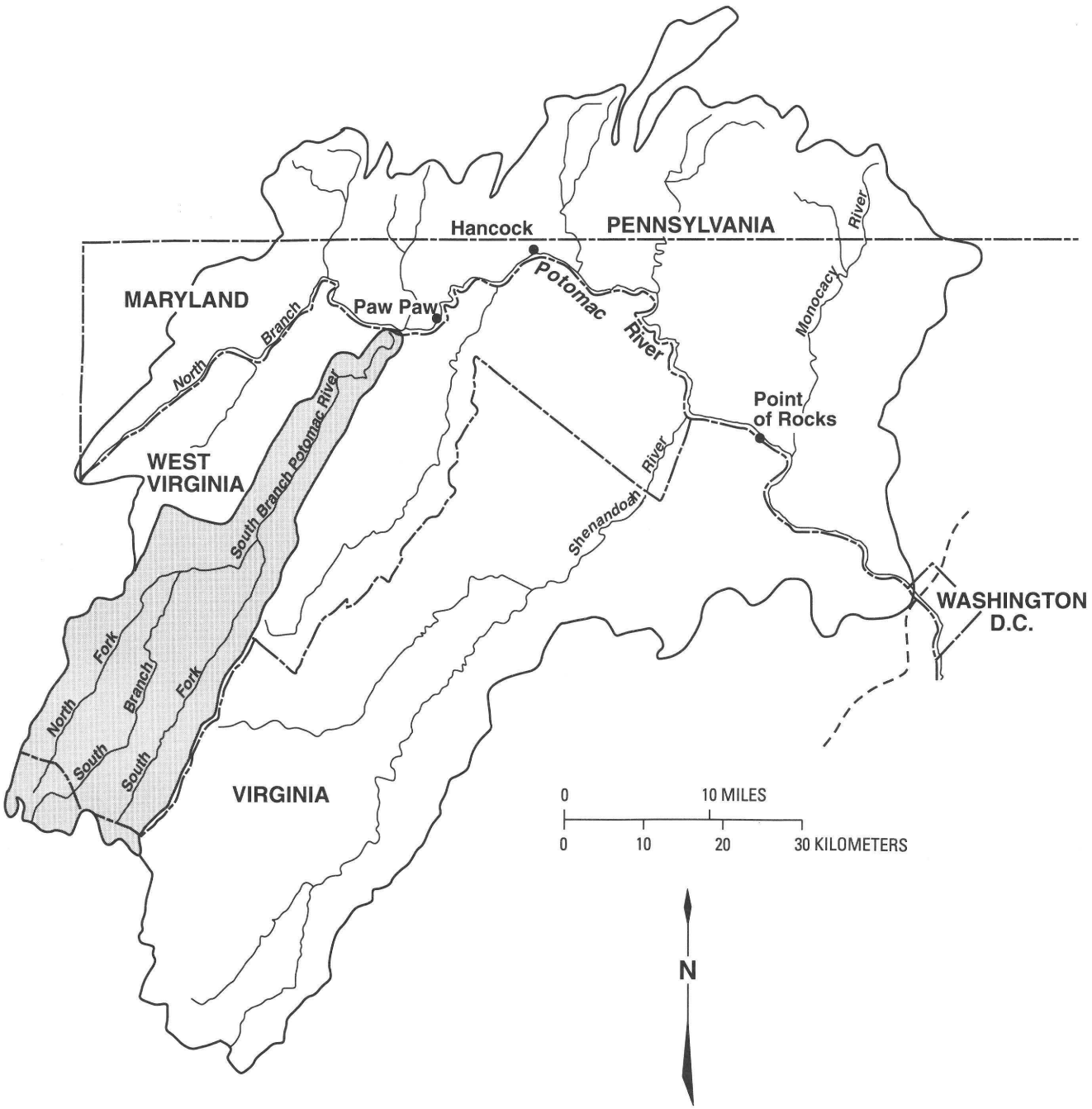

Figure 2. Potomac River basin. The shaded area is the South Branch Potomac River basin.

channels to their former courses, although the channels themselves were often widened substantially and denuded of vegetation. Debris and large boulders were generally cleared from the channel, and thick lobes of sediment on the flood plain were scraped off and piled along channel margins to form levees.

Few reliable observations of flow patterns and processes were obtained during the flood, and flood-plain and channel rehabilitation efforts quickly erased or obscured much of the physical evidence. An excellent documentary record was preserved, however, in aerial photographs (average scale about 1:8,000) flown for the West Virginia Department of Highways within 5 days following the flood. Although intended for assessment of road damage, the photographs show the intensity and spatial distribution of a series of erosion and deposition features formed by the flood on valley floors throughout the South Branch Potomac River basin. Most of these bear some resemblance to features that have been described in the literature before; however, we know of no previous flood in which the visual evidence of valley-floor erosion was both so widespread and so well documented. Although this report is concerned

Figure 3. Property damage on flood plain, looking upstream along valley of North Fork South Branch Potomac River immediately upstream of North Fork Gap. The river is located to the left of the field of view. Photograph by F.N. Scatena.

Figure 4. Trailer frame wrapped around tree by floodwaters. Note severely damaged house in background. Photograph by D. Lafon, U.S. Army Corps of Engineers.

primarily with the South Branch basin, the aerial photographs of the Cheat River basin have superior resolution, and some have been used to illustrate type examples of particular erosion and deposition features.

Purpose and Scope

The primary purpose of this report is to describe the November 1985 flood and its geomorphic impacts on valley floors in the South Branch Potomac River basin. This is an essential prerequisite to more detailed analysis of the factors controlling spatial distribution and morphology of fluvial erosion and deposition features of the flood.

The report concentrates on the South Branch, North Fork South Branch, and South Fork South Branch Potomac Rivers between the Virginia–West Virginia border and the confluence of the South Branch and the South Fork South Branch Potomac Rivers at Moorefield. Some additional information has been compiled for the South Branch downstream of Moorefield. We first visited the field area in December 1985 as part of a reconnaissance study for the Interstate Commission on the Potomac River Basin (Scatena, 1986). Subsequent to this trip, we visited the study area many times beginning in the spring of 1986. Much of the analysis is based on examination of preflood and postflood aerial photographs.

Organization

The report is organized as follows.

- Discussion of bottomland morphology in the study basin and of the interaction between boundary conditions and flood hydraulics;
- Presentation of hydrologic and hydraulic data for the November 1985 flood in the South Branch Potomac River basin;
- Brief description of erosion and deposition features observed at the mouths of tributaries to the three forks of the South Branch Potomac River;
- Description and classification of channel and floodplain erosion features formed in the November 1985 flood;
- Description and classification of channel and floodplain deposition features formed in the flood;
- Definition of a simple four-part hierarchical system for classifying erosion patterns in order to map their spatial distribution at basin scale;
- Description and analysis of the spatial distribution of erosion classes along the three forks of the South Branch Potomac River;
- Discussion and conclusions.

Previous studies that discuss aspects of the fluvial geomorphology of the South Branch basin include Fridley (1939, 1940), Ver Steeg (1940), Hack and Goodlett (1960), Clark (1967, 1987), Sites (1973), and Hack (1973). References on bedrock geology and hillslope geomorphology are provided by Jacobson and others (chapter C, this volume). Background data on basin hydrology are reported in Baloch and others (1971), Hobba and others (1972), and Friel and others (1975). Preliminary observations on the aftermath of the 1985 flood are reported in Scatena (1986), Clark and others (1987), Kite (1987), and Kite and Linton (chapter D, this volume).

BOTTOMLAND MORPHOLOGY

The trajectory of flood flow and resulting patterns of erosion and deposition appear to have been guided by the shape and orientation of the valley boundaries as well as the channel boundaries. Local valley topography and spatial configuration of roughness elements in the path of the flow also played an important role in determining where the flood had the greatest impact on the valley floor. The following discussion focuses on aspects of bottomland morphology that apparently influenced the spatial distribution and intensity of flood impacts in November 1985 in the South Branch basin.

Structural Control of Drainage

The South Branch Potomac River basin (fig. 1, pl. 1) is primarily in the Valley and Ridge physiographic province; the western tributaries to the North Fork drain the Appalachian Plateau. Drainage forms a trellis pattern, with the three main forks of the South Branch following parallel trends approximately N30°E. Valleys are underlain mostly by shale and limestone, and intervening ridges are capped by sandstone. Although the valleys run dominantly along strike, local structural weaknesses (Clark, 1967) have allowed river channels to cut paths transverse to strike, forming prominent water gaps (fig. 5*A*) where streams flow across ridge-forming sandstones and quartzites. The strike valleys are narrow but generally have some alluvial bottomland. There are also several extended valley reaches parallel to strike where the rivers run through bedrock canyons; but even in the canyons, the lithologies exposed in the channel and valley walls are variable. Geologic structure exerts a dominant but poorly understood influence on valley morphology in this region, one of the most complex areas of the Appalachians; some of the structural features have yet to be resolved (C. Scott Southworth, U.S. Geological Survey, written communication, 1987; Gerritsen and Dunne, 1988).

Channel gradients along the three forks of the South Branch upstream of Moorefield generally range from 0.002 to 0.009, and gradients in the bedrock canyons typically are steeper than reaches immediately upstream and downstream. The North Fork is steeper than either the South Fork or the South Branch (fig. 6, table 3), and this difference

probably accounts in part for greater erosion in the North Fork valley during the November 1985 flood. Between Moorefield and the confluence with the North Branch Potomac River, the gradient of the South Branch becomes much gentler, with an average value of 0.0009.

Patterns of Valley Width

Average valley widths upstream of the confluences of the North Fork with the South Branch and of the South Fork with the South Branch generally range between 200 and 400 m for drainage areas up to about 800 km^2. Although a few locations have valley floors up to 1,000 m wide, geologic structure effectively prevents any systematic increase in width of the three valleys of the South Branch as drainage area increases. Downstream of the major confluences the valleys broaden locally; the valley floor at Petersburg is almost 1,400 m wide at its broadest point (fig. 5*A*), and the valley floor downstream of Moorefield broadens to more than 1,700 m (fig. 5*B*). However, broad flood plains continue to alternate with constricted valley floors and bedrock canyons. Along the South Branch downstream of Moorefield, average valley-floor widths range from 95 to 1,250 m; from Romney to the confluence with the North Branch, the valley floor is generally 350 to 500 m wide.

Figure 7 illustrates the spatial distribution of average valley widths and of constrictions and canyon reaches along the three forks of the South Branch between the Virginia State line and Moorefield (also see pl. 1). In the canyons oriented along strike and in the water gaps cut through prominent ridges, the valley floors often are 125 m or less in width. Even where the river does not flow through a canyon or a major water gap, alternating expanding and contracting reaches are characteristic of these valleys and appear to have had an important influence on flow hydraulics during the 1985 flood. In some reaches, resistant bedrock spurs form local constrictions where the valley floor is no more than 50–70 m wide. Local constrictions may also be created by terraces or by fans at the mouths of tributaries, as can be seen along some parts of the North Fork valley (fig. 8). In some cases, valley-floor width varies by an order of magnitude within a longitudinal distance of 1 km.

Geomorphic Surfaces

Valley-floor topography and large roughness elements strongly influenced both depth and direction of flood flow and local patterns of erosion and deposition in the November 1985 event. At some locations, planform of the flooded area and the spatial pattern of features providing flow resistance changed significantly with flood stage. Features contributing to elevation and roughness variations included secondary channels, topographic steps, roads, bridges, fence lines, and patches of forest. Flow often separated around buildings or trees, affecting erosion and deposition nearby; in some cases, flow separated around a local topographic rise on the valley floor. Although preexisting overflow channels and tributaries were eroded in many places, new channels also formed at sites throughout the basin. Our discussions of flood-plain erosion and deposition forms include numerous illustrations and qualitative information about the role of these features.

The bottomlands inundated in the 1985 flood generally consist of two main geomorphic surfaces. One surface appears to be a flood plain and is 2.5–4 m above the low-water channel; this surface occupies the majority of the valley floor in most reaches. Local residents have stated that this surface was flooded in 1949 and 1985 but that only the swales and overflow channels incised in this surface were flooded in other events. At some locations this surface was not flooded even in 1949. Although it is generally relatively flat, the surface sometimes tilts either laterally or downvalley, and therefore its elevation above the channel may vary along a reach that is several hundred meters in length. Furthermore, debris fans and colluvial deposits commonly grade to the valley floor, creating local areas of greater relief. Although this surface does not conform strictly to the flow criterion used for defining a flood plain (Wolman and Leopold, 1957), it is not a well-defined terrace either. Subsequent use of the term "flood plain" in this report includes this surface.

A lower surface is present at many sites but is much less extensive and appears to occupy channel-margin belts and point-bar locations. It is most prominently developed in the South Fork basin. Whereas the upper surface is generally cleared for pasture or crops, the lower surface (1–1.5 m above low water) is commonly forested. Coarse particle sizes, hummocky surface relief, and greater frequency of inundation make this surface less suitable for agriculture than the higher surface. The low surface may be characterized either as flood plain or as active channel shelf, a geomorphic surface that is inundated during semiannual high-flow events (Osterkamp and Hedman, 1977); correlations with specific flow durations are not available at present to make a distinction between these possibilities. At some locations during the 1985 flood, especially where the main thread of flow was diverted around or away from the forested area, the low surface was marked by debris jams wrapped around trees, but relatively little erosion occurred. Other locations experienced complete devastation as the forest cover and underlying materials were stripped away.

Channel Pattern

The North Fork, South Branch, and South Fork can be classified as either confined (Lewin and Brindle, 1977), restrained (Lane, 1957), or partially confined (Nanson,

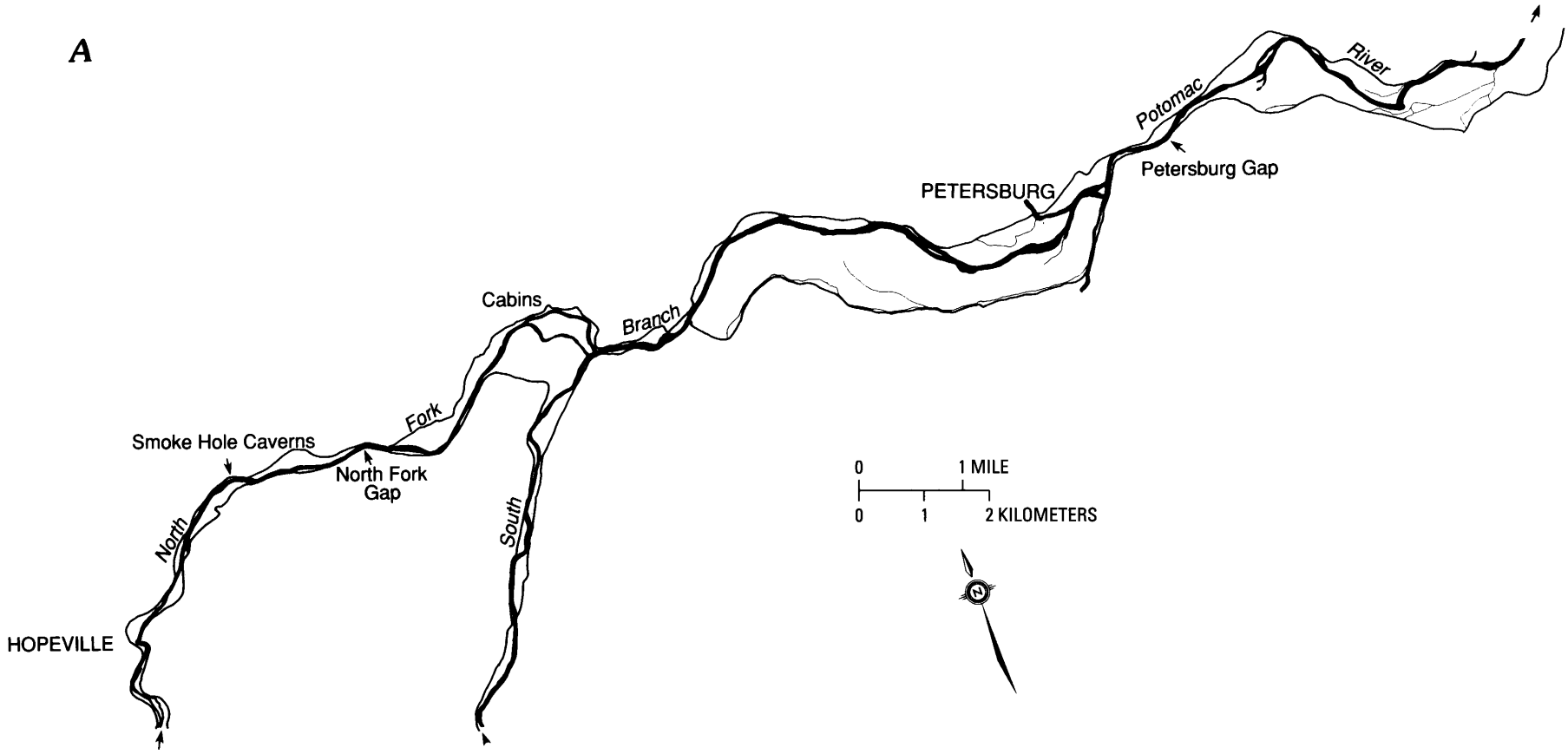

Figure 5. Sketch maps illustrating river channels and valley-floor outlines. (*A*) North Fork South Branch and South Branch Potomac Rivers upstream of their confluence, to South Branch Potomac River downstream of Petersburg Gap. (*B*) South Branch Potomac River, from downstream of Petersburg Gap to Sector, downstream of the Trough.

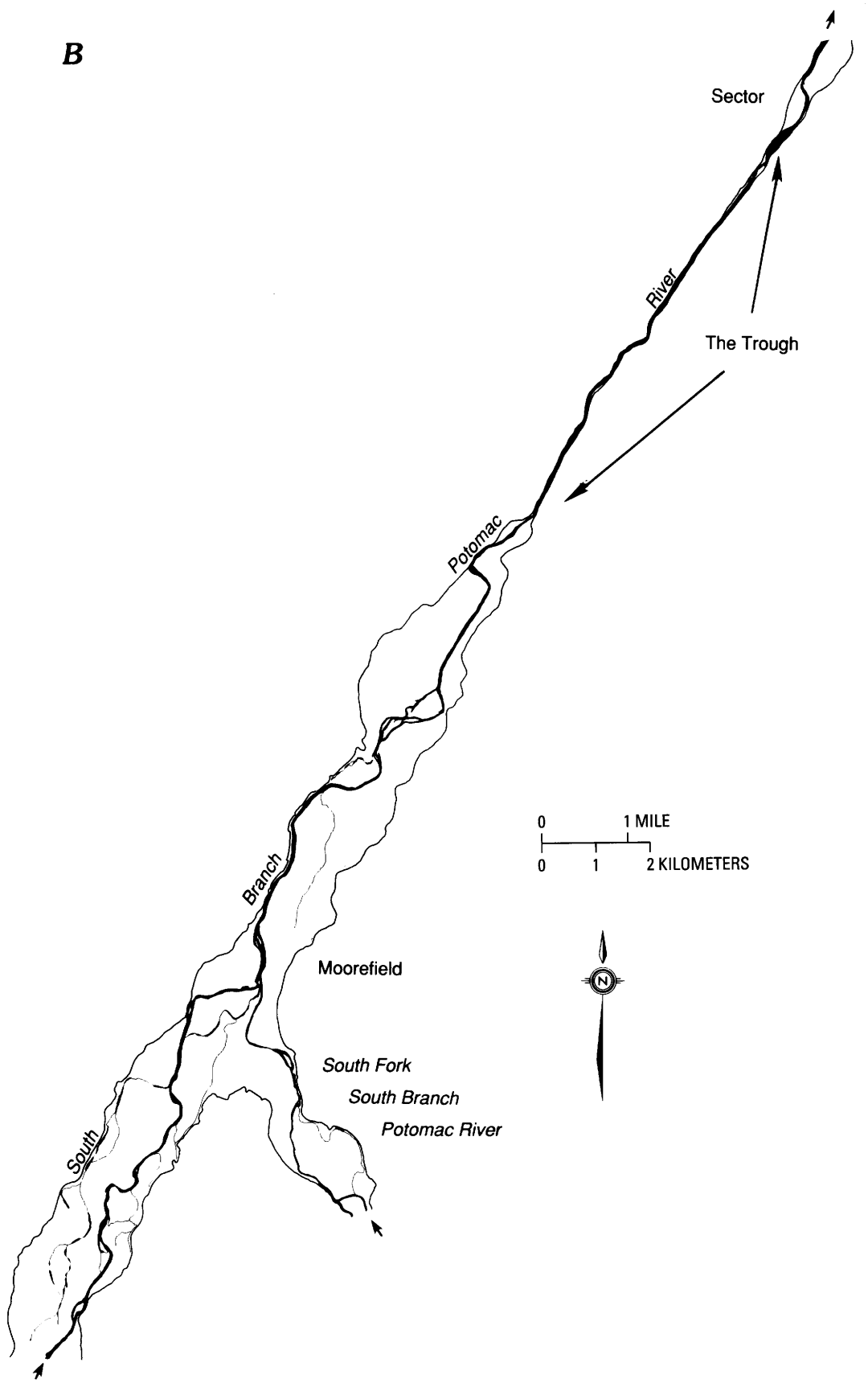

Figure 5. Continued.

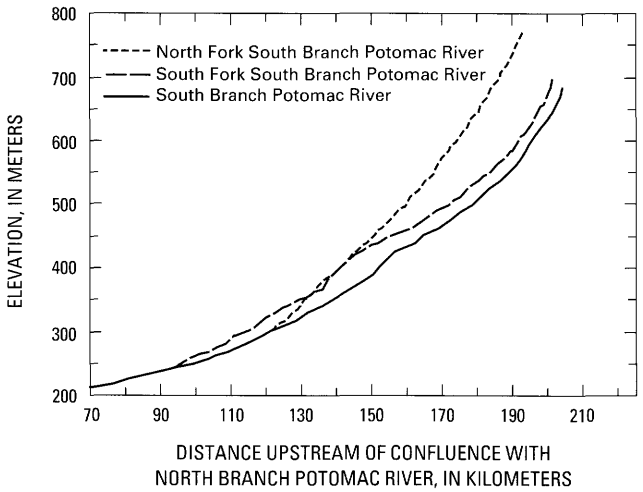

Figure 6. Longitudinal profiles of North Fork South Branch, South Branch, and South Fork South Branch Potomac Rivers upstream of Moorefield.

Table 3. Channel gradients along the three forks of the South Branch Potomac River

Extent	Gradient	Distance (km)
North Fork South Branch Potomac River from Laurel Fork to confluence with South Branch near Cabins	0.0065	70.9
South Branch Potomac River from Virginia State line to confluence with North Fork near Cabins	.0047	83.3
South Branch Potomac River from confluence with North Fork near Cabins to confluence with South Fork at Moorefield	.0021	28.8
South Fork South Branch Potomac River from Virginia State line to confluence with South Branch at Moorefield	.0036	104.9
South Branch Potomac River from confluence with South Fork at Moorefield to confluence with North Branch Potomac River	.0009	92.8

1986) meandering rivers whose ability to migrate laterally is limited by the presence of resistant valley walls. Valley confinements in the South Branch drainage encompass a range of types: channels entrenched in bedrock and lacking significant bottomland development; channels with isolated flood-plain segments alternating from one side of the valley to the other; channels that abut a valley wall or terrace scarp at least once in every meander crossing; channels that occupy relatively broad bottomlands but whose migration is constrained by valley walls at critical locations (figs. 5, 8). Channels commonly have bedrock floors veneered with coarse sediment, and measured thickness of alluvial fill beneath flood plains in the Petersburg and Moorefield areas is generally less than 6 m (Jacobson and others, 1989).

The channels and the valleys they occupy have relatively low sinuosity, generally ranging from 1.05 to 1.25. Some of the broader valley reaches have multiple anabranching or anastomosing channels, and tributary channels commonly run parallel to the main river along the valley wall for some distance. The anastomosing channel patterns typically approach a major confluence or a major constriction in the valley walls (fig. 5). Most of these are sites where a relatively broad valley experienced comparatively minor geomorphic changes during the November 1985 flood. However, at other sites, unstable multiple-channel patterns were created by the 1985 flood. The phenomenon of erosional anastomosis or braiding by an extreme flood is also described by Carson (1984, p. 14) from the Canterbury Plains of New Zealand: "Many presently meandering rivers on the Plains have, at previous times this century, been exposed to high return-period floods that have rutted large parts of the floodplain, as well as producing rapid bend migration and concomitant dissection of wide point bars. The result has been a braided appearance that only slowly reverts to the single-thread mode as ruts heal with sediment accretion and vegetation regrowth."

The creation of new channels by the 1985 flood suggests that some of the secondary channels on flood plains in the South Branch basin before 1985 were themselves the remnants of overflow channels eroded in previous extreme floods rather than stable channels in an aggrading reach. At several locations, comparison of preflood and postflood aerial photographs reveals that these channels, partially filled in but persisting as depressions on the flood plain, were reoccupied and redissected in the 1985 flood (fig. 9).

HYDROLOGY OF THE NOVEMBER 1985 FLOOD IN THE SOUTH BRANCH POTOMAC RIVER BASIN

Peak Discharge

Discharge values at peak flood were estimated by the U.S. Geological Survey using indirect methods following the flood (Lescinsky, 1987). Estimated values of peak discharge at the six gage sites in the South Branch basin are listed in table 1; gage locations are shown in plate 1 and figure 1. Of the six gages, one (North Fork South Branch Potomac River at Cabins) was discontinued prior to November 1985, one (South Branch Potomac River at Petersburg) was destroyed by erosion of the river bank during the flood, three were disabled by rising floodwaters and failed to record peak or falling stages, and one (South Fork South Branch Potomac River at Brandywine) recorded a complete stage hydrograph but required a revised rating. At five of the six stations, the November 1985 flood exceeded the previous flood of record by ratios of 1.68 to 2.93; peak discharge at the sixth station (Brandywine) was almost identical to the value recorded for the record flood of June

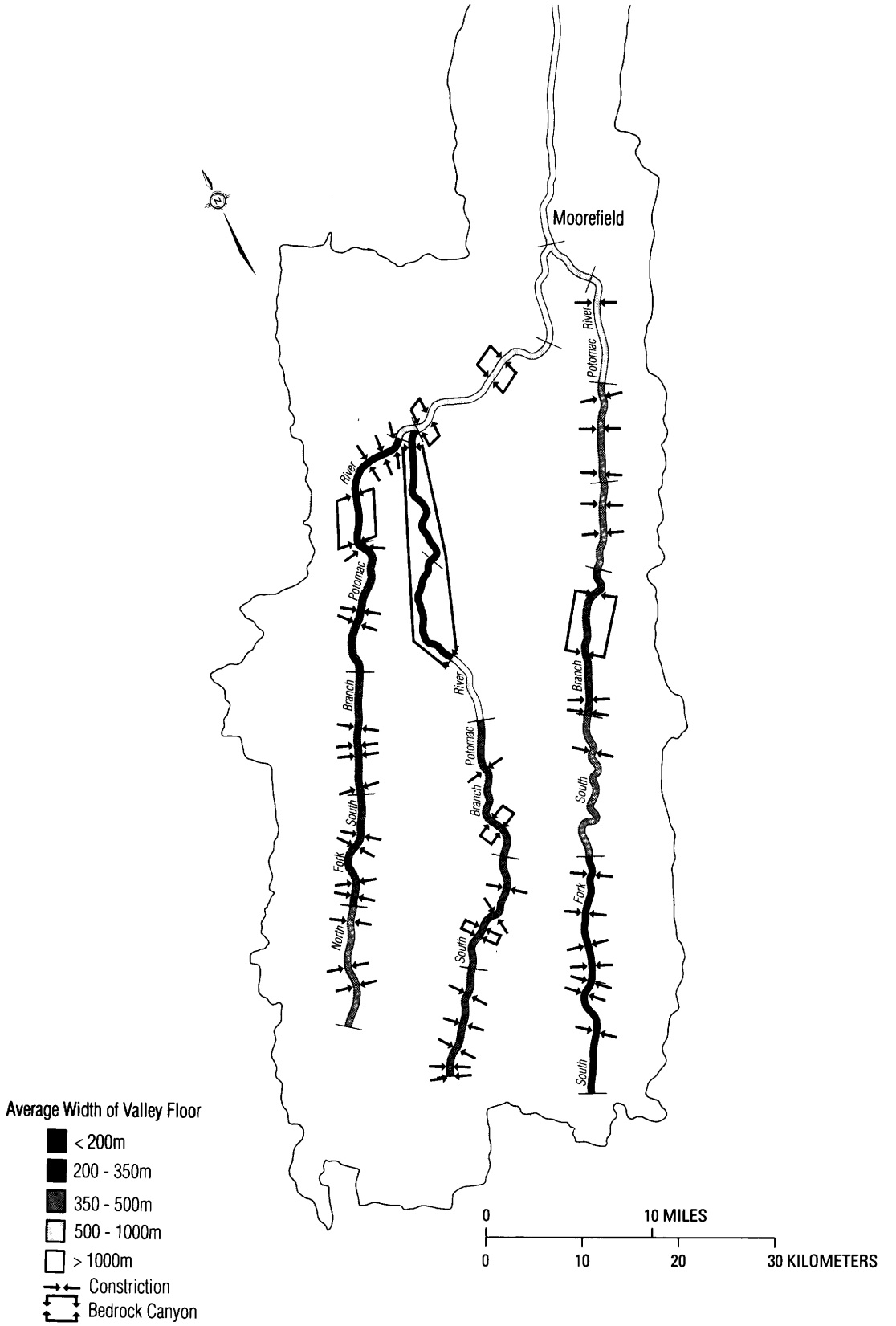

Figure 7. Sketch map showing locations of valley constrictions and bedrock canyons and average width of valley floor along the three forks of the South Branch Potomac River upstream of Moorefield. Constrictions are defined as valley cross sections that are no more than one-third as wide as the valley along the reach immediately downstream.

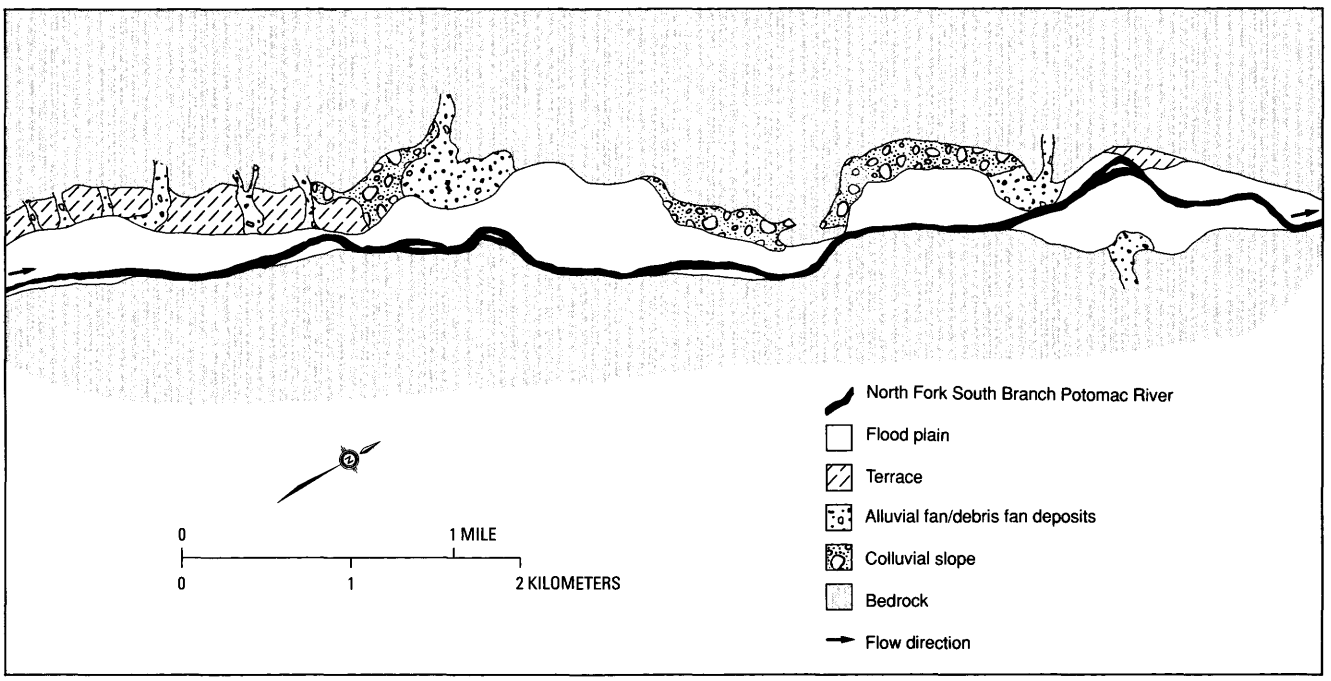

Figure 8. Photointerpretive sketch showing valley planform and associated geomorphic features along the North Fork South Branch Potomac River downstream of Riverton; morphology based on preflood aerial photography.

1949. Unit discharge values ranged from 1.78 to 4.34 $m^3/s/km^2$ (163–397 $ft^3/s/mi^2$). These are among the largest values ever recorded for comparable drainage areas in this part of the United States, but they fall well within the envelope curve defined in figure 10.

Unit discharge values were highest on the South Fork at Brandywine and Moorefield, despite the fact that much of the east side of the South Fork basin is regulated by a series of Soil Conservation Service flood-control dams. Most of these dams overflowed, and a few experienced severe spillway erosion (fig. 11). Estimates of peak discharge were computed by the Soil Conservation Service for four of the tributaries that have flood-control dams; these are listed in table 4. Inflow to the reservoir above each dam was derived using unit hydrograph routing techniques for the upstream drainage area, and outflow from each dam was based on crest stage measurements and design ratings for the dam spillway. Unit discharge values calculated from the inflow data range from 4.4 to 7.2 $m^3/s/km^2$ (398 to 660 $ft^3/s/mi^2$); outflow unit discharges range from 2.1 to 4.7 $m^3/s/km^2$ (191 to 427 $ft^3/s/mi^2$).

Peak unit discharge on the North Fork at Cabins was lower than at Brandywine or Moorefield but higher than at the other stations (table 1). The unit discharge with the next to highest value was measured along the South Branch near Franklin. Although the official peak discharge for the Franklin gage is 1,250 m^3/s (44,000 ft^3/s), the actual slope-area measurement was made in a short canyon several kilometers downstream of the gage, and the discharge estimate was adjusted downward to account for the smaller drainage area at Franklin. The peak discharge value at the measurement site was 1,520 m^3/s (53,500 ft^3/s). If the drainage area of the South Branch produced this unit discharge uniformly, it would have delivered 2,300 m^3/s (81,300 ft^3/s) peak discharge at the North Fork confluence. Furthermore, if the flood crests on the North Fork and the South Branch arrived at the confluence simultaneously, the peak discharge at the Petersburg gage would have been about 4,800 m^3/s (170,000 ft^3/s). However, the discharge measured just upstream of the Petersburg gage was only 3,700 m^3/s (130,000 ft^3/s). The discrepancy may be attributable to (1) uncertainty in estimating peak discharge at one or more of the gage sites, (2) flood waves on the North Fork and South Branch above their confluence that were out of phase, (3) attenuation of the flood wave moving down the South Branch as it traversed the reach between Franklin and the confluence with the North Fork, or (4) a combination of two or more of these possibilities. Given the rapid rise and fall of water level in the flood, a peak discharge value at the Petersburg gage smaller than the arithmetic sum of the tributary peaks would be generated if the two tributary peaks were out of phase by as much as a couple of hours. In addition, attenuation of the flood wave on the South Branch could have occurred as the combined result of valley widening in the reach upstream of Upper Tract and ponding at the entrance to the Smoke Hole canyon just below Upper Tract (figs. 12, 13). Backwater above the entrance to the canyon caused the stage on the South Branch at Upper Tract

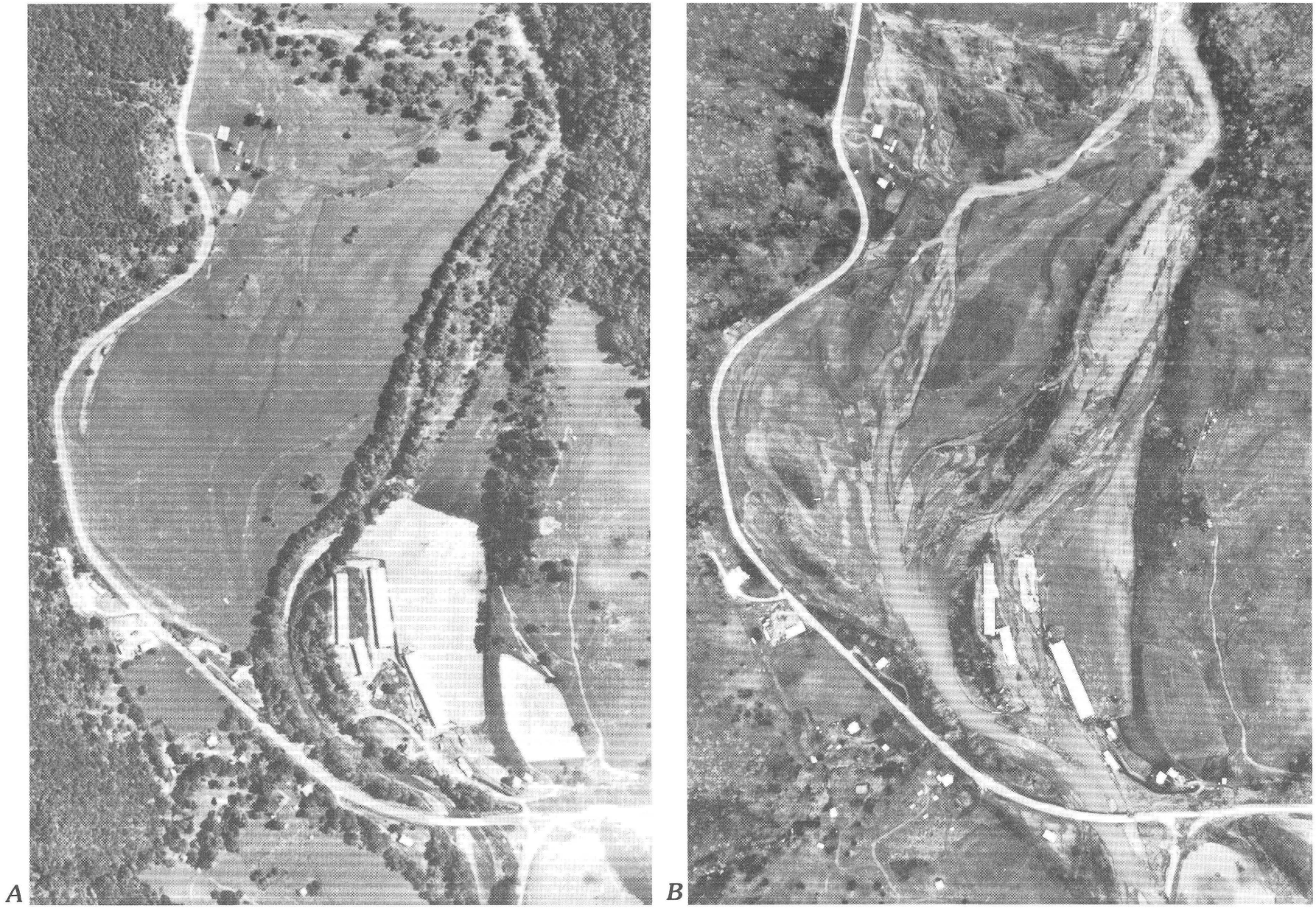

Figure 9. Aerial photographs illustrating reoccupation and incision of old flood-plain channels: (*A* and *B*) North Fork South Branch Potomac River at Judy Gap, May 1980 and November 1985; flow is from bottom to top. Field of view is 780 m wide. (*C* and *D*) South Fork South Branch Potomac River near Milam, May 1980 and November 1985; flow is from bottom to top. Field of view is 780 m wide.

D

C

Figure 9. Continued.

to rise high enough that water flowed over the divide from the South Branch valley into the North Mill Creek drainage; an assumption that flow was critical over the divide yields a maximum overflow discharge value of about 140 m^3/s. Ponding at the entrance to Smoke Hole presumably slowed the arrival of peak discharge at the confluence with the North Fork and reduced the magnitude of the hydrograph peak while spreading it over a longer time interval.

A similar case may be made in comparing peak discharges at the Petersburg, Moorefield, and Springfield gages. Peak discharge at the Springfield gage was estimated at 6,800 m^3/s (240,000 ft^3/s), equal to the sum of the peaks at Petersburg and Moorefield; yet those two sites account for only 63 percent of the drainage area at Springfield. Witnesses report that the South Branch and the South Fork reached crest stage within half an hour of each other at Moorefield, indicating that peak discharge at the confluence may have exceeded the peak at Springfield. Even assuming that the area downstream of Moorefield received less precipitation and experienced lower unit discharges than the areas monitored by the upstream gages, the available evidence suggests attenuation of the flood wave between Moorefield and the Springfield gage site. Ponding above valley constrictions may have been partially responsible; the Trough, a bedrock canyon downstream of Moorefield (fig. 5*A*), is particularly narrow, and the high-water marks surveyed after the flood clearly indicate that floodwaters entering this canyon were ponded at its upstream end (see the following section).

The correspondence between peak discharge and spatial patterns of precipitation is uncertain at best. The isohyets in plate 1 show that the highest precipitation values within the study area are centered over the South Branch

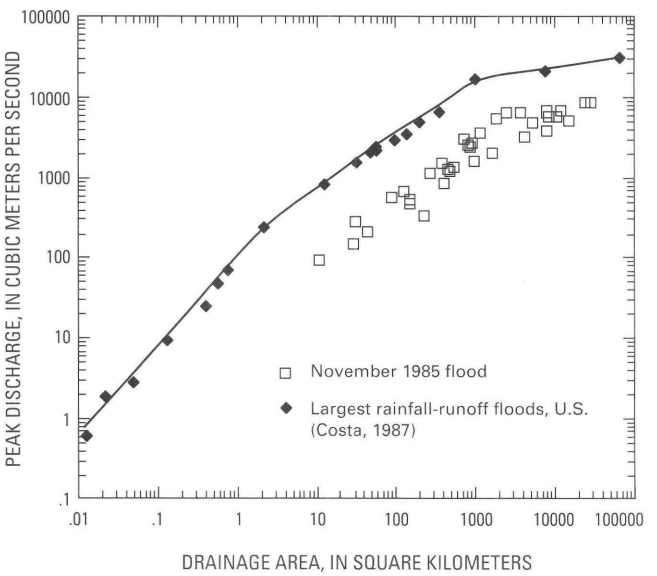

Figure 10. Peak discharge versus drainage area for the November 1985 flood, compared with the largest rainfall-runoff floods recorded for the United States (after Miller (1990); printed by permission of John Wiley and Sons). Data from Costa (1987) and Lescinsky (1987).

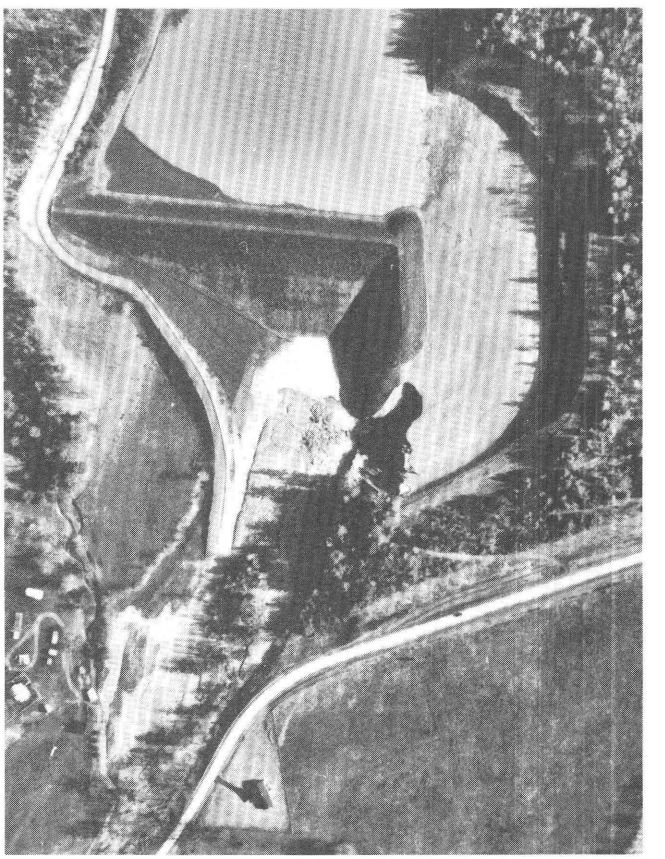

Figure 11. Soil Conservation Service flood control dam on Little Fork with eroded spillway following November 1985 flood. Valley of South Fork South Branch Potomac River, 11 km upstream of Brandywine. Field of view is 500 m wide.

Table 4. Peak discharge estimates for four Soil Conservation Service flood-control reservoirs: November 1985 flood, South Fork South Branch Potomac River basin

Watershed	Drainage area		Peak inflow		Inflow unit discharge		Peak outflow		Outflow unit discharge	
	km^2	mi^2	m^3/s	ft^3/s	$m^3/s/km^2$	$ft^3/s/mi^2$	m^3/s	ft^3/s	$m^3/s/km^2$	$ft^3/s/mi^2$
10	6.94	2.68	50.1	1,770	7.2	660	30.6	1,080	4.4	403
14	14.37	5.55	102.5	3,620	7.1	652	67.1	2,370	4.7	427
17	44.73	17.27	194.8	6,880	4.4	398	93.2	3,290	2.1	191
19	39.24	15.15	206.1	7,280	5.3	481	145.0	5,120	3.7	338

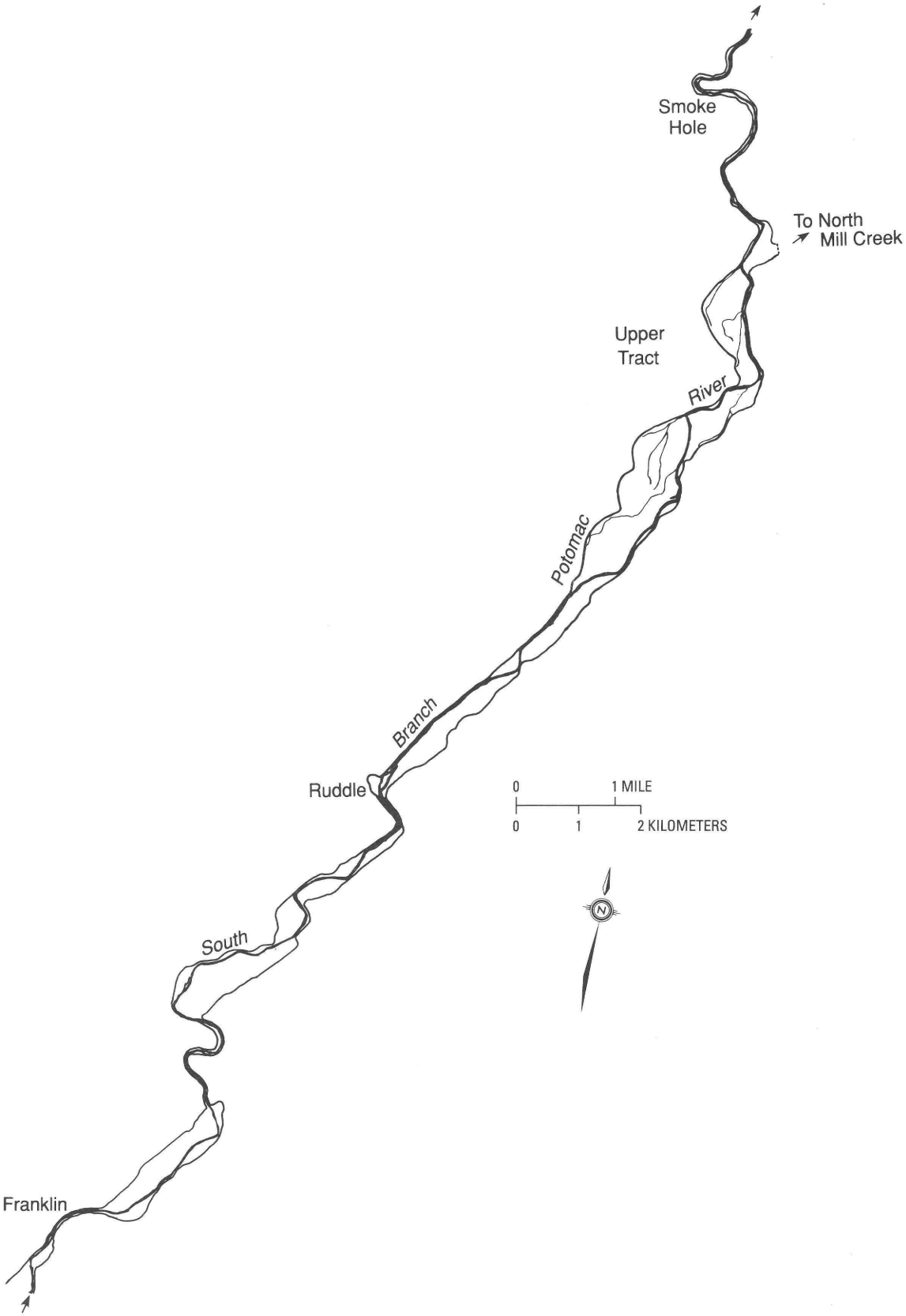

Figure 12. Sketch map illustrating river channel and valley-floor outline along South Branch Potomac River from Franklin to Smoke Hole canyon. Some of the flow from the South Branch crossed over the divide near Upper Tract and was diverted into the valley of North Mill Creek for approximately 5 h on the night of November 4–5, 1985.

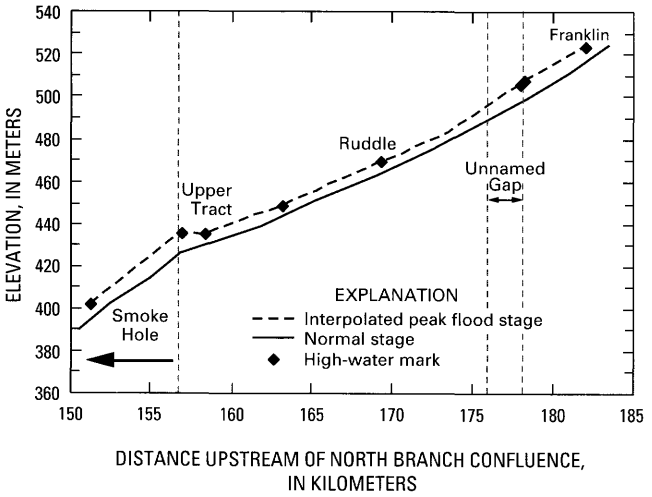

Figure 13. Longitudinal profiles of November 1985 flood crest and low-water stage along South Branch Potomac River from Franklin gage to Smoke Hole downstream of Upper Tract.

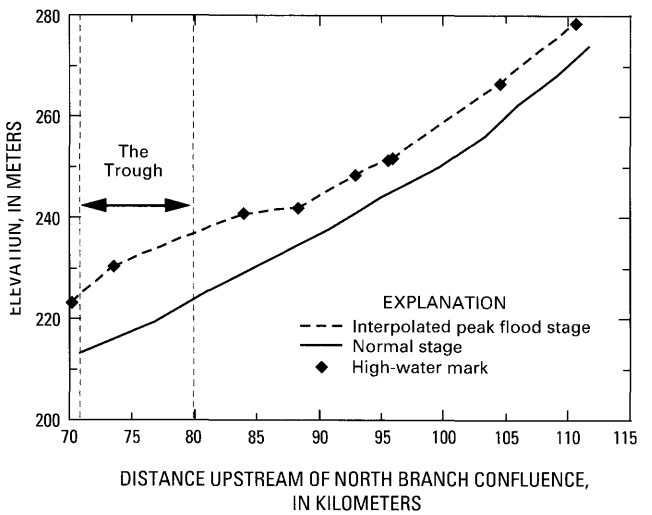

Figure 14. Longitudinal profiles of November 1985 flood crest and low-water stage along South Branch Potomac River from downstream of Petersburg Gap to Sector (downstream end of the Trough).

between Franklin and Upper Tract. Precipitation values are lower over the South Fork drainage, where the highest unit discharge estimates were made. Cumulative volumes of precipitation upstream of the gages in the South Branch basin have been calculated, yielding average rainfall depths of 158–220 mm (table 1); no correlation between average depth and peak unit discharge is apparent. Colucci and others (chapter B, this volume) emphasize that, although the network of rain gages in this area is sparse, unofficial results of a bucket survey conducted by the Soil Conservation Service tend to confirm the general patterns shown in the contour map based on official data. However, it is possible that one or more small cells generating intense precipitation over the mountains on the east side of the basin went undetected by either the rain gage network or the bucket surveys.

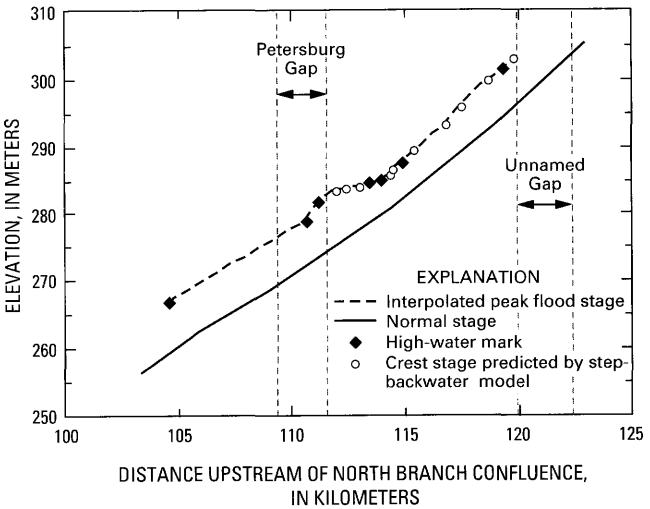

Figure 15. Longitudinal profiles of November 1985 flood crest and low-water stage along South Branch Potomac River from unnamed gap upstream of Petersburg to downstream end of Petersburg Gap. Step-backwater estimates of peak stage provided by Army Corps of Engineers.

Crest Stage and Longitudinal Profiles

Floodwaters at crest stage were deep enough that virtually the entire valley floor was inundated along all three forks of the South Branch from the Virginia State line to Moorefield and along the South Branch from Moorefield to the confluence with the North Branch Potomac River. Elevations of high-water marks at selected sites were surveyed after the flood by U.S. Geological Survey field crews. Additional water surface elevations for the areas near Petersburg and Moorefield were generated by step-backwater modeling performed in the preliminary phase of an Army Corps of Engineers flood-control study; the model output data are generally in agreement with measured high-water marks. These data, together with cross sections surveyed by the U.S. Geological Survey for slope-area discharge estimates, were used to construct generalized longitudinal profiles of peak flood stage (figs. 13–16).

Comparisons of peak flood stages with topographic contours reveal that water depths above low-flow stages along the South Branch and its main forks ranged from less than 4 m to 12.7 m. Variations in flow depth over the valley floor were controlled largely by valley contractions and expansions. The deepest flows along the South Branch Potomac River occurred in the Trough (fig. 14).

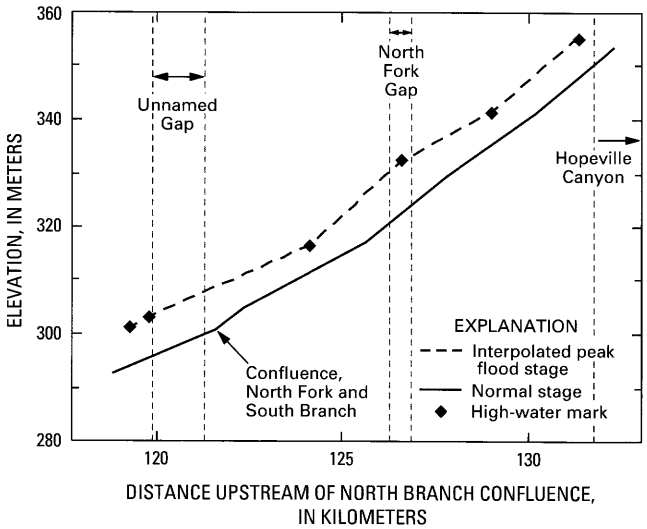

Figure 16. Longitudinal profiles of November 1985 flood crest and low-water stage along North Fork South Branch Potomac River from Hopeville to confluence with South Branch Potomac River, and extending along the South Branch Potomac River to the site of the Petersburg gaging station.

Along the South Branch near Moorefield, average water depth at peak stage was about 7 m; but as the valley narrowed approaching the Trough, backwater above the entrance caused a rapid increase in depth. Although the data are too sparse to construct a detailed water-surface profile along the Trough, deep flows appear to have persisted along much of its length (fig. 14).

The South Branch valley near Petersburg is quite broad but is bounded by two bedrock constrictions: an unnamed gap at its upstream end and Petersburg Gap at its downstream end (fig. 5*A*). Flow depths above low water decreased slightly downstream along the upper two-thirds of the reach, from about 6.5–7.5 m just below the unnamed gap to 5–6 m at the widest part of the valley, which is a short distance upstream of Petersburg (fig. 15). From there to Petersburg Gap, flow depth increased sharply to about 8.6 m above low water owing to backwater effects of the constriction. Maximum water depths at peak stage decrease almost immediately below the entrance to Petersburg Gap.

Along the South Branch valley between Franklin and the Smoke Hole (fig. 12), data on crest stages are too sparse to define a detailed profile, but the general trend (fig. 13) is consistent with the results described above. The valley in the vicinity of Upper Tract is relatively wide (average width 530 m), with a river gradient between 0.002 and 0.003. The sharp gradient break in the low-water profile 2 km downstream of Upper Tract marks the entrance to Smoke Hole. The abrupt constriction of the valley at this site caused ponding at peak stage, with water reaching depths of 8–9 m at the canyon entrance, as compared with estimated depths between 5 and 6 m above low water in the canyon and 4–5 m above low water farther upstream at Ruddle. The measured elevation of the high-water mark at the Upper Tract bridge actually was slightly greater than the elevation of the next high-water mark upstream; although one or the other of these marks may be in error, there is little doubt that the general slope of the water surface at peak stage flattened out in the immediate vicinity of the bridge. Ponded water reached a maximum depth of 1.2 m over the drainage divide between the South Branch and North Mill Creek valleys, and one eyewitness stated that water flowed over the divide for approximately 5 h, from 8 p.m. to 1 a.m. on the night of November 4–5. The overflow eroded ditches along the road and caused damage to some buildings, but no significant geomorphic impacts were observed.

The examples cited above illustrate a pattern of variation in water depth at crest stage that was repeated at other sites throughout the basin; additional examples are illustrated for the South Branch between the Franklin gage and an unnamed gap 4 km downstream of the gage (figs. 12, 13) and for the North Fork between Hopeville Canyon and the confluence with the South Branch (figs. 5*A*, 16). In all cases a tight constriction in the valley caused backwater effects and ponding upstream, with declining stage in and downstream of the constriction itself. This clearly affected the spatial distribution of energy expenditure along the valley.

Timing of Flood Wave and Shape of the Hydrograph

Peak flow along the middle reaches of the three forks of the South Branch occurred during the night of November 4–5. Because instrument records and precise, reliable eyewitness reports are scarce, information about the timing of the flood wave and the shape of the hydrograph is spotty at best. The following discussion incorporates available information from instrument records and recollections of residents.

The only available complete-stage hydrograph of the flood in the South Branch basin is from the South Fork at Brandywine (fig. 17). Crest stage was 3.63 m above bankfull, and the rising limb of the hydrograph was particularly steep in the last few hours before the flood crest. Records indicate that stage rose 1.88 m in the last 1.5 hours before the hydrograph peak and fell by about the same amount during the 6 h following the peak. Bankfull stage was exceeded for 27 h, but floodwaters were more than 1 m above bankfull for only 14 of those 27 h.

At the Franklin gage on the South Branch the stage recorders were disabled before the flood crest arrived, but the rising limb apparently was as steep as or steeper than that at the Brandywine gage (fig. 17). The last recorded stage was 4.87 m at 7 p.m. on November 4; peak stage of 6.88 m, according to an unconfirmed report by a resident,

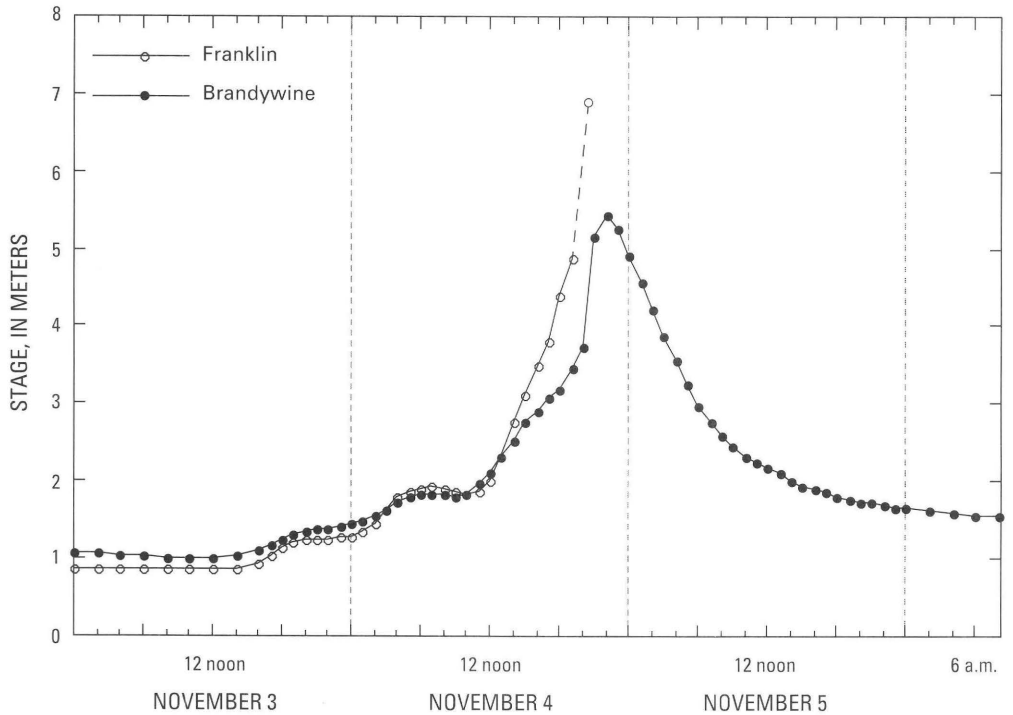

Figure 17. Stage hydrographs for the November 1985 flood at Brandywine, W. Va. (complete stage record), and at Franklin, W. Va. (incomplete stage record; time of peak is indicated by dashed line and is estimated from eyewitness accounts).

occurred between 8 and 9 p.m. Assuming that the flood peaked at 8:30 p.m., a rise of 2 m occurred in the last 1.5 h before the peak. The peak could not have occurred much later, as the crest stage at Upper Tract (about 24 km downstream) apparently occurred between 10 and 11 p.m.

Most observers from other locations in the North Fork and South Branch valleys recall that the water rose very rapidly. It is likely that there were also local surges due to the extremely turbulent nature of the flow. Abrupt changes in velocity and stage probably accompanied failure of small debris jams at many sites, and changes in flow pattern associated with scouring of new channels across the valley floor would have had similar effects.

The sequence of events at Petersburg is a case in point. Residents stated that a sudden surge caused a rapid increase in water level some time after the river overflowed its banks. Furthermore, the surge that inundated most of the valley floor was described as spreading from the South Petersburg flood plain rather than from the channel of the South Branch itself. This account is consistent with the geomorphic evidence. Flow emerging from the gap upstream eroded the channel banks, causing the channel to widen by a factor of 2 or 3 and destroying the Petersburg gage and several houses. After the river overflowed its banks, a major component of flow headed southeast, away from the channel, and scoured a broad, shallow trough leading toward the south side of the valley (fig. 18). Flow that followed this trajectory combined with overbank flow concentrated along several other swales on the valley floor and reached the channel of Johnson Run, which lies along the southern margin of the South Branch flood plain. Presumably, the scouring of the valley floor upstream diverted a large amount of water toward Johnson Run shortly after the South Branch reached flood stage, thus causing the surge mentioned above. Similar events must have occurred throughout the basin as flow patterns changed with rising and falling stage and with erosional and depositional modification of the valley bottom.

An approximate chronology of the progress of the flood crest is based on the recollections of witnesses (fig. 19). Bearing in mind that the crest occurred late at night, it is not surprising that some of these reports yield inconsistent and sometimes contradictory results. Nevertheless a plot of the reported time of the crest against distance upstream of Moorefield can be used to estimate average flood-peak celerity, with calculated values ranging from 3 m/s to as much as 6 m/s.

Recurrence Intervals

Discharge values corresponding to probabilities of 0.01 (recurrence interval 100 yr) and 0.002 (recurrence interval 500 yr) have been calculated at all six gage sites for comparison with 1985 flood peaks (table 2). Discharges

Figure 18. Valley floor upstream of Petersburg at the site where flood flow emerged from an unnamed gap (at left). This is the site where the Petersburg gage on the South Branch was destroyed, along with several houses. Note the erosional trough just left of center that carried flow across the flood plain toward Johnson Run, on the south side of the valley. Other flow paths visible in the photograph also indicate diversion of a significant component of the flood flow away from the South Branch channel and convergence toward the south side of the valley. Field of view is 3,000 m wide.

were calculated using the method outlined by the Interagency Advisory Committee on Water Data (1982) and using regional flood-frequency curves for the Potomac Highlands region of West Virginia (Runner, 1980). Skew coefficients for the first set of estimates were weighted averages based on both systematic station records and regionalized skew coefficients. The systematic station records (including the November 1985 flood) were adjusted to account for historical data. After examination of historical records, we

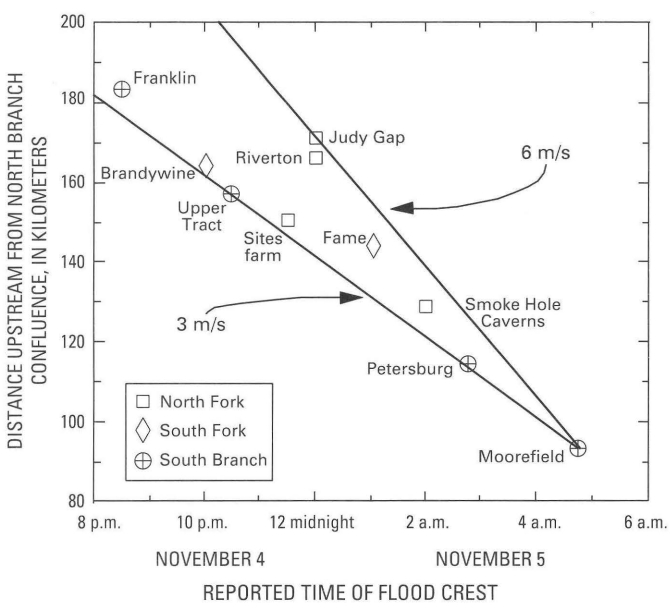

Figure 19. Plot of estimated time of flood crest versus distance upstream of the confluence of the South Branch and North Branch Potomac Rivers. Data on timing of flood crest from all three forks of the South Branch Potomac River are based on eyewitness accounts; some observations may be in error by 1–2 h. The slopes of the two trend lines drawn through the data points represent maximum and minimum interpretations of flood-wave celerity, assuming constant celerity upstream of Moorefield. ▶

Table 5. Hydraulic parameters calculated for U.S. Geological Survey gage sites

Station	Mean velocity[1]		Maximum velocity[2]				Maximum Froude number[5]	
	Channel (m/s)	Complete section (m/s)	Channel (m/s)	Complete section (m/s)	Mean width[3] (m)	Mean depth[4] (m)	Channel	Complete section
South Branch Potomac River at Franklin, W.Va.	4.6	3.7	5.3	4.0	72	5.7	0.61	0.54
North Fork South Branch Potomac River at Cabins, W.Va.	3.9	3.2	4.2	3.4	165	4.9	.47	.48
South Branch Potomac River near Petersburg, W.Va.	4.2	4.2	4.6	4.6	118	7.2	.53	.53
South Fork South Branch Potomac River near Moorefield, W.Va.	3.2	2.2	3.4	2.4	552	2.4	.50	.50
South Branch Potomac River near Springfield, W.Va.	4.2	3.8	4.4	4.0	201	8.5	.63	.45

[1] Three cross sections surveyed at each site; mean velocity is the mean of three cross sections.

[2] Maximum velocity refers to the largest value among the three cross sections surveyed. Maximum velocities within any single cross section are not known.

[3] Mean top width of the inundated area for three cross sections at each site.

[4] Mean depth for each cross section calculated as the ratio of cross-sectional area to top width; results for individual cross sections were averaged at each site.

[5] Maximum Froude number is the largest value among the three cross sections at each site.

assumed that the November 1985 flood was the largest since 1877 at all stations except Brandywine; for Brandywine, we assumed that the June 1949 flood was the largest since 1877. The 1877 flood was exceeded by the 1985 flood and by the June 1949 flood at those stations where historical records are available, but we lack data to extend the historical record any further back. Datable materials associated with prehistoric high-magnitude floods have not been found in this basin, and therefore we have not had an opportunity to apply techniques of paleoflood hydrology to revise these estimates.

The November 1985 flood exceeded the 100-yr flood estimated at all six stations by both methods. The November 1985 flood also exceeded the 500-yr flood peak estimated at four of the six stations by either method. Further downstream on the main stem of the Potomac River, the recurrence interval of the 1985 flood decreased with increasing drainage area; at Point of Rocks, Md., and Washington, D.C., the recurrence interval was only 25 yr (Lescinsky, 1987). From the available data, it is apparent that this was a rare event, but it was most unusual in drainage basins with areas ranging between 300 and 5,000 km^2 (Miller, 1990).

Hydraulic Parameters

Because of the tremendous destruction caused by this flood, data on flow hydraulics are of considerable interest. Velocity, water-surface slope, energy slope, Froude number, and unit stream power (defined by equations (1) and (2) below) can be derived at the sites where indirect discharge estimates were made. These parameters may be useful in comparing this flood with other extreme floods (tables 5, 6). Hydraulic data are available for five of the six gage sites where indirect discharge estimates were made; the South Fork at Brandywine is not represented because a complex flow cross section and the presence of a bridge and tributary inflow make calculation of hydraulic parameters difficult and unreliable.

Velocities were calculated separately for the complete cross section and for the channel at each gage site. Average velocity over three cross sections at each of the five gage sites ranged from 2.2 to 4.2 m/s, and average channel velocity ranged from 3.2 to 4.6 m/s. The highest estimate of average channel velocity for any single cross section was 5.3 m/s at Franklin. Average cross-section values of Froude number (Chow, 1959) ranged from 0.39 to 0.54, and the cross section with the highest average velocity had a channel Froude number of only 0.63. Although the average values of depth and velocity indicate that flow was not supercritical (i.e., Froude number >1.0) across the entire cross section at any of the indirect discharge measurement sites, local areas of critical or supercritical flow may have existed along irregular boundaries or around obstructions in the path of the flood.

Power supplied to the column of fluid per unit of bed area is a useful parameter for evaluating the ability of rivers to erode and transport sediment (Bagnold, 1966). This quantity, often referred to by subsequent authors as unit stream power, has been cited in discussions of high-magnitude floods in terms of competence and capacity to

Table 6. Unit stream power calculated for U.S. Geological Survey gage sites

Station	Energy gradient	Unit stream power (W/m^2)					
		Complete section		Channel		Flood plain	
		Minimum	Maximum	Minimum	Maximum	Minimum	Maximum
South Branch Potomac River at Franklin, W.Va.	0.0048	956	1,035	1,286	1,971	448	588
North Fork South Branch Potomac River at Cabins, W.Va.	.0034	441	607	676	1,165	57	204
South Branch Potomac River near Petersburg, W.Va.	.0017	464	586	—	—	—	—
South Fork South Branch Potomac River near Moorefield, W.Va.	.0023	114	133	276	347	83	119
South Branch Potomac River near Springfield, W.Va.	.0013	400	419	524	627	151	162

"Minimum" and "maximum" indicate range of values calculated for the three cross sections used in slope-area discharge computations at each gage site. Dash indicates that cross sections were not subdivided in original slope-area computations; unit stream power was calculated for complete cross sections only.

transport sediment (Costa, 1983; Baker and Costa, 1987). Unit stream power is calculated either as the product of boundary shear stress (τ) and velocity (v),

$$\omega = \tau v \tag{1}$$

or as the product of discharge (Q), unit weight of water (γ), and energy slope (s), divided by flow width (w):

$$\omega = \frac{\gamma Q s}{w} \tag{2}$$

The largest values of unit stream power and boundary shear stress are developed in bedrock canyons, where the boundaries are resistant to erosion and the flow cross section cannot adjust its width to accommodate extreme discharges. Conversely, wide reaches of alluvial valley bottom are expected to have the lowest values of unit stream power.

Average values of unit stream power, based on three cross sections each at U.S. Geological Survey gage sites in the South Branch basin, ranged from 125 to 988 W/m^2 (the range of values for each site is listed in table 6). Separate computations for channel and overbank flow at individual cross sections yielded values for channel unit stream power as high as 1,971 W/m^2 (South Branch near Franklin) and 1,165 W/m^2 (North Fork above Cabins); values for overbank flow ranged between 83 W/m^2 (South Fork above Moorefield) and 588 W/m^2 (South Branch near Franklin). Some of the more prominent erosion features observed in the South Branch basin were generated by flows moving out of the channel and across the valley floor just downstream of a constricted reach. These features are probably associated with high values of unit stream power developed in the upstream constriction. Scour forms commonly produced in other settings are probably associated with lower values of unit stream power, comparable to those calculated for overbank flow. Improved assessment of the relation between unit stream power and flood- plain erosion will require detailed information about how flow patterns are affected by planform and topographic characteristics of valley boundaries.

Along the North Fork valley, in and below Hopeville Canyon, were several large boulders with maximum diameters of 2.5–2.8 m, resting on smaller imbricated boulders. In some cases, other objects underneath the smaller boulders, such as cut boards, indicated that the boulders were transported by the flood. The average intermediate axis of the five largest boulders believed to have moved was 1,700 mm. Using an empirical equation of Costa (1983),

$$v = 0.18 d_I^{0.487} \tag{3}$$

the average velocity at this site was 6.7 m/s. Costa (1983) also presented an empirical formula for calculating the minimum value of unit stream power needed to transport boulders of a given size:

$$\omega = 0.009 d_I^{1.686} \tag{4}$$

Using the same particle size as before, we obtain a unit stream power value of 2,500 W/m^2 for the mouth of Hopeville Canyon. This exceeds the values cited previously but is of the same order of magnitude as the maximum values obtained at Franklin and Cabins (table 6). As Komar (1988) presents evidence suggesting that many of the empirical formulas of flow competence tend to overestimate the threshold shear stress for transport of coarse particles, both the velocity and the unit stream power value calculated here should be regarded as maximum estimates. An independent estimate of unit stream power at the mouth of Hopeville Canyon, based on channel gradient, width at the exit constriction, and a discharge slightly less than the peak at Cabins, yields a value of about 1,650 W/m^2.

The values of unit stream power derived here are unremarkable by comparison with the values tabulated by Baker and Costa (1987) in their discussion of the most extreme floods recorded; of the 35 events they cited, only 4 have values of unit stream power less than 1,000, and the maximum value is 18,582 W/m^2. On the other hand, only 8 of 35 entries had drainage areas greater than 100 km^2, and 2 of those were floods from dam breaks. Extreme values of unit stream power apparently occur less often at sites with large drainage areas than at sites with small drainage areas. What is unusual about the hydraulics of the November 1985 flood in the South Branch basin is the occurrence of relatively high values of unit power in environments where well-developed, erodible alluvial bottomlands were exposed to the flow.

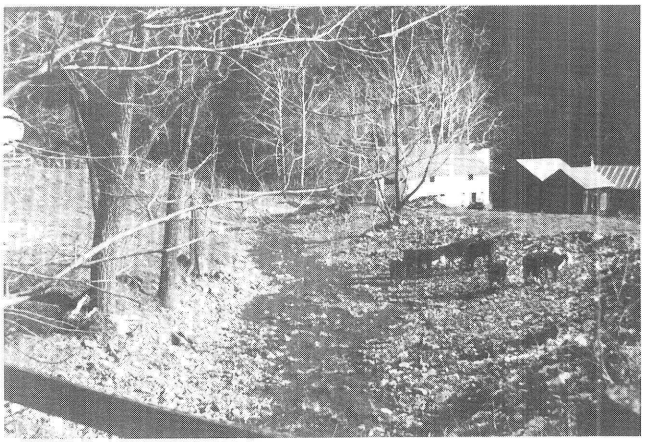

Figure 20. Scouring and widening of small tributary to the North Fork South Branch Potomac River between Judy Gap and Riverton.

Sediment Loads

The only sediment data available for comparison with previous floods were collected far downstream on the main stem Potomac River. At Point of Rocks, Md., 203 km downstream of the confluence of the South Branch with the North Branch, 3.09 megagrams (3.4 million tons) of suspended sediment were carried past the gage over a period of 3 days (James and others, 1987). The November 1985 flood carried the largest load of any flood since 1961, when daily suspended sediment records were initiated, even though it was not the greatest flood measured during that period. Tropical Storm Agnes in June 1972 had a peak discharge of 9,830 m^3/s (347,000 ft^3/s), 12.3 percent larger than the peak discharge during the 1985 flood (8,750 m^3/s). Suspended load passing the Point of Rocks gage during Agnes, however, was 1.24 million tonnes, or only 40.1 percent of the load measured for the 1985 flood. The load measured at Point of Rocks probably represents only a small fraction of the total sediment eroded from slopes and valley floors in the South Branch basin and elsewhere in the Potomac River basin. Much of the coarse fraction of sediment entrained by floodwaters in the South Branch basin remained in the basin, forming extensive deposits in all of the main valleys. Although much of the silt and clay component of the sediment load probably traveled further, flood-plain deposits composed largely of fine-grained sediment were observed along the South Branch downstream of its confluence with the South Fork and along the main stem Potomac downstream of the confluence of the South Branch with the North Branch.

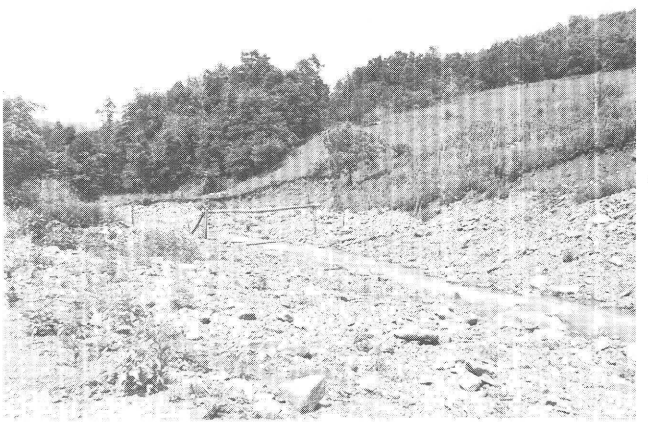

Figure 21. Scoured channel and exposed colluvium of adjacent slope, along Dry Run about 1 km upstream of confluence with North Fork South Branch Potomac River (7.5 km upstream of Circleville). Flow is from right to left.

FLOOD IMPACTS

Erosion and Deposition at Tributary Confluences

Aerial photographs of the three main forks of the South Branch allow identification of tributaries whose lower reaches were disturbed by the flood and that may have delivered large amounts of sediment. Slope failures along the walls of the main valleys were rare in this event, and tributaries were the primary conduits for entrainment and delivery of sediment derived from landslides that occurred in selected areas of the basin. The sediment derived from landslides was augmented by scouring of headwater channels and adjacent bottomlands (Jacobson and others, chapter C, this volume).

Many small tributary channels were scoured and widened during the flood, leaving a characteristic U-shaped cross section floored by cobbles and boulders. Small streams like the ones shown in figures 20 and 21 have no true bottomland, and channel widening occurred at the expense of adjacent colluvium or fan deposits. In many cases the angular clasts visible in the channel were derived from scouring and undercutting of adjacent slopes (fig. 21).

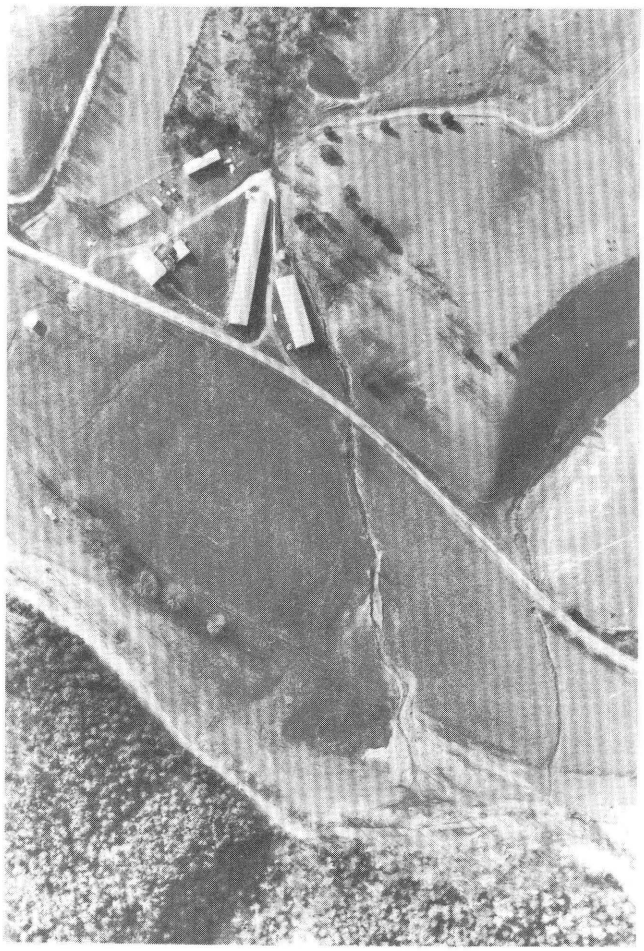

Figure 22. Incised channel and birds-foot delta at confluence of small unnamed intermittent stream with South Fork South Branch Potomac River at Palo Alto, 4 km downstream of the Virginia–West Virginia border. Flow along South Fork is toward lower right. Field of view is 430 m wide.

Tributaries subject to differing amounts of disturbance delivered varying amounts of sediment to the main valley. In some cases a tributary incised its bed but the zone affected by channel erosion was quite narrow, and much of the sediment mobilized by the stream was deposited at its mouth (fig. 22). Other, higher order tributaries exhibited more extensive scouring and reworking and appear to have delivered more sediment to the main channel (fig. 23).

Delta Forms

High flood stage and local ponding on or adjacent to the main stem river caused deposition and storage of sediment emanating from tributaries, forming small deltas at several locations in the South Branch basin. Although morphology may resemble the characteristic planform of a birds-foot delta (fig. 22), the term is used here primarily to distinguish coarse sediments deposited as a result of ponding from fan deposits left behind by diverging flow on a sloping surface. Despite the influence of backwater on deposition at tributary mouths, these deposits contain little silt and clay, suggesting that even under ponded conditions, local eddy velocities were sufficient to keep fines in suspension.

Figure 24 shows a series of bars, about 1–1.5 m thick, deposited on the valley floor at the mouth of an unnamed tributary of the South Branch Potomac River in Smoke Hole canyon. The presence of undisturbed trees suggests that this site probably was occupied by a slowly recirculating eddy separate from the main thread of flow at high stage; the opposite bank of the South Branch was exposed to the main flow and was completely stripped of vegetation. Aerial photography of the site shows the sediment emerging from the tributary to form several discrete lobes (fig. 25). Field examination revealed that although the

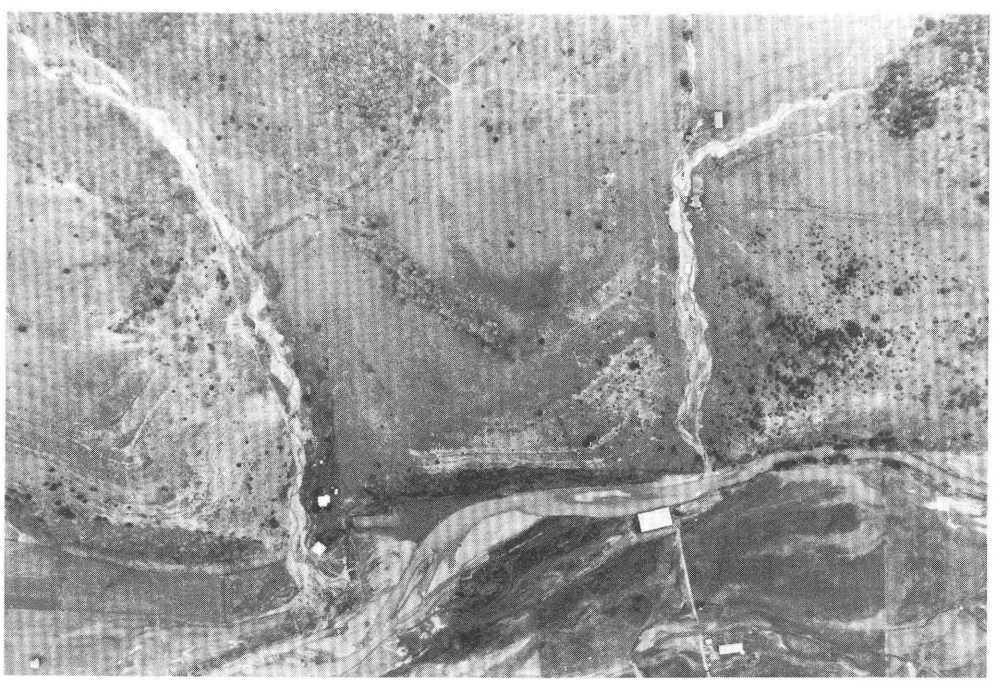

◀ **Figure 23.** Valleys of two unnamed tributaries to the South Branch Potomac River near the Virginia–West Virginia border. Reworking of bottomland deposits by stripping and deposition of coarse sediment occurred along most of the meander belt in both valleys; valley walls were undercut at several locations. Both tributaries delivered sediment directly to South Branch. Flow along South Branch is from right to left. Field of view is 660 m wide.

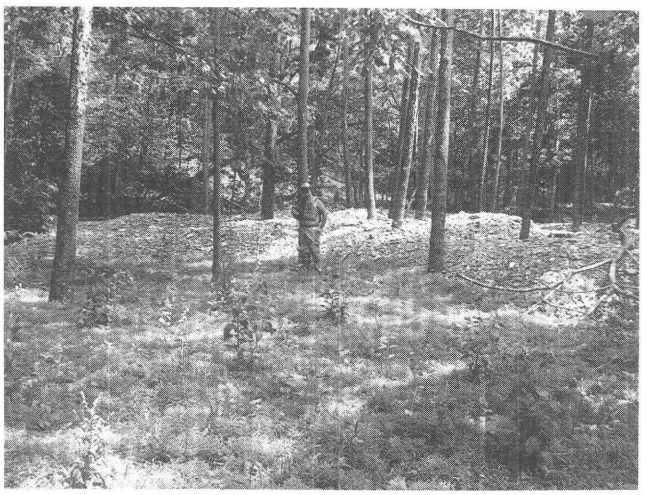

Figure 24. Delta formed at mouth of unnamed tributary to the South Branch Potomac River at Blue Rock in Smoke Hole canyon. Poorly sorted deposits bury trees to depths of approximately 1 m.

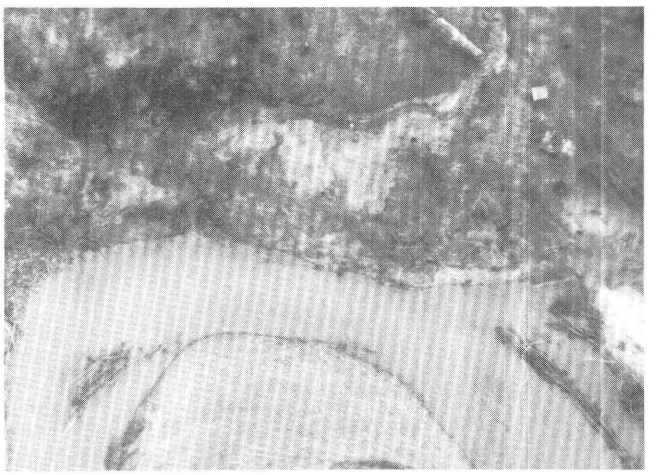

Figure 25. Aerial view of delta shown in figure 24 (see top center). Flow along South Branch is from right to left. Note that the point bar along the left bank (bottom center) was stripped of vegetation, whereas vegetation along the right bank was left intact. Field of view is 250 m wide.

morphology suggests a series of braid bars with steep slipfaces, there is no imbrication or internal stratification. Furthermore, the surface layer of angular gravel mantles a deposit with a large component of poorly sorted sand-sized fragments. We interpret this deposit as a mass of sediment carried by the tributary and rapidly emplaced on the flood plain under slack-water conditions. Flow in the eddy or emanating from the tributary winnowed sands from the surface layer; with declining flood stage, the deposit was incised and partially reworked by flow draining toward the main channel.

At the mouth of Redman Run, which also drains into the South Branch in Smoke Hole canyon (fig. 26), a poorly sorted gravel deposit as much as 1 m thick buried the bases of trees adjacent to the channel. This deposit has a relatively flat surface about 2 m above the low-water channel and gradually thins in the upstream direction. High-water marks indicate that peak stage was no more than 0.5 m above the surface of the deposit at its downstream end. Postflood reworking created a lower gravel bar emanating from the mouth of Redman Run into the channel of the South Branch.

Fan Deposits

Many of the larger tributaries of the three forks of the South Branch have built fans extending across the valley from the slope break at the mountain front. Major valley constrictions are formed by these fans. Extensive deposition

Figure 26. Delta at the mouth of Redman Run, tributary to South Branch Potomac River in Smoke Hole canyon. Sediment up to 1 m thick buries bases of trees growing on the pre-1985 surface. The approximate elevation of this surface is indicated by the tree on the edge of the deposit, just right of the center of the photograph. Much of the underlying material probably was delivered by a debris avalanche that occurred in June 1949. Flow along South Branch is from right to left.

Figure 27. Erosion and deposition on fan at the mouth of Nelson Run, tributary to North Fork South Branch Potomac River between Circleville and Judy Gap. Flow along North Fork is from right to left. Field of view is 750 m wide.

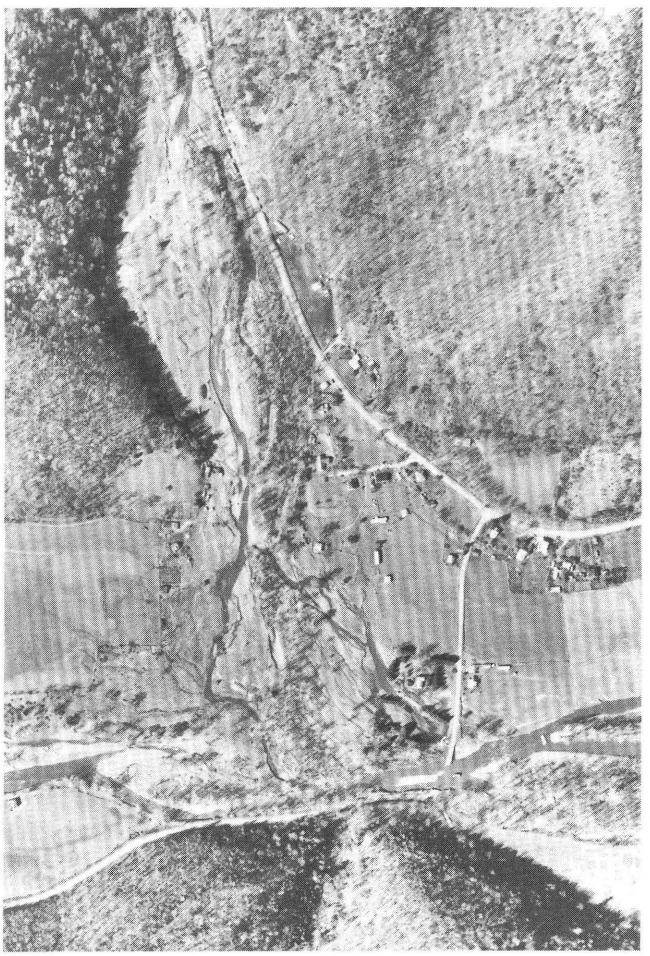

Figure 28. Incision of fan and flood-plain deposits by anastomosing channel system at the confluence of Big Run and the North Fork South Branch Potomac River, about 11 km downstream of the Virginia–West Virginia border. Flow along North Fork is from left to right. Field of view is 890 m wide.

and incision occurred on some fan surfaces during the flood, especially where tributaries were subjected to intensive scour and widening. A prominent example is Nelson Run, a tributary of the North Fork between Circleville and Judy Gap (fig. 27). Some of the flow emanating from Nelson Run evidently moved down the steepest part of the fan (to the right along the base of the mountain slope in the figure) and then crossed the flood plain along the base of the fan. On this fan, as on others in the South Branch basin, some sediment clearly reached the main channel, but a substantial amount of the sediment coming out of the tributary appears to have been deposited on the fan or on the flood plain at the base of the fan.

Fanlike accumulations also occurred at the mouths of larger tributaries. Many of these form anastomosing patterns at the confluence and may be analogous to the anastomosing systems described by Smith (1983). At the junction of Big Run with the North Fork (fig. 28), an actively anastomosing channel system incised the valley floor. The possibility that major sediment contributions from tributary valleys influenced the extent and pattern of erosion and deposition along the main river at downstream locations is considered in more detail by Jacobson and others (chapter C, this volume).

Erosion Features on Bottomland

Widespread erosion on the bottomlands of the three forks of the South Branch took a variety of forms, many of which resemble erosion features reported in the geomorphic literature (Collins and Schalk, 1937; Jahns, 1947; Wolman and Eiler, 1958; Hack and Goodlett, 1960; Stewart and LaMarche, 1967; Baker, 1977, 1978, 1984, 1988; Sullivan, 1983; Ritter and Blakely, 1986; Nanson, 1986; Kresan, 1988; Ritter, 1988) or small-scale features reported in the sedimentology literature (Dzulynski and Sanders, 1962; Karcz, 1967, 1968; Allen, 1971, 1982, 1985; Paola and others, 1986). In the present discussion, we recognize

erosion features ranging from localized disruptions of the surface (longitudinal grooves and scour marks) to dissection and stripping of much or all of the valley floor. In almost all cases the bottomland surface is occupied by vegetation, with pasture and cropland predominating over forest vegetation on the higher surface and woody vegetation more common on the lower surface. As a result of the resistance offered by dense networks of roots, the strength of the turf layer or of the root system appeared critical in determining the extent of erosion at many sites during the flood. Once a surface layer was breached, the underlying deposits in some areas were subject to rapid scour and incision.

Subsurface stratigraphy is highly variable: at some locations a cobble pavement is found within 10–15 cm of the surface, whereas other sites are underlain by as much as 2 m of cohesive alluvial soil composed largely of silty sand. Even the finer cohesive deposits may have cobble lenses or boulders occurring above basal channel gravels and cobbles. Stratigraphic heterogeneity in some cases is related to the spatial distribution of preflood overflow channels or buried scour-and-fill sequences. At several locations a partially indurated paleosol was exposed in the channel bed and banks by vertical incision during the flood. A similar paleosol, revealed during excavations on the South Branch flood plain near Petersburg, was estimated, on the basis of radiocarbon dates, to be 7,000 yr old (Jacobson and others, 1989).

The heterogeneous character of the valley floor resulted in a patchy distribution of erosion and deposition features. However, although bottomlands in the South Branch basin are less homogeneous than the substrates used in flume experiments reported in the sedimentology literature, the sedimentological studies provide information that is relevant to our understanding of the morphology and genesis of erosion features. In the ensuing discussion, we seek to draw analogies between features observed in the aftermath of this flood and erosion processes described in the sedimentology literature.

Dzulynski and Sanders (1962) characterize erosion features on firm mud bottoms as either (1) scour marks, which are created by turbulent flow patterns impinging on an erodible bed, or (2) tool marks, which result from impact on an erodible bed by an object or particle entrained in the flow. Our observations indicate that both types of features formed on valley floors in the study area during the November 1985 flood. Allen (1971) suggests that most scour features formed in cohesive substrates are associated with flow separation; that flow separation may be produced by upward or downward steps on the bed, by obstructions in the path of the flow, by flow expansions, or by other types of irregularities or defects in the bed; and that maximum turbulent stress occurs where the separated flow becomes reattached to the bed. Observations of flood-generated features in the South Branch basin indicate that flow separation around obstructions, local heterogeneity in the resistance of the valley floor to erosion, and topographic irregularities influencing the pattern of surface drainage are all important in determining the pattern of erosion. Trees and structures such as fences, roads, buildings, and bridges often form the locus for initiation of separated flow, which may lead to creation of erosion and deposition forms.

Longitudinal Grooves

Elongate linear grooves were eroded by the flood at many sites within the study area. These typically are parallel or subparallel to the local direction of flood flow and extend down the valley floor tens to hundreds of meters. They generally appear in groups of parallel grooves and may be regularly spaced at intervals of 0.5–3 m. Size varies, from depths and widths measured in centimeters to depths and widths exceeding 1 m (fig. 29). Gravel and cobbles are commonly found embedded in or deposited on the floors of grooves; trenching of the surface beneath and adjacent to the groove reveals that the coarse material was emplaced during the flood. Although they are often found in close proximity to sites of severe erosion, longitudinal grooves also are found in areas where the valley floor is otherwise almost completely intact. We therefore associate these features with inception and early stages of bottomland erosion.

In some cases the grooves clearly are tool marks or drag marks made by objects, usually uprooted trees, entrained in the flow (figs. 29*A*, 30; also see Kite and Linton, chapter D, this volume, fig. 5). Diagnostic evidence includes grooves that are parallel to uprooted trees lying on the valley floor, pits (possible gouge marks) along the trend of a set of grooves, and grooves that cross one another. In other cases the grooves are incised along trends that run parallel to crop rows or other preexisting weaknesses in the surface that may be preferred sites for incision (fig. 29*C*). Figure 31 shows an example where some grooves run along crop rows but others cut across these rows at oblique angles.

Longitudinal grooves often occur in straight, parallel sets oriented along the direction of flow and unrelated to crop patterns or other artifacts (figs. 29*B*, 32). Similar elongate linear features, both erosional and depositional, have been described in a broad range of environments (see Allen, 1982, pp. 24–52). Longitudinal grooves sculpted in cohesive river beds under the influence of bedload transport typically contain sand and gravel, which presumably were used as cutting tools in groove formation. An experimental study by Shepherd and Schumm (1974) of channel incision on a cohesive bed yielded longitudinal grooves and potholes in the early stages of erosion; the grooves eventually coalesced and ultimately a single narrow, deep inner channel formed. Similar features, formed on a much larger scale

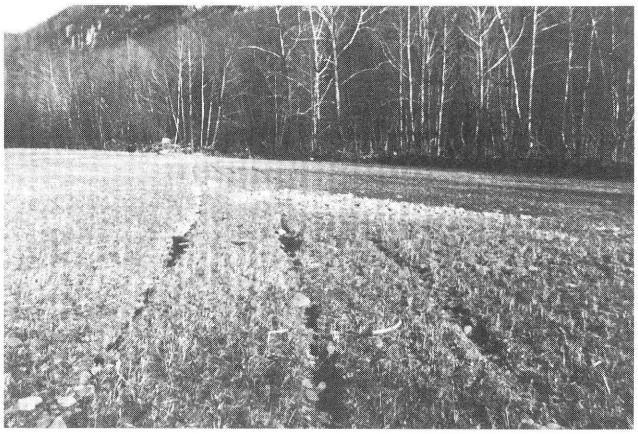

A

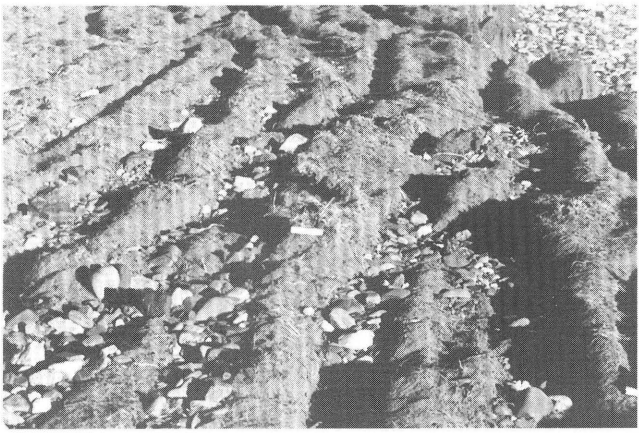

B

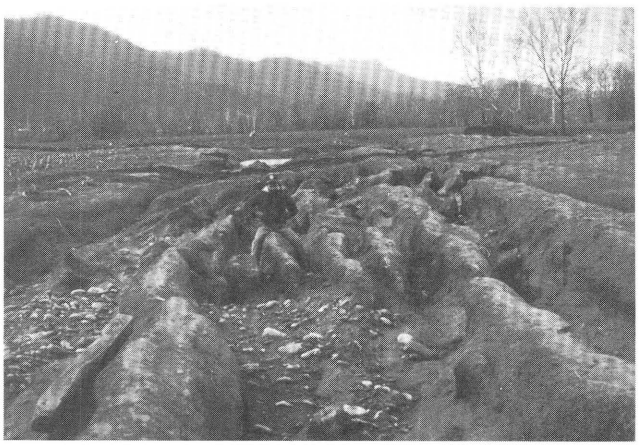

C

Figure 29. Longitudinal grooves (*A*) formed by the limbs of a tree dragged across valley floor, North Fork South Branch Potomac River about 0.6 km upstream of Seneca Rocks; (*B*) oriented along direction of flow, unrelated to crop patterns. Ruler is 15 cm long. North Fork South Branch Potomac River near Zeke Run, about 10 km upstream of Hopeville; (*C*) incised along crop rows, South Branch Potomac River near Fisher, several kilometers upstream of Moorefield. Photograph by R. Gray, U.S. Soil Conservation Service.

by Pleistocene glacial meltwater floods, have been described by Baker (1978) and by Kehew and Lord (1986).

Longitudinally oriented erosion and deposition forms may generally be attributed to secondary flows consisting of paired longitudinal vortex tubes with opposite directions of rotation (Allen, 1982). An array of helical vortices of this type can develop in straight stream channels (Einstein and Li, 1958). Allen (1985) suggests that in the absence of bedload, furrows will develop on a soft mud bed by fluid stripping where the vortices descend toward the bed and then diverge, but that corrasion in the presence of bedload could produce furrows along zones of converging and rising flow instead (fig. 33). Our observations of cobbles and gravels on the floors of some grooves (fig. 29) suggest that corrasion by coarse clasts embedded in the vortex was one of the mechanisms involved in groove formation during the 1985 flood.

Scour Marks

Scour marks are erosion features that range in shape from small circular or elliptical pits, to elongate parabolic or spindle-shaped marks, to irregular shapes formed by lateral erosion and uneven headcut retreat (figs. 34–38). Some examples observed in the field were smaller than 1 m in diameter and shallower than 0.3 m, but the largest examples were tens to hundreds of meters long and tens of meters wide. The largest of the observed scour features are referred to below as flood channels or chutes.

Many of the observed scour marks had spoon-shaped long profiles that were steepest at the head of the scour. In this respect they are reminiscent of the idealized form of flute marks described by Allen (1971, 1982); however, some examples had stepped profiles and complex internal structure resembling discontinuous gully systems. Scour marks, like longitudinal grooves, were found in association with severe disruption of the valley floor but also occurred as isolated forms on otherwise undisturbed bottomland. Most scours observed in the study area appear to be associated with some form of flow separation and vortex action. Similar features formed on the Connecticut River flood plain in the flood of March 1936 were described by Collins and Schalk (1937) as "swirl pits"; macroturbulent vortex action or "kolking" (Matthes, 1947) was identified as the probable cause of other circular or elliptical scours described by Ritter and Blakely (1986) and Baker (1978).

One of the more common types of scour marks observed in the aftermath of the November 1985 flood was created by flow separation around individual obstacles projecting above the flood-plain surface. Most of the obstacles were trees (fig. 39*A*), but the same effect was

Figure 30. Grooves formed as drag marks by trees entrained in flood flow. South Fork South Branch Potomac River, 2 km upstream of Milam; flow along South Fork is from left to right. Field of view is 460 m wide.

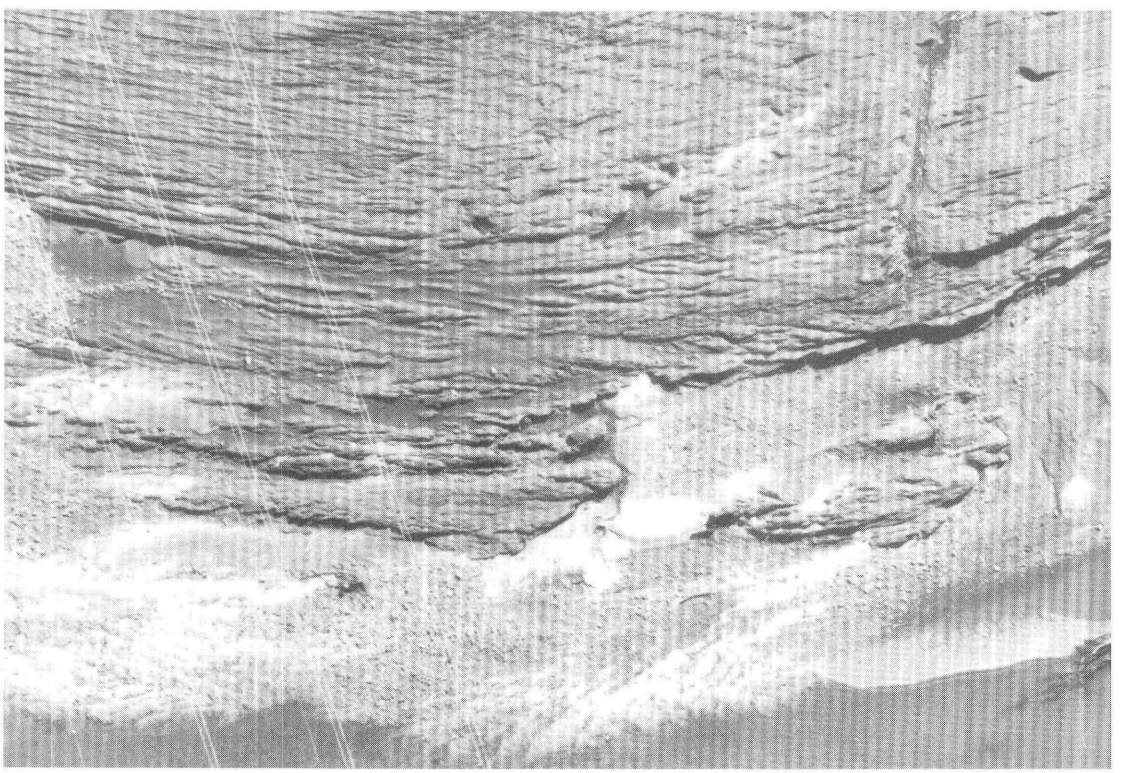

Figure 31. Deeply incised grooves oriented subparallel to crop rows, Cheat River about 2 km upstream of Rowlesburg. Flow is from right to left. Diagonal white lines on left side of photograph are power transmission lines suspended across the river. Field of view is 140 m wide.

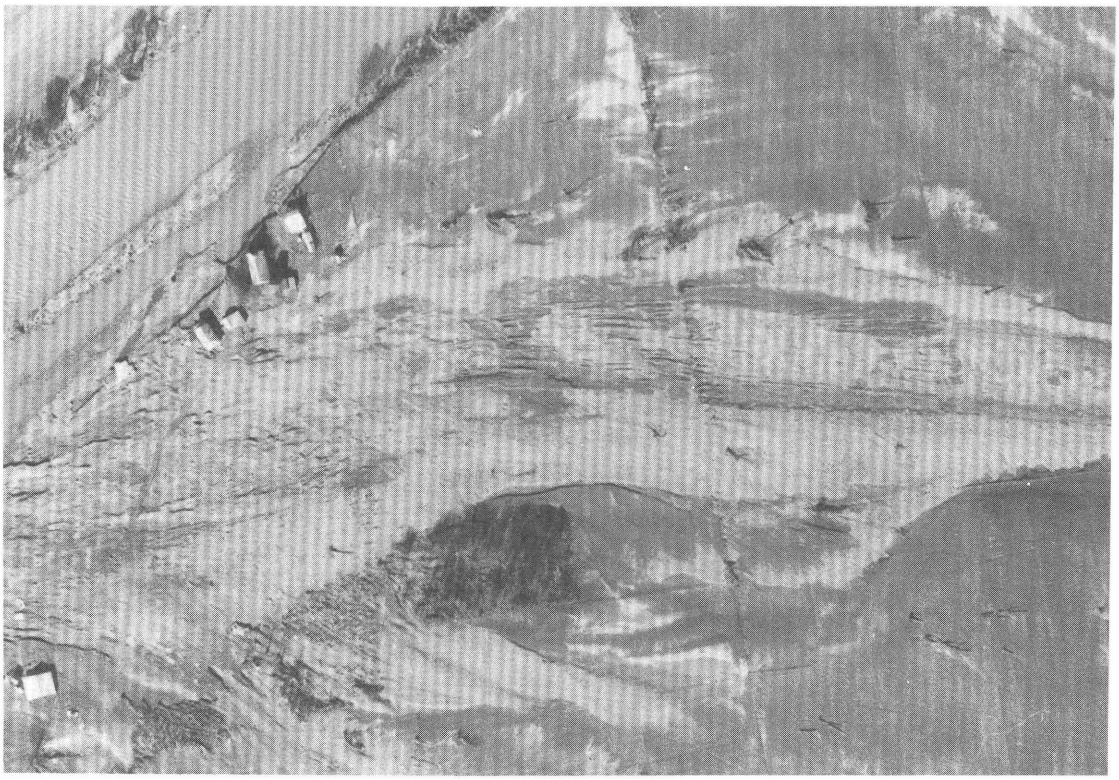

Figure 32. Grooves incised along trend of shallow erosional trough, South Branch Potomac River just downstream of Petersburg gaging station (station was destroyed in the flood). Flow along South Branch is from left to top center. Field of view is 790 m wide.

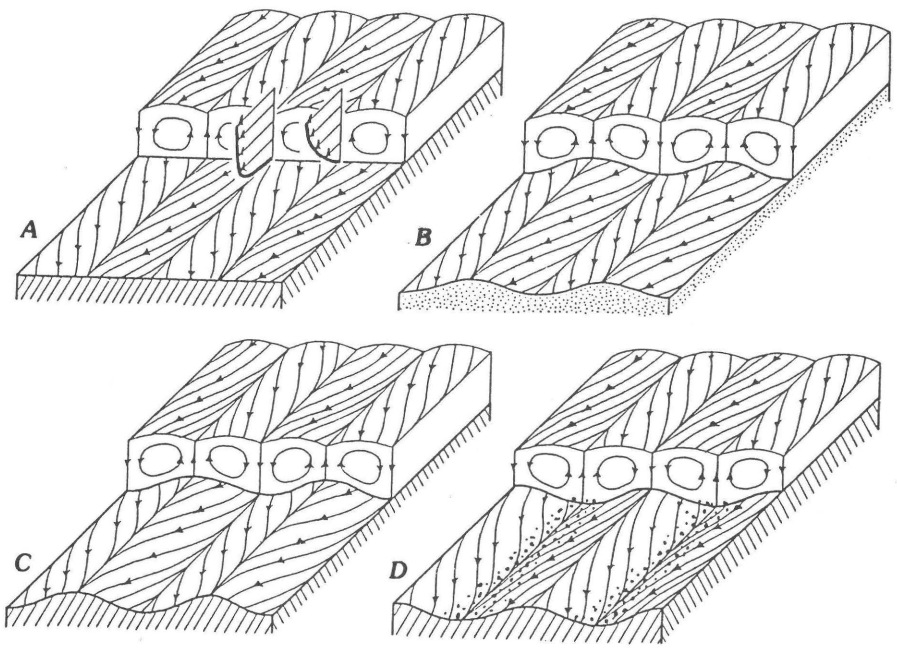

Figure 33. Drawing showing flow pattern of longitudinal corkscrew vortices and their hypothesized effects on the shape of the underlying bed (from Allen, 1985, p. 211; used by permission). (*A*) General character of motion, (*B*) shape of deformable granular surface adjusted to the motion, (*C*) shape of a mud bed adjusted to the motion in the absence of bedload, and (*D*) shape of a mud bed adjusted to the motion in the presence of bedload particles.

A

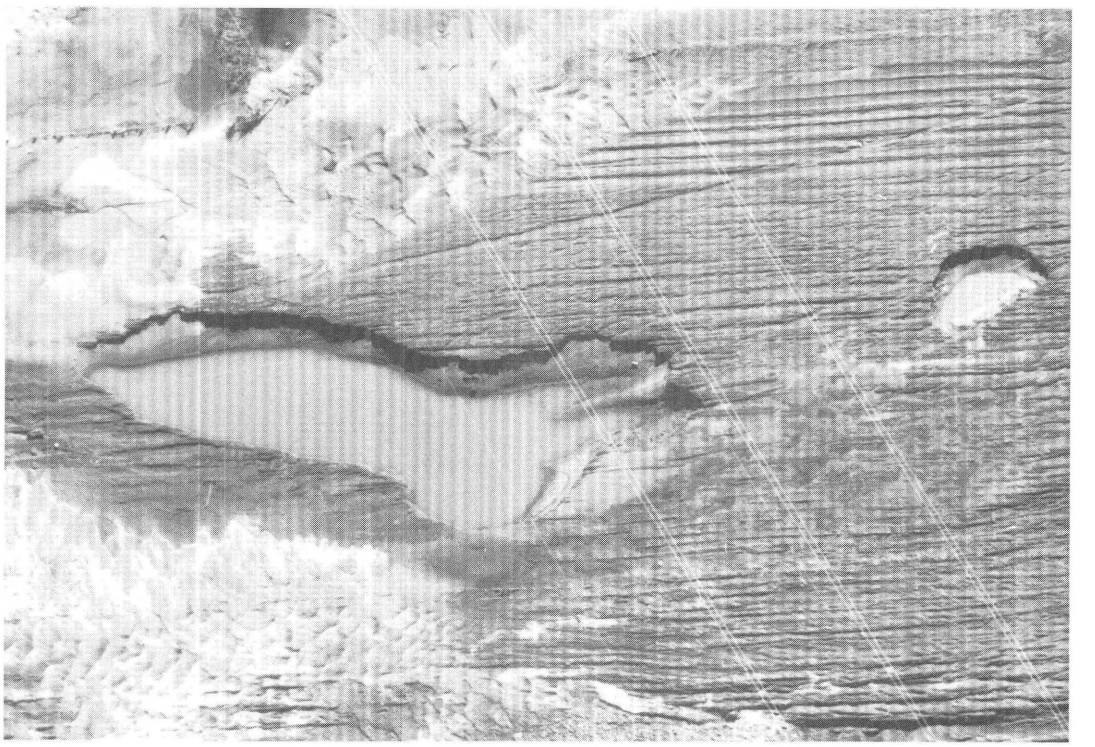

B

Figure 34. (*A*) Small elliptical scour on valley floor along South Branch Potomac River between Redman Run and Austin Run, 5 km upstream of confluence with North Fork. Flow was from upper right to lower left. (*B*) Elliptical (see right edge) and elongate or spindle-shaped (see center) scour marks on the Cheat River flood plain, about 2 km upstream of Rowlesburg. Flow was from right to left. Note longitudinal grooves incised along crop rows; also note sand dunes at top and bottom of photograph. White lines running from top center to lower right are power transmission lines. Field of view is 100 m wide.

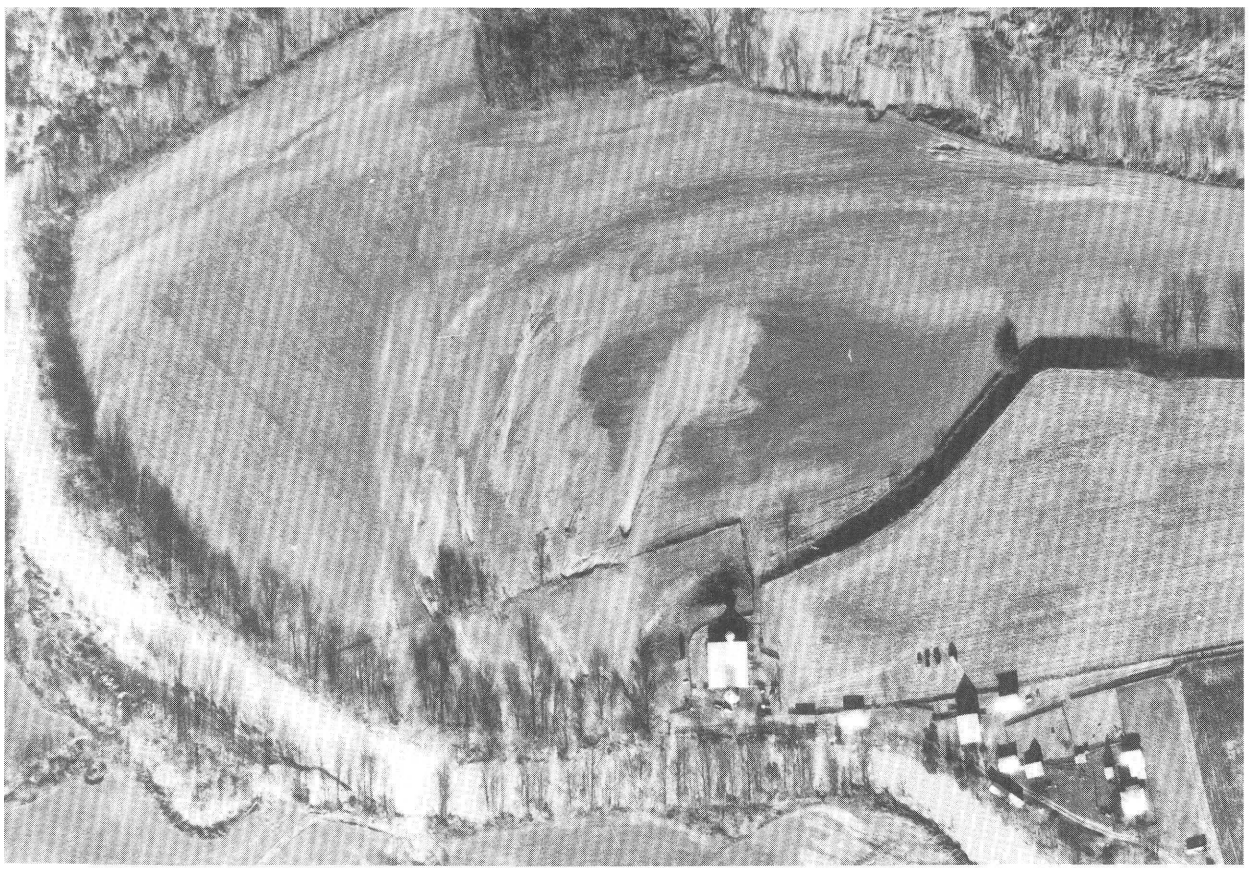

Figure 35. Elongate scour marks along South Fork South Branch Potomac River, 7 km downstream of Brandywine. Note that the heads of the scour marks are located just downstream of a fence line, which may have been a site for initiation of separated flow. Flow in channel enters at lower right and follows meander clockwise to upper right, but overbank flow during the flood cut across the valley floor from bottom center. Field of view is 760 m wide.

sometimes observed around buildings (fig. 39*B*). The pattern of flood flow around a tree is analogous to the generalized pattern of flow around a rounded, blunt body protruding vertically into the flow, which has been described in great detail. The typical horseshoe-shaped scour was given the name "current crescent" by Peabody (1947); structures formed by scour and deposition associated with flow around an obstacle were described by Dzulynski and Walton (1965) as obstacle marks. Additional discussions of these features have been presented by Karcz (1968), Baker (1978), Allen (1982), Sullivan (1983), Ritter and Blakely (1986), Paola and others (1986), and Baker and Kochel (1988). Similar phenomena associated with scour at bridge piers have been discussed in the engineering literature (Laursen, 1960; Moore and Masch, 1963; Shen, 1971).

A horseshoe vortex typically forms by separation of the boundary layer on the upstream side, which rolls up and is stretched or wrapped around the obstacle (Shen, 1971, fig. 23–4; also see Baker, 1978, p. 102; Allen, 1982, fig. 5–2; and Paola and others, 1986, fig. 2). The limbs of the vortex reattach at some distance downstream, leaving a zone of separated flow in the wake of the obstacle. As Allen (1982, fig. 5–10) and Paola and others (1986) indicate, and as our observations confirm, erosion commonly occurs in the region of vortex flow on the upstream side. If the obstacle is a tree, scour around the base may partially undermine it and allow the flow to uproot or topple it (fig. 40).

Debris accumulations around trees (figs. 39*A*, 41) increase the cross-sectional area of the obstacle offered to the flow and therefore increase the size of the area of separated flow. In some cases this may protect the tree from the immediate effects of basal scour, but in other cases the debris may be responsible for increasing the shear exerted on the tree by floodwaters, thus leading to toppling of the tree. Similar effects were observed along the valley of Plum Creek in Colorado in the aftermath of a catastrophic flood occurring in 1965 (W.R. Osterkamp, U.S. Geological Survey, personal communication, 1988; flood described by Osterkamp and Costa, 1987).

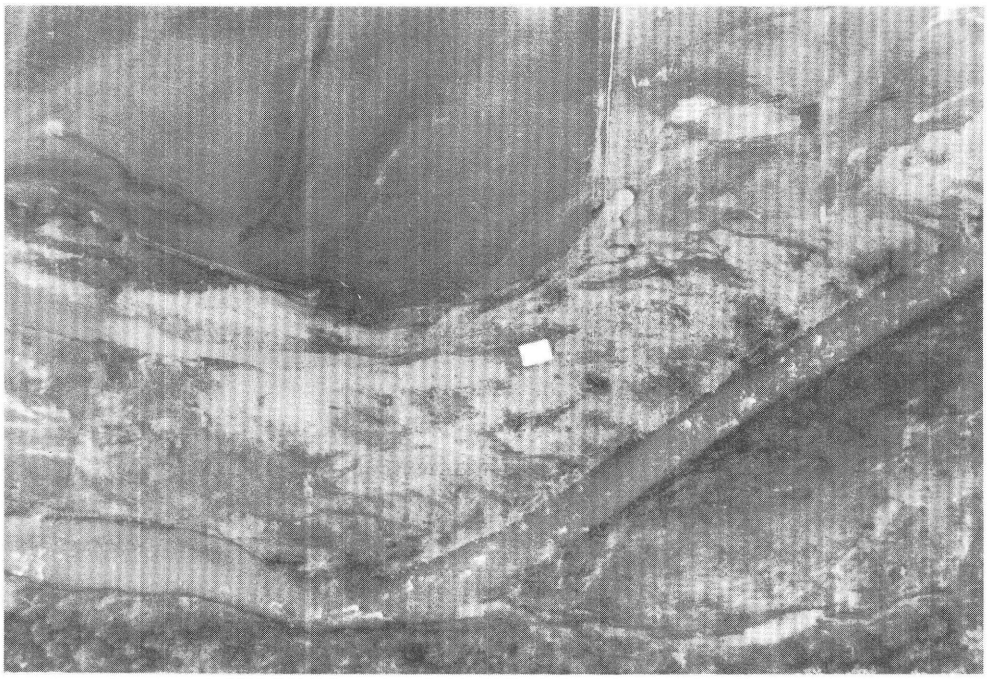

A

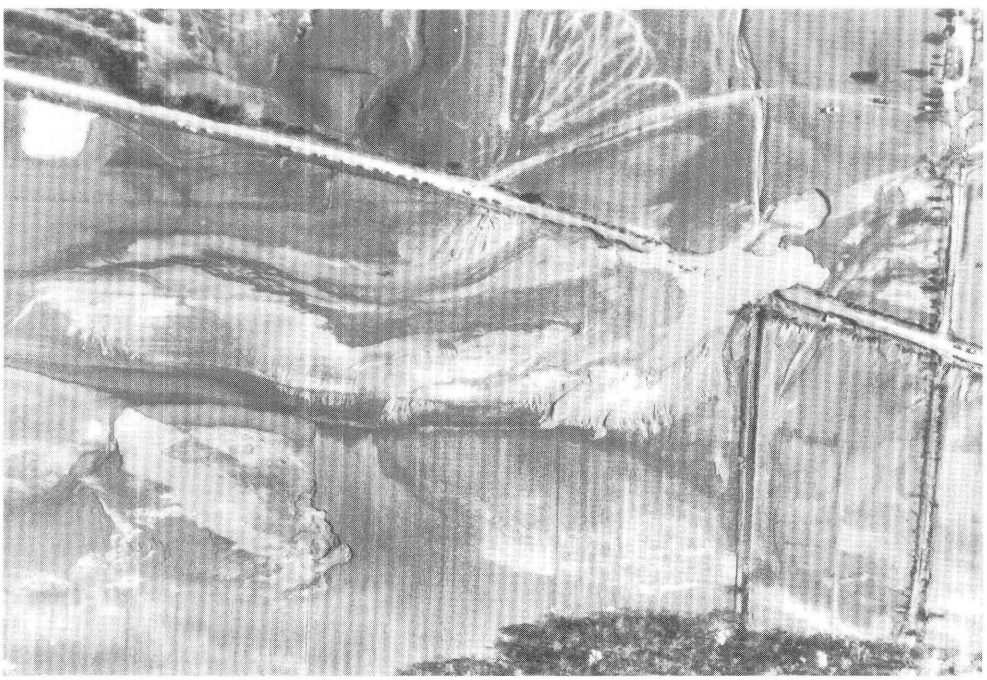

B

Figure 36. (*A*) Headward branching scour on North Fork flood plain, about 2 km downstream of Circleville. The two headcuts diverge at the location of a fence line, which may have been a site of initiation of flow separation before the scour retreated headward. Field of view is 390 m wide. (*B*) Several scour features in this photograph appear to have retreated headward from linear flow obstructions. Flow was from upper right to lower left; the river channel is out of view at the bottom of the picture. South Fork flood plain, 13 km upstream of confluence with South Branch at Moorefield. The road is elevated 2–3 m above the flood plain and served to block floodwaters until it was overtopped and breached; the resulting scour, at right center, then retreated headward and formed two prominent headcuts. Another, broader headcut is visible at lower left and appears to have started at a fenceline oriented perpendicular to the flow, which was from right to left on this portion of the flood plain. Splay deposits also are clearly visible. Field of view is 620 m wide.

Figure 37. Headward-eroding scour formed where overbank flow drained back into the river channel (center of picture). Flow is from left to right. North Fork at Bennett Gap, 1.5 km downstream of Riverton. Field of view is 380 m wide.

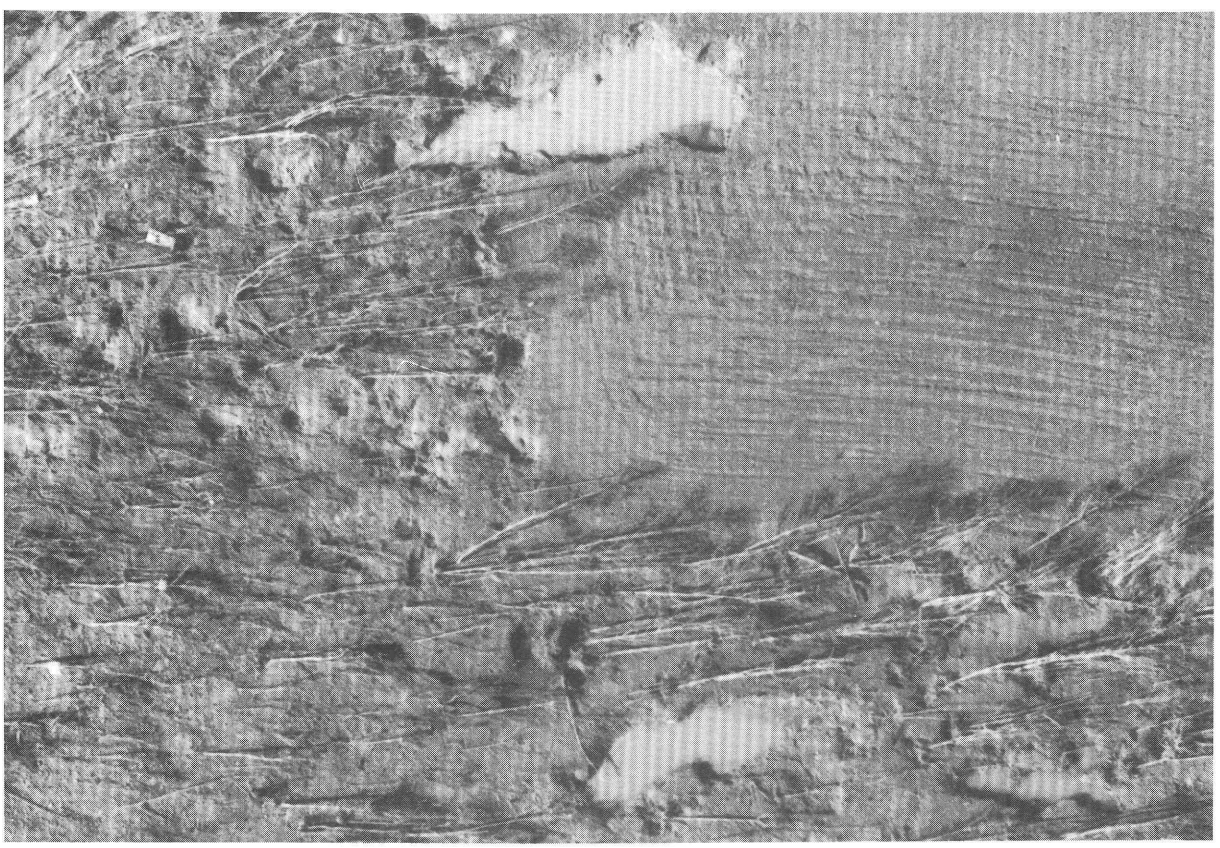

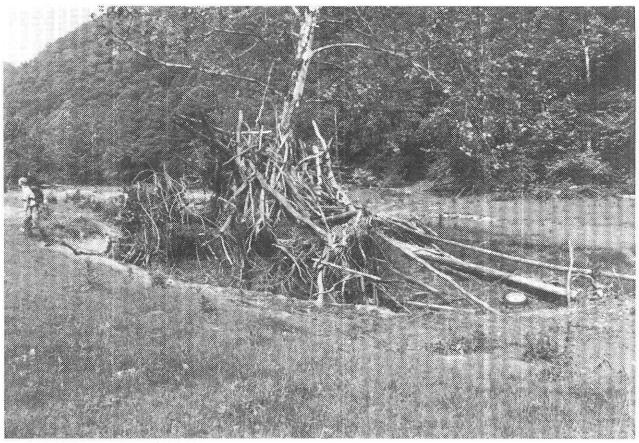

A

B

Figure 39. Scour marks created by flow separation around isolated objects on the flood plain. (*A*) Tree with accumulated debris and elliptical scour, South Branch Potomac River between Redman Run and Austin Run, 5.7 km upstream of confluence with North Fork; flow was from left to right. (*B*) Scour mark formed around upstream side of house on the flood plain of the Black Fork River, tributary to Cheat River, 1 km upstream of Parsons. Field of view is 95 m wide. Flow direction is from left to right.

◀ **Figure 38.** Irregular scour pattern on forested surface upstream of a field cleared for row crops. Virtually every tree in the forested area has been knocked down and many have been uprooted, leaving small circular or elliptical pits. Several pits have been enlarged to form elongate scour marks. At top center, a turbulent thread of flow emerging from the forested area onto the open field has left an irregular scour mark, whose outline bears a strong resemblance to the shape of a turbulent jet emerging from an orifice (illustrated in Allen, 1985, fig. 11.10, p. 206). Flow is from left to right. Cheat River, 10 km upstream of Rowlesburg. Field of view is 110 m wide.

◀ Figure 40. Fallen tree flanked by a pair of elliptical scour marks, Cheat River about 8 km downstream of Parsons. The scours appear to make up the limbs of a horseshoe, but they do not quite meet on the upstream side of the tree, and the scour on the left side leads into an elongate erosional trough that extends downstream. Note cutbank on left side of photograph where channel widening occurred in the flood. Flow along Cheat is toward the top. Field of view is 100 m wide.

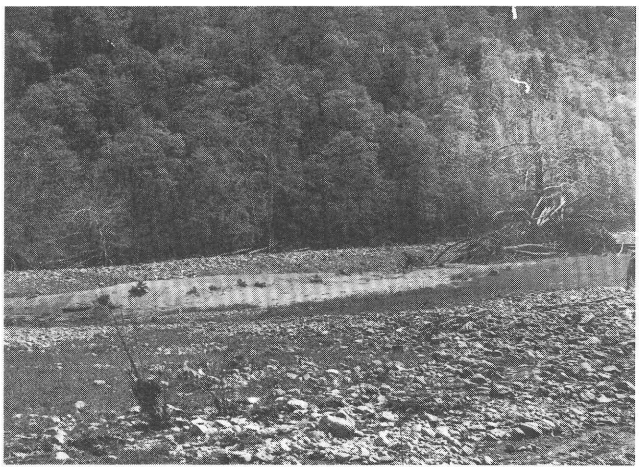

Figure 42. Sand deposit formed in the lee of a standing tree, South Branch Potomac River between Redman Run and Austin Run.

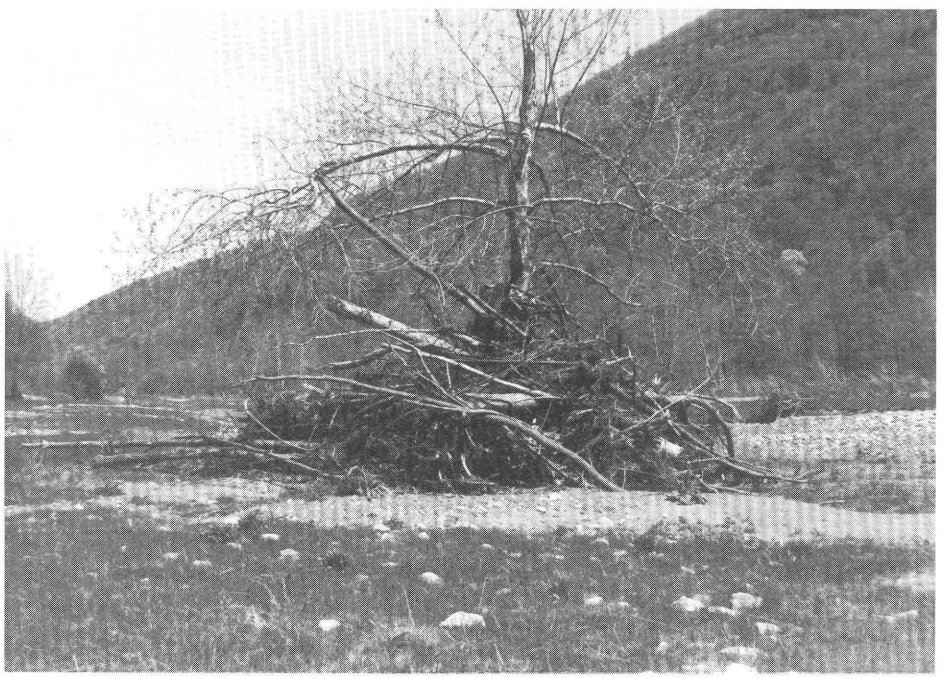

Figure 41. Debris jam formed on upstream side of tree during the flood. South Branch Potomac River between Redman Run and Austin Run, about 5.4 km upstream of confluence with the North Fork.

Patterns of erosion and deposition in the separation zone and immediately downstream of the reattachment point also may vary considerably (Allen, 1982, fig. 5–10, p. 185). In some cases there is an elliptical scoured zone that gradually shallows downstream (fig. 39*A*). In other cases a remnant of undisturbed bottomland is found along the centerline of flow downstream of the obstacle, flanked by scour zones; sometimes there is a mound of sediment deposited over undisturbed bottomland within the region of flow separation (fig. 42). The transition from conditions favoring deposition to conditions favoring erosion in the lee of the obstacle apparently occurs with increasing strength of the wake-vortex system at very high flow velocities (Shen, 1971; Baker, 1978).

Although scour marks formed in the November 1985 flood were commonly found in association with isolated flow obstructions such as trees or buildings, linear features crossing the flood plain perpendicular to the main flow also acted as initiation sites for flow separation and scour. Multiple parallel scour marks were found extending downstream from roads, fence lines, rows of trees, and topographic steps on the valley floor (figs. 35, 43). Scour marks also were located preferentially in local topographic lows, where floodwaters were deeper and shear stresses were greater than at adjacent high points. Some of these scours may have reoccupied the sites of old abandoned scour marks formed in past floods.

Elongate scour marks observed in the study area resemble parabolic or spindle-shaped transverse erosional marks described by Allen (1971) (figs. 34*B*, 35, 43). Allen's (1971) experiments demonstrated that an original circular or elliptical pit could become an elongate scour mark by progressive erosion in the downstream direction. The upstream end of the pit is the site of initiation of separated flow; the rate of bed erosion by fluid-stressing (i.e., shear stress exerted by the overlying fluid) is greatest near the point of reattachment (Allen, 1971, p. 227). As erosion progresses, the separated zone becomes longer and the locus of maximum bed erosion shifts downstream (Allen, 1982, fig. 7–27). Thus, some of the elongate scour marks observed in the South Branch basin, like the features developed in Allen's (1971) experiments, may have formed by downstream extension of smaller, initially elliptical or irregularly rounded scour pits.

Some elongate scour marks appear also to have grown upstream by headcut retreat along existing swales and depressions; branching patterns resembling a simple drainage network were observed at several locations (fig. 36). The headcuts at such locations were amphitheater shaped with well-developed plunge pools. Fluvial erosion by water converging toward and draining over the lip of the scour is considered the most likely cause here, given the rapid recession of floodwaters and the fact that the underlying alluvium often contained strata that were either quite cohesive or too coarse to be eroded and transported downstream by sapping. Headcut retreat is strongly indicated where the head of a scour mark is located upstream of a linear feature identified as the probable locus of flow separation responsible for initiating the scour (fig. 36). Similar headcuts have been observed forming knickpoints in cohesive alluvium underlying new channels cut by the November 1985 flood (fig. 44).

Irregular, patchy patterns of scour were generated by highly turbulent flow on bottomlands with hummocky topography and numerous local obstructions of varying shapes and sizes (figs. 38, 43, 45). These examples attest to the extraordinary complexity of the flow fields that develop at some sites.

Bank Erosion and Channel Widening

Bank erosion was common along all three forks of the South Branch Potomac River during the November 1985 flood. Many fresh cutbanks were formed, exposing alluvium, colluvium, and debris-fan deposits in cross section. In some cases, where a large component of the flood flow left the channel, the preflood channel remained virtually unmodified despite major impacts on the adjacent bottomland. However, where channel flow impinged against one bank or the other, the resulting erosion was often dramatic, doubling or tripling the width of the channel at the expense of the flood plain (figs. 46*A–D*).

The positions of preflood banks are sometimes marked in the aerial photographs by a line of trees or organic debris in the water (figs. 46*A*, *B*). Often a cutbank is flanked by an area along the channel margin where alluvium has been partially stripped away. Downstream, the stripped areas commonly grade into sandy to gravelly splay deposits (figs. 47, 48). In some instances an example of radical channel widening is associated with multiple chutes or erosion channels on the valley floor or with formation of bars and remnant islands in the channel belt (figs. 47, 49).

Where the channel was flanked by forested bottomland rather than by flood plains cleared for agriculture, channel widening sometimes was accompanied by irregular scouring and abrasion of the adjacent surface. The resistance to flow offered by the trees and the anchoring effect of their roots may have prevented more extensive bank erosion at such sites, even though many of the trees were knocked down by the force of the flow (fig. 50). However, presence or absence of forest was not a clear determinant of the extent of channel widening or of other forms of erosion. Gallery forests or lines of trees bordering the channel were present along most of the length of each of the three forks of the South Branch prior to the flood, and the trees were completely removed at many sites. Dense stands of trees failed to prevent channel widening or stripping of the

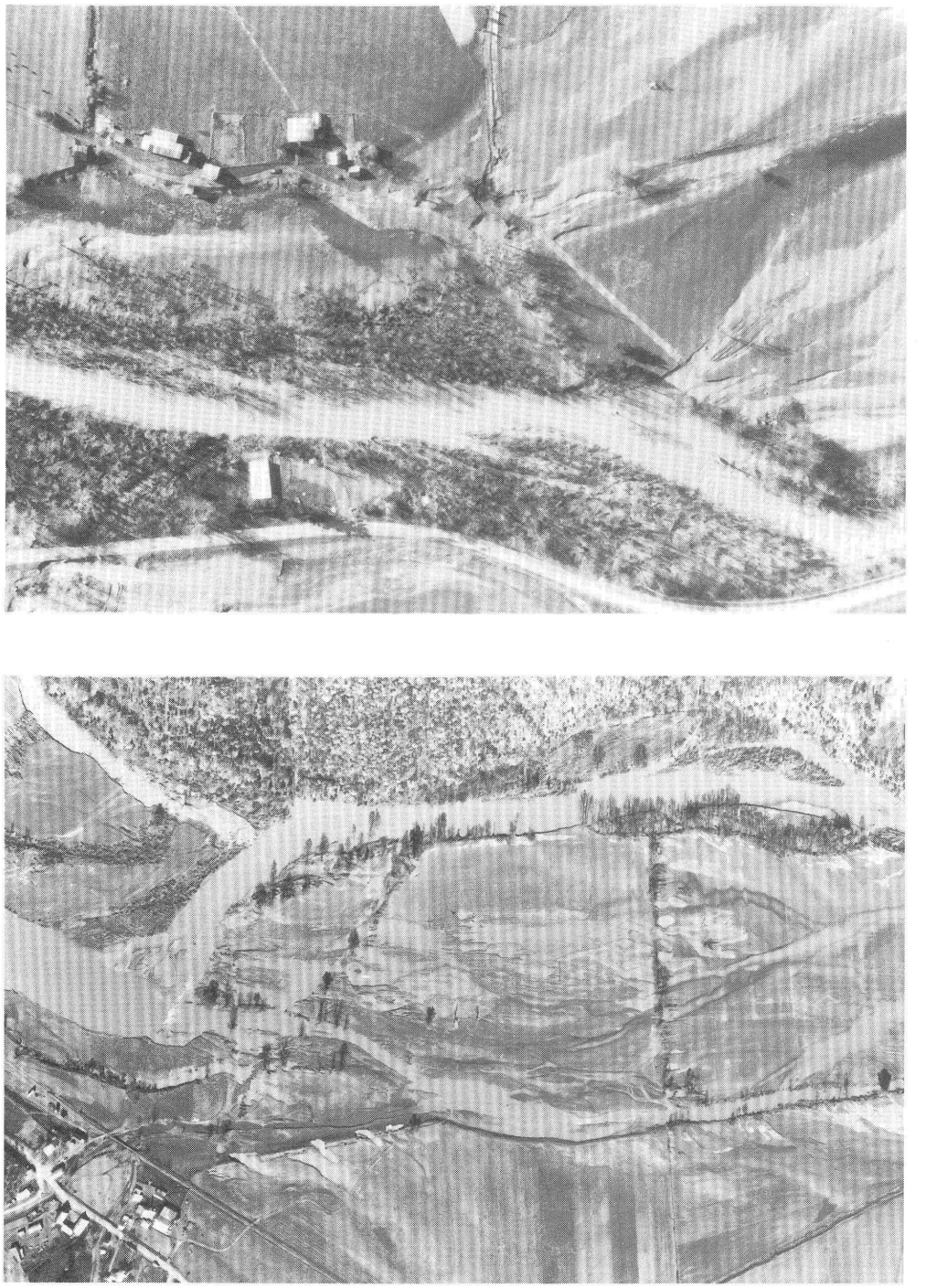

Figure 43. Scour marks associated with flow obstructions: (*A*) South Fork South Branch Potomac River at Brandywine; flow is from left to right. Note elongate scours initiated where flood flow crossed over the road just right of the center of the photograph and also where the road approaches the river channel at lower right. Field of view is 640 m wide. (*B*) South Branch Potomac River near Durgon, 9 km downstream of Petersburg; flow is from left to right. Complex pattern of channel widening and flood-plain erosion, with elliptical and elongate scours formed downstream of fence lines, rows of trees, and topographic steps. Note area marked by both scour marks and longitudinal grooves in cultivated field at the center of the photograph. Several larger channels incised along the flood-plain margins also are visible. Field of view is 1,400 m wide.

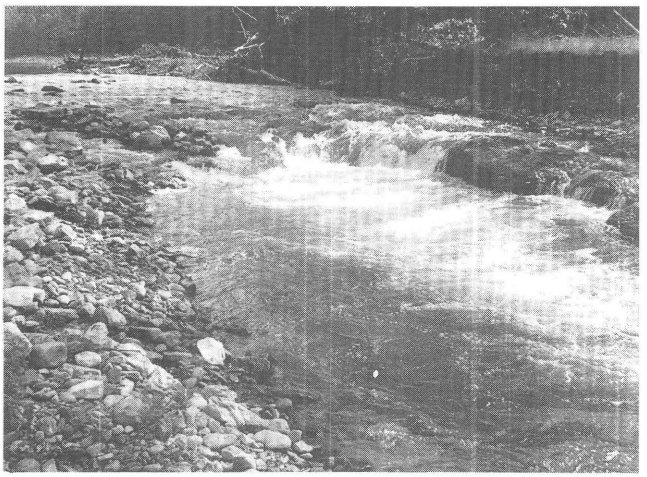

Figure 44. Headcut in a new channel actively retreating upstream at low flow in the summer of 1987. Vertical drop in bed level over the ledge is about 1.5 m. South Branch Potomac River downstream of Austin Run, 4.4 km upstream of confluence with the North Fork.

bottomland surface at those sites where stresses imposed by flood flows were most intense (fig. 51).

Channel widening occurred at several sites where bridges influenced flow hydraulics, and it may have been caused by a combination of accelerated flow through the contracted opening beneath the bridge and turbulent eddies spawned by flow separating over and around the edges of the bridge (fig. 52). Similar occurrences have been reported previously; Ritter and Blakely (1986) describe an instance of extreme scour that they attribute to macroturbulent vortex action spawned by a bridge during a flood that was not considered competent to cause comparable erosion under natural conditions. Where Route 33 crosses the South Fork at Brandywine, channel widening and scour of the valley floor occurred downstream of the bridge, and a prominent arcuate scour formed along the right bank upstream of the bridge (fig. 53). The latter could have formed under a turbulent vortex generated by shear between flow moving through the bridge and flow piled up behind the bridge and road embankment along the right bank; alternatively, it might have formed by headcut migration under the influence of flow draining off the flood plain and back into the channel of the South Fork.

Stripping

General scouring and removal of vegetation and fine-grained alluvium from the valley floor that is not restricted to a well-defined scour mark or erosion channel is here referred to as "stripping." Stripping usually involved removal of a veneer of silty to sandy overbank deposits to reveal an underlying pavement of cobbles and boulders (figs. 54*A–C*, 55). At some locations, tree trunks were snapped or sheared off above the base, leaving behind stumps whose roots were exposed following removal of the surrounding soil (fig. 56).

The depth of stripping generally ranged up to 1.5 m, depending primarily on the depth of the contact between any fine-grained sediment and the coarse pavement underneath. Stripping occurred most often on point bars, channel islands, and bottomland segments in or immediately downstream of canyon reaches.

The coarse pavement presumably represents a channel lag deposit such as is normally found at the base of the alluvial sequence underneath a flood plain. Imbrication of cobbles and boulders exposed on the postflood surface, with some clasts resting against remnant clumps of vegetation (fig. 55), indicates that considerable reworking of this layer often occurred at sites where it was exposed by stripping of the surface layer. At some sites in the study area, cobbles and boulders were deposited on top of soil without stripping, leaving a continuous carpet of imbricated clasts that looks virtually identical to the layer exposed at other sites by stripping. Positive evidence for stripping is provided by erosional remnants of fine-grained cohesive material adjacent to the stripped surface (figs. 54*A*, *B*).

Few sites are characterized exclusively by erosion or by deposition, however. More commonly there is a transition from one to the other. At sites such as those illustrated in figure 57 and in figure 9 of Kite and Linton (chapter D, this volume), the stripped surface appears to ramp upward from the area along the channel margin, where the depth of scour is greatest, to its downstream terminus. Fresh lobes of coarse material, derived from stripping or from bedload already in transit, form splay deposits that obscure the transition from an erosional surface to a surface affected only by deposition. Bedload transport of gravel along ramp surfaces has been described as a common mechanism for moving coarse materials onto upper point-bar and low flood-plain surfaces (Ritter, 1975; Knox, 1987).

The process involved in stripping appears to be a combination of (1) surficial abrasion and gouging by sediment particles, trees, and other objects entrained in the flow and (2) fluid-stressing, which tends to cause failure of cohesive beds along planes of shearing or tearing (Allen, 1971, p. 201). The reports cited by Allen (1971) include an experimental study of cohesive mud bottoms by Dunn (1959), who derived an expression for critical bed shear as a function of vane shear strength. In the present instance the critical shear stress is that required to tear the vegetation mat or turf layer from the underlying material. This process is facilitated if the turf has already been broken; the turf layer may then be undermined or rolled up by the flow (fig. 58). As turf is removed, other turf edges are exposed, and eventually a large portion of the flood-plain surface becomes unraveled. Grass-covered surfaces are more vulnerable to this type of erosion than forested surfaces, where turf removal is minimized by the flow resistance of standing

Figure 45. Complex pattern of scour and incision, flood plain of Black Fork River at Hendricks (tributary to Cheat River). Lobe of coarse sediment at left is derived from a stripped area just upstream (see Kite and Linton, chapter D, this volume, fig. 8). Enlarged view of debris jam around house at lower right is shown in Kite and Linton (chapter D, this volume, fig. 11). Flow is from left to right. Field of view is 600 m wide.

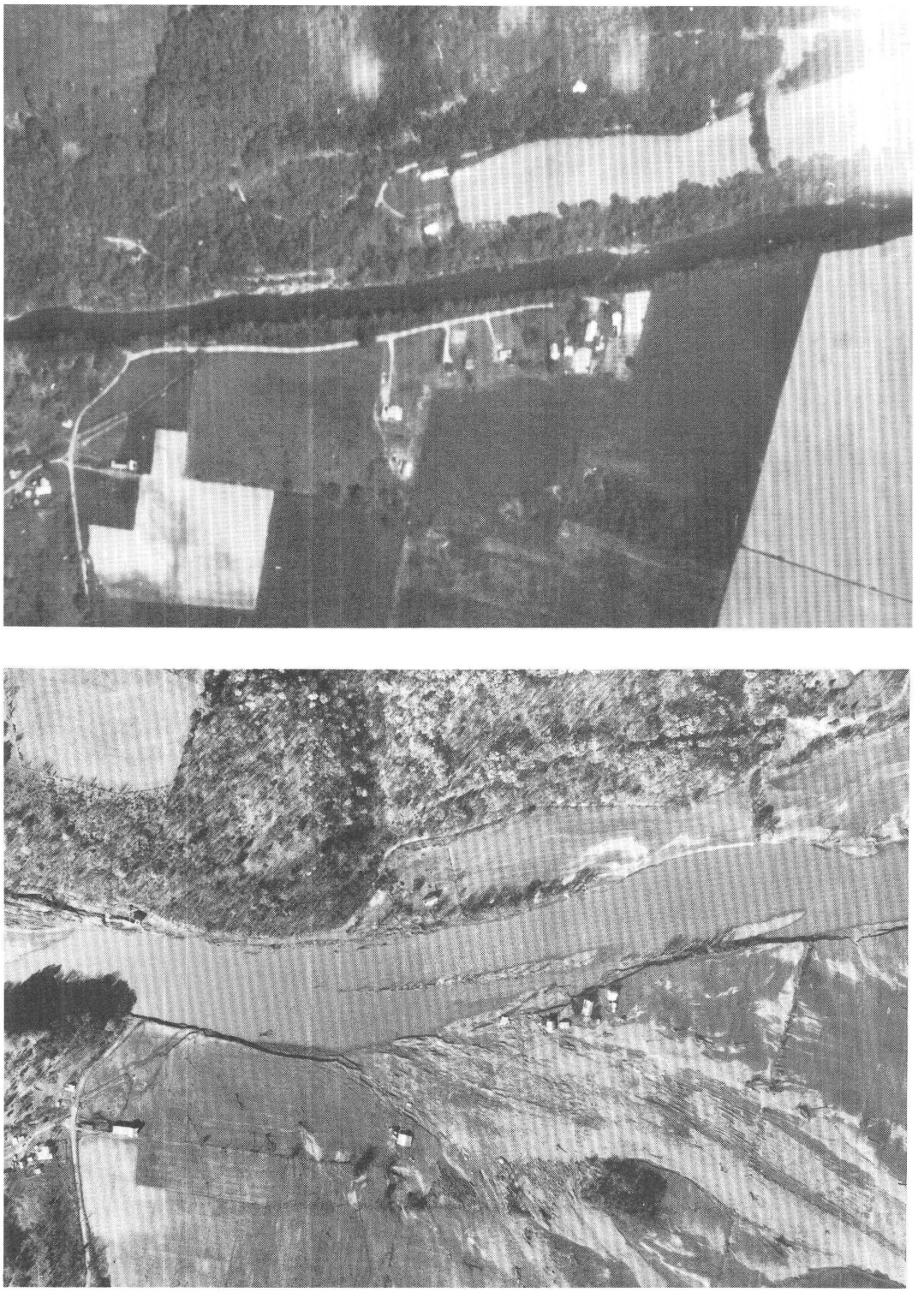

Figure 46. Before-and-after views illustrating channel widening. (*A* and *B*) Location along the South Branch where flow emerges from the unnamed gap upstream of Petersburg; flow is from left to right. The Petersburg gage and several houses on the right bank were destroyed as the channel more than doubled its width. Location is 2.1 km downstream of the confluence with the North Fork. Field of view is 1,000 m wide. (*C* and *D*) Site along the South Fork about 6 km downstream of Milam. Flow is from left to right. Note that the large scored area in upper right center was part of a topographic surface that was lower than the adjacent flood plain; along the South Fork this surface was often more heavily scored than the rest of the valley floor. Field of view is 770 m wide.

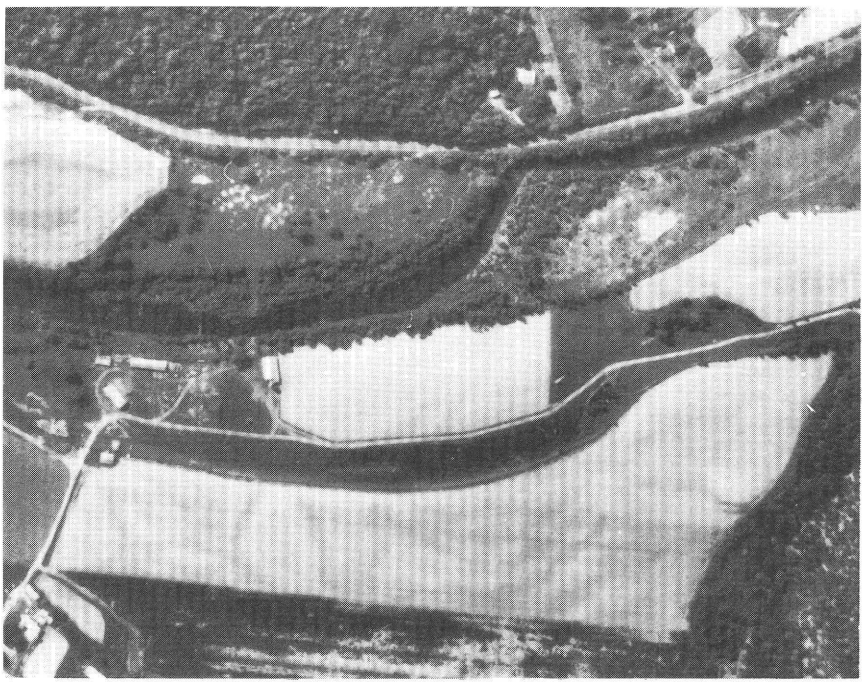

C

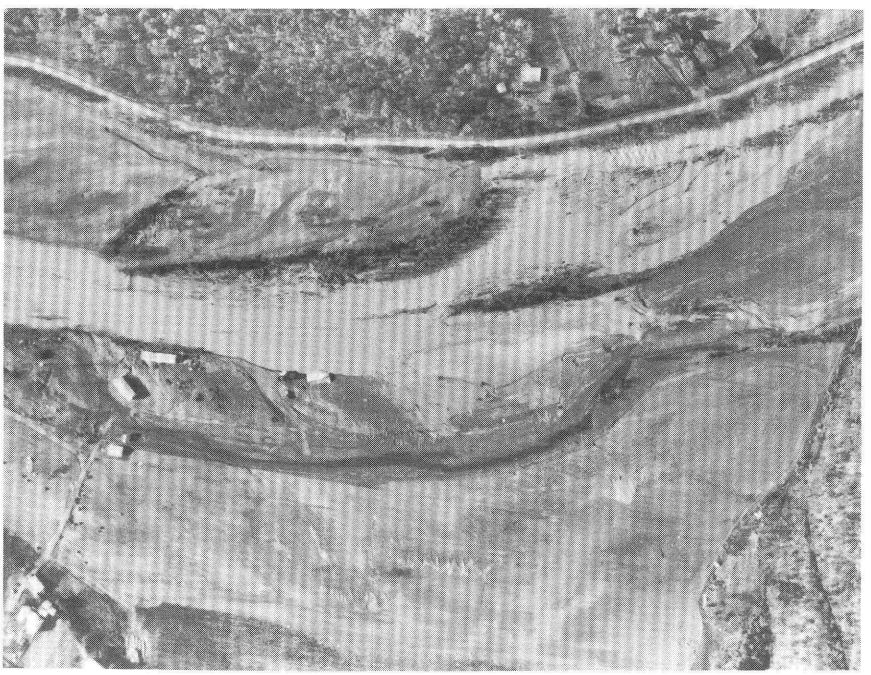

D

Figure 46. Continued.

Figure 47. Oblique aerial photograph showing channel widening along the North Fork at Macksville, 4.7 km upstream of Seneca Rocks. Note the surviving trees standing on stripped flood-plain remnants in the widened channel. A scour channel with amphitheater-shaped headcut extends headward between two buildings at right center. Photograph by E. Propst, Clarksburg Publishing Company.

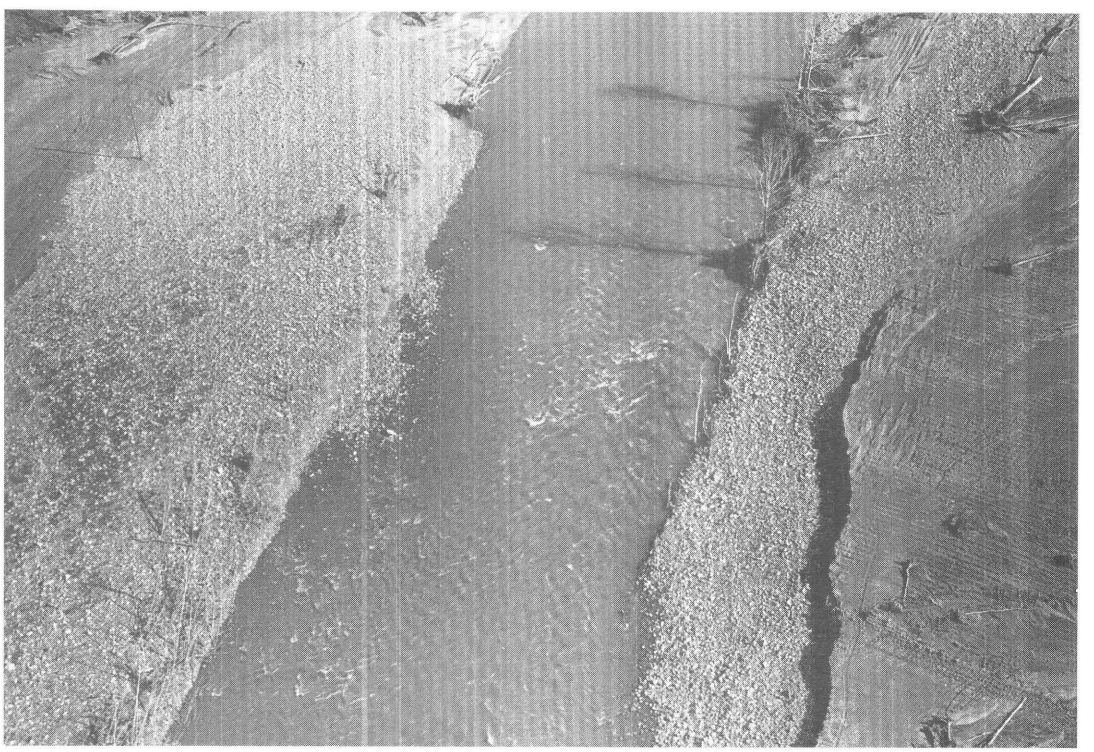

Figure 48. Channel of South Branch downstream of confluence with North Fork; exact location unknown. Steep cutbank at right grades into a stripped area at top right, where flow left the channel and crossed the flood plain. Photograph by W. E. Duliere, West Virginia Advocate.

A B

Figure 49. North Fork near Tool Run, 8.4 km upstream of Hopeville (*A*) before and (*B*) after the flood. Flow is from bottom center to top left. Channel widening has left a broad stripped remnant in the channel at the apex of the bend. The preflood view in (*A*) suggests that this remnant may have been an old bar that had become attached to the flood plain. Note also the shift in the channel toward the right bank and the large body of sediment deposited along the left bank just downstream of the bend. Field of view is 670 m wide.

trees and by the tensile and shear strength of root systems. As was mentioned previously, however, the power of the 1985 flood was sufficient at many sites to overcome resistance by grass or standing trees. Many of the stripped areas were densely vegetated before the flood, and some thick groves of trees were removed without a trace (fig. 51). Trees located along the margins of the main flow were much more likely to survive the flood than were trees in its direct path.

Chutes

Concentrated flow on the flood plain often produced a well-defined channel rather than stripping the entire surface. These channels, many of which were comparable in cross-section dimensions to the preflood river channel (fig. 59), are referred to here as chutes. They were commonly several hundred meters in length; the largest example identified on postflood aerial photographs was about 800 m long and 50 m wide. Splay deposits often extended onto the flood plain adjacent to the margin of the chute, and lineations on their surfaces indicate flow divergence outward and away from the longitudinal trend of the chute (fig. 60). Some chutes were reoccupied swales or back channels that were incised and widened during the flood; others formed at sites lacking evidence of a preexisting channel.

Incipient chute forms were seen at several locations in the South Branch drainage. In plan view they resembled scalpel points protruding into the bottomland and tapering to a point at the downstream end, with adjacent splay deposits (fig. 61). The term "incipient" is used here because these forms are interpreted as occurring in settings where the erosive power of overbank flow was insufficient to cut a longer channel across the valley floor. Fully developed chutes may have cut across a point bar or meander loop,

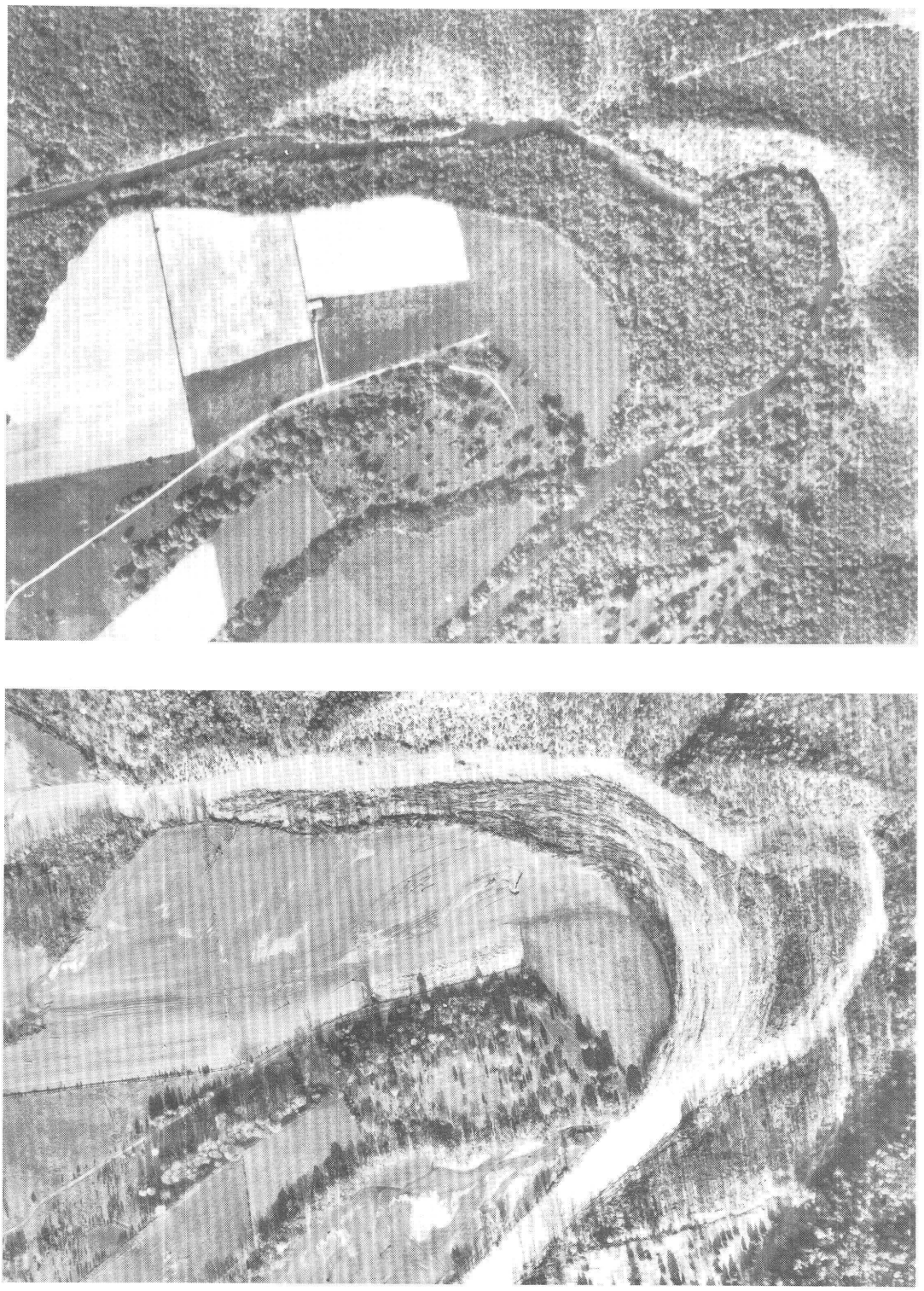

Figure 50. (*A*) Before and (*B*) after views showing scour of forested channel margins and low flood plain along South Fork, 2 km upstream of Milam. Flow is from bottom center. Several shallow channels were cut across the forested area at right center, and a large portion of the valley floor was stripped. The upper flood-plain surface was affected primarily by formation of scattered longitudinal grooves and scour marks. Field of view is 1,100 m wide.

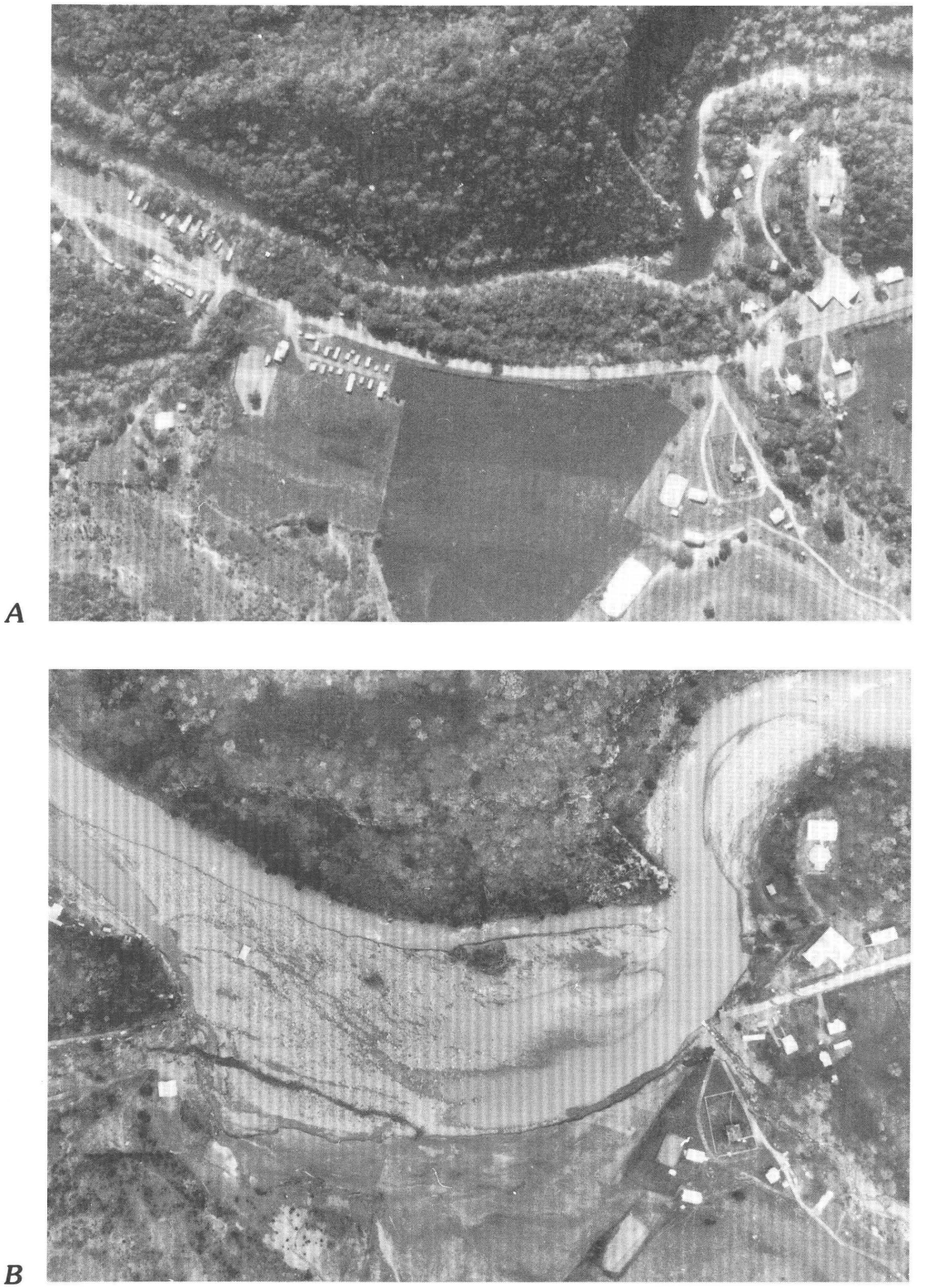

Figure 51. (*A*) Before and (*B*) after views of the North Fork at Hopeville. Flow is from upper right to upper left. The bedrock constriction at the exit of Hopeville canyon is about 60 m wide, and flow emerging from this constriction stripped away a large grove of trees and the underlying flood plain. Eleven lives were lost at the site of the house and trailer park seen at left center of (*A*). This surface is about 6–7 m above the low-water channel, and local residents noted that it had not been reached by floodwaters in the previous record flood of June 1949. Field of view is 770 m wide.

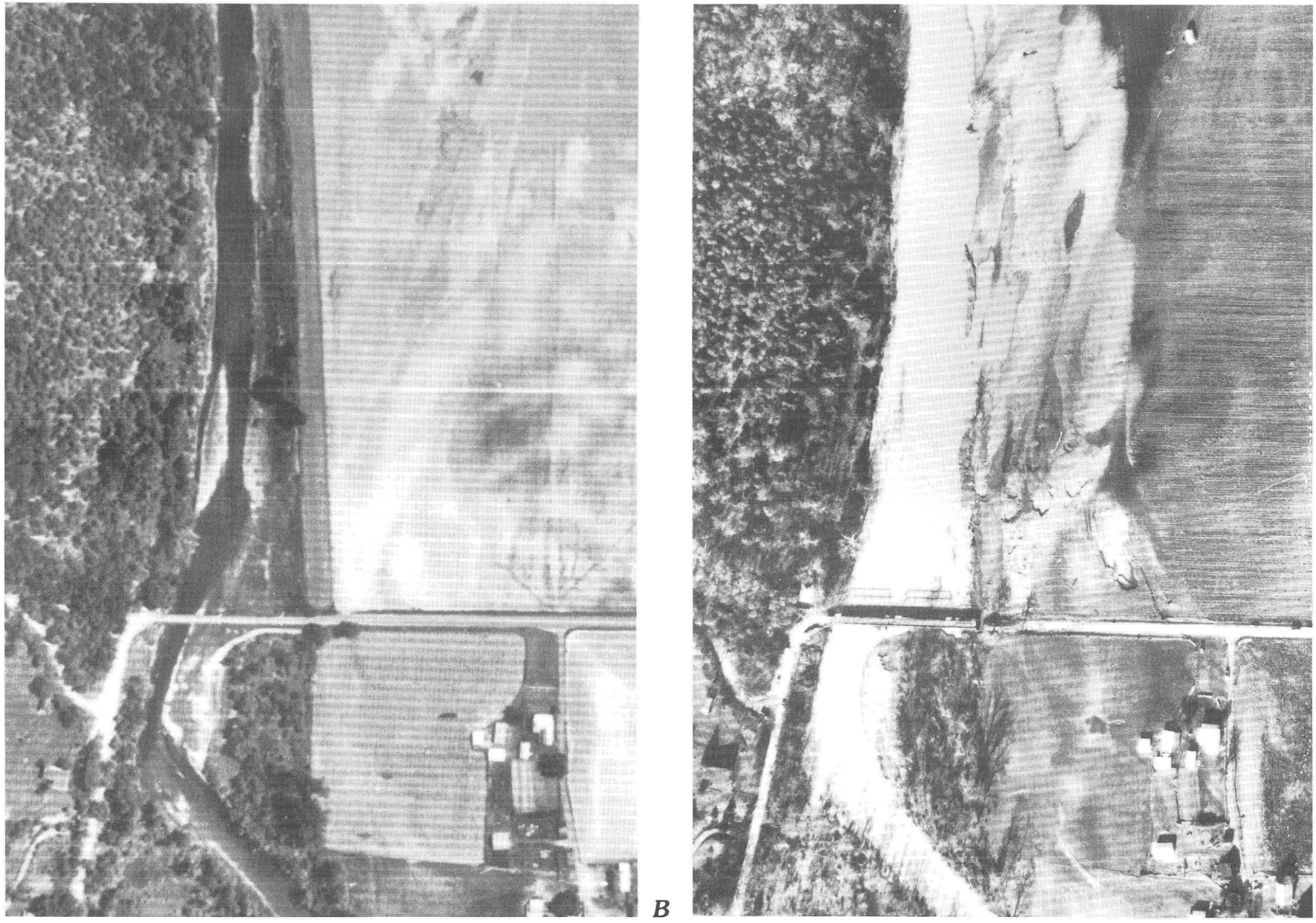

Figure 52. (*A*) Before and (*B*) after views showing channel widening downstream of a bridge crossing the South Fork at Fort Seybert, 14 km downstream of Brandywine. Flow is from bottom to top. Channel widening affected the lower topographic surface; note that the scarp separating the lower surface from the upper flood plain in (*A*) coincides with the position of the channel margin after the flood in (*B*). A large splay was deposited on the flood plain adjacent to the eroded area. Several prominent scour marks are visible in (*B*) on the upper flood plain in the center of the photograph. Their origin may be related to turbulent eddies spawned by flow over the road. Field of view is 400 m wide.

Figure 53. Channel widening and flood-plain scour, South Fork at Brandywine gaging station. Flow is toward the top. Field of view is 300 m wide.

intersecting the river channel at one or both ends (fig. 60), but there were also well-developed examples with upstream or downstream termini that did not intersect the channel (fig. 62).

Most chutes formed at locations where a major component of flow followed a straight or slightly curved trajectory parallel with the valley walls, crossing the flood plain rather than negotiating a bend in the channel. Such chutes may have been initiated by erosion of the river bank at the upstream end of a flood-plain segment, followed by scour and incision of the flood plain progressing in the downstream direction. A chute believed to have formed in this way is illustrated in figures 63 and 64: here the upstream end of the chute marks the point where the main body of flow left the channel, and the attitude of the fallen trees (fig. 64) indicates progressive downstream scour rather than headcut retreat. In other cases there was initial abrasion of the flood-plain surface to form a shallow trough, followed by incision of a deeper channel within the area of the trough and upstream growth of this channel by headcut retreat. In the right center part of figures 99*B* and *C*, the area where flood flow crossed onto the flood plain is occupied by a shallow trough with scattered scour marks and longitudinal grooves; this is separated from the upstream end of the main chute by a vertical headcut that branches into discrete lobes. Initial formation of a shallow scoured zone followed by incision of an inner channel was observed in flume studies by Shepherd and Schumm (1974), and a similar sequence of events was proposed by Kehew and Lord (1986) for the evolution of channels formed by glacial meltwater floods.

At several sites where one or more chutes formed below the confluence of a tributary with one of the main rivers, flow from both sources contributed to the pattern of erosion (figs. 62, 65). In such cases the main body of the chute branches upstream into discrete headcuts, at least one of which captured flow from and retreated headward along swales crossing the surface of a fan built by the tributary. Lobate headcuts were not restricted to the upstream ends of chutes; some also had multiple lobes radiating from the channel walls (figs. 62, 99*B*, *C*). The lobate scours probably were initiated where shallow swales carrying concentrated flow across the flood plain were truncated by incision of deeper chute channels. Flow cascading over the wall of a chute would have caused headcut retreat along the trend of the swale until flood stage declined below some threshold level capable of sustaining the erosion process.

Chutes inspected in the field generally had steep banks. Those that did not intersect the river channel at the downstream end gradually shallowed downstream until they merged with the surrounding undisturbed valley floor; sometimes the transition was obscured by splays deposited at the downstream end of the chute. Chute floors usually were flat (fig. 66), but some had uneven or stepped bed topography with inner and outer channels (fig. 59).

Most chutes were floored by imbricated cobbles and boulders (fig. 66). Although many of the cobbles and boulders appeared to have moved during the flood, the fact that cobble splays observed following the flood generally were contiguous to areas of channel or flood-plain scour (from which they presumably were excavated) suggests that most probably did not move further than a few hundred meters. Much of the floor material may have been composed of slightly reworked lag deposits: older sediments exposed in some chute walls were composed of rounded cobbles, gravel, and small boulders in a sandy matrix (fig. 67) and were similar in texture to the fresh deposits on the adjacent valley floor. Along one 126-m section of chute (figs. 66 and 67), 63 percent of the bank length contained imbricated gravel, cobbles, and boulders; gravel lenses at this site were up to 14 m long and 1 m thick (Scatena, 1986). That such coarse material should be found at such shallow depth beneath the flood-plain surface suggests that large floods may have played an important role in shaping

A

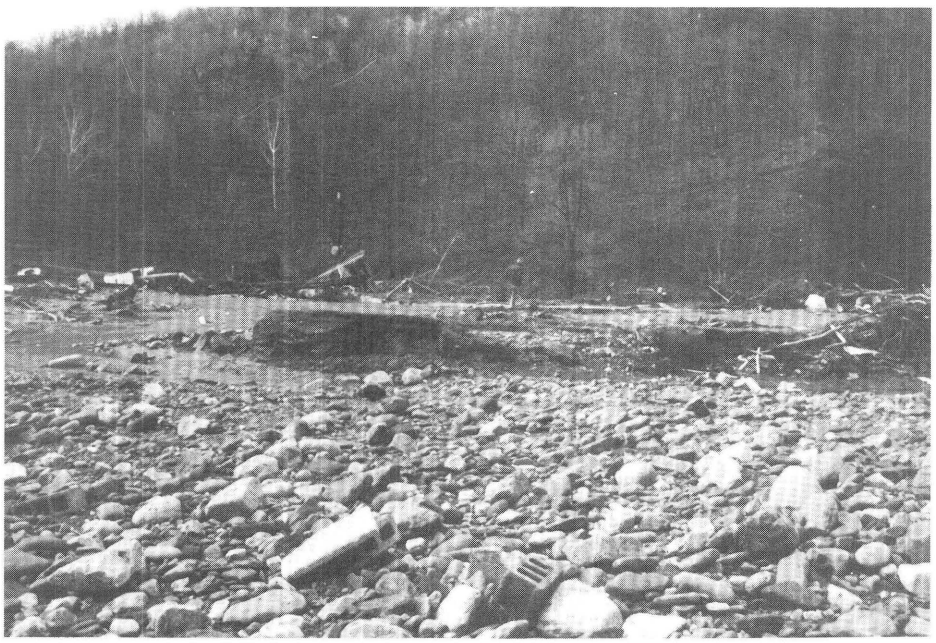

B

Figure 54. Three examples of flood-plain stripping: (*A*) North Fork in Hopeville canyon, 0.9 km upstream of Hopeville (photograph by F.N. Scatena). The view is looking upstream. The channel is about 40 m wide. The point bar in the foreground was a pasture before the flood. As much as a meter of alluvium was stripped away; erosion scarps are visible on the remnants of the original surface. Figures 55 and 56 show the area upstream and around the bend from this location. (*B*) North Fork near North Fork Gap. The remnant of flood-plain alluvium is virtually all that remains of the original surface at this location. (*C*) South Branch, 0.8 km downstream of the Trough. Flow is from right to left. Photograph by W.E. Duliere, West Virginia Advocate.

C

Figure 54. Continued.

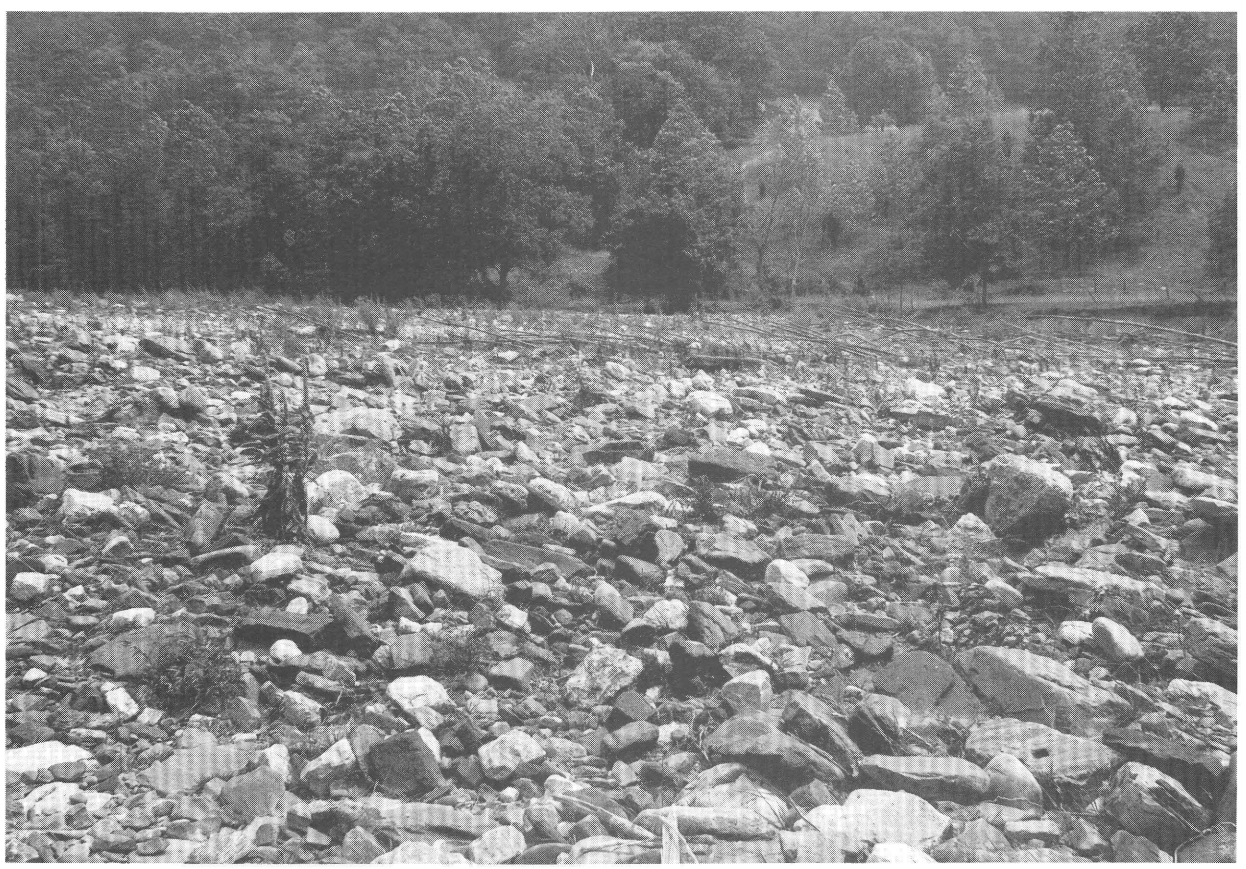

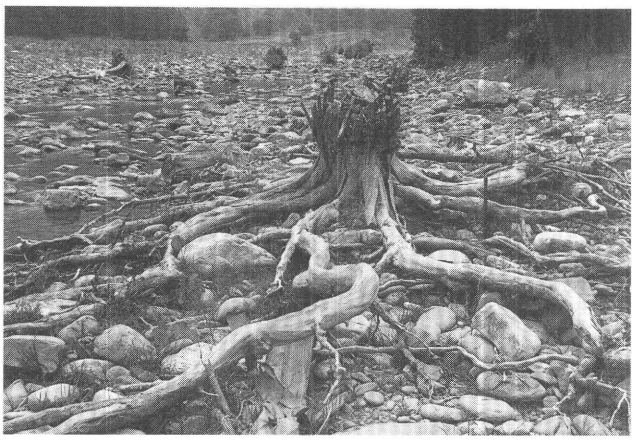

Figure 56. North Fork in Hopeville canyon at same location as figure 55. View is facing upstream. Stump is standing next to the low-water channel.

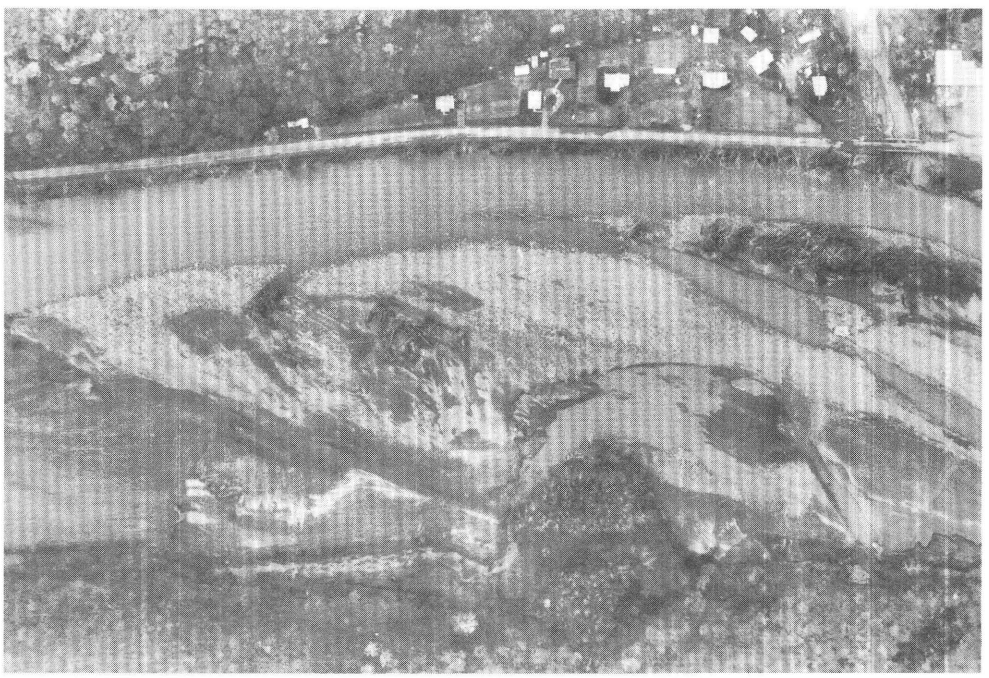

Figure 57. Gradation from stripped surface to depositional lobe derived from stripped material; North Fork at Jordan Run, 2.5 km downstream of Hopeville. Flow is from left to right. The feature protruding from the valley wall at bottom center is a probable debris-flow lobe emplaced in June 1949. Note scour caused by flow diverted around this lobe. Long dimension of field of view is 670 m.

◀ Figure 55. Imbricated pavement of cobbles and boulders on stripped flood plain. North Fork in Hopeville canyon, 1.7 km upstream of Hopeville. Flood flow was from right to left. Note the fallen trees in the middle background and the cutbank marking the edge of the stripped area in the background at the right. This was a pasture before the flood.

Figure 58. Mounds of rolled-up turf located around margins of an elongate scour mark. This photograph was taken about 18 months after the flood, and the margins of the scoured area were covered by grass. South Branch flood plain between Redman Run and Austin Run, 5.1 km upstream of confluence with North Fork.

the present form of the flood plain. However, cobbles and boulders are not equally important components of the subsurface at all locations. In some chute walls and river bank exposures a vertical section of fine-grained alluvium with interbedded gravel lenses was observed (figs. 68, 69). Similar alluvial sequences were observed by Costa (1974) and by Ritter (1975) and were interpreted as evidence for large rare floods in an environment otherwise characterized by long-term accumulation of sandy or silty lateral and vertical accretion deposits.

Chutes on forested bottomlands were generally narrower and not so well defined as those formed on land cleared for agriculture (fig. 70). Their characteristics may have been controlled in part by the flow resistance and resistance to scour offered by tree trunks and tree roots. Furthermore, many of the forested bottomlands along the three forks of the South Branch are at lower elevations than adjacent areas cleared for agriculture, and they may in fact have been allowed to remain in forest precisely because they lack more than a veneer of fine alluvial sediment to cover a pavement of cobbles and boulders. Flows powerful enough to overcome the resistance offered by trees in this setting may strip the surface rather than form well-defined channels (fig. 50).

Anastomosing Channels and Jet-Shaped Erosion Forms

Dissection of bottomlands by anastomosing flood channels was observed at several locations in the South Branch basin in November 1985. In some places, two or more distinct chutes parallel each other across the valley floor (fig. 9). Elsewhere, an anastomosing pattern occurs within a relatively narrow belt along the preflood river channel; such patterns are associated with incomplete channel widening that creates remnant islands in the expanded channel (fig. 71). The most dramatic examples involve dissection and reworking of much of the width of the valley floor (figs. 72*A–D*). The catastrophic erosion at such sites, and the limited number and spatial extent of the areas affected, indicate that this pattern signals the crossing of a significant geomorphic threshold in the balance between flood hydraulics and resistance to erosion. We do not yet have sufficient information to quantify this threshold reliably, but previous computations of unit stream power suggest energy expenditures in excess of several hundred W/m^2 may lead to catastrophic erosion of the valley floor.

Patterns of erosional anastomosis observed here bear some morphologic resemblance to channel systems eroded by glacial meltwater floods (Bretz, 1923, 1928, 1959; Baker, 1978; Kehew and Lord, 1986), but spatial scale of the erosion forms and magnitude of the formative event are clearly much smaller. Transient braided patterns described by Carson (1984) also were formed by erosion during major

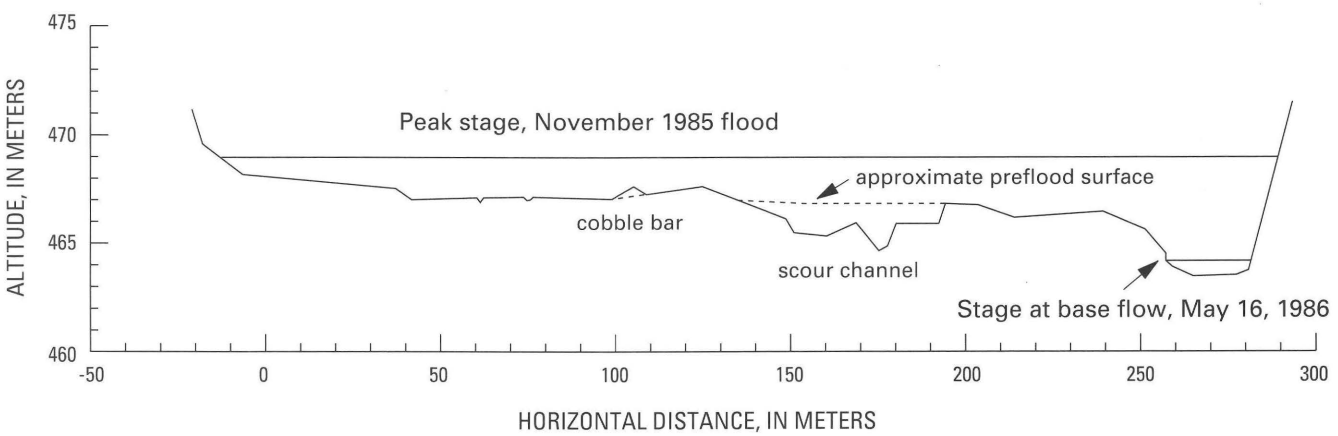

Figure 59. Postflood cross section of North Fork valley at Seneca Rocks Visitor Center. Chute formed in the flood is comparable in width to the preflood river channel. Figure 62 is an aerial photograph of this chute (after McKoy, 1987).

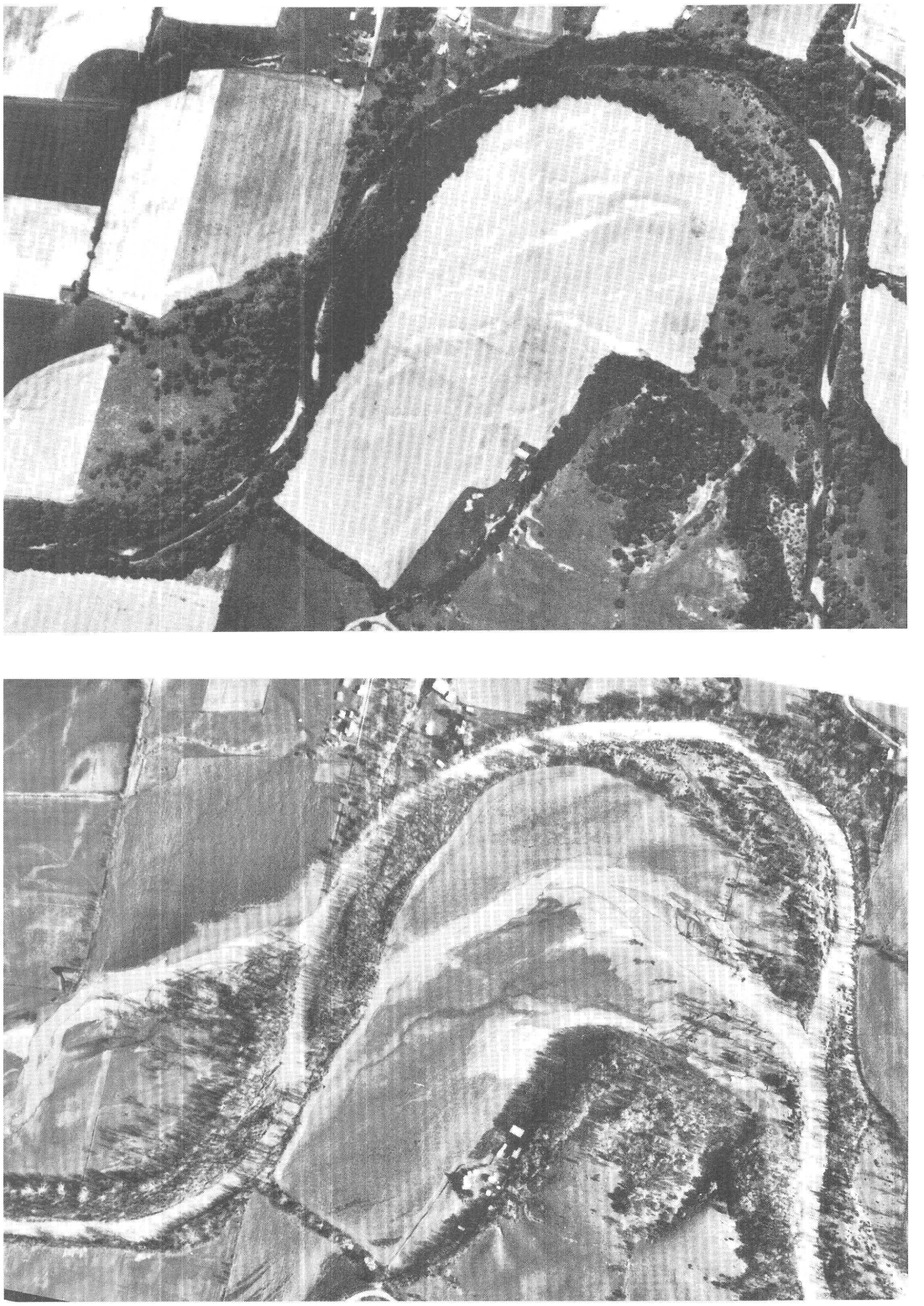

Figure 60. South Fork near Fort Seybert (*A*) before and (*B*) after the flood. Location is 12 km downstream of Brandywine. Prominent chutes formed during the flood were incised along the trends of swales visible in preflood photograph. Flow is from right to left. Field of view is 1,200 m wide.

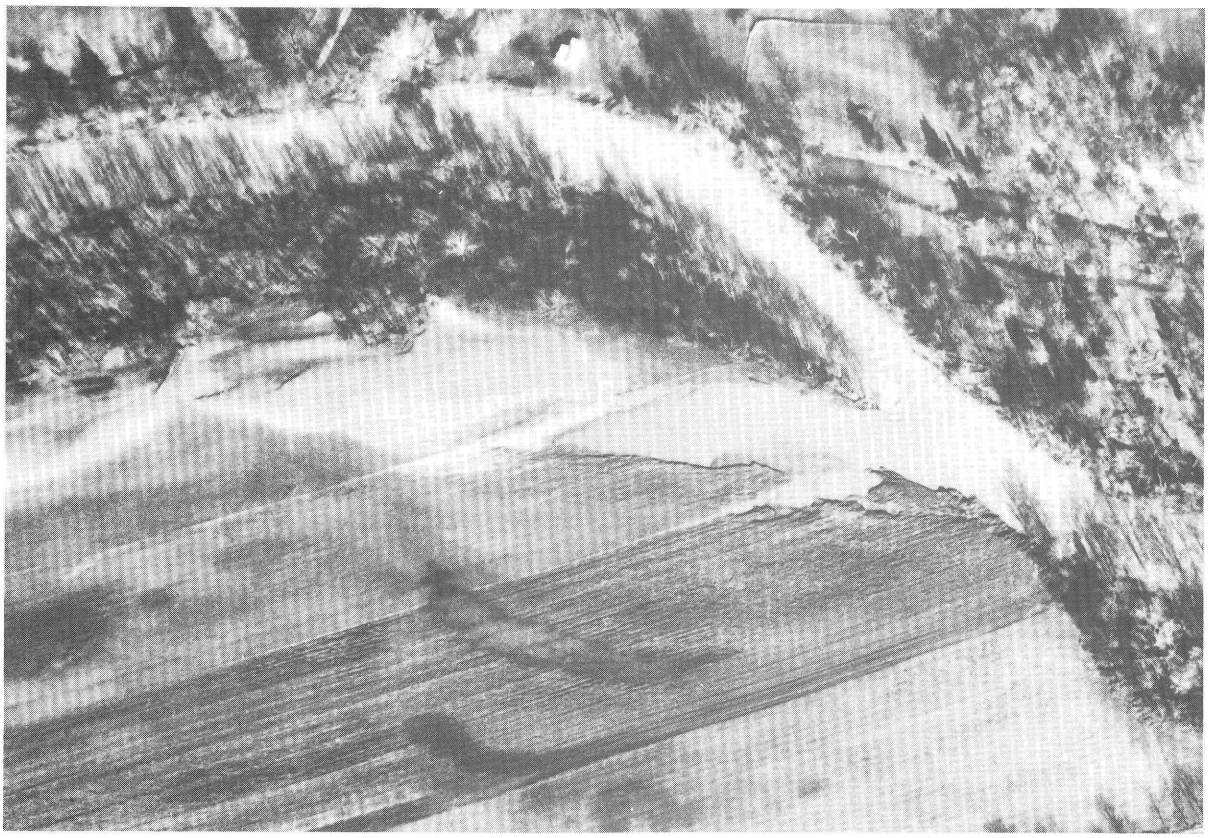

Figure 61. Incipient chute eroded in South Fork flood plain near Oak Flat, 9.3 km downstream of Brandywine. Flow is from right to left. Width of field of view is 460 m.

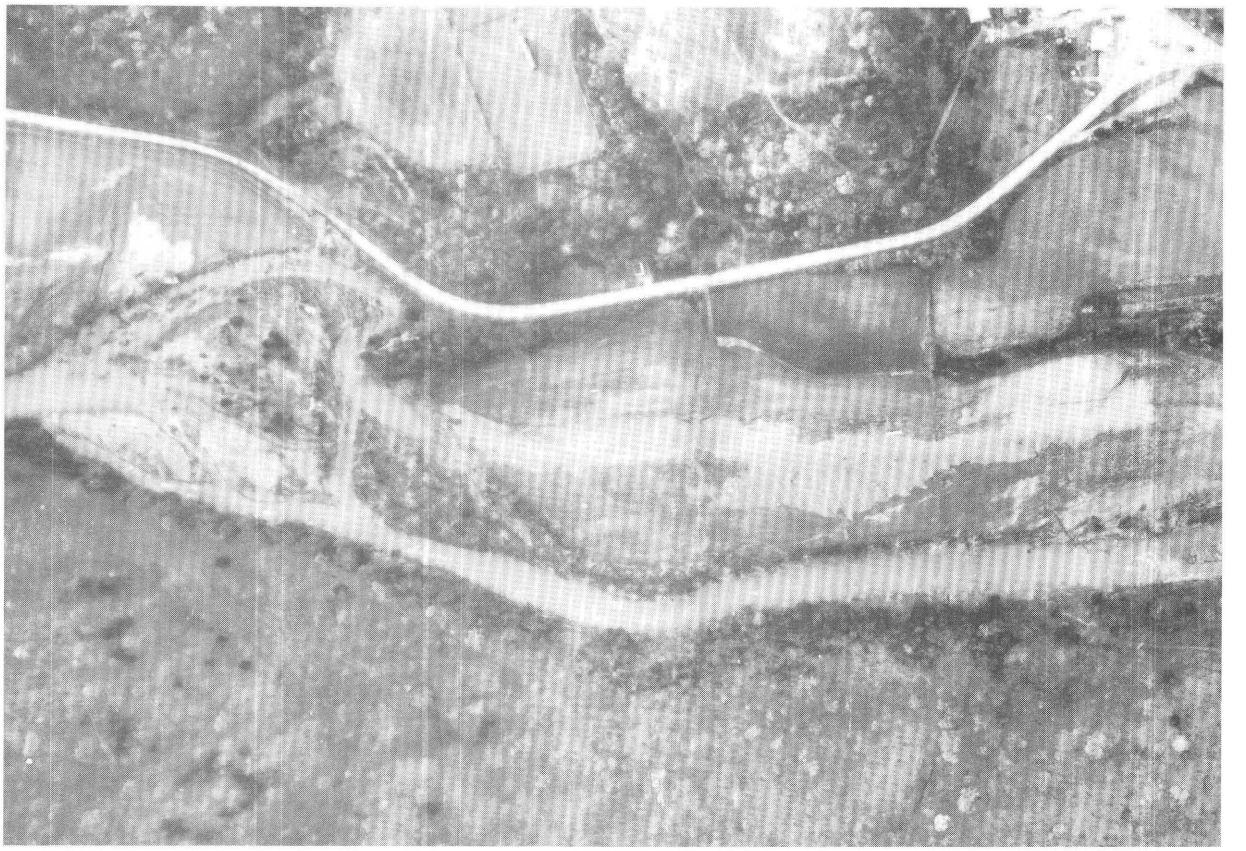

Figure 63. Chute on flood plain of North Fork about 0.6 km upstream of Seneca Rocks. Flow forced around a bedrock outcrop scoured the upstream end of the chute; incision proceeded from upstream to downstream, where a coarse splay deposit flares out over the adjacent valley floor. Flow is from left to right. Field of view is 930 m wide.

◀ **Figure 62.** Chute on flood plain of North Fork at Seneca Rocks Visitor Center, 0.6 km downstream of Seneca Rocks. Flow is from left to right. Seneca Creek joins the North Fork just to the left of the area shown in this picture; the headcut oriented toward the upper left corner of the photograph evidently was exploited by flow coming from Seneca Creek. The cross section shown in figure 59 extends across the flood plain at this site from a point about halfway between the two parking loops at top left center to a point on the right bank of the North Fork just upstream of the bend in the channel. Field of view is 650 m wide.

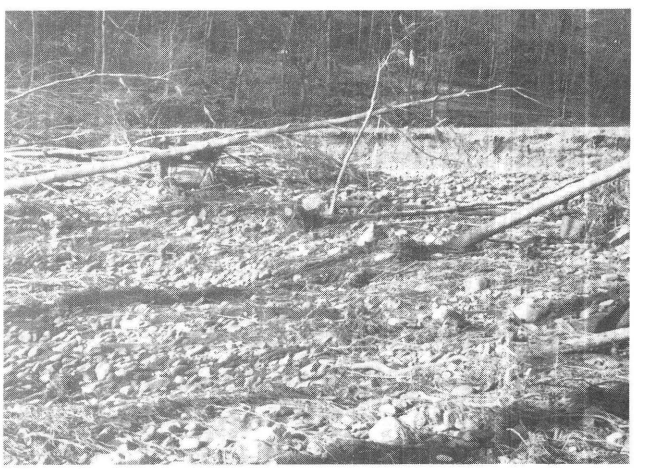

Figure 64. Ground view of upstream end of chute illustrated in figure 63. Tilted and uprooted trees indicate current direction and indicate that erosion of the channel proceeded from upstream to downstream rather than by upstream migration of headcuts.

Figure 65. Chute with branching headcuts, South Branch at Smith Creek, about 3.5 km upstream of Franklin. Flow along the South Branch is from right to left. Prominent headcuts in the foreground were created by flow emerging from Smith Creek. Photograph by E. Propst, Clarksburg Publishing Company.

Figure 66. Chute in figures 63 and 64, shown looking downstream. This chute was about 40 m wide, 1.5 m deep, and 500 m long.

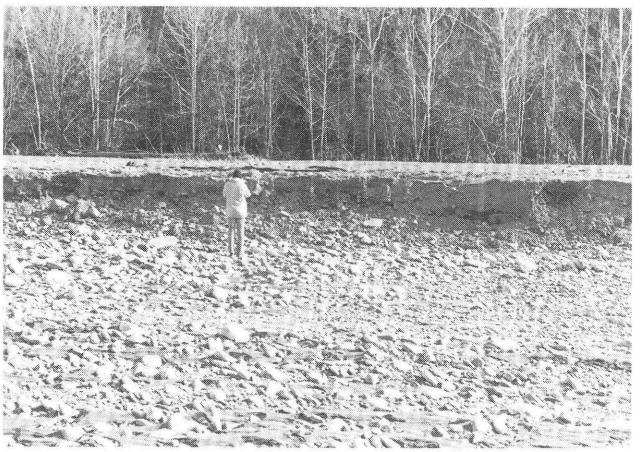

A

B

Figure 67. Two views of the right bank of the chute seen in figure 66. (*A*) A flat bed of imbricated cobbles and a bank about 1.5 m high; the trees in the background are standing on a lower surface, and the North Fork is on the other side of the trees. (*B*) A closer view of the bank section, indicating that the flood plain is underlain by a sequence of cobbles and gravel that generally resembles the material exposed on the floor of the chute.

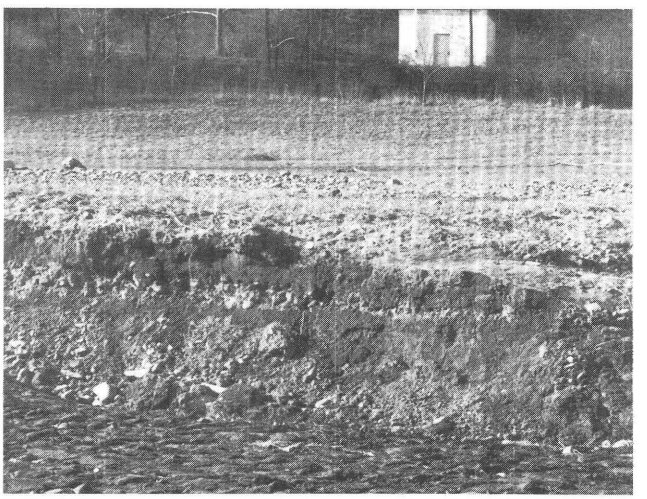

Figure 68. The left bank of the chute illustrated in figures 66 and 67 exposes a sequence of fine-grained alluvium with interbedded gravel lenses resembling those described by Ritter (1975). The gravel lens exposed in cross section presumably was deposited by a past flood in much the same way as the gravel lens on the surface was deposited by the November 1985 flood.

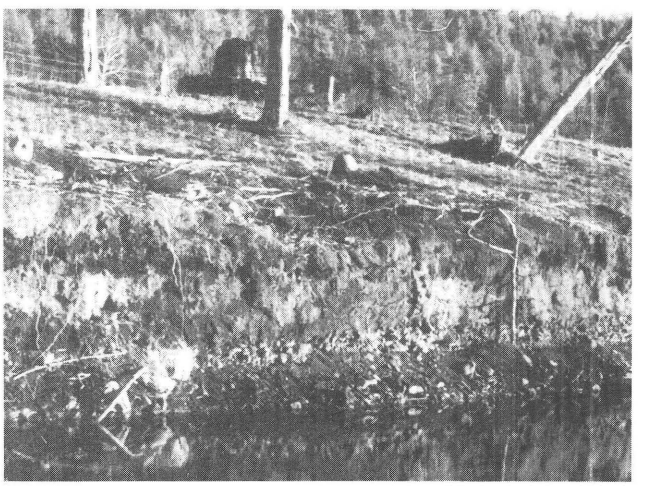

Figure 69. The left bank of the South Fork at Brandywine exposes a gravel lens (near the base) that resembles the lenses shown in figure 68. Such deposits may be common in the flood plains of the three forks of the South Branch. The bank is about 2–2.5 m high.

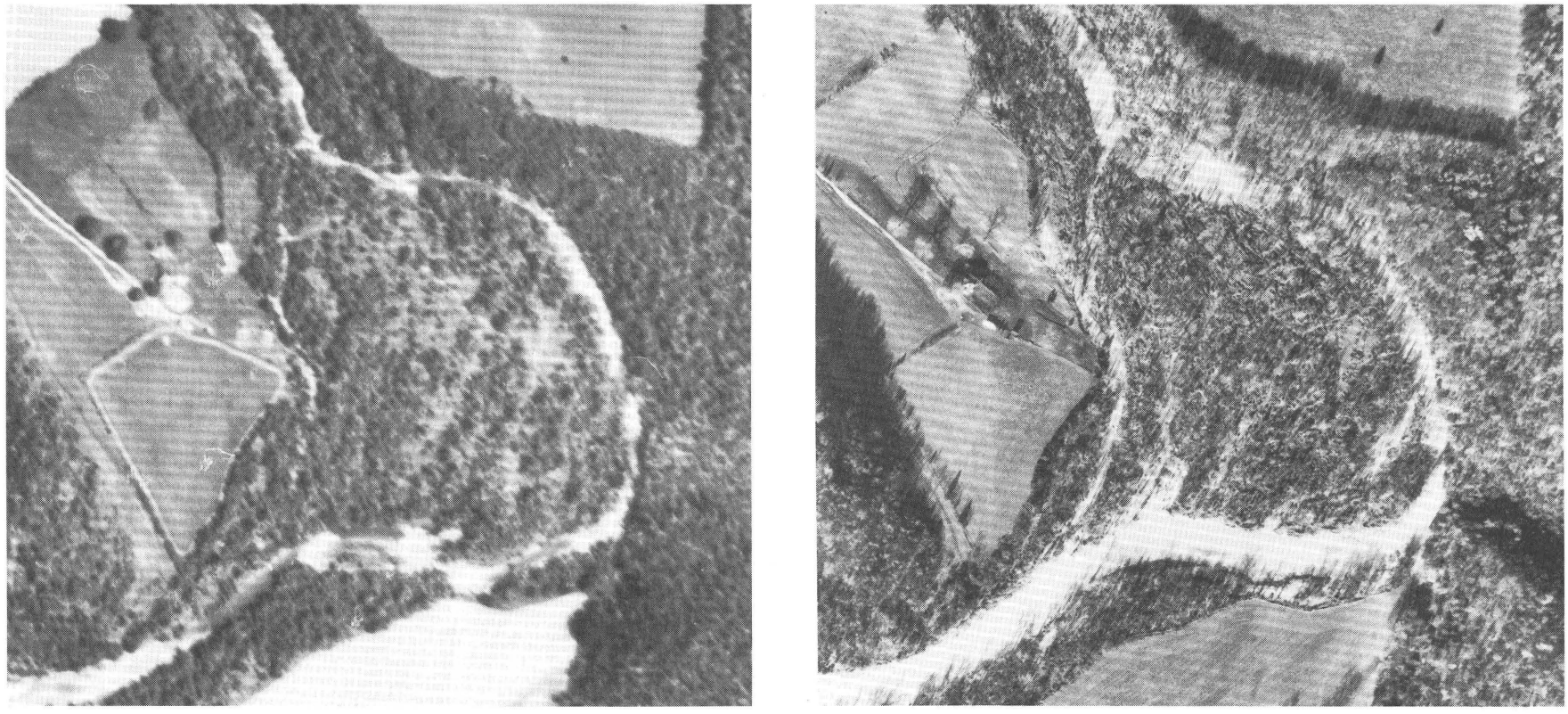

A *B*

Figure 70. South Fork, 1.9 km downstream of Brandywine gaging station, seen (*A*) before and (*B*) after the flood. Flow is from bottom left to top center. Chutes running across this forested bottomland (actually the lower of the two surfaces described previously) are generally narrower than, and not as well defined as, chutes running across cleared fields. The examples shown here were enlarged by the flood, but their existence predates the flood. Field of view is 630 m wide.

A

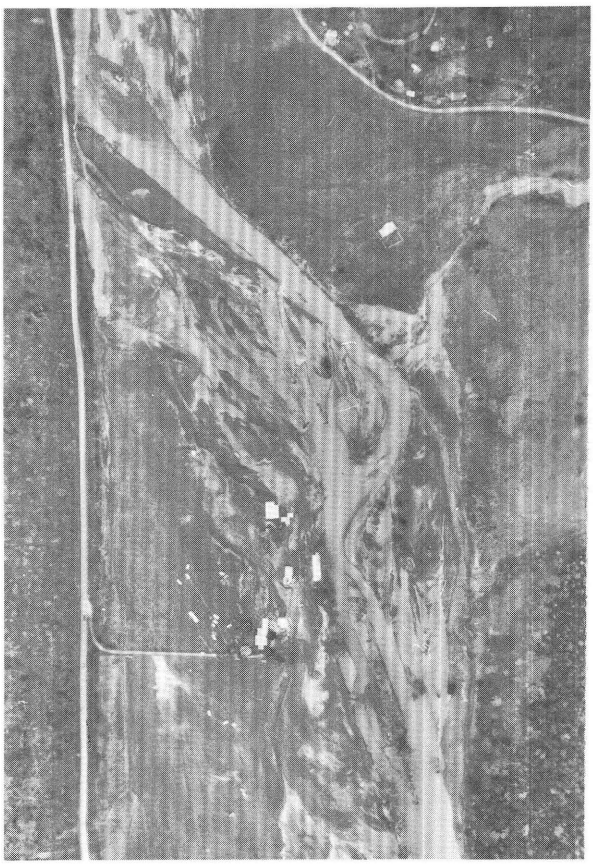

B

Figure 71. South Branch flood plain, about 3 km upstream of Franklin. Flow is from bottom to top. Channel widening and dissection of the flood plain left several large remnant islands separated by a set of anastomosing channels. The new channels shown in (*B*) appear to occupy the trends of swales and abandoned channels visible before the flood (*A*). Field of view is 690 m wide.

floods. Although these gradually heal with deposition of sediment and growth of vegetation, any remaining topographic depression may be a preferred path for overbank flow in subsequent floods and could be excavated again if an event of comparable magnitude were to occur.

At sites of erosional anastomosis in the study area, many residual islands are found in groups separated by closely spaced channels, are diamond-or rhomboid-shaped, and resemble braid bars in gravel-bed streams that have been truncated in the falling stages of a flood (figs. 72*B*, *D*). Island forms described in the literature (Chorley, 1959; Baker, 1978; Komar, 1983; Kehew and Lord, 1986; Osterkamp and Costa, 1987) sometimes bear strong resemblance to the lemniscate loop, a minimum-drag shape describing airfoils and other streamlined forms. Most of the residual islands at sites of erosional anastomosis in the South Branch basin were more irregular than those showing lemniscate forms. Kehew and Lord (1986, p. 167) suggest that groups of erosion residuals that are dominantly elongated, quadrilateral, or irregular in shape, rather than approaching the equilibrium streamline form, result from short-duration flow and represent "an initial or early stage of erosional development which would occur where a large discharge of water has suddenly flowed over an area of underfit or nonintegrated drainage." Evidently, the short duration and rapid stage changes of the November 1985 flood did not allow the resulting erosion and deposition forms to reach an equilibrium shape.

Another form of catastrophic erosion observed at several locations in the study area resembled a plane jet formed by an expanding stream of fluid emerging from an orifice or constriction (figs. 73*A–H*). This type of erosion typically occurred in expanding reaches downstream of valley constrictions. At sites where the river channel below the constriction flowed along the left or right valley wall rather than down the center of the valley floor, the high-velocity core of flow emerging from the constriction left the channel and followed a trajectory directed downvalley. The resulting erosion channel typically was several times as wide as the preflood river channel and expanded slightly with increasing distance downstream, with coarse splays and debris flaring outward in all directions. As the flow

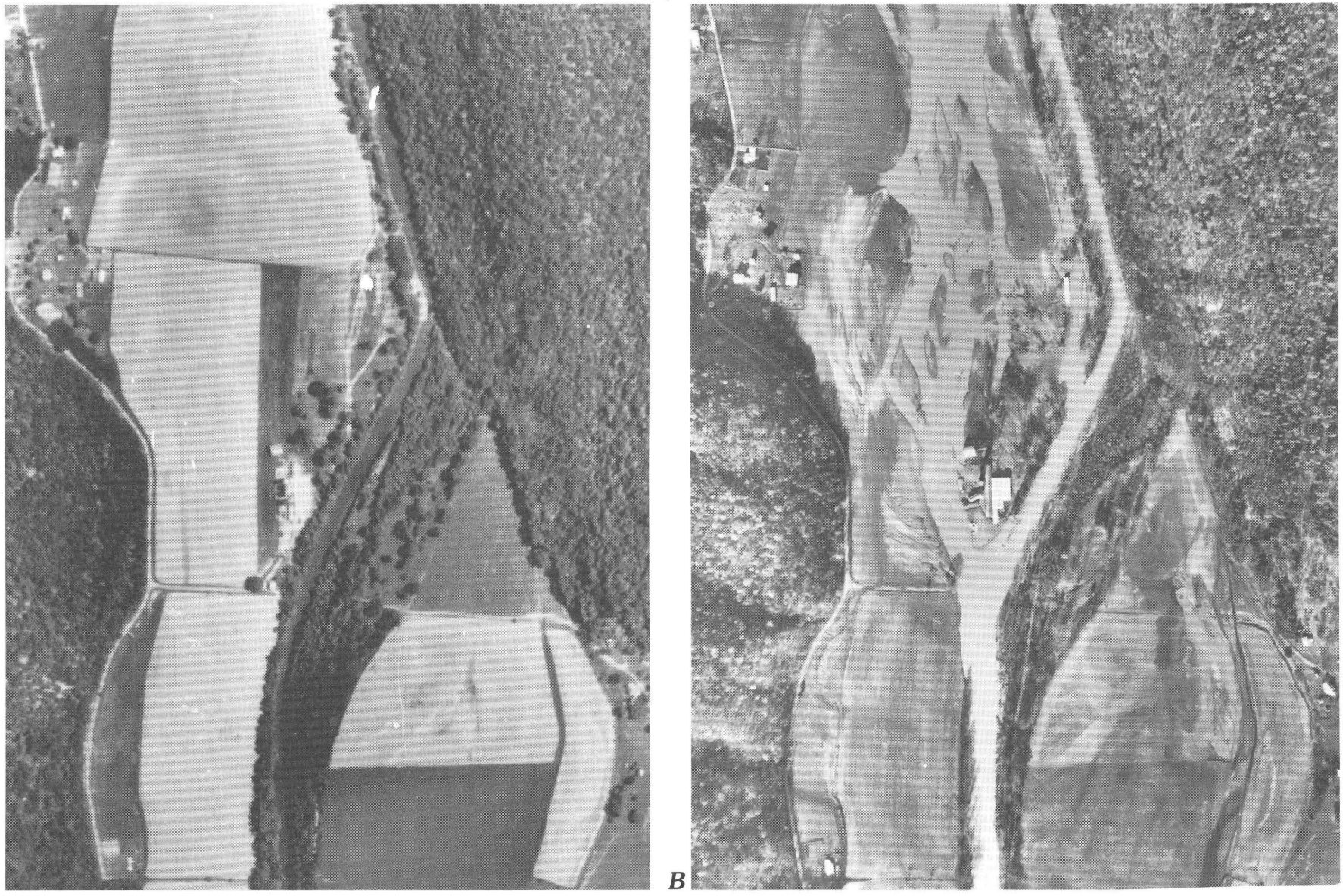

Figure 72. Examples of valley floors extensively dissected by anastomosing erosion channels. (*A*) Before and (*B*) after views of the Adamson dairy farm on the South Fork flood plain at Fame, 6 km downstream of Fort Seybert. Flow is from bottom to top. The South Fork emerges from a bedrock constriction about 3 km upstream of the dairy, but the channel follows a straight path from the constriction until it reaches the location shown here. Field of view is 870 m wide. (*C*) Before and (D) after views of the North Fork South Branch Potomac River valley near Zeke Run, 12 km downstream of Seneca Rocks and 10 km upstream of Hopeville. Flow is from bottom to top. The undisturbed area to the right of the channel is a terrace several meters higher than the main valley floor to the left of the channel, which was dissected during the flood. Field of view is 670 m wide.

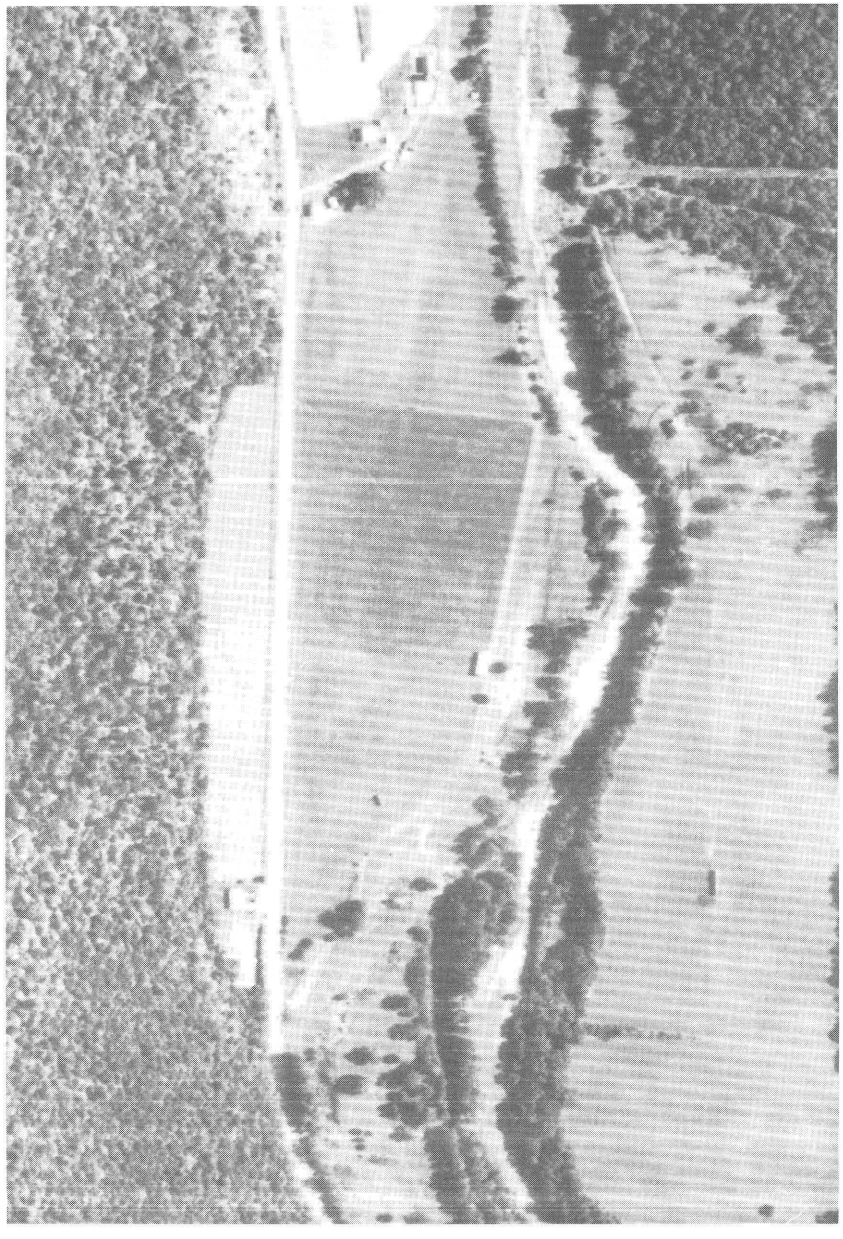

C

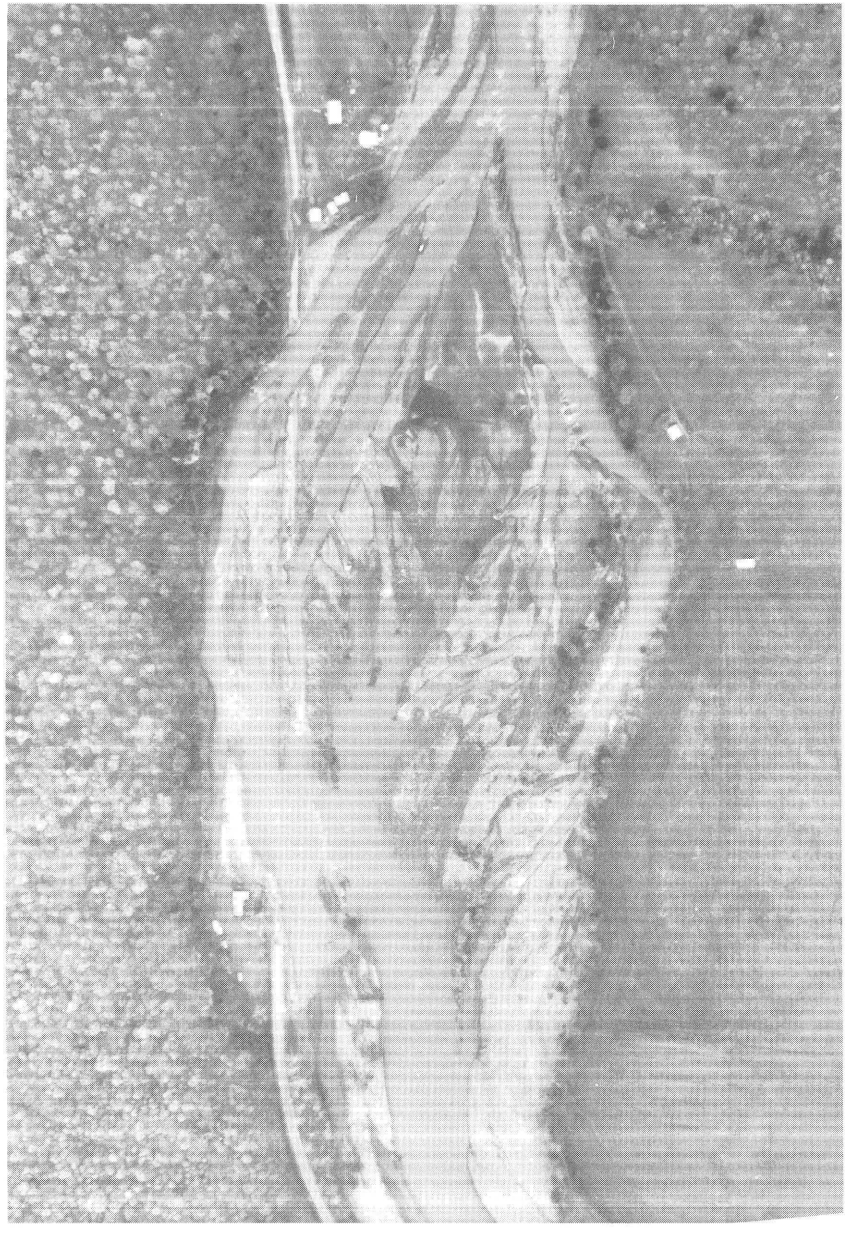

D

Figure 72. Continued.

A

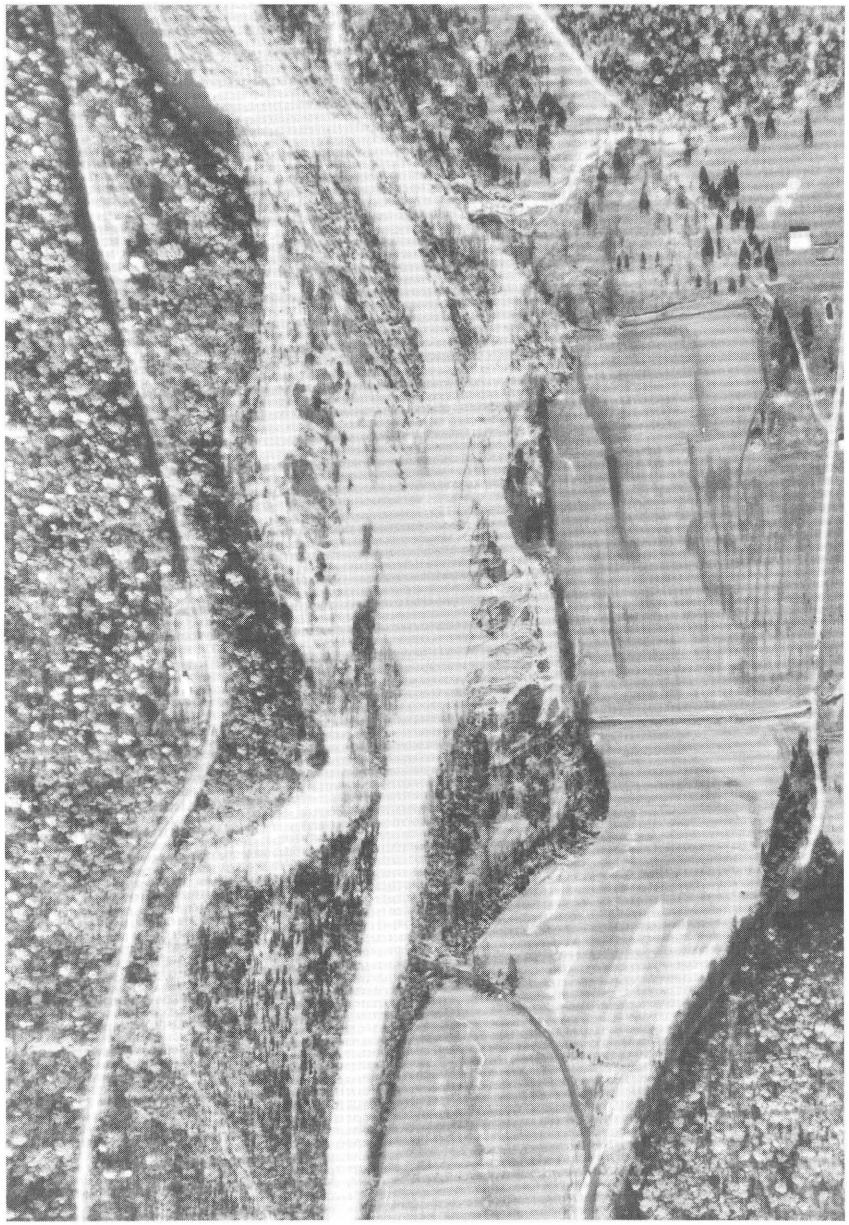

B

Figure 73. Examples of jet-shaped erosion forms. (*A*) Before and (*B*) after views of the South Fork South Branch Potomac River valley at a site about 3 km downstream of Brake. Flow is from bottom to top. The preflood photograph shows a complex valley form with multiple abandoned or inactive overflow channels and several forested bars or channel islands. Field of view is 690 m wide. (*C*) Before and (*D*) after views of the North Fork South Branch Potomac River valley at a site 3 km downstream of Seneca Rocks. Flow is from bottom to top. Field of view is 640 m wide. (*E*) Before and (*F*) after views of the North Fork South Branch Potomac River valley about 8 km downstream of Seneca Rocks and 14 km upstream of Hopeville. Flow is from bottom to top. Field of view is 670 m wide. (*G*) Before and (*H*) after views of the South Branch Potomac River valley about 5 km downstream of Franklin. Flow is from top to bottom. Field of view is 700 m wide.

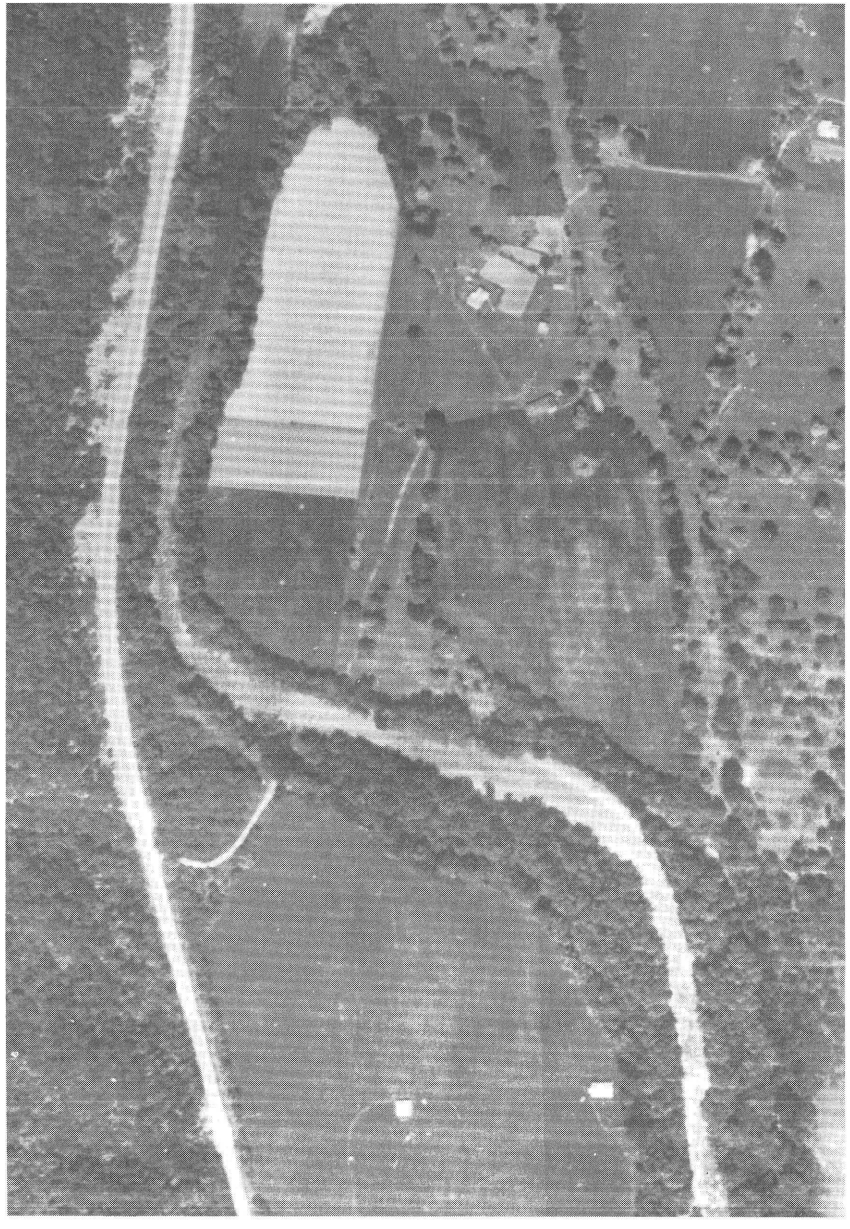

C

D

Figure 73. Continued.

F

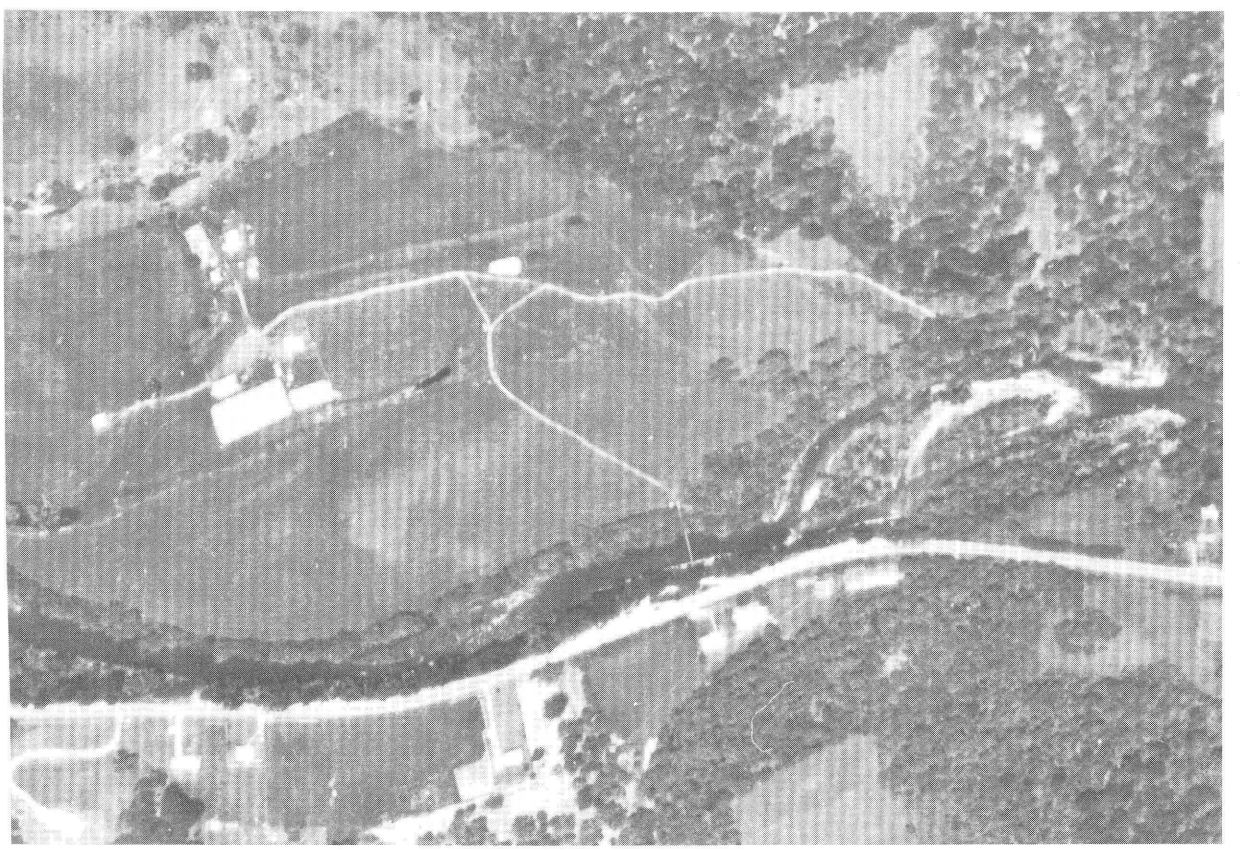

E

Figure 73. Continued.

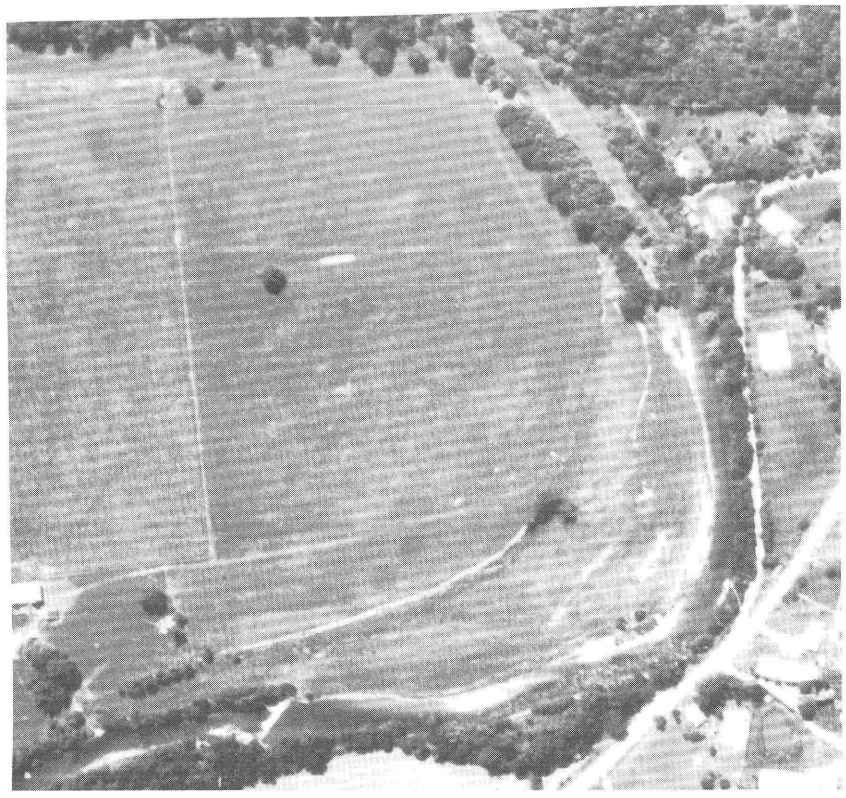

G

H

Figure 73. Continued.

continued to spread out, velocity and power per unit width of the flow decreased. Deposition occurred where the spreading flow was no longer competent to erode the underlying surface or to transport the material entrained. At its downstream end the erosion channel ended abruptly by splitting into multiple secondary channels diverging away from the center, dissecting splay deposits, and leaving residual bars and islands surrounding the eroded area. Downstream of the jet-shaped area of erosion, flow generally converged and drained back into the preflood channel. The flow patterns and morphology are similar to those illustrated for erosional anastomosis (fig. 72), the primary difference being the dominant central erosion channel. Maximum length of the area of valley affected either by erosional anastomosis or jet-shaped erosion forms was about 1,000 m; maximum width of the central erosion channel was about 220 m, and maximum width of the area affected (including secondary erosion channels and splays) was about 350 m.

Deposition Features

A wide variety of deposition forms were found along the valleys of the three forks of the South Branch Potomac River following the flood. Although local patterns of deposition were extremely heterogeneous, several important trends were noted. The following summary is based on our field reconnaissance and on observations by Scatena (1986) and by M.L. McKoy and R. Fonner (West Virginia Geological Survey, written communication, 1986).

Valley-floor deposits upstream of Petersburg and Moorefield were dominated by coarse sediment. The largest boulders believed to have moved had long axes of more than 2.4 m, and boulders with long axes of 1 m were frequently observed. Many deposits were composed largely of cobbles and small boulders, with pebbles and granules between the larger grains. Sand deposits were found most often along the margins of flow, or where velocity declined as a result of backwater upstream of a barrier or valley constriction, diverging flow on a broad valley floor, or flow separation in the lee of an obstacle. Although silt- and clay-sized sediment was contributed by mass movement and fluvial processes in tributary valleys, and by erosion of alluvium in the larger valleys, mud deposits were rare. Conditions apparently were too turbulent to allow settling of silt and clay, even in eddies where velocities were lower than in the surrounding flow.

Deposition along these valleys was patchy and discontinuous, occurring predominantly as cobble, gravel, and sand splays, sheets, and ribbons in proximity to erosion sites. Sediment thicknesses were variable; the thickest observed accumulation was a bar that protruded as much as 4 m above low-water stage in the South Branch channel downstream of the North Fork confluence. Splay deposits up to 1.5 m thick occurred on flood plains at several locations. Isolated gravel and cobble bars on bottomlands and along channel margins were 0.5–1 m thick, and sand dunes with amplitudes up to 1 m were observed in backwater areas or along the margins of the flooded area. These thicknesses, however, represent extreme values rather than the norm. Sand and gravel sheets and ribbons, which were really the most extensive deposits, generally were less than 10 cm thick. Many areas that were unaffected by erosion also experienced negligible deposition.

Downstream of the confluences of the North Fork and the South Fork with the South Branch, particle size of flood-plain deposits decreased. Mud deposits were more common on the Petersburg flood plain than further upstream, and deposition of silt and clay occurred mostly along the reach downstream of Moorefield. Residents of both towns had to clean substantial accumulations of mud from homes and businesses (fig. 74). Gravel and cobble splays were less common in the lower South Branch basin than they were further upstream. Although overbank deposition of mud was more widespread, deposition rarely exceeded 10 cm and probably averaged less than 1 cm. Thicker deposits were found in backwater areas or in local depressions; for example, mud accumulations of 15–25 cm were found along the South Branch valley between Moorefield and the Trough, and silt accumulations of 30–50 cm covered part of the valley floor immediately upstream of the constriction at Blues Beach (14 km north of Romney).

Along the main stem Potomac River, downstream from the South and North Branches, little erosion occurred on flood plains, and the impact of the flood was primarily depositional. No gravel deposits were observed on the valley floor. A 250-m transect across the left flood plain at a site near Hancock, Md., showed an average of 3.6 cm of silt deposited by the 1985 flood (fig. 75). Far downstream, at the mouth of the Monocacy River, mud coatings were left behind on the trees, and 2–5 cm of mud were deposited in the picnic area near the Monocacy aqueduct (fig. 76).

In the air photographs, it was possible to distinguish sand bodies from coarser deposits on the basis of image tone and texture, but sediment finer than sand was not recognizable. The discussion below focuses on deposition patterns in the valleys upstream of Moorefield, where deposition of fine-grained sediment was relatively uncommon.

Channel Bars

Although much of the coarse sediment transported in the flood was carried by in-channel flow, more of the well-defined gravel deposits detectable in the postflood aerial photographs were on flood plains. Perhaps high river stages obscured the visibility of channel deposits at the time the photographs were taken. It is also possible that competence and transport capacity of deeper flow in the main channels were sufficient to carry most of the sediment

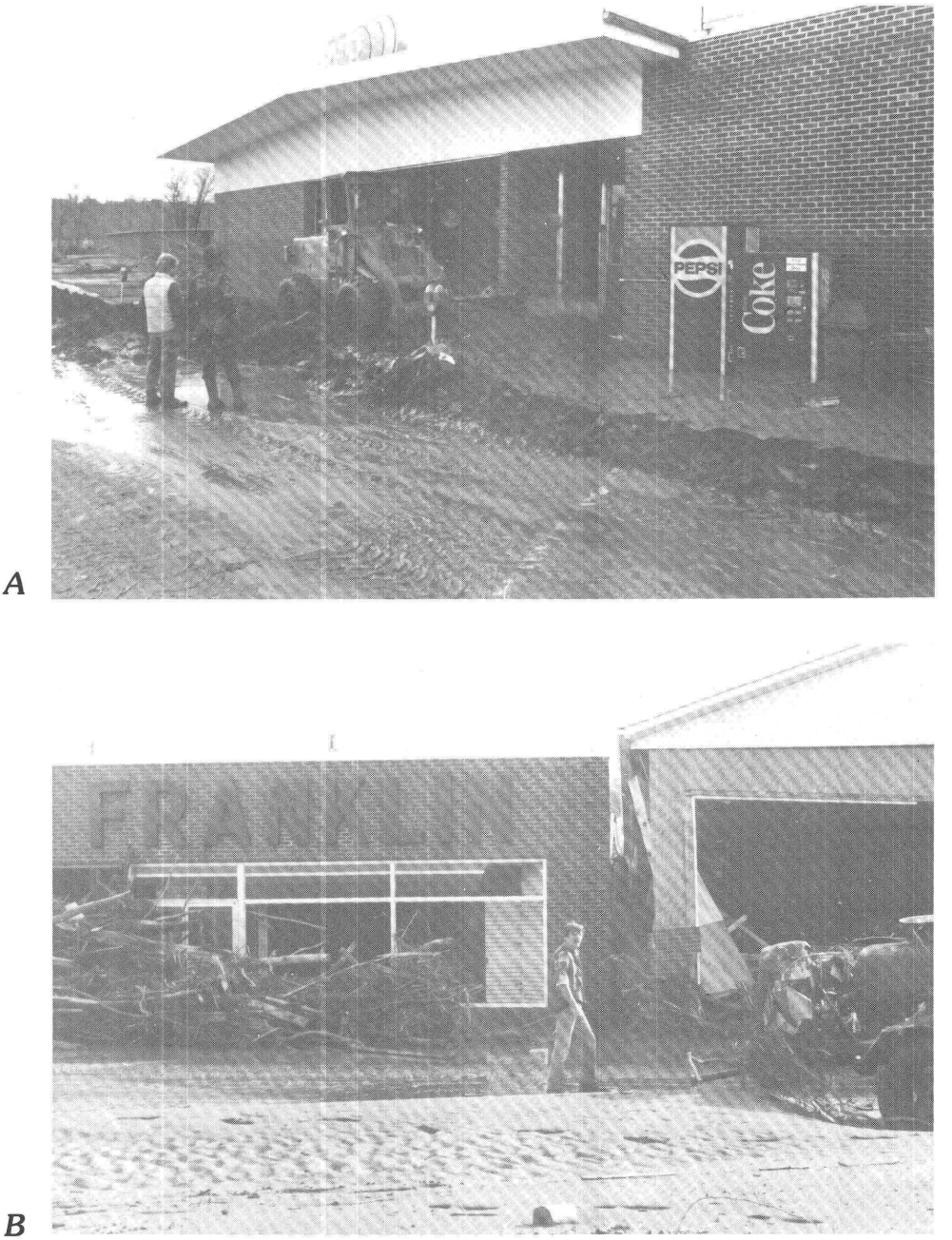

A

B

Figure 74. Two views of sediment deposited in the streets of Petersburg, W. Va. (*A*) Mud deposits about 30 cm deep. (*B*) Ripple marks in sand. Note also organic debris piled up in front of the store entrance. Photographs by Paul Porter.

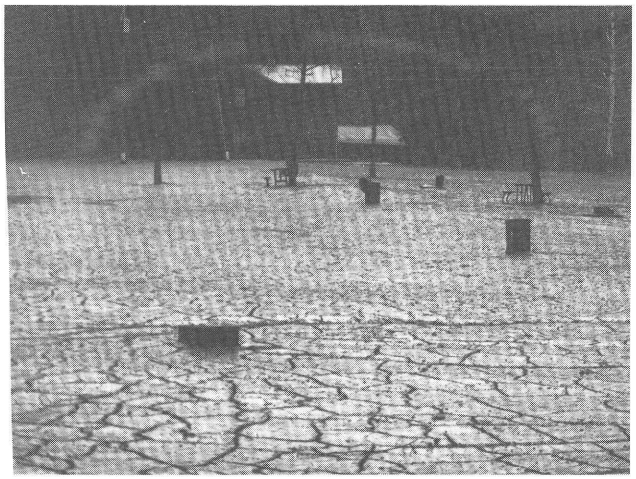

Figure 75. Mud deposited on flood plain of Potomac River near upstream end of C&O Canal tunnel, 2 km downstream of Paw Paw, W. Va. Average depth of mud was about 5 cm.

Figure 76. Mud deposited on flood plain and "bathtub ring" formed by silt marks on vegetation (note light gray color in bottom half of photograph), indicating elevation of high water during the November 1985 flood. Photograph taken from Monocacy Aqueduct, junction of Monocacy River with Potomac River.

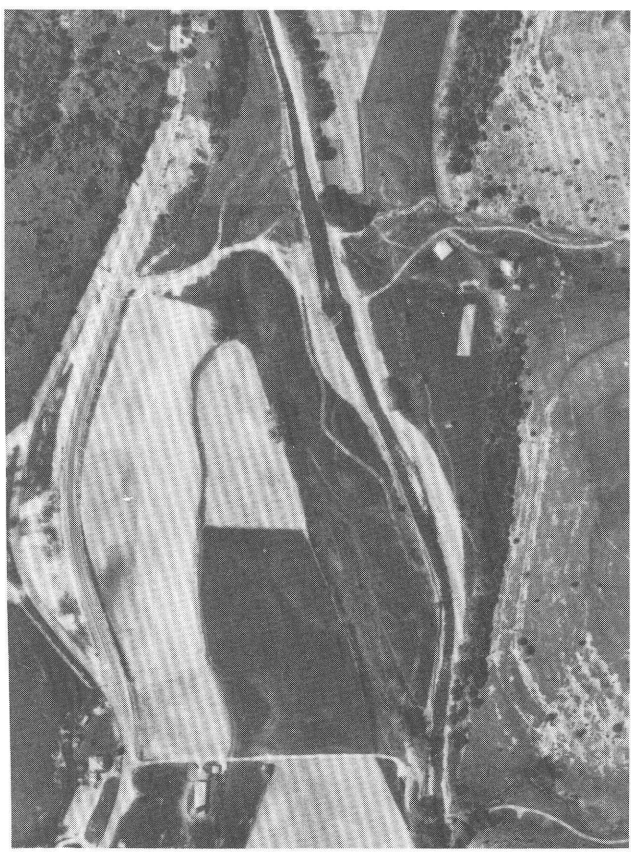

A

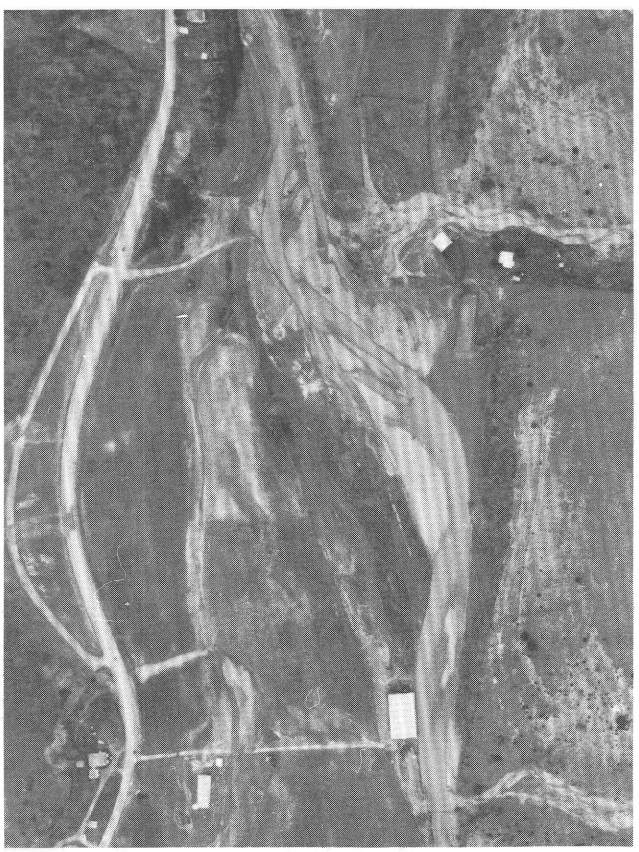

B

Figure 77. (*A*) Before and (*B*) after views of South Branch Potomac River near the Virginia–West Virginia boundary. Flow in South Branch is from bottom to top. Although some of the coarse material visible in the channel may have been delivered from heavily reworked tributary valleys seen at the right in (*B*), much of the exposed sediment appears to be a lag deposit derived from stripping of the flood plain; note that the channel in (*B*) is 3–4 times as wide as in (*A*). Field of view is 590 m wide.

supplied, whereas the combination of sediment supplied from the channel and excavated from the flood plain more often exceeded the transport capacity of shallower flow over hydraulically rough valley floors.

Some of the sediment deposited in channel bars may have been derived from tributary contributions, but most of the gravel bars visible in the channel were at locations where substantial channel widening and bottomland erosion occurred. At these sites, gravel bars were difficult to distinguish from stripped flood-plain remnants (figs. 49, 77–79).

Church and Jones (1982) point out that gravel bars typically occur in a limited range of settings, the principal categories being (1) areas of channel widening, (2) channel junctions where backwater from the main river ponds a tributary, and (3) apices of channel bends, where resistance to flow increases and slack water may occur along the convex bank. Bars in these settings are associated with diverging flow, succeeded immediately downstream by converging flow and increased shear stress. For the most part this statement is sufficient to characterize sites of bar formation in the channels of the three forks of the South Branch Potomac River in the 1985 flood. Most bars observed in the postflood river channel are oriented along the direction of flow with a streamlined form that tapers to a point. Depending on position and shape, gravel bars may be classified following the nomenclature adapted by Church and Jones (1982) after Smith (1974) and Krigstrom (1962). However, as Ashmore (1982) points out, most bar forms reflect the influence of postdeposition modification (fig. 80).

Lateral bars are attached to one bank, usually with a narrow trough between bar and bank extending along most of the length of the bar. The most prominent examples are found at locations where the bottomland on the opposite side of the channel has been severely eroded; in figures 49, 78, and 81, the concave, or outer, bank has been eroded and the bar is attached to the convex, or inner, bank just past the apex of a bend in the channel. In other cases, lateral bars are found along relatively straight channel reaches where no significant channel widening has occurred (fig. 82). Both examples shown here are attached to a bank with a slightly convex planform.

Other bar forms less common in the South Branch basin than lateral bars include longitudinal bars, which occur at sites of channel widening upstream of a zone of converging flow. Typical planform of longitudinal bars observed in the study area is tapered to a point at the downstream end with straight lateral margins and a diffuse, somewhat blunt, upstream border (fig. 83). Complex or compound bar types (figs. 84, 85) may incorporate both newly deposited sediment and eroded remnants of the adjacent bottomland. A fan-shaped gravel sheet in the channel marks the terminus of a jet emerging from a bedrock constriction (fig. 73*H*).

Bottomland Deposits

As noted above, the dominant particle sizes deposited on bottomlands upstream of the major confluences were sand and gravel. For the most part, gravel was deposited contiguous to or in proximity to source areas, whereas sand was carried in suspension farther from the source before being deposited. As a result, longitudinal sorting of deposits is common downstream of an area of stripping or channel widening.

Bottomland deposits that can be distinguished on postflood aerial photographs generally fit into one of four categories: (1) lobate gravel splays, gravel sheets, and sand splays; (2) isolated gravel bars; (3) wake deposits, formed in regions of separated flow downstream of flow obstructions; and (4) backwater deposits formed in regions of reduced velocity upstream of a major flow constriction or a local barrier. Although dunes and ripples are not generally distinguishable in aerial photographs of the South Branch basin, several spectacular examples of bedforms can be seen in the larger scale aerial photographs of the Cheat River basin (Kite and Linton, chapter D, this volume, fig. 7).

Splay deposits are associated with severe channel or flood-plain erosion (figs. 52, 57, 60, 61, 63, 73*F*, 86). Gravel splays are contiguous with the edge of the eroded area. In some instances the broadly curved lobate form has a dentate outer margin formed by a series of smaller lobes within the larger sediment body. The surface of the deposit forms a series of scrolled ridges and troughs that curve outward, with a convex profile terminating almost perpendicular to the main flow (figs. 87*A–C*). Surficial topography varies from one splay to another and may reflect reworking and incision by water draining over the margins of the deposit at falling stage. The upstream edge of the splay may be a poorly defined transitional boundary from a region of stripping (fig. 87*B*; also see Kite and Linton, chapter D, this volume, fig. 8), but the downstream terminus of the lobe is abrupt and generally is marked by a steep slipface (fig. 88). Preservation of the slipface may indicate that downstream migration of the lobe was by progressive avalanching, with the steep front remaining at the angle of repose after the stage fell or after the flow was no longer competent to transport cobbles over the surface.

Locally, the valley floor is covered by a gravel and cobble veneer (fig. 89) that lacks the distinctive features of the lobate splay deposits. As these are sometimes found flanking the river channel, they may in some cases be characterized as levee deposits. Gravel sheets most often are downstream of and contiguous with broad areas of channel widening and stripping.

Sand deposits often exhibit the lobate shape of a gravel splay but occur farther from the source area. Some sand lobes are separated from a gravel splay or from the

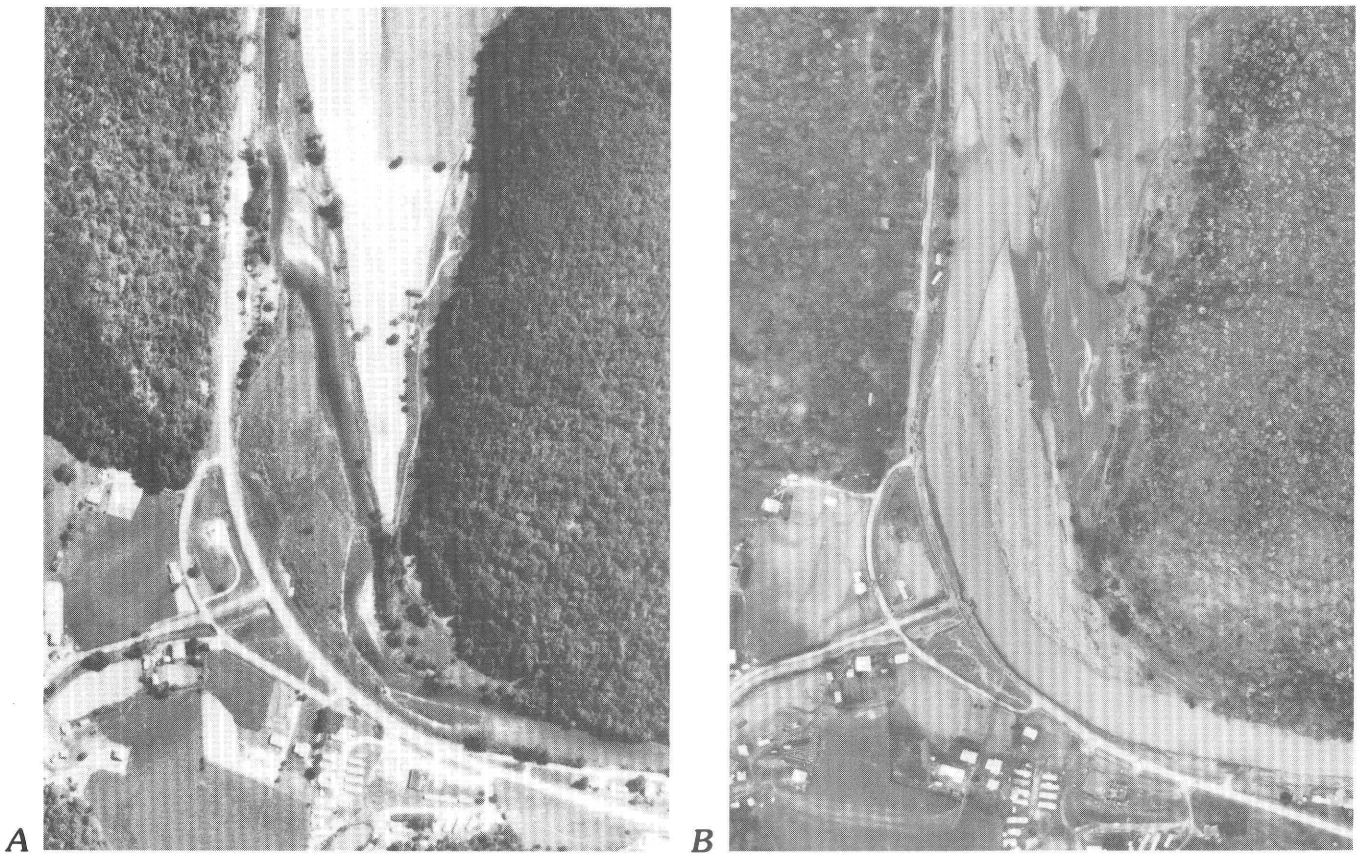

Figure 78. (*A*) Before and (*B*) after views of South Branch Potomac River at Ruddle. Flow is from lower right. Note erosion of valley floor along left bank of river and formation of large bar along right bank and smaller bar along left bank downstream. Field of view is 650 m wide.

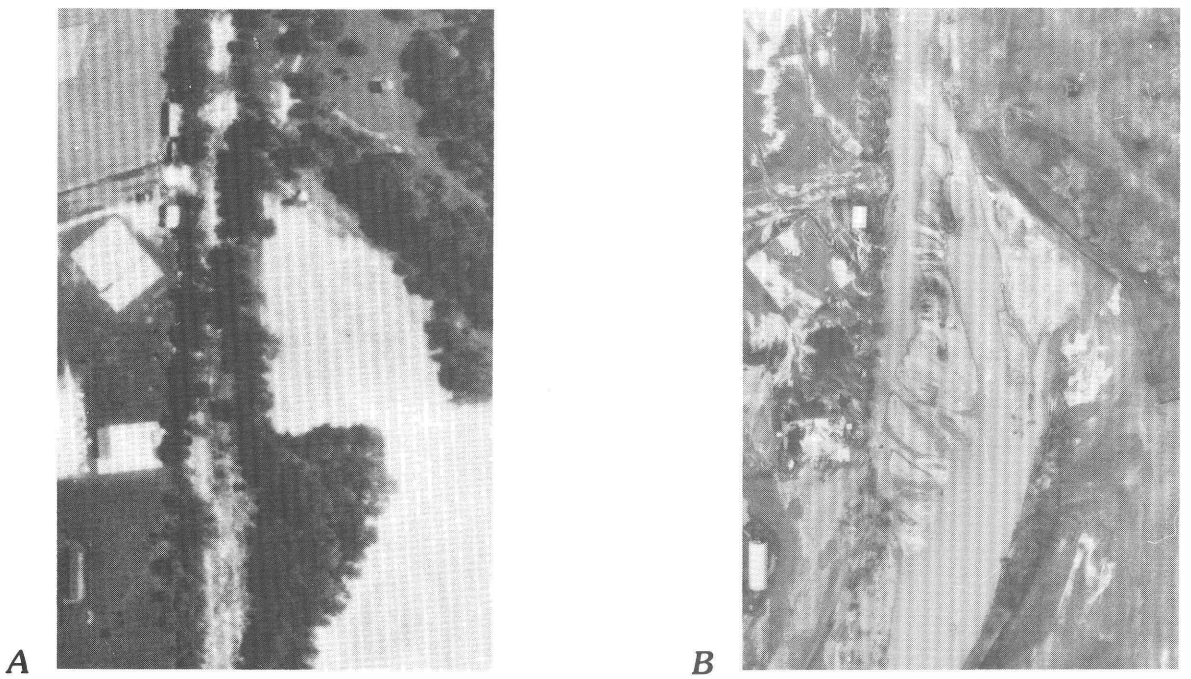

Figure 79. (*A*) Before and (*B*) after views of South Branch Potomac River at Franklin. Flow is from bottom to top. Channel islands visible in (*B*) look like gravel bars in a braided river but probably are stripped and dissected remnants of the valley floor. Field of view is 270 m wide.

Figure 80. Gravel bar in South Branch channel, 1 km downstream of confluence between South Branch and North Fork. Highest point on bar is about 4 m above low water. Flow is from right to left. Steep side profile of this bar appears to result from scour following peak flood discharge; this process probably continued during subsequent high flows.

sediment source by an area lacking significant deposition (fig. 90). In many cases the sand deposit has a feathered or dentate outline (figs. 90, 91*A–D*). This shape resembles the furrowed margins at the edges of some gravel splays and reflects either a pattern of outward-draining flow, which became less competent and deposited sand as it spread out, or a swash mark left behind as the water reversed direction and drained back toward the channel following the flood crest.

Isolated gravel bars on the valley floor are similar to but smaller than the gravel splays described above. These bars generally are downstream of a scour mark and are composed primarily of material excavated from the scour. Longitudinal sorting, with finer sediment accumulating toward the downstream end (McKoy, 1987), may reflect selective transport of the excavated material or may result from trapping of sediment from the surrounding flow in the zone of lower velocity at the lee of the bar.

Wake deposits, either gravel or sand, occur in the lee of flow obstructions throughout the study area. Examples of deposits in the lee of isolated trees or localized clumps of

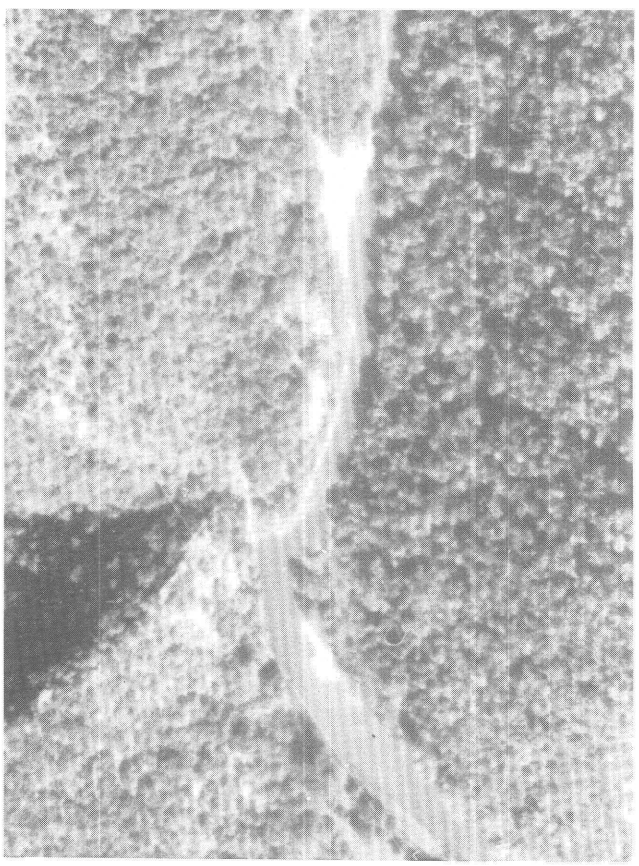

A

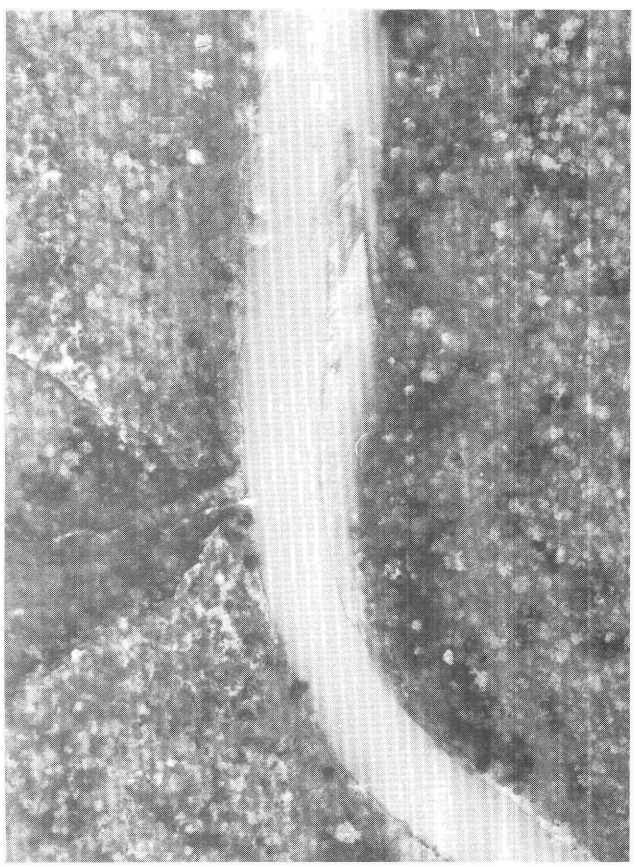

B

Figure 81. (*A*) Before and (*B*) after views of South Branch Potomac River at the mouth of Redman Run, about 6 km upstream of the confluence with the North Fork. Flow is from the lower right. Note that the bottomland along the left bank was completely eroded by the November 1985 flood and that the bar along the right bank was formed in the same event. The section of bottomland removed in 1985 was not present in 1945; it was emplaced by a debris avalanche emerging from the mouth of Redman Run during the flood of June 1949 and remained in place for 36 yr until the 1985 flood removed it. Field of view is 390 m wide.

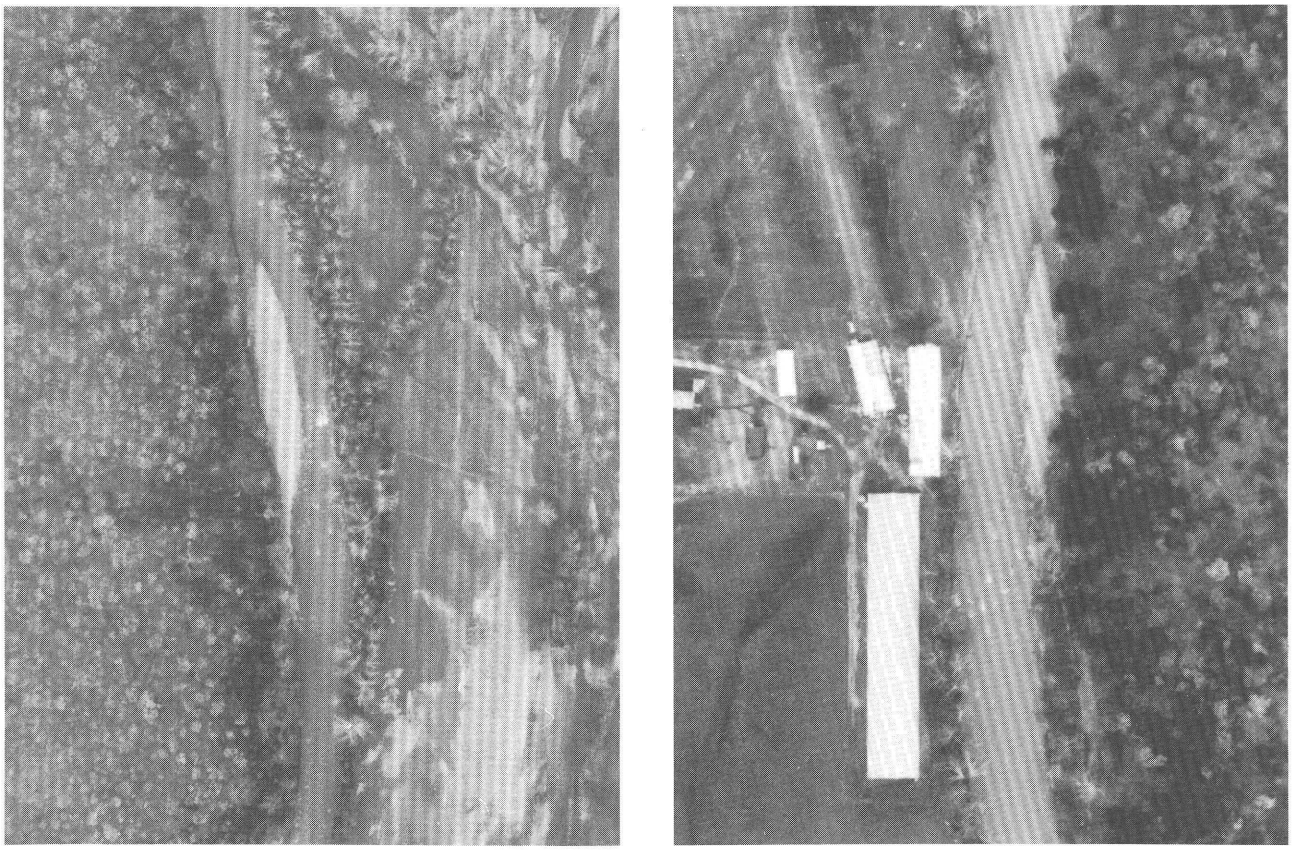

A B

Figure 82. Lateral bars attached to slightly convex banks. (*A*) North Fork, 2.7 km downstream of Circleville. Field of view is 310 m wide. (*B*) North Fork, 0.8 km downstream of Riverton. Field of view is 270 m wide. Flow is from bottom to top in both (*A*) and (*B*).

vegetation are shown in figures 42 and 92. Another type of deposition pattern occurs where a line of trees bordering the channel acts as a baffle, slowing the flow as it leaves the channel and causing deposition of a series of subparallel sand or gravel bodies. These deposits may be aligned with gaps between the trees, or they may be at sites of flow separation behind trees or vegetation clumps (fig. 93). This type of feature is found wherever there is intact vegetation along the margins of the path taken by the main body of the flood and, because of its location, may also be described as a levee deposit. A similar series of small lobate forms is seen at the right edge of figure 36*B*, where deposition occurred at a downward step from a road to the flood plain. As there are no visible gaps in the road other than the large scour mark at the left, the lobate pattern probably was created by longitudinally oriented vortices generated at the downward step.

Ponding of floodwater by a local barrier or by a valley constriction may cause a reduction in velocity that allows sand to drop out of suspension. We refer to the sediment bodies formed by this process as backwater deposits, as opposed to slack-water deposits, which are ponded deposits that may be preserved as paleohydrologic indicators of flood stage (Stedinger and Baker, 1987) in tributary valleys or bedrock alcoves. Sediment bodies that are identifiable from aerial photographs as backwater deposits are rare in the study area, although backwater effects occurred upstream of valley constrictions at several locations. Two examples of backwater deposits are shown here. The first occurred upstream of a valley constriction where the entrance to a short bedrock gorge was the site of an elevated road embankment that ponded water on the flood plain (figs. 94, 95). Sand deposits along the right bank were mostly less than 10 cm thick. The dunes in figure 96 were formed on the flood plain to the left of the channel; they indicate that the reduced velocity of flood flow caused sand to be transported as bedload rather than as suspended load. Silt and clay remained in suspension.

The second example (fig. 97) is a site where a thick grove of trees accumulated a large amount of floating organic debris that formed a barrier to flow crossing the flood plain. A broad, nearly continuous blanket of sand was deposited just upstream of this barrier; note that the barrier

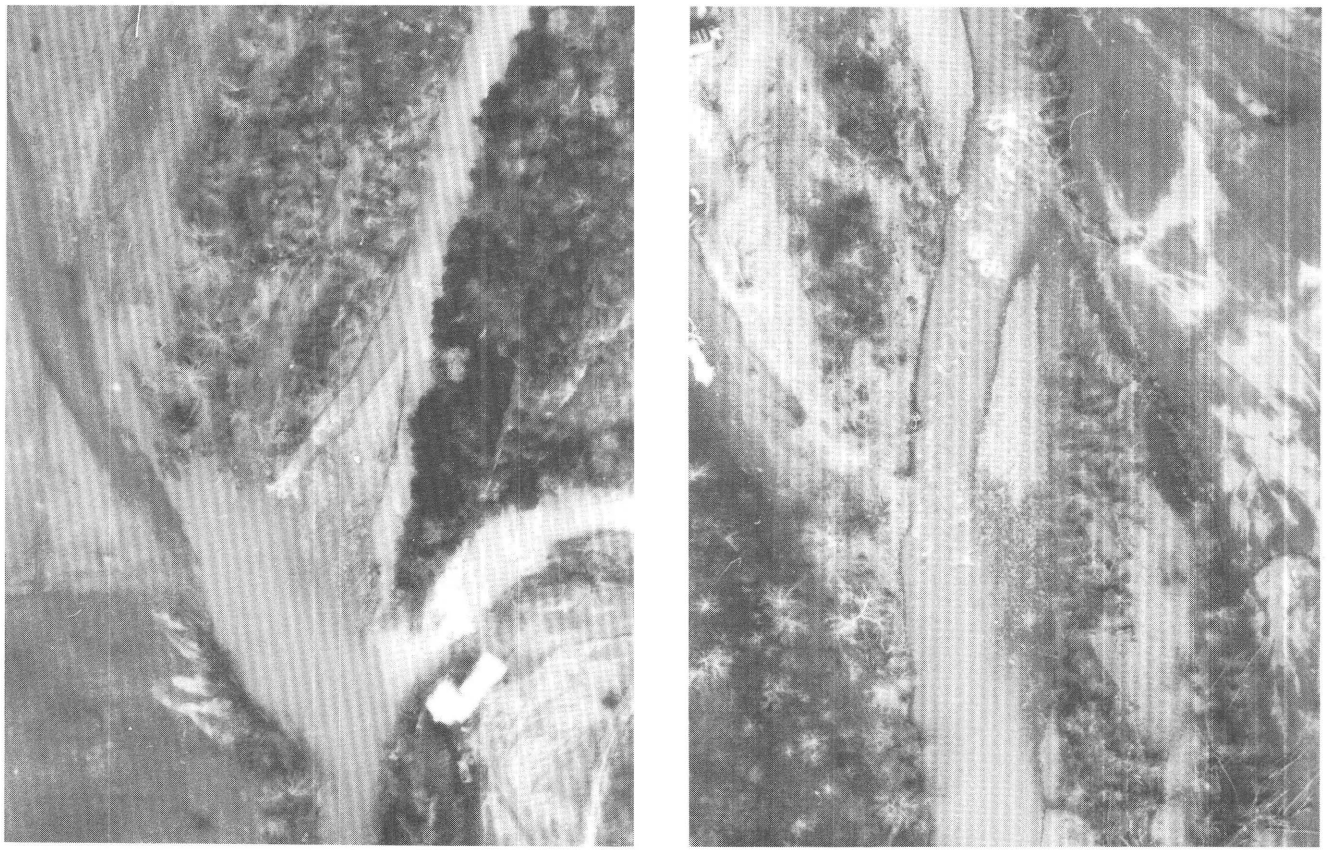

A *B*

Figure 83. Longitudinal bars (not attached to channel banks) with blunt, somewhat diffuse upstream borders. (*A*) South Branch, about 5 km upstream of Franklin. Field of view is 220 m wide. (*B*) North Fork, about 2 km upstream of Seneca Rocks. Field of view is 190 m wide. Flow is from bottom to top in both (*A*) and (*B*).

was breached at one point and that a headward-retreating gully formed where flow accelerated through the opening.

Patterns of sand deposition on the valley floor did not always conform to one of the types described above; in some broad or expanding valley reaches, stringers and irregularly shaped patches of sand were deposited in or on the margins of multiple shallow depressions that served as overflow channels.

CLASSIFICATION OF IMPACTS ON THE VALLEY FLOOR

The intensity of valley-floor erosion caused by the 1985 flood varied considerably throughout the South Branch basin. Because the erosion and deposition forms created in the flood were influenced by interactions between highly turbulent flow and local boundary conditions, explanation of the detailed pattern of erosion would require intensive site-specific investigations. Broad spatial trends exist as well, however, and these can be described in a simple classification scheme. To map the distribution of erosion damage at a scale of 1:250,000, we devised a simple hierarchy of four erosion categories. Individual valley reaches were classified from preflood and postflood aerial photographs, but the assignment of each reach to a category was subjective because the boundaries between classes are necessarily gradational. The criteria used for the erosion mapping are described in table 7.

The flood occupied the entire valley floor at most sites, and its path was guided both by the valley walls and by the river channel. Consequently, erosion features were most prominent at or below valley crossings, or at sites where the channel and the valley thalweg were oriented transverse to one another. For the incipient to moderate erosion class, scour features were concentrated where flow first crossed from the river channel onto the alluvium of the adjacent flood plain or at sites of flow obstructions such as roads and buildings (fig. 98). Erosion was less significant where the channel and valley were parallel and was confined mostly to areas along the channel margin, with isolated scour marks or sets of longitudinal grooves scattered across an otherwise intact valley floor.

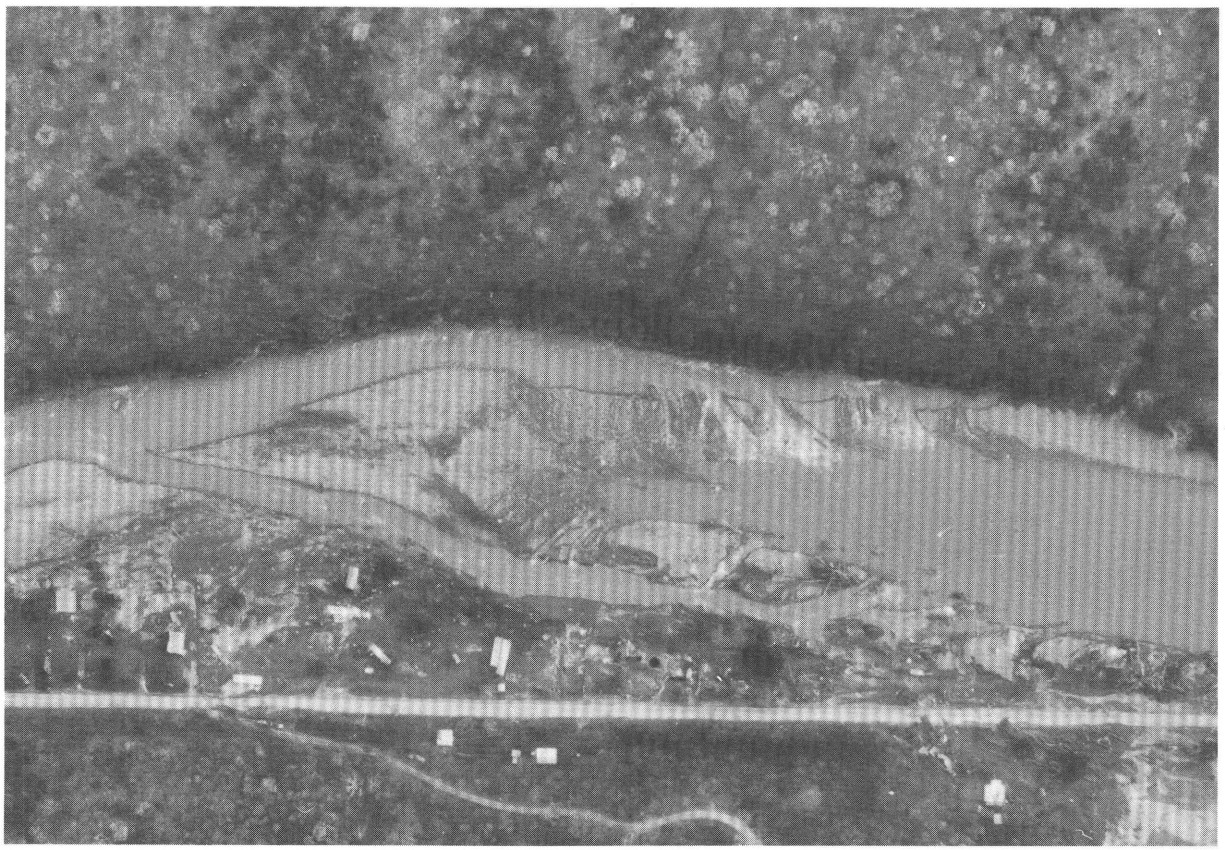

Figure 84. Compound bar formed from dissected flood-plain remnants and freshly deposited gravels. North Fork, about 1 km upstream of the Cabins gage site and 5 km downstream of Hopeville. Flow is from right to left. Note the area of diverging flow through drainage channels separating dissected flood-plain remnants and converging flow around the streamlined downstream end of the bar. Field of view is 630 m wide.

Erosion features associated with severe erosion (class C) characteristically extended farther downstream from a valley crossing than those associated with incipient to moderate erosion. Some examples exhibit relatively simple patterns of chute formation with marginal splays (fig. 60), leaving the majority of the inundated valley floor unaffected. Other examples reveal a more intricate pattern of dissection (fig. 99). Prominent erosion features at the site illustrated are (1) a broad stripped area surrounding irregularly shaped remnants of the eroded surface, which grades into a splay deposit that overlaps the intact portion of the valley floor; and (2) a chute, nearly as wide as the preflood channel of the North Fork and about 450 m long, with marginal amphitheater-shaped headcuts branching off along both sides. In addition, there are multiple scour marks, longitudinal grooves, and sediment deposits of various sizes, shapes, and textures scattered along this section of the valley. The large island in the middle of the reach, previously attached to the flood plain along the left bank, was created by a chute cutoff.

Classification is based on presence or absence of characteristic features within a valley reach; thus a site where two different topographic surfaces were affected by the flood in different ways is assigned to a single category. In figure 50, cultivated fields on a low terrace experienced local formation of scour holes and longitudinal grooves. A lower, forested surface was modified by formation of multiple narrow, shallow chutes, with a central area of more intense stripping and removal of vegetation just upstream of the apex of the bend in the channel. Additional chutes were incised in the valley floor along the right bank entering and leaving the meander. Erosion in this reach was mapped as class C.

Examples of catastrophic erosion most often were associated with expanding flow emerging from a valley constriction (figs. 51, 72, 73, 100, 101). The most severe impacts typically were confined to the area upstream of the widest point in the valley expansion. The pattern of flow emanating outward from a central scoured zone must have been accompanied by powerful macroturbulent eddies with

Table 7. Definition of erosion classes

Class	Definition	Characteristic features
A	Minimal erosion	Little or no modification of channel or valley floor; minor erosion of cut banks but without significant channel widening.
B	Incipient to moderate erosion	Uprooted trees; longitudinal grooves and scour marks on flood plains; pitted or abraded areas along channel margins, with debris accumulations and chaotic surface texture; incipient chutes; localized stripping of point bars; channel widening by up to 100 percent. Gravel deposits common.
C	Severe erosion	One or more fully developed flood-plain chutes; stripping of alluvium from a significant portion of the valley floor; extreme channel widening by combined stripping and lateral bank retreat; may include any or all features from previous class. Extensive gravel splays contiguous with erosion features.
D	Catastrophic erosion	Extensive dissection of valley floor by a set of anastomosing channels or by a jet-shaped erosion feature; or destruction of most of the width of an alluvial bottomland by combined stripping and channel widening. (Latter criterion not applicable in canyon settings where preflood alluvial bottomland is only 1–2 channel widths across.)

a significant head loss between the center and the margins of the scoured zone.

SPATIAL DISTRIBUTION OF EROSION CLASSES

The mapping procedure involved stereo viewing of postflood aerial photographs and annotation of 7½-min topographic quadrangles to indicate location, morphology, and scale of all identifiable erosion and deposition features. The valleys were divided into longitudinal segments and classified after comparing preflood and postflood aerial photographs with the features identified on the maps. Segment boundaries and classes were compiled on a 1:250,000-scale base map. Valley-floor margins were identified by stereo viewing and were traced onto 7½-min quadrangles. Average width along each valley segment was calculated by measuring area between the valley-floor margins and dividing by longitudinal distance along the valley thalweg.

Two maps depicting the distribution of erosion classes are reproduced in this report. The first (pl. 1) shows locations of individual valley segments and is coded to indicate the class to which each segment is assigned. Plate 1 also shows locations of bedrock canyons and valley constrictions along the three forks of the South Branch Potomac River. A simpler map at smaller scale is provided in figure 102. On this map, each of the three forks of the South Branch is divided into several long reaches whose boundaries coincide with the reach boundaries in figure 7; only those reaches upstream of the South Branch-South Fork confluence at Moorefield are shown on this map. The combined percentage of each reach assigned to the severe and catastrophic erosion classes is indicated and provides an index of erosion severity.

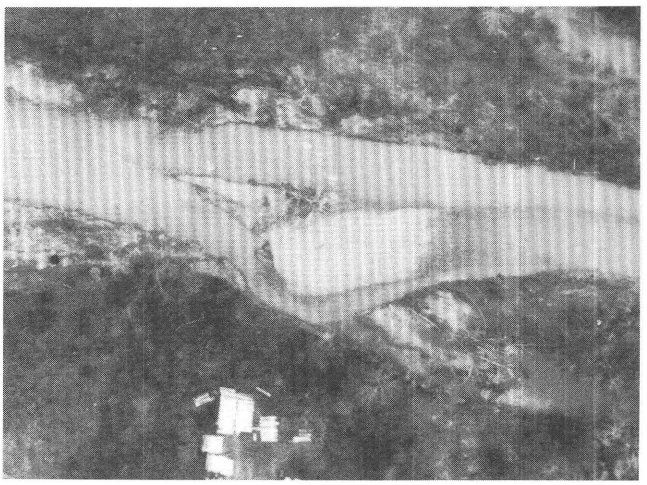

Figure 85. Compound bar form with blunt, rectangular upstream section and streamlined downstream section. North Fork, about 2 km upstream of Riverton. Flow is from right to left. Field of view is 250 m wide.

Valley constrictions were defined in plate 1 as sites where the valley floor was constrained to a width less than one-third the width along the reach downstream; thus, the area immediately downstream of a location marked on the plate by a pair of arrows would be an area of flow expansion or divergence during a flood of the stage reached in November 1985. Significant flow contractions and expansions occurred at other sites that did not meet the criterion of the 1:3 ratio; however, the width of the valley floor is so variable along the three forks of the South Branch that a larger ratio, such as 1:2, would not be effective in discriminating changes that significantly influenced flood hydraulics.

Of 17 sites in plate 1 that were assigned to class D (catastrophic erosion), 14 are downstream of valley constrictions or at the mouths of bedrock canyons. In one case (fig. 72*B*) the constriction is about 3 km upstream of the site where the most severe erosion occurred. The channel follows a straight path emerging from the constriction, and dissection of the flood plain by a series of anastomosing channels occurred only where the channel changed direction and the main thread of flow continued straight along the flood plain. In a second case (fig. 72*D*), erosion occurred at a valley expansion that did not meet the 1:3 ratio criterion used in mapping. In a third case (fig. 73*D*) the width of the

Figure 86. Gravel splays derived from bottomland erosion downstream of bridge, South Branch Potomac River, 1 km upstream of Romney. Flow is from left to right. Photograph by W.E. Duliere, West Virginia Advocate.

valley floor upstream of the site of most severe erosion does not indicate a constriction, but a low terrace occupies much of the valley. Although there was shallow flow over this surface, most of the flow was confined within the lower area bordered by the terrace scarp. The pattern of erosion suggests that a jet formed where flow emerged from the confined portion of the valley section. This example demonstrates that the definition of a flow constriction varies with flood stage and depth of water on different topographic surfaces. Simple quantitative indices for mapping constrictions at a scale of 1:250,000 are thus inadequate for detailed explanation of the controls on flow patterns and are used here only to illustrate general trends.

In compiling figures 7 and 102, we initially located reach boundaries where major shifts in erosion pattern or in the trend of valley width were observed, but the boundaries were modified to make reach lengths less variable. Summary data on erosion classes for these reaches are listed in table 8. Along 384.4 km of mapped channel reachesupstream of the confluence with the North Branch Potomac River, 318.2 km, or 82.8 percent, were mapped as experiencing at least incipient erosion. Classes representing severe or catastrophic erosion accounted for 116.2 km, or 30.2 percent of the total, and class D alone (catastrophic erosion) accounted for 21.8 km or 5.7 percent of the total.

Examination of the erosion maps reveals several trends:

- Erosion was much more severe along the North Fork than along the other two forks of the South Branch or along the South Branch downstream of Moorefield, with 41.1 percent and 18.1 percent of the valley mapped as class C and class D, respectively. Corresponding values for the South Branch above the South Fork confluence are 20.6 percent and 4.1 percent and for the South Fork are 26.4 percent and 4.2 percent. Along the South Branch downstream of Moorefield, 14.8 percent of the valley was mapped as class C; class D erosion was not observed.
- Along each of the three forks of the South Branch, the reach farthest upstream experienced minimal erosion by comparison with other reaches.
- Erosion generally increased in severity in the downstream direction along the North Fork valley, except for a drop from 84.2 to 55.8 percent classified as severe or catastrophic in the lower two reaches above the confluence with the South Branch.

A

B

C

Figure 87. Gravel splays with dentate outer margins. Scrolled ridges and troughs curve outward and appear to be sculpted by flow that drained away from the channel. (*A*) South Branch Potomac River, about 4 km upstream of confluence with North Fork. Flow is from bottom to top. Field of view is 360 m wide. (*B*) North Fork South Branch Potomac River, 10 km downstream of Seneca Rocks and 12 km upstream of Hopeville. Flow is from bottom left. The area immediately to the right of the channel has been stripped; lateral transition from an area of net erosion to an area of net deposition is poorly defined. Field of view is 380 m wide. (*C*) South Fork South Branch Potomac River near Fort Seybert. Flow is from bottom to top. The channel shown here is a chute incised into the valley floor during the flood (see fig. 60). The fallen trees on the surface of the splay deposit at left center provide flow vectors. Field of view is 260 m wide.

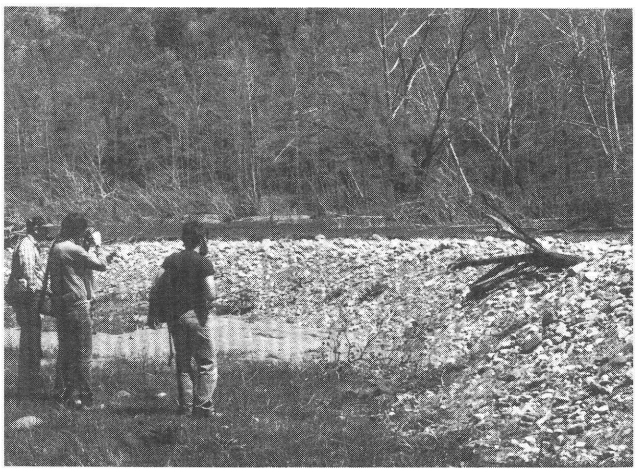

Figure 88. Steep slipface about 1.5 m high at downstream end of gravel splay deposit. Although the area upstream of the deposit was stripped, the downstream end buries an intact surface, as indicated by the turf in left foreground. Flood flow was from right to left. South Branch Potomac River, 5.5 km upstream of the confluence with the North Fork. A similar deposit is described by Ritter (1988, figs. 9, 10).

- A similar downstream trend toward increasing severity of erosion occurred along the South Fork valley, but a marked decrease in erosion severity was observed along the last two reaches upstream of Moorefield.
- Along the South Branch, the highest percentage of the valley classified as severe or catastrophic occurred upstream of Franklin. Erosion severity then declined in the downstream direction, reaching a minimum in the upper part of the Smoke Hole canyon near Upper Tract. Percent of valley reach classified as severe or catastrophic rose again in the lower part of the canyon and on the South Branch below the North Fork confluence.
- Along the South Branch approaching Moorefield and downstream of the confluence with the South Fork at Moorefield, the percent of valley length assigned to severe or catastrophic erosion classes was low. Severe erosion between Moorefield and the confluence of the North and South Branch Potomac River was limited to areas at or just below major valley constrictions and bedrock canyons.

Factors that are potentially important in explaining broad spatial patterns of flood-generated erosion include channel gradient, valley width, discharge, and erosion resistance of the valley floor. Channel gradient and valley width were estimated using topographic maps and aerial photographs (table 8), but peak discharge measurements for the November 1985 flood were made at only a few points in the basin, and values for other locations were calculated by interpolation. Erosion resistance has not been quantified, and its role is poorly understood.

Despite these uncertainties, we suggest explanations for some of the spatial trends outlined above:

- The difference between the North Fork and the other forks of the South Branch with respect to the spatial extent of severe erosion is in part a function of differences in gradient. The North Fork, with a gradient of 0.0065, is significantly steeper than the South Branch above its confluence with the North Fork (0.0047) or the South Fork above Moorefield (0.0036). The gradient of the South Branch between the North Fork confluence and Moorefield is gentler (0.0021) than any of the three forks, and the South Branch downstream of Moorefield has the gentlest gradient of all (0.0009).
- Discharge peaks are comparatively small along the steepest valley reaches, which drain headwater basins with small contributing areas. Longitudinal trends in the extent of severe erosion along a single valley cannot be explained by gradient alone because discharge tends to increase with increasing drainage area as gradient decreases. If the rate of downstream increase of discharge is greater than the rate of downstream decrease in gradient, and if lithologic controls prevent any systematic downstream increase in valley width, then unit stream power should increase in the downstream direction.

  Along the North Fork, we observe no systematic increase in valley width (fig. 7, table 9), and the gradient remains steep as discharge increases. If we assume constant unit discharge for all parts of the North Fork basin (using the value from the Cabins site), we can estimate peak discharges at the midpoint of each reach that can be combined with other data to estimate reach-average values of unit stream power. Average channel gradient for each reach is used to approximate average energy gradient during the flood. The values in table 9 show the expected downstream increase in average unit stream power, paralleling the downstream trend toward increasing erosion. The anomalous decline in extent of severe erosion in reach 5 is a result of erosion resistance; the canyon upstream of Hopeville has little erodible bottomland. If the canyon portion is excluded from the reach, severe and catastrophic erosion classes account for 79.6 percent of reach 5 rather than 55.8 percent (table 9).
- Average valley widths have a greater range and show less consistent trends along the South Fork than along the North Fork (table 9, fig. 7). Gradient decreases along the first few reaches and then alternately increases and decreases in subsequent reaches. Average gradient, however, is less variable than average width. Using a value of unit discharge based on measurements at the two gages in the basin, we estimated peak discharge as a function of cumulative drainage area for each reach. Reach-average values of unit stream power were calculated and compared with the percent reach length

Table 8. Summary data on erosion classes

Area	Cumulative length (km)					Percentage of total length			
	Class A	Class B	Class C	Class D	Total	Class A	Class B	Class C	Class D
North Fork	4.7	24.0	28.9	12.7	70.3	6.7	34.1	41.1	18.1
South Branch above North Fork confluence	18.7	45.6	16.0	3.8	84.1	22.2	54.2	19.0	4.5
South Branch between North Fork confluence and South Fork confluence	.0	21.4	7.6	.8	29.8	.0	71.8	25.5	2.7
South Fork	24.2	49.4	28.0	4.5	106.1	22.8	46.6	26.4	4.2
South Branch below South Fork confluence	18.6	61.6	13.9	.0	94.1	20.4	65.4	14.8	.0
All rivers combined	66.2	202.0	94.4	21.8	384.4	17.2	52.5	24.6	5.7

Table 9. Physiographic parameters, reach-average values of unit stream power, and spatial extent of severe erosion for individual valley reaches along the three forks of the South Branch Potomac River

North Fork South Branch Potomac River

Reach[1]	Reach length (km)	Channel slope	Mean width of valley floor (m)	Estimated discharge[2] (m^3/s)	Reach-average unit stream power[3] (W/m^2)	%(C+D)[4]
1	13.8	0.0092	355	595	151	18.6
2	12.0	.0077	243	986	306	65.4
3	12.3	.0058	264	1,535	330	70.5
4	16.2	.0051	288	2,050	356	84.2
5	16.0	.0051	251	2,363	471	55.8

South Branch Potomac River upstream of confluence with South Fork

Reach[1]	Reach length (km)	Channel slope	Mean width of valley floor (m)	Estimated discharge[2] (m^3/s)	Reach-average unit stream power[3] (W/m^2)	%(C+D)[4]
1	12.6	0.0094	261	510	180	0.0
2	13.8	.0060	231	930	237	63.2
3	17.1	.0039	334	1,435	164	25.7
4	7.9	.0029	530	1,716	92	11.8
5	13.7	.0047	85	1,558	844	5.0
6	19.0	.0029	125	1,671	380	26.8
7	18.2	.0025	726	4,097	138	44.5
8	11.6	.0015	1,539	4,568	44	.0

South Fork South Branch Potomac River

Reach[1]	Reach length (km)	Channel slope	Mean width of valley floor (m)	Estimated discharge[2] (m^3/s)	Reach-average unit stream power[3] (W/m^2)	%(C+D)[4]
1	13.8	0.0073	121	377	223	15.3
2	16.6	.0042	192	836	179	20.6
3	20.0	.0029	461	1,439	89	22.0
4	16.9	.0044	238	1,999	362	50.5
5	10.4	.0030	368	2,408	192	57.3
6	10.0	.0033	352	2,720	250	60.0
7	9.8	.0027	482	3,041	167	20.7
8	8.6	.0028	925	3,194	95	.0

[1] Reach numbers increase in the downstream direction for each river; all reaches identified are upstream of Moorefield.

[2] Discharge estimates based on application of unit discharge values from gage sites; each value estimated for midpoint of reach.

[3] Reach-average unit stream power calculated as product of estimated discharge, channel slope, and unit weight of water divided by mean width of valley floor.

[4] %(C+D) represents cumulative percentage of reach assigned to erosion classes C and D.

A

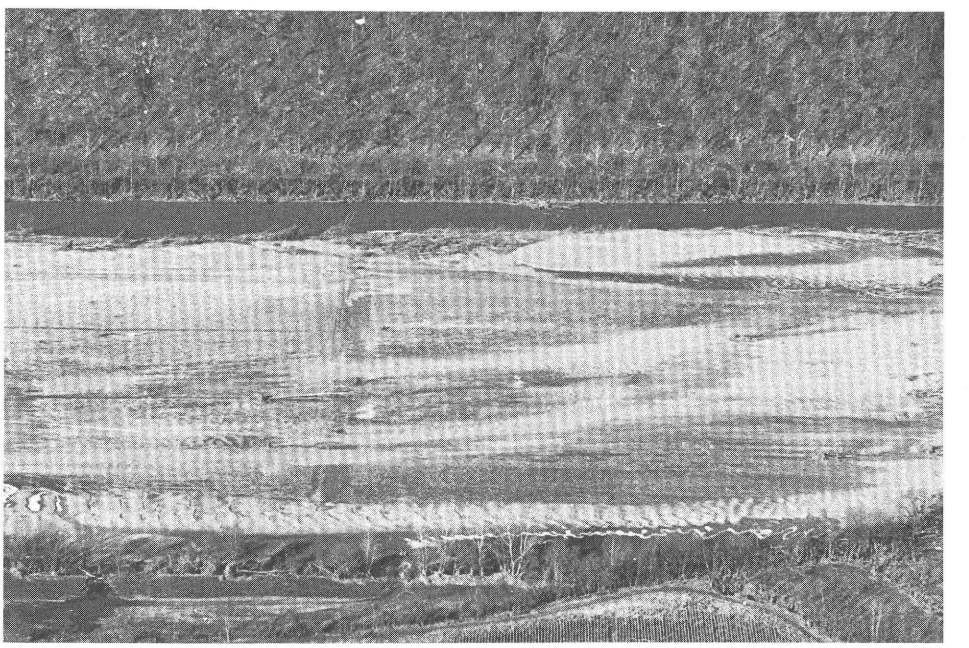

B

Figure 89. Gravel sheets flanking the main river channel. (*A*) North Fork South Branch Potomac River, 3.6 km upstream of Seneca Rocks. Flow is from right to left. Photograph by F.N. Scatena. (*B*) South Branch Potomac River downstream of the Trough. Flow is from left to right. Photograph by W.E. Duliere, West Virginia Advocate.

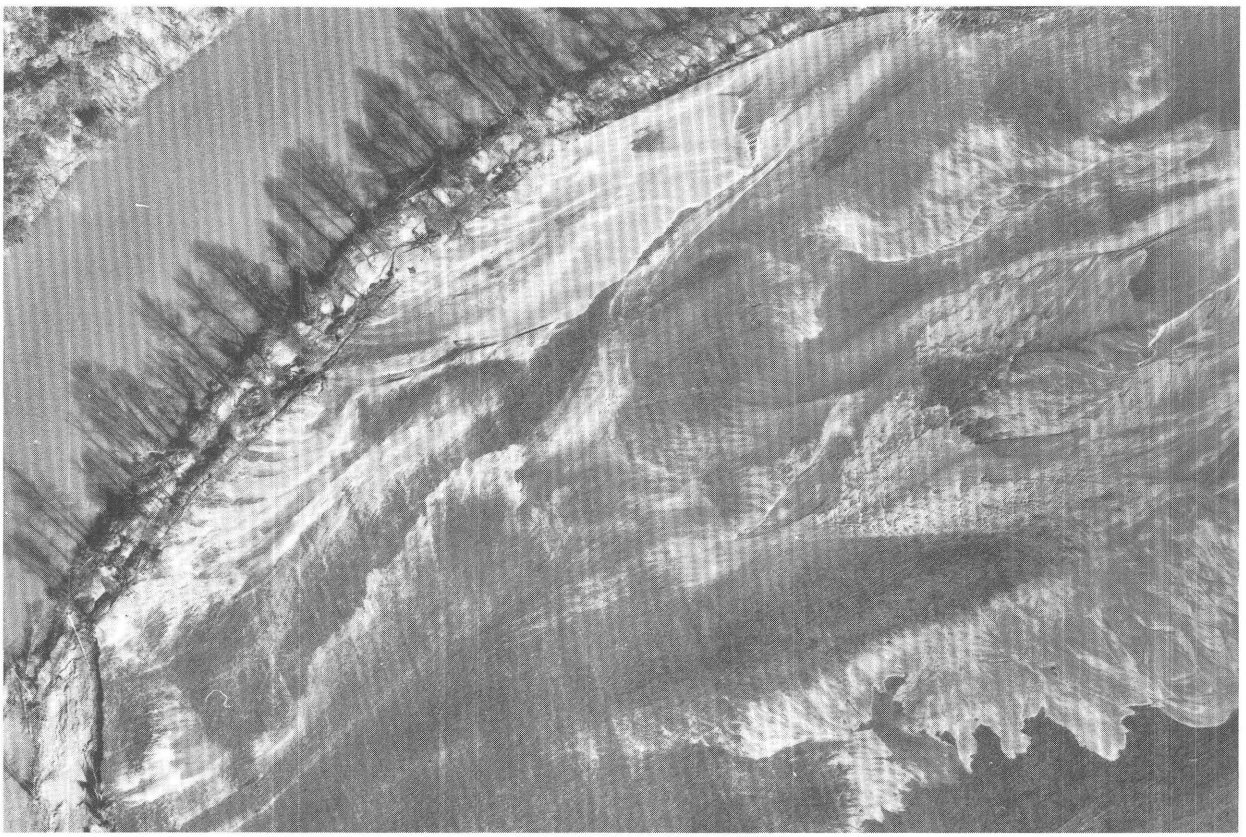

Figure 90. Levee deposits bordering the channel and sand splays on the flood plain; Cheat River, 8 km downstream of Parsons. Flow is from lower left. Field of view is 380 m wide.

assigned to the severe and catastrophic erosion classes. The relationship between these variables shows no clear trend (table 9). Some of the discrepancy probably is due to variations in erosion resistance; for example, reach 4, like reach 5 along the North Fork valley, includes several kilometers of bedrock canyon with little erodible bottomland. Further explanation of the erosion pattern clearly would require closer attention to local conditions within each of the long reaches described here.

- The pattern of erosion along the South Branch valley is the most difficult to explain using the information available. To synthesize values of unit stream power for comparison with erosion statistics, we estimated peak discharge using unit discharge based on the Franklin indirect discharge measurement for reaches 1 and 2 and using weighted average unit discharge for the measurements from Franklin and Petersburg for reaches 3–6. For reaches 7 and 8, additional increments of discharge were based on a weighted average using the Petersburg and Springfield measurements. When the reach-average values of unit stream power calculated using these discharge estimates are compared with corresponding values of percent reach length assigned to the severe and catastrophic erosion classes, no significant correlation is found. Evidently, local variations in boundary conditions affecting flood hydraulics and erosion resistance need to be taken into account. Closer examination suggests a partial explanation for the observed erosion patterns.

Between reach 2 and reach 4, average valley width more than doubles, and between reach 1 and reach 4, average channel gradient declines from 0.0094 to 0.0029. These changes, together with the backwater effects caused by the constriction at the entrance to the Smoke Hole reach just below Upper Tract, appear to explain the sharp decline in severe erosion from reach 2 to reach 4. On the other hand, the causes for increases in severe erosion from reach 1 to reach 2 are unclear. Although the difference between reach-average values of unit stream power for these two reaches (182 W/m^2 for reach 1 and 239 W/m^2 for reach 2) appears insufficient to explain the difference in the amount of flood erosion, the average stream-power values are predicated on the assumption that peak discharge per unit of drainage area was the same in both reaches. If tributaries instead had contributed higher unit discharge to reach 2, the reach-average value of unit stream power along this reach would be larger.

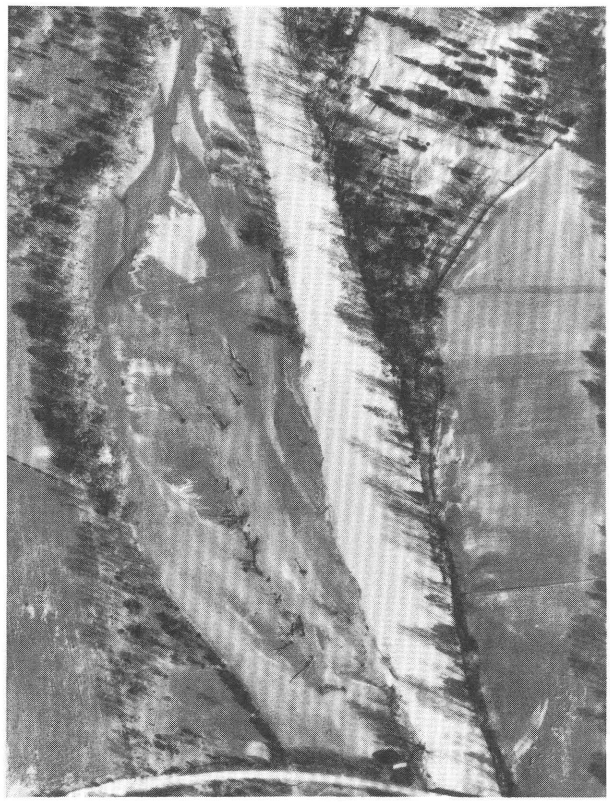

A

B

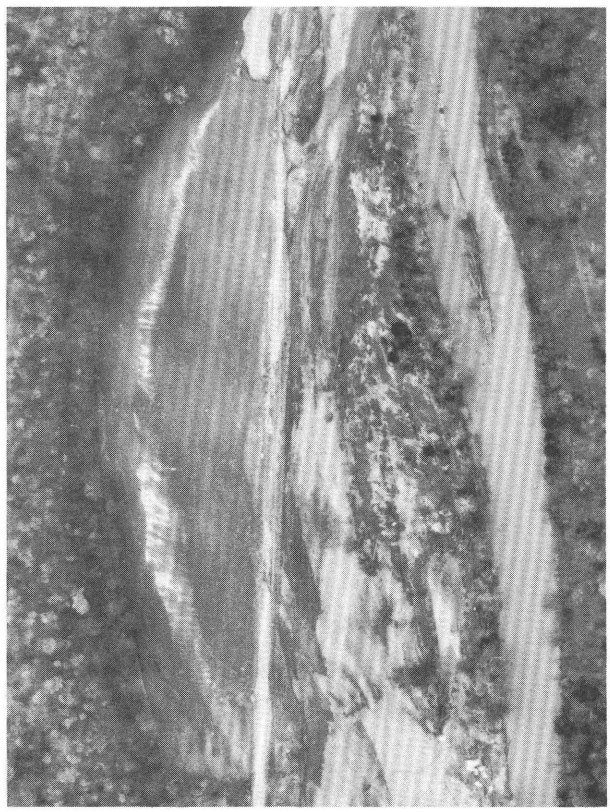

C

D

◀ **Figure 91.** Feathered or dentate sand deposits on the valley floor; flow in each case is from bottom to top. (*A*) South Fork South Branch Potomac River, 2 km upstream of Milam. Note sand deposits at left center. Field of view is 500 m wide. (*B*) South Fork South Branch Potomac River, 6 km downstream of Milam. Note dentate sand deposits to the right of the channel, at the center of the photograph. Field of view is 360 m wide. (*C*) North Fork South Branch Potomac River, 9 km downstream of Seneca Rocks. Note the sand deposits to the left of the road. Field of view is 400 m wide. (*D*) South Fork South Branch Potomac River, 8.5 km downstream of Brandywine. Field of view is 460 m wide.

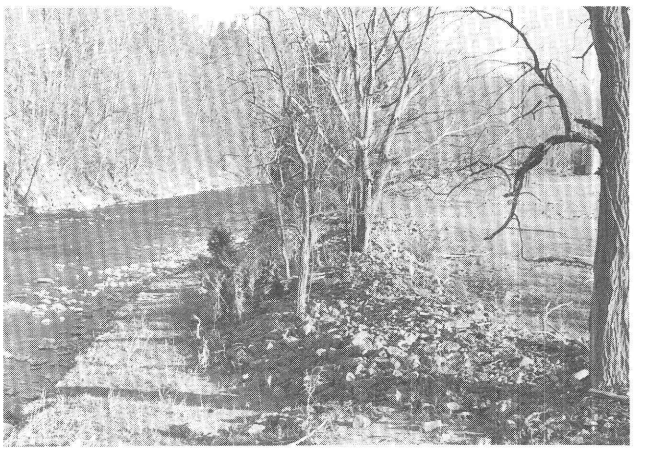

Figure 92. Gravel levee formed as a wake deposit around a small group of trees. Looking upstream on South Branch Potomac River, 4 km upstream of Franklin. Photograph by F.N. Scatena.

A

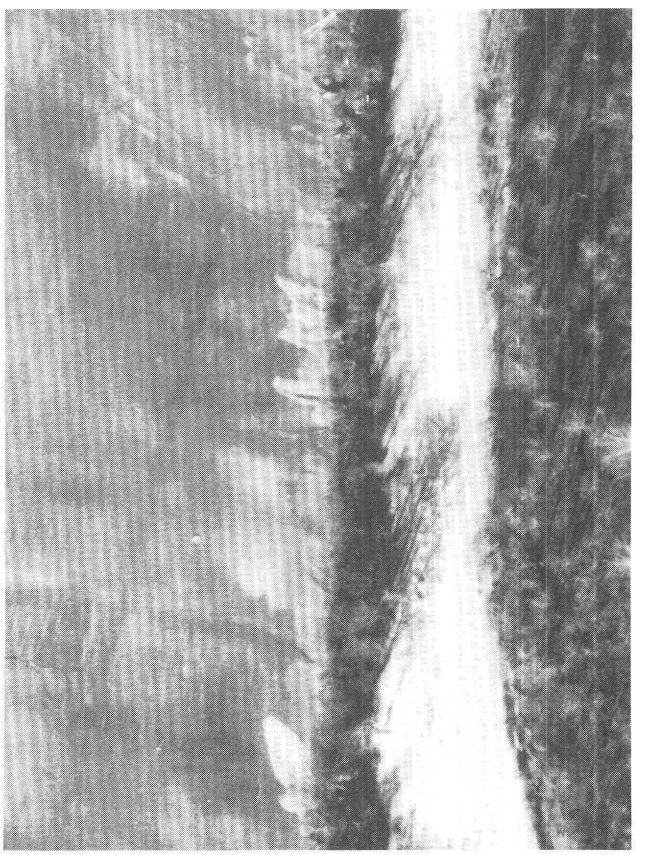

B

Figure 93. Sand levees formed as wake deposits associated with flow obstruction by trees bordering the channel. Flow is from bottom to top in each case. (*A*) South Branch Potomac River, about 20 km upstream of the confluence with the North Fork. Field of view is 420 m wide. (*B*) South Fork South Branch Potomac River at Fort Seybert. Note the discrete lobes of sand emerging from between the trees and oriented almost perpendicular to the channel. Field of view is 150 m wide.

Figure 94. Backwater deposits upstream of a road embankment at the entrance to a bedrock gorge; South Branch Potomac River, about 2 km downstream of Franklin. Flow is from bottom to top. Field of view is 290 m wide.

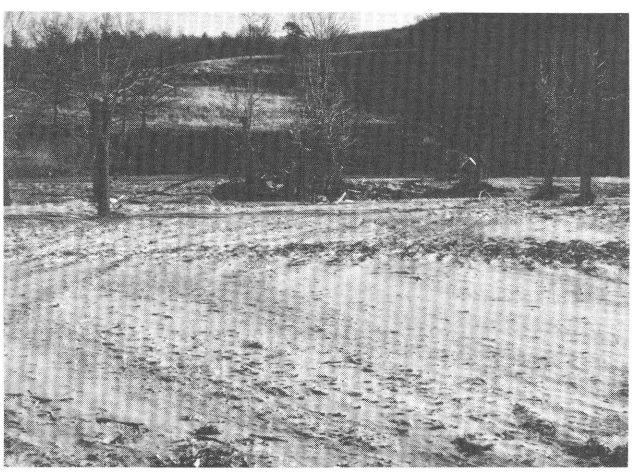

Figure 95. Sand sheet on right bank of South Branch Potomac River at the site shown in figure 94. View is toward the right valley wall.

Figure 96. Sand dunes near left bank of South Branch Potomac River at the site shown in figure 94.

Figure 97. Sand deposits on right and left banks of South Branch Potomac River, 0.8 km upstream of the confluence with the North Fork. Flow is from bottom to top. Backwater deposits formed on the valley floor to the right of the channel, where flow was blocked by trees and by a debris jam lodged against the trees at the downstream end of the open field. Note headcut on gully formed at breach in tree line just right of center. Wake deposits formed on the left side of the channel where trees retarded overbank flow. Field of view is 370 m wide.

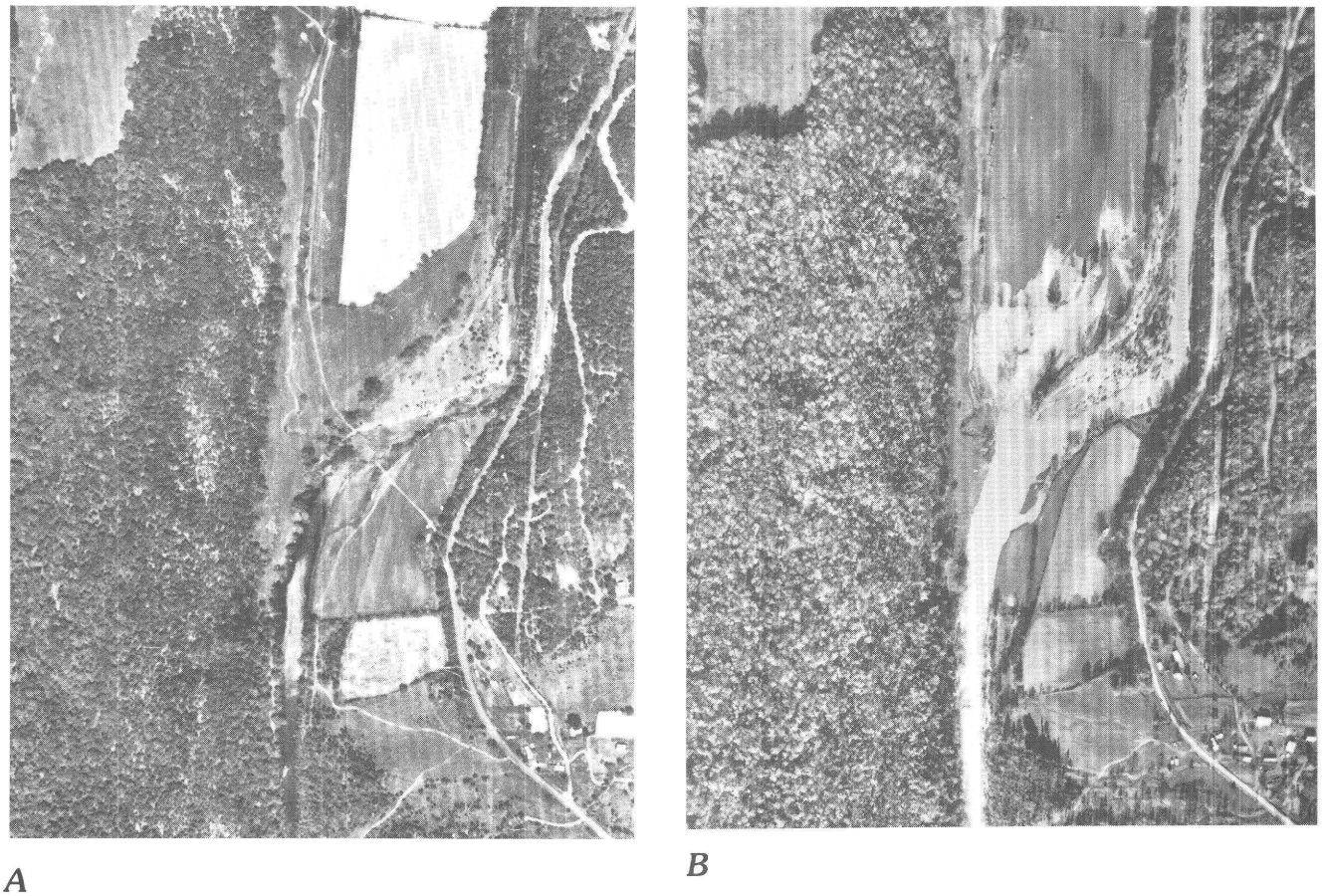

A B

Figure 98. (*A*) Before and (*B*) after views of the South Fork South Branch Potomac River at a site just downstream of the Moorefield stream gage and about 8 km upstream of the confluence with the South Branch Potomac River. Flow is from bottom to top. This site is an example of erosion class B. Field of view is 950 m wide.

High unit stream power coincides with modest erosion in the upper part of the Smoke Hole canyon (reach 5) because the reach is narrow and lacks bottomland for development of the geomorphic features typical of the severe and catastrophic erosion classes. As the canyon broadens approaching the North Fork confluence, increased bottomland development is subject to erosion, and the extent of severe erosion increases. Below the confluence, the combined flood discharges of the North Fork and South Branch flowed through two narrow gaps, causing extensive erosion on the broad valley floors downstream of each gap. The average value of unit stream power calculated for this reach (138 W/m^2) is deceptive, given the spatial variability of hydraulic conditions between the gaps and the broader portions of the valley. Thus we need to supplement reach-average values of unit stream power with more detailed information on local maximum values.

DISCUSSION

The preceding paragraphs suggest that, for both the South Fork and the South Branch, longitudinal trends in the severity of erosion along a single valley are heavily influenced by local conditions and are not readily explained by a single parameter such as reach-average unit stream power. Pooling of data from all of the valley reaches described in table 9 reveals some general trends, however. For example, the extent of severe erosion reaches a peak for valley reaches in an intermediate range of valley widths (fig. 103). All valley reaches with more than 50 percent of their length mapped in the severe and catastrophic erosion classes had mean widths between 230 and 370 m; the sole outlier approaching 50 percent was the South Branch below its confluence with the North Fork. As noted above, this is a broad reach punctuated by two narrow gaps.

The trend illustrated in figure 103 may be explained as follows. For fixed values of peak discharge and gradient, a wider valley generally will have lower velocities and lower values of unit stream power; thus the widest valley reaches are unlikely to experience severe erosion. A narrower valley will be subjected to higher velocities and higher unit power. However, the narrowest valley reaches are bedrock canyons with limited bottomland. Because of

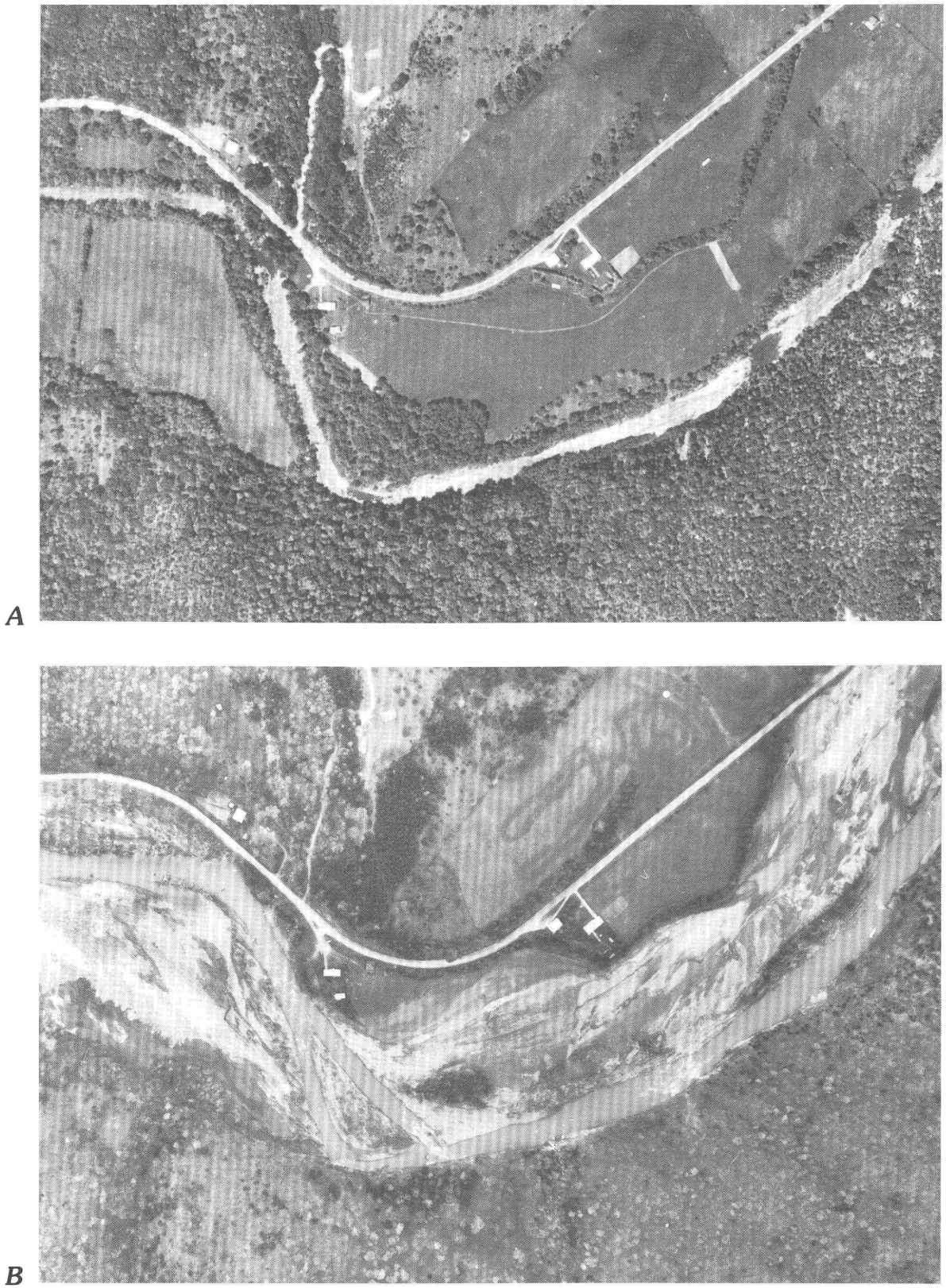

Figure 99. (*A*) Before and (*B*) after views of the North Fork valley about 10 km downstream of Seneca Rocks and 12 km upstream of Hopeville. (*C*) Photointerpretive sketch identifying erosion and deposition features. Flow is from left to right. This site is an example of erosion class C; features include a chute about 450 m long (right center), an area of flood-plain stripping (adjacent to the channel at left center), an island formed by cutting of a new channel (bottom center), and numerous scour marks, longitudinal grooves, and areas of uprooted vegetation. Field of view is 1,200 m wide.

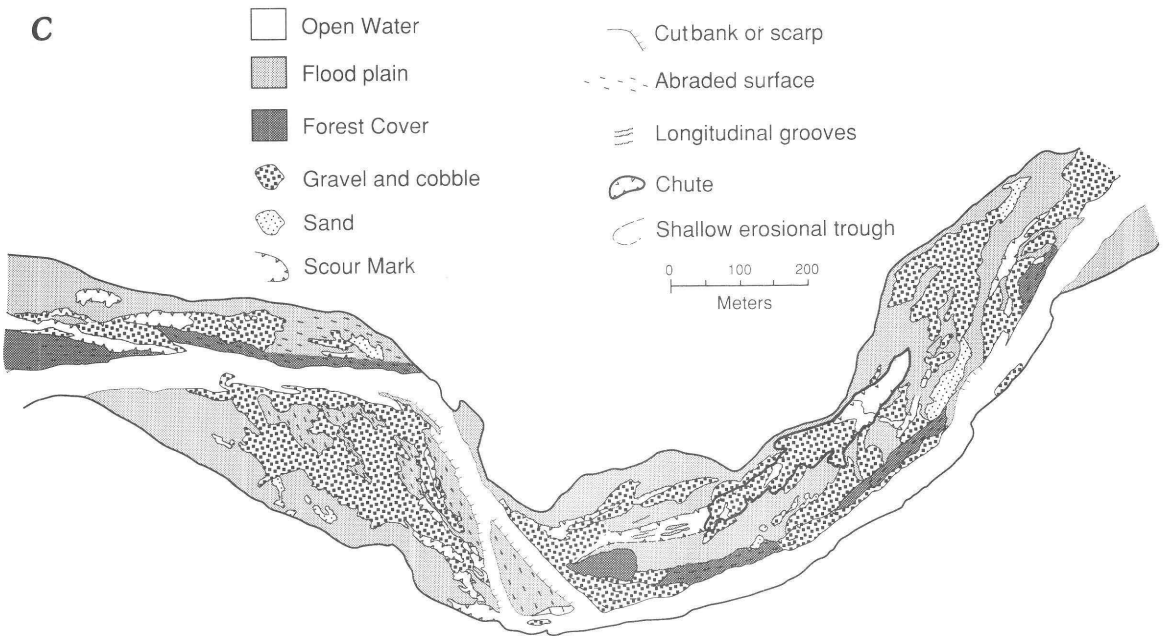

Figure 99. Continued.

their greater resistance to erosion, these also experience relatively little change even in an extreme flood.

Although the relation between reach-average unit stream power and percent of reach length assigned to the severe and catastrophic erosion classes appears weak for individual valleys, a scatterplot based on the pooled data does reveal a trend (fig. 104). The data appear to define an envelope curve for this flood, and along this curve the extent of severe erosion increases sharply with increasing unit power. Reaches with more than 50 percent of their length mapped in the severe and catastrophic erosion classes are associated with reach-average unit stream power values in the range of 200–500 W/m^2. If valley reaches with average widths of 200 m or less are assumed to be partly constrained by bedrock and thus more resistant to erosion, we can isolate the points representing those reaches and examine the other points on the plot. Although the majority of these points still lie below the envelope curve, the general trend is in much closer agreement with the shape of the envelope.

The explanation of spatial patterns of fluvial erosion presented here is a preliminary analysis of a complex process. Studies in progress are intended to provide a comprehensive approach to defining the physiographic, hydraulic, and hydrologic constraints on severe erosion of the valley floor. Miller (1990) concluded that meteorologic and hydrologic conditions associated with the November 1985 event were no more severe than conditions during several other events occurring in other areas of the central Appalachians during the preceding 50 yr. Unusual impacts associated with this flood are attributable to the juxtaposition of an extreme meteorologic event with a particular pattern of valley physiography. Details of the interaction of the flood flow with the boundary conditions in any given valley reach remain to be explored, and threshold hydraulic conditions associated with different levels of erosion intensity remain to be defined.

Although we primarily describe how the November 1985 flood affected the valleys of the South Branch Potomac River, our observations have a bearing on broader questions of Appalachian geomorphology and hazards.

In some environments, river channels and flood plains appear to be equilibrium landforms sculpted by frequently recurring events of moderate intensity rather than by rare, extreme events. This paradigm, stated by Wolman and Miller (1960), is supported by published observations of the modest, relatively short-lived effects of large floods occurring in areas of temperate climate and moderate relief (Wolman and Eiler, 1958; Costa, 1974; Gupta and Fox, 1974; Moss and Kochel, 1978). The November 1985 flood and others reported in the literature (Hack and Goodlett, 1960; Stewart and LaMarche, 1967; Williams and Guy, 1973; Baker, 1977; Shroba and others, 1979; Gupta, 1983; Nanson, 1986) appear to be counterexamples, leading observers to suggest that in some steep, narrow valleys the infrequent extreme events may be dominant in forming the landscape. Examples from sand-bedded streams in arid and semiarid piedmont or plains environments indicate that a large enough flood may cause spectacular channel widening in these settings as well, and that subsequent recovery or continued channel widening is dependent on the sequence of flood flows occurring over periods of several decades

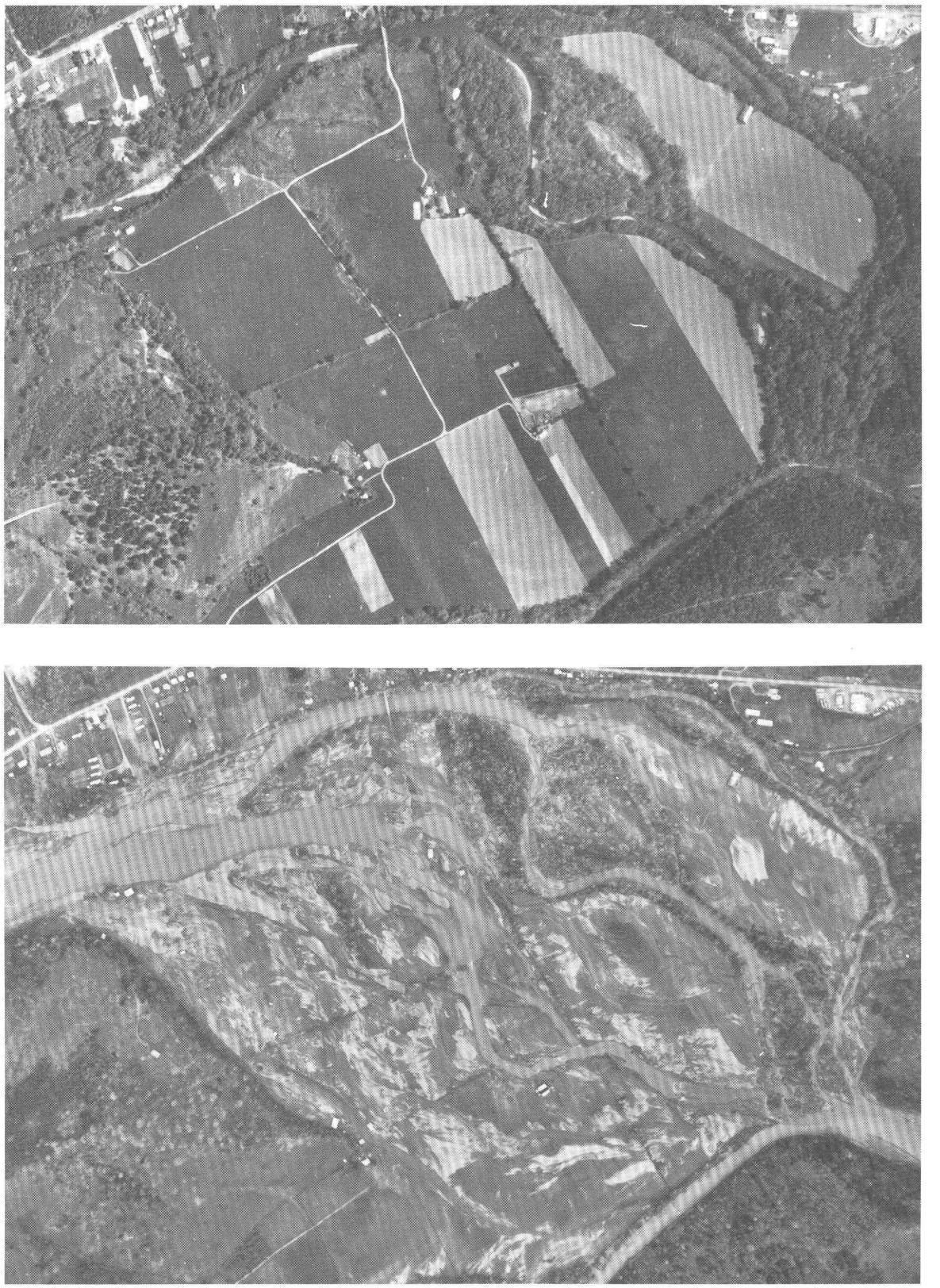

Figure 100. (*A*) Before and (*B*) after views of the confluence of the North Fork South Branch and South Branch Potomac Rivers. The North Fork enters from the upper left, and the South Branch enters from bottom center. This is an example of erosion class D; note the extent of flood-plain dissection accomplished by the North Fork upstream of the confluence. Note also the presence of patchy sand deposits over much of the valley floor. Field of view is 1,900 m wide.

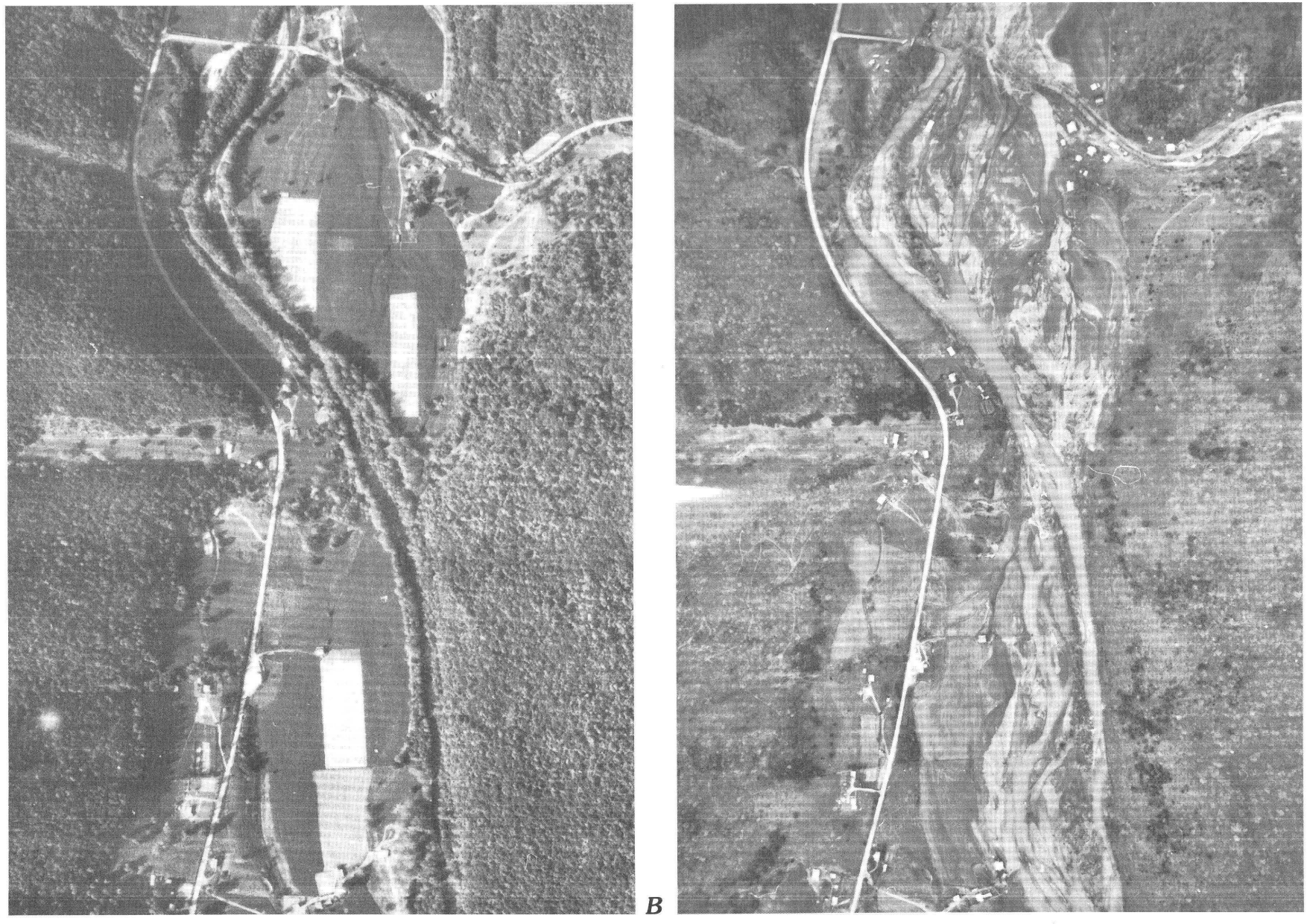

Figure 101. (*A*) Before and (*B*) after views of the North Fork valley, about 7 km upstream of Seneca Rocks. Flow is from bottom to top. This is an example of erosion class D. Field of view is 1,200 m wide.

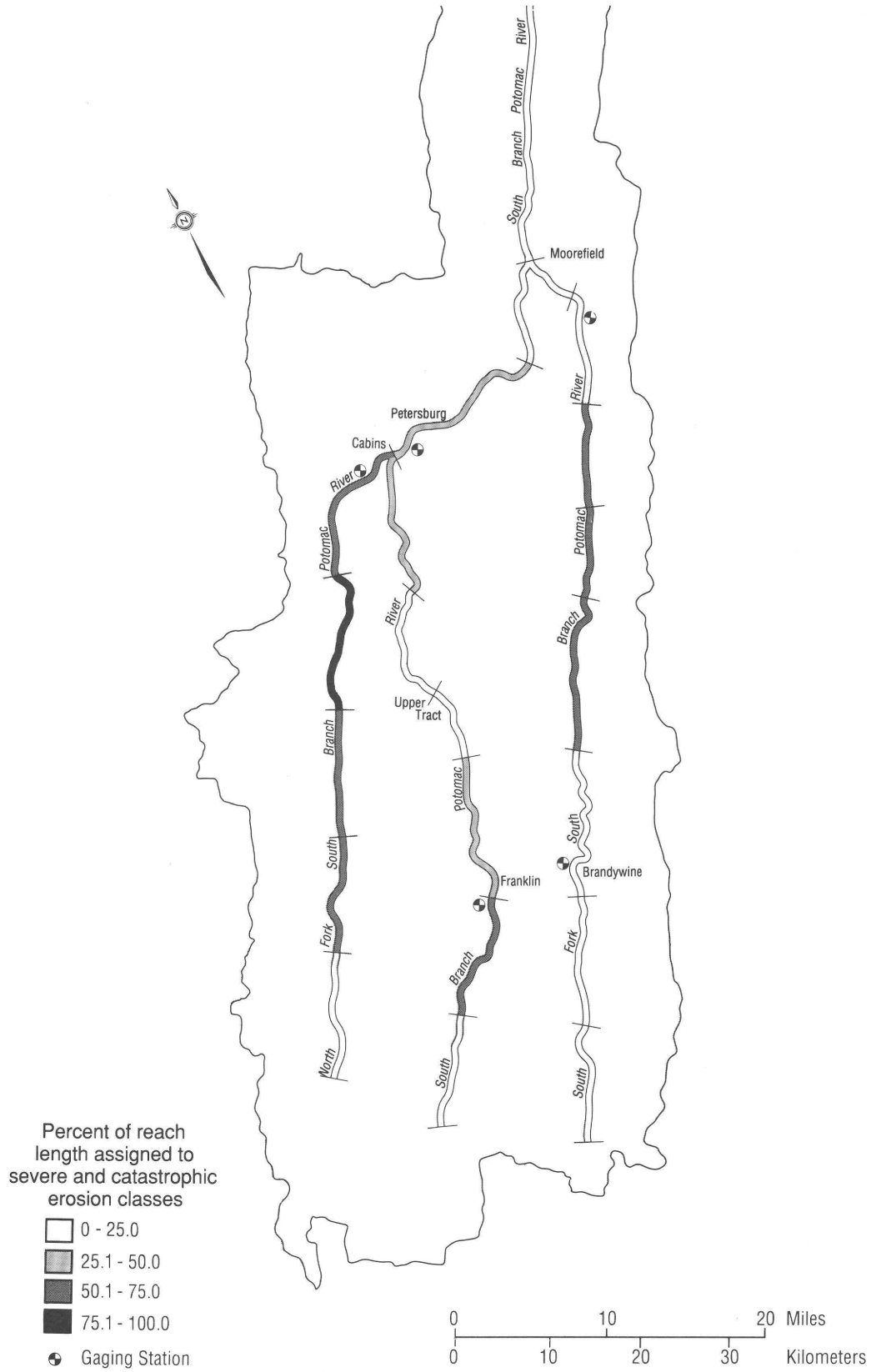

Figure 102. Map showing generalized spatial distribution of severe valley-floor erosion.

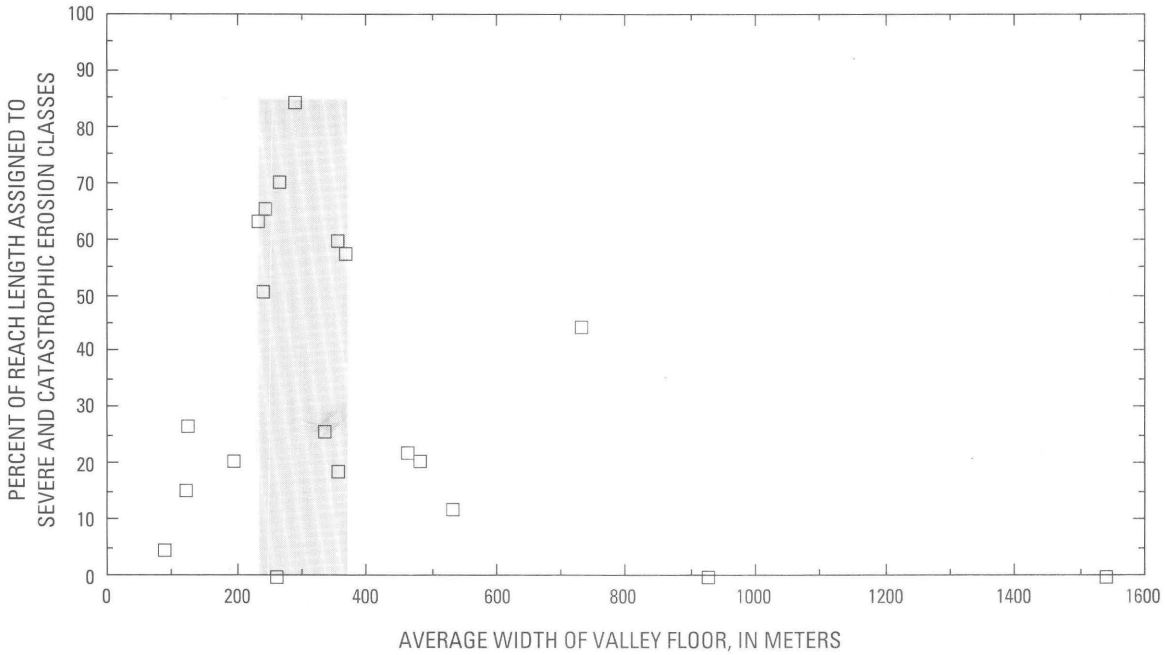

Figure 103. Plot of percent reach length assigned to erosion classes C and D versus average width of valley floor. The highest percentages are associated with a narrow range of valley widths (shaded area).

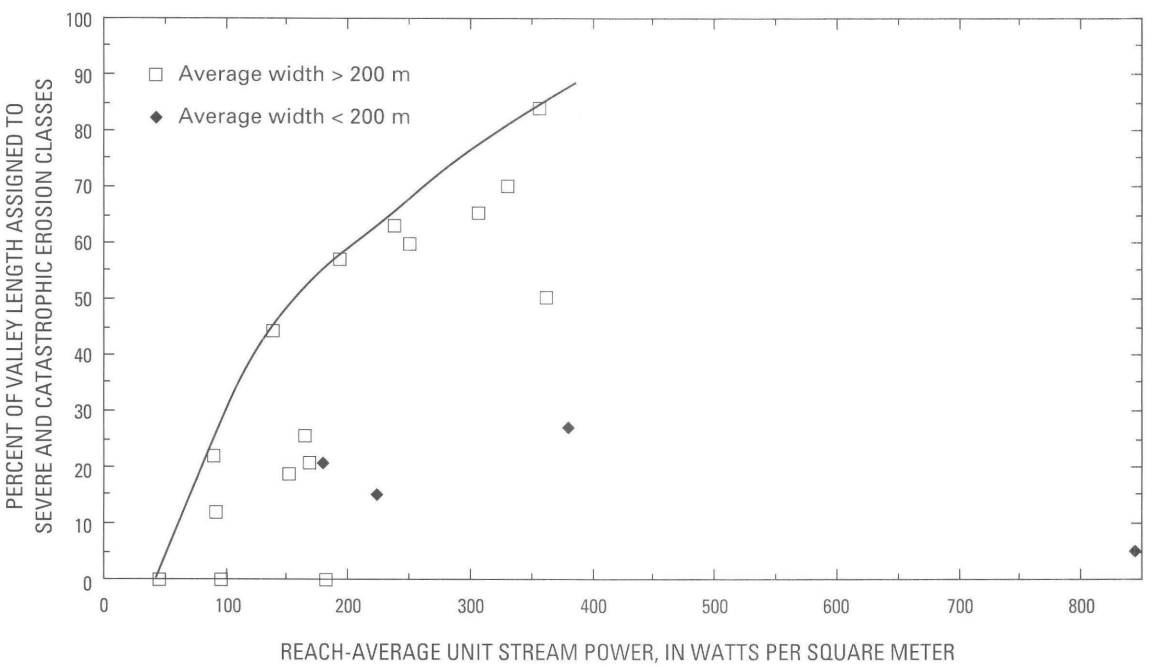

Figure 104. Plot of percent reach length assigned to erosion classes C and D versus reach-average values of unit stream power.

(Schumm and Lichty, 1963; Burkham, 1972; Osterkamp and Costa, 1987; Kresan, 1988). Wolman and Gerson (1978), recognizing that the paradigm described by Wolman and Miller (1960) did not account for these observations, described the relative effectiveness of large floods in terms of the comparison between recurrence interval and recovery time.

Rehabilitation efforts following this and other extreme floods tend to limit observations of natural recovery processes. Therefore, to test hypotheses about the relative importance of extreme floods in valley-floor evolution, it may be necessary to develop models for interpreting the geologic record of past floods. Conceptual models of flood-plain morphology and stratigraphy might incorporate features analogous to those created in the November 1985 flood. For example, extreme heterogeneity of sediment textures is to be expected, such as cobbles and boulders in or adjacent to erosion channels that are filled with finer sediment deposited during subsequent floods of lower magnitude. Nanson (1986) described geomorphic and stratigraphic patterns in valleys where channel and flood plain evidently do not reach equilibrium form over an extended period of time; his conceptual model posits a cyclical pattern of vertical aggradation punctuated by catastrophic erosion and reworking of older sediments. The age of the deposits buried beneath the flood-plain surface may vary greatly within a single valley cross section, depending on the history of erosion and subsequent aggradation. Hack and Goodlett (1960) suggested that a similar type of disequilibrium form may be common in the Appalachians.

Observations of this flood have implications for the evaluation of potential hazards. The costs associated with "ordinary" floods often involve property loss due to inundation by water and deposition of sediment, as well as disruption of utility service and contamination of water supplies. These costs are concentrated in urban areas, as private property is concentrated in these areas. Thus, planning for flood control and mitigation of flood losses traditionally is focused on protection of population centers. Mapping programs for prediction of areas subject to inundation in flood events with recurrence intervals of 100 yr have been undertaken by the U.S. Geological Survey and the Federal Emergency Management Agency.

Examination of the costs of the November 1985 flood (see Jacobson, chapter A, this volume) suggests that policymakers need a better understanding of the potential hazards and costs of rare floods. Costs from the flood are associated with extensive damage to infrastructure, including road networks, bridges, dams, and buildings. These costs were distributed over a broad area. Long-term loss of agricultural production was another result of the flood; without substantial infusion of Federal funds, many farms on valley floors in the South Branch basin might have been unproductive for centuries. Even after massive rehabilitation, some of these farms will never return to previous levels of productivity. Although it is unlikely that society can be fully protected from events of this type, public agencies, individuals, and businesses may benefit from an improved ability to predict what locations are potentially at risk from catastrophic erosion or sedimentation during an extreme flood. This information can be used in siting of roads, bridges, homes, and businesses. In some instances a difference in location of only a few hundred meters may be sufficient to avoid the most severe impacts of another flood like the November 1985 event; note, for example, that the houses destroyed at the site illustrated in figures 46*A* and *B* were in the direct path of flow emerging from a bedrock constriction. The turkey sheds in figure 9*B* were also in a vulnerable position with respect to the pattern of flood flow emerging from a constriction.

The utility of selecting a single recurrence interval that would be uniform for all flood-hazard zoning also may be questioned in the aftermath of the 1985 flood. The most severe impacts and the greatest risks to life and property are not necessarily limited to the area inundated by events with 100-yr recurrence intervals; nor are all sites within the confines of such an area actually exposed to the same kinds of hazards. In high-gradient, high-energy river basins the prevailing hydraulic conditions during any one event may vary greatly, both longitudinally along the valley and laterally across the valley. Instead of identifying the areas affected by a particular design storm, it may be more sensible to provide the public with information on hazards associated with flows of specified recurrence interval at any given site, or to provide estimates of the recurrence intervals associated with particular kinds of hazards.

Erosion and deposition associated with manmade structures and land-use patterns show that flood-flow hydraulics are substantially influenced by the cumulative effects of human activity on the valley floor. For example, bridges and road embankments clearly affect flow patterns and are in turn affected by them. Other human impacts extend beyond local effects of engineering structures. Clearing of forested valley floors reduces roughness and also reduces resistance to erosion. Changes in channel pattern and gradient following local channel diversion, clearing, and straightening have undoubtedly affected hydraulic characteristics of flood waves in many valleys. Artificial filling of overflow channels and construction of buildings on the fill may retard or divert flow during a large flood and could lead to extensive damage on the valley floor.

Although recent studies have improved understanding of impacts of drainage modifications on channel evolution (Schumm and others, 1984; Simon and Hupp, 1986), the effects of channel work or valley-floor modification on patterns of overbank flow and the potential for valley-floor erosion have yet to be thoroughly investigated. In regions where extreme floods have the potential for causing this type of damage, agencies charged with public safety and

hazard mitigation have reason to be interested in achieving a better understanding of such effects.

SUMMARY AND CONCLUSIONS

It is clear from examination of the hydrologic data and the geomorphic evidence that the November 1985 flood was a rare event. Indeed, although channel widening and valley-floor erosion have been reported in the aftermath of other floods, we have not found documentation of such intense valley-floor modification occurring over such a large area. Similar events certainly have occurred in the past and will occur in the future. In the case of the November 1985 flood, availability of large-scale aerial photographs covering most of the affected area allowed documentation of the various flood impacts and their spatial extents. As such opportunities are rare, a primary goal of this paper is to provide information that may serve as a useful point of reference for investigators studying similar events occurring in other times and places.

The November 1985 flood was the largest recorded in the South Branch Potomac River basin, with discharges exceeding values estimated for a recurrence interval of 500 yr at four of six gage sites. Flow velocities in the channel were as high as 4.6 m/s and locally may have exceeded 6 m/s; estimated values of unit stream power at U.S. Geological Survey gage locations were as high as 988 W/m^2 and may have exceeded 2,500 W/m^2 at some locations. Hydraulic conditions during the flood were heavily influenced by valley physiography, which in turn was influenced by the bedrock structure of this part of the Valley and Ridge. Because of the presence of numerous valley constrictions and expansions, very large discharges were forced through relatively small valley cross sections. Evidence collected after the flood demonstrates that bedrock canyons were responsible for ponding of floodwaters upstream and that flow emerging from canyons and valley constrictions caused severe erosion at many sites.

Geomorphic impacts of the flood included an array of erosion features, including longitudinal grooves, scour marks, extensive channel widening, stripping of alluvium from the valley floor, bottomland dissection by anastomosing erosion channels, and jet-shaped erosion forms. Widespread deposition of coarse sediment was heavily concentrated at locations laterally contiguous with eroded areas. Newly formed channel bars were observed at several locations but were relatively uncommon. Splay deposits, gravel and sand sheets, isolated gravel bars and sand dunes, wake deposits, and backwater deposits were left behind by the flood at many locations along the flood plain. Particle size of flood-plain deposits along the three forks of the South Branch Potomac River ranged from sand to boulders, with some transported particles exceeding 1 m in diameter; particle sizes decreased downstream along the main stem Potomac River, consisting primarily of fine-grained sediment.

Mapping of erosion damage by classes along 384 km of channel and valley floor between the Virginia–West Virginia border and the confluence of the North and South Branches of the Potomac River revealed that 82.8 percent of the valley length experienced at least incipient erosion, 30.2 percent experienced severe erosion, and 5.7 percent experienced catastrophic erosion of the valley floor. Valley reaches with at least 50 percent of their length classified as experiencing severe erosion generally fell in a narrow range of average valley-floor widths (between 230 and 370 m). Reach-average values of unit stream power were calculated from estimates of peak discharge, valley width, and channel gradient; severe erosion percentages of 50 percent or more were associated with reach-average values of unit stream power of 200–500 W/m^2. The results suggest that it should be possible to define threshold conditions for severe bottomland erosion. Further research is required to provide more detailed information on relations between hydrologic inputs, valley physiography, flood hydraulics, and geomorphic impacts on valley floors in extreme floods.

REFERENCES CITED

Allen, J.R.L., 1971, Transverse erosional marks of mud and rock, Their physical basis and geological significance: Sedimentology, v. 5, p. 167–385.

———1982, Sedimentary structures, Their character and physical basis: Developments in sedimentology, v. 30A–30B: New York, Elsevier.

———1985, Principles of physical sedimentology: London, Allen & Unwin, 272 p.

Ashmore, P.E., 1982, Laboratory modelling of gravel braided stream morphology: Earth Surface Processes and Landforms, v. 7, p. 201–225.

Bagnold, R.A., 1966, An approach to the sediment transport problem from general physics: U.S. Geological Survey Professional Paper 422–I, 37 p.

Baker, V.R., 1977, Stream channel response to floods with examples from central Texas: Geological Society of America Bulletin, v. 88, p. 1057–1071.

———1978, Paleohydraulics and hydrodynamics of Scabland floods, *in* Baker, V.R., and Nummedal, D., eds., The channeled scabland: Washington, D.C., National Aeronautics and Space Administration, p. 59–115. (Reprinted in Baker, V.R., ed., 1981, Catastrophic flooding, The origin of the channeled scabland: Benchmark Papers in Geology, v. 55: Stroudsburg, Pa., Dowden, Hutchinson and Ross, 361 p.)

———1984, Flood sedimentation in bedrock fluvial systems, *in* Koster, E.H., and Steel, R.J., eds., Sedimentology of gravels and conglomerates: Canadian Society of Petroleum Geologists Memoir 10, p. 87–98.

———1988, Flood erosion, *in* Baker, V.R., Kochel, R.C., and Patton, P.D., eds., Flood geomorphology: New York, John Wiley and Sons, p. 81–95.

Baker, V.R., and Costa, J.E., 1987, Flood power, *in* Mayer, L., and Nash, D., eds., Catastrophic flooding: London, Allen and Unwin, p. 1–21.

Baker, V.R., and Kochel, R.C., 1988, Flood sedimentation in bedrock fluvial systems, *in* Baker, V.R., Kochel, R.C., and Patton, P.C., eds., Flood geomorphology: New York, John Wiley and Sons, p. 123–137.

Baloch, M.S., Henry, E.N., and Dickerson, W.H., 1971, Streamflow characteristics of the Potomac River: Charleston, W. Va., West Virginia Department of Natural Resources, Division of Water Resources and West Virginia University, 276 p.

Bretz, J.H., 1923, The channeled scablands of the Columbia Plateau: Journal of Geology, v. 31, p. 617–649.

———1928, The channeled scabland of eastern Washington: Geographical Review, v. 18, p. 446–477.

———1959, Washington's channeled scabland: Washington Division of Mines and Geology Bulletin 45, p. 7–57.

Burkham, D.E., 1972, Channel changes of the Gila River, Safford Valley, Arizona, 1846–1970: U.S. Geological Survey Professional Paper 655–G, 24 p.

Carson, M.A., 1984, Observations on the meandering-braided river transition, the Canterbury Plains, New Zealand: New Zealand Geographer, v. 40, p. 12–17, 89–99.

Chorley, R.J., 1959, The shape of drumlins: Journal of Glaciology, v. 3, p. 339–344.

Chow, V.T., 1959, Open-channel hydraulics: New York, McGraw-Hill, 680 p.

Church, M., and Jones, D., 1982, Channel bars in gravel-bed rivers, *in* Hey, R.D., Bathurst, J.C., and Thorne, C.R., eds., Gravel-bed rivers: New York, John Wiley and Sons, p. 291–324.

Clark, G.M., 1967, Structural geomorphology of a portion of the Wills Mountain Anticlinorium, Mineral and Grant Counties, W. Va.: University Park, Pennsylvania State University, Ph.D. thesis, 165 p.

———1987, Some major topographic and drainage relationships in the North Fork Mountain-Smoke Hole area, Grant and Pendleton Counties, W. Va., *in* Kite, J.S., ed., Research on the Late Cenozoic of the Potomac Highlands, Southeastern Friends of the Pleistocene, v. 1: Morgantown, W. Va., West Virginia Geological and Economic Survey Open-File Report OF–88–2, p. 67–77.

Clark, G.M., Jacobson, R.B., Kite, J.S., and Linton, R.C., 1987, Storm-induced catastrophic flooding in Virginia and West Virginia, November 1985, *in* Mayer, L., and Nash, D., eds., Catastrophic flooding: London, Allen & Unwin, p. 355–379.

Collins, R.F., and Schalk, M., 1937, Torrential flood erosion in the Connecticut Valley, March 1936: American Journal of Science, v. 34, p. 293–307.

Costa, J.E., 1974, Response and recovery of a Piedmont watershed from tropical storm Agnes, June 1972: Water Resources Research, v. 10, p. 106–112.

———1983, Paleohydraulic reconstruction of flash-flood peaks from boulder deposits in the Colorado Front Range: Geological Society of America Bulletin, v. 94, p. 986–1004.

———1987, A comparison of the largest rainfall-runoff floods in the United States with those of the People's Republic of China and the world: Journal of Hydrology, v. 96, p. 101–115.

Dunn, L.S., 1959, Tractive resistance of cohesive channels: Proceedings of the American Society of Civil Engineers, Journal of the Soil Mechanics and Foundations Division, v. 85, p. 1–24.

Dzulynski, S., and Sanders, J.E., 1962, Current marks on firm mud bottoms: Transactions of the Connecticut Academy of Arts and Sciences, v. 42, p. 57–96.

Dzulynski, S., and Walton, E.K., 1965, Sedimentary features of flysch and graywackes: New York, Elsevier.

Einstein, H.A., and Li, H., 1958, Secondary currents in straight channels: Transactions of the American Geophysical Union, v. 39, p. 1085–1088.

Fridley, H.M., 1939, Solution and stream piracy: Journal of Geology, v. 47, p. 177–188.

———1940, Watergaps by solution and piracy, A reply: American Journal of Science, v. 238, p. 226–233.

Friel, E.A., Hobba, W.A., and Chisholm, J.L., 1975, Records of wells, springs, and streams in the Potomac River Basin, West Virginia: Morgantown, W. Va., West Virginia Geological and Economic Survey Basic Data Report 3.

Gerritsen, S., and Dunne, W.M., 1988, Reexamination of the Smoke Holes, W. Va., and the role of faulting in cover deformation within the central Appalachians [abs.]: Geological Society of America Abstracts with Programs, v. 20, p. 266.

Gupta, A., 1983, High-magnitude floods and stream channel response, *in* Collinson, J.D., and Lewin, J., eds., Modern and ancient fluvial systems: International Association of Sedimentologists Special Publication 6, p. 219–227.

Gupta, A., and Fox, H., 1974, Effects of high-magnitude floods on channel form, A case study in the Maryland Piedmont: Water Resources Research, v. 10, p. 499–509.

Hack, J.T., 1973, Drainage adjustment in the Appalachians, *in* Morisawa, M. E., ed., Fluvial geomorphology: Binghamton, N.Y., Publications in Geomorphology, p. 51–69.

Hack, J.T., and Goodlett, J.C., 1960, Geomorphology and forest ecology of a mountain region in the central Appalachians: U.S. Geological Survey Professional Paper 347, 66 p.

Hobba, W.A., Jr., Friel, E.A., and Chisholm, J.L., 1972, Water resources of the Potomac River Basin, West Virginia: Morgantown, W. Va., West Virginia Geological and Economic Survey, River Basin Bulletin 3.

Interagency Advisory Committee on Water Data, 1982, Guidelines for determining flood flow frequency: U.S. Geological Survey Office of Water Data Coordination, Bulletin 17B.

Jacobson, R.B., Linton, R.C., and Rubin, Meyer, 1989, Alluvial stratigraphy of the Potomac River valley bottom near Petersburg and Moorefield, W. Va.: U.S. Geological Survey Open-File Report 89–485, 27 p.

Jahns, R.H., 1947, Geologic features in the Connecticut Valley, Massachusetts, as related to recent floods: U.S. Geological Survey Water-Supply Paper 996, 158 p.

James, R.W., Jr., Simmons, R.H., and Strain, B.F., 1987, Water resources data, Maryland and Delaware, Water year 1986: U.S. Geological Survey Water-Data Report MD–DE–86–1, 316 p.

Karcz, I., 1967, Harrow marks, current-aligned sedimentary structures: Journal of Geology, v. 75, p. 113–121.

———1968, Fluviatile obstacle marks from the wadis of the Negev (southern Israel): Journal of Sedimentary Petrology, v. 38, p. 1000–1012.

Kehew, A.E., and Lord, M.L., 1986, Origin and large-scale erosional features of glacial-lake spillways in the northern Great Plains: Geological Society of America Bulletin 97, p. 162–177.

Kite, J.S., ed., 1987, Research on the Late Cenozoic of the Potomac Highlands, Southeastern Friends of the Pleistocene, v. 1: Morgantown, W. Va., West Virginia Geological and Economic Survey Open-File Report OF–88–2.

Knox, J.C., 1987, Stratigraphic evidence of large floods in the upper Mississippi Valley, *in* Mayer, L., and Nash, D., eds., Catastrophic flooding, London, Allen & Unwin, p. 155–180.

Komar, P.D., 1983, The shapes of streamlined islands on Earth and Mars, Experiments and analysis of the least-drag form: Geology, v. 11, p. 651–654.

———1988, Sediment transport by floods, *in* Baker, V.R., Kochel, R.C., and Patton, P.C., eds., Flood geomorphology: New York, John Wiley and Sons, p. 97–111.

Kresan, P.L., 1988, The Tucson, Arizona, Flood of October 1983— Implications for land management along alluvial river channels, *in* Baker, V.R., Kochel, R.C., and Patton, P.C., Flood geomorphology: New York, John Wiley and Sons, p. 465–489.

Krigstrom, A., 1962, Geomorphological studies of sandur plains and their braided rivers in Iceland: Geografiska Annaler, v. 44, p. 328–346.

Lane, E.W., 1957, A study of the shape of channels formed by natural streams flowing in erodible material: Omaha, Nebr., U.S. Army Engineer Division, Mississippi River Corps of Engineers, Sediment Series 9.

Laursen, E.M., 1960, Scour at bridge crossings: Journal of the Hydraulics Division, Proceedings of the American Society of Civil Engineers, v. 86, p. 39–54.

Lescinsky, J.B., 1987, Flood of November 1985 in West Virginia, Pennsylvania, Maryland, and Virginia: U.S. Geological Survey Open-File Report 86–486.

Lewin, J., and Brindle, B.J., 1977, Confined meanders, *in* Gregory, K.J., ed., River channel changes: New York, Wiley-Interscience, p. 221–233.

Matthes, G.H., 1947, Macroturbulence in natural stream flow: Transactions of the American Geophysical Union, v. 28, p. 255- 262.

McKoy, M.L., 1987, Flood flow hydrology at Seneca Rocks, *in* Kite, J.S., ed., Research on the Late Cenozoic of the Potomac Highlands, Southeastern Friends of the Pleistocene, v. 1: Morgantown, W. Va., West Virginia Geological and Economic Survey Open-File Report OF–88–2, p. 78–85.

Miller, A.J., 1990, Flood hydrology and geomorphic effectiveness in the central Appalachians: Earth Surface Processes and Landforms, v. 15, p. 119–134.

Moore, D.G., and Masch, F.D., 1963, Influence of secondary flow on local scour at obstructions in a channel: U.S. Department of Agriculture Miscellaneous Publication 970, p. 314–320.

Moss, J.H., and Kochel, R.C., 1978, Unexpected geomorphic effects of the Hurricane Agnes storm and flood, Conestoga drainage basin, southeastern Pennsylvania: Journal of Geology, v. 86, p. 1–11.

Nanson, G.C., 1986, Episodes of vertical accretion and catastrophic stripping, A model of disequilibrium flood plain development: Geological Society of America Bulletin, v. 97, p. 1467–1475.

Osterkamp, W.R., and Costa, J.E., 1987, Changes accompanying an extraordinary flood on a sand bed stream, *in* Mayer, L., and Nash, D., eds., Catastrophic flooding: London, Allen & Unwin, p. 201–224.

Osterkamp, W.R., and Hedman, E.R., 1977, Variation of width and discharge for natural high-gradient stream channels: Water Resources Research, v. 13, p. 256–258.

Paola, C., Gust, G., and Southard, J.B., 1986, Skin friction behind isolated hemispheres and the formation of obstacle marks: Sedimentology, v. 33, p. 279–293.

Peabody, F.E., 1947, Current crescents in the Triassic Moenkopi formation: Journal of Sedimentary Petrology, v. 17, p. 73–76.

Ritter, D.F., 1975, Stratigraphic implications of coarse-grained gravel deposited as overbank sediment, southern Illinois: Journal of Geology, v. 83, p. 645–650.

———1988, Floodplain erosion and deposition during the December 1982 floods in southeast Missouri, *in* Baker, V.R., Kochel, R.C., and Patton, P.C. eds., Flood geomorphology: New York, John Wiley and Sons, p. 243–259.

Ritter, D.F., and Blakely, D.S., 1986, Localized catastrophic disruption of the Gasconade River flood plain during the December 1982 flood, southeast Missouri: Geology, v. 14, p. 472–476.

Runner, G.S., 1980, Runoff studies on small drainage areas (Technique for estimating magnitude and frequency of floods in West Virginia): U.S. Geological Survey Open-File Report 80–1218.

Scatena, F. N., 1986, Flood plain reconnaissance study, November 1985 flood, Potomac River Basin: Interstate Commission on the Potomac River Basin Technical Report 86–5, 32 p.

Schumm, S.A., Harvey, M.D., and Watson, C.C., 1984, Incised channels: Morphology, dynamics and control: Littleton, Colo., Water Resources Publications, 200 p.

Schumm, S.A., and Lichty, R.W., 1963, Channel widening and flood-plain construction along Cimarron River in southwestern Kansas: U.S. Geological Survey Professional Paper 352–D, p. 71–88.

Shen, H.W., 1971, Scour near piers, *in* Shen, H.W., ed., River mechanics: Ft. Collins, Colo., Colorado State University, p. 23.1–23.25.

Shepherd, R.G., and Schumm, S.A., 1974, Experimental study of river incision: Geological Society of America Bulletin, v. 85, p. 257–268.

Shroba, R.R., Schmidt, P.W., Crosby, E.J., and Hansen, W.R., 1979, Storm and flood of July 31–August 1, 1976, in the Big Thompson River and Cache la Poudre River basins, Larimer and Weld Counties, Colorado, Part B, Geologic and geomorphic effects in the Big Thompson Canyon area, Larimer County: U. S. Geological Survey Professional Paper 1115, p. 87–152.

Simon, A., and Hupp, C.R., 1986, Channel evolution in modified Tennessee channels, *in* Proceedings of the Fourth Federal Interagency Sedimentation Conference, v. 2: Subcommittee on Sedimentation of the Interagency Advisory Committee on Water Data, p. 5-71–5-82.

Sites, R.S., 1973, Geology of the Smoke Hole region of West Virginia: Southeastern Geology, v. 15, p. 153–167.

Smith, D.G., 1983, Anastomosed fluvial deposits: modern examples from western Canada, *in* Collinson, J.D., and Lewin, J., eds., Modern and ancient fluvial systems, International Association of Sedimentologists Special Publication 6, Blackwell Scientific Publications, p. 155–168.

Smith, N.D., 1974, Sedimentology and bar formation in the upper Kicking Horse River, A braided outwash stream: Journal of Geology, v. 82, p. 205–223.

Stedinger, J.R., and Baker, V.R., 1987, Surface water hydrology, Historical and paleoflood information: Reviews of Geophysics, v. 25, p. 119–124.

Stewart, J.H., and LaMarche, V.C., 1967, Erosion and deposition produced by the flood of December 1964 on Coffee Creek, Trinity County, California: U.S. Geological Survey Professional Paper 422–K, 22 p.

Sullivan, J.E., 1983, Geomorphic effectiveness of a high-magnitude rare flood in central Texas: University of Texas at Austin, unpublished Master's thesis, 214 p.

Ver Steeg, K., 1940, The formation of watergaps by solution and piracy: American Journal of Science, v. 238, p. 32–41.

West Virginia Advocate, 1986, The West Virginia killer flood of 1985: Flood Commemorative Issue, 96 p.

Williams, G.P., and Guy, H.P., 1973, Erosional and depositional aspects of Hurricane Camille in Virginia, 1969: U.S. Geological Survey Professional Paper 804, 80 p.

Wolman, M.G., and Eiler, J.P., 1958, Reconnaissance study of erosion and deposition produced by the flood of August 1955 in Connecticut: American Geophysical Union Transactions, v. 39, p. 1–14.

Wolman, M.G., and Gerson, R., 1978, Relative scales of time and effectiveness of climate in watershed geomorphology: Earth Surface Processes, v. 3, p. 189–208.

Wolman, M.G., and Leopold, L.B., 1957, River flood plains, Some observations on their formation: U.S. Geological Survey Professional Paper 282–C, p. 87–107.

Wolman, M.G., and Miller, J.P., 1960, Magnitude and frequency of forces in geomorphic processes: Journal of Geology, v. 68, p. 54–74.

☆ U.S. G.P.O. 1993-342-389:80004